Development of an immunocompetent model of oncolytic adenoviral gene therapy for ovarian cancer

Anna-Mary Young

A thesis submitted to the University of London (Faculty of Science) for the degree of Doctor of Philosophy

August 2012

Centre for Molecular Oncology
Bart's Cancer Institute
Bart's & The London School of Medicine & Dentistry
Charterhouse Square, London EC1M 6BQ

I, Anna-Mary Young, hereby confirm that the work presented in this thesis is original and is my own. Work undertaken by others in contribution to this thesis has been clearly indicated. Where information has been derived from other sources, this has been acknowledged and appropriately referenced.

Acknowledgements

First and foremost huge thanks go to my supervisor Iain McNeish without whom none of this would have been possible. I am tremendously grateful to him for the opportunity to come to the lab and I hope to put to good use the skills acquired therein. Sincere thanks also go to him for his tenacity and harassment during the writing of this thesis - I could not have done it without him. Huge thanks to all those in the lab who came to my aid on innumerable occasions; all of Team McNeish – Sarah, Maggie, Lynda, Karin, Katrina, Laura , Lynsey, Michael - along with Barbara, Gioia, Rathi, Pam and many more. To the boys, Ming, Mo, Mark, Daniel and Jim for top tips, cloning advice and football banter. Thanks must also go to CRUK without whose funding this work would not have been possible and who continue to fund cancer research despite the difficult economic climate.

I should like to dedicate this thesis to several people. Firstly to my mother who has been a constant inspiration to me despite leaving this world far too soon; to my long-suffering family- my father and stepmother and my “double trouble” Olivia and James. They have manfully weathered the ups and downs of this doctoral thesis and have kept me sane. The laughter and the tears have been a great antidote to the stresses and strains of the work-life balance.

Finally I should like to thank the staff and patients with whom I have had the privilege to work. They are a constant source of inspiration. All I can say is, “Together we will beat it…..”

Abstract

Oncolytic adenoviral gene therapy has potential as a novel anti-cancer agent for ovarian cancer. Host immune responses are thought to contribute to its therapeutic effects. However further evaluation has been hampered by the lack of an immunocompetent animal model. This is predominantly because human adenovirus is highly species-specific and replicates poorly in murine cells.

The second generation human adenovirus (hAd5) type 5 mutant *dl*922-947 contains a deletion in the E1A CR2 region which allows it to replicate selectively in cells with Rb pathway abnormalities, a finding observed in >90% of human cancers. Previous work has shown that *dl*922-947 has considerable activity in ovarian cancer and is more potent than E1A wild-type adenoviruses and the E1B-55K mutant *dl*1520 (Onyx-015, H101). Unfortunately, like its wild-type counterpart, *dl*922-947 replicates poorly in murine cells and infectious virion progeny are not generated.

Mechanisms for the failure of infectious virion formation remain unclear and have been investigated as part of this project. I have found that murine malignant cells can be infected readily with hAd5 vectors. Both early and late viral genes are transcribed and there is evidence of viral genome replication. However, a profound failure of infective virion production is observed together with low levels of late viral protein expression. Ribosome fractionation assays show reduced viral mRNA loading in murine cells, resulting in failure of translation, especially of late transcripts. Aberrant function of the non-structural L4 protein 100K has been identified as a major hurdle to successful viral replication in murine cells. Ectopic expression of L4 100K promotes translation of viral late mRNA and increases expression of late viral proteins and virion production. However, these increases are only partial.

Table of Contents

Table of Figures

Abbreviations

aa	amino acid residue
AAV2	Adeno-Associated Virus-2
Ad2	Human adenovirus serotype 2
Ad5	Human adenovirus serotype 5
Ad48	Human adenovirus serotype 48
AdCre	Cre recombinase adenovirus
ADP	Adenovirus death protein
AKT	serine/threonine specific protein kinase
ALD	adrenoleukodystrophy
ALT	Alanine Transaminase
ATCC	American Type Culture Collection
ATM	Ataxia-Telangiectasia mutated protein kinase
ATR	ATM and RAD-3 related protein kinase
AUG	nucleotide sequence for methionine; start codon for mRNA translation
BAX	Bcl-2–associated X protein
Bcl-2	B-cell lymphoma 2 protein
BLAST	Basic Local Alignment Search Tool
BLD	below the limit of detection
BRAF	v-Raf murine sarcoma viral oncogene homolog B1
BRAF	serine/threonine-protein kinase B-Raf
BRCA1/2	gene encoding breast cancer type 1/2 susceptibility proteins
BSA	bovine serum albumin
C57Bl/6	C57 black 6 laboratory mice
$CaCl_2$	calcium chloride
CAR	Coxsackievirus and Adenovirus Receptor
CBP	complement binding protein
CCR	coiled-coiled region
cDNA	complementary 1st strand DNA
CIC	Cortical inclusion cyst
CIN	chromosomal instability
CMT64	murine alveogenic lung carcinoma tumour cell line
CMT93	murine rectal carcinoma cell line
CMV	cytomegalovirus
CPE	cytopathic effect

CsCl	caesium chloride
C_T	cycle threshold
CTL	cytotoxic T lymphocyte
DBP	DNA binding protein
DE1/2	downstream element 1/2
DEFA/B	transcription factor complexes A/B
DMEM	Dulbecco's Modified Eagle Medium
DMSO	dimethyl sulfoxide
DNA	deoxyribonucleic acid
dsDNA	double stranded deoxyribonucleic acid
dsRNA	double stranded ribonucleic acid
E2F	E2F family of transcription factors
EDTA	ethylenediaminetetraacetic acid
EGFR	epidermal growth factor receptor
eIF	eukaryotic initiation factor
EMT	epithelial mesenchymal transition
ERK1/2	extra-cellular signal-related kinase
EtBr	ethidium bromide
FACS	fluorescence activated cell sorting
FADD	Fas-associated death domain
FasL	Fas ligand
FVII, FIX, FX	clotting factors VII, IX and X
FCS	foetal calf serum
FTE	fallopium tube epithelium
GDP	guanosine diphosphate
GFP	green fluorescent protein
GM-CSF	granulocyte-macrophage colony-stimulating factor
GOG	Gynaecologic Oncology Group
GTP	guanosine triphosphate
H2A	histone 2A
H_2O	distilled water
HCV	hepatitis C virus
HEK 293	Human Embryonic Kidney 293 cells
HER2	human epidermal growth factor 2
hMLP	human adenoviral major late promoter

Hox	homeobox gene
h.p.i.	hours post infection
HR	homologous recombination
HRP	horseradish peroxidase
HSPG	heparan sulphate proteoglygcans
HSV	Herpes simplex virus
hTPL	human adenoviral tripartite leader
HVR	hypervariable regions
IAP	inhibitor of apoptosis
IC_{50}	inhibitory concentration required for a 50% reduction in cell survival
ICON	International Collaborative Ovarian Neoplasm study
IgM	immunoglobulin M
IGROV1	human epithelial ovarian cancer cell line
Il-1/1β/6	interleukin (various)
TNF-α	tumour necrosis factor -α
IRES	internal ribosomal entry site
INR	initiator element
IP	intraperitoneal
ISH	In-situ hybridisation
IT	intratumoral
ITR	inverted terminal repeat
IV	intravenous
KC	Kuppfer cells
KCL	potassium chloride
kDa	kilodaltons
KDS	potassium dodecyl sulphate
KRAS	V-Ki-ras2 Kirsten rat sarcoma viral oncogene homolog protein
LAR	Luciferase Assay Reagent II
LB	Lysogeny broth
LRP	lipoprotein receptor-related protein
MAPK	mitogen-activated protein kinase
MAV-1	Murine adenovirus type 1
MBMEC	mouse brain microvascular endothelial cells
Mdm2	murine double minute tumour suppressor protein
Mcl-1	induced myeloid leukaemia cell differentiation protein

MEK1/2	mitogen-activated protein kinases MAP2K1 and 2
$MgCl_2$	magnesium chloride
$MgSO_4$	magnesium sulphate
MISIIR	Mullerian inhibitory substance type II receptor
MLP	major late promoter
MLTU	major late transcription unit
mMLP	Murine adenoviral major late promoter
Mnk-1	MAP kinase-interacting serine/threonine-protein kinase 1
mo.	months
MOI	multiplicity of infection
MOSEC	mouse ovarian surface epithelial cell line
MOVCAR	murine ovarian carcinoma cell line
MRN	Mre-11-Rad50-Nbs-1 complex
mRNA	messenger ribonucleic acid
mTPL	murine adenoviral tripartite leader
MTT	3-2,5-diphenyltetrazolium bromide
n.s.	not significant
Na_2HPO_4	sodium phosphate dibasic
NaCl	sodium chloride
NaOH	sodium hydroxide
NCR	non-coding region
NDV	Newcastle Disease Virus
NES	nuclear export signal
NFI/II/III	nuclear factor I/II/III transcription factors
NFκB	nuclear factor kappa-light-chain-enhancer of activated B cells
NIH 3T3	fibroblast cell line established from Swiss mouse embryo tissue
NLS	nuclear location signal
NTC	non-template control
NTR	non-translated region
OD_{260}	optical density at 260 nanometers
ORF	open reading frame
OSE	ovarian surface epithelium
OS	overall survival
p53/TP53	tumour protein 53 (tumour suppressor protein)
pAA	plasmid encoding hAd5 MLP and TPL

pAM	plasmid encoding hAd5 MLP and MAV-1 TPL
PABP	poly (A) binding protein
PARP	poly ADP ribose polymerase
PBS	phosphate buffered saline
PCNA	antibody to proliferating cell nuclear antigen
PCR	polymerase chain reaction
PFS	progression-free survival
PFU	plaque-forming units
p.i.	post infection
PI3K	phosphoinositide-3-OH kinase
PKR	protein kinase R
PLB	passive lysis buffer
pMA	plasmid encoding MAV-1 MLP and hAd5l TPL
PML	Promyelocytic leukaemia
pMM	plasmid encoding MAV-1 MLP and TPL
PRMT1	protein-arginine methyltransferase-1
pTEN	Phosphatase and tensin homolog tumour suppressor protein
qPCR	quantitative polymerase chain reaction
qRT-PCR	quantitative reverse polymerase chain reaction
RACE	Rapid Amplification of cDNA Ends
Rb	Retinoblastoma tumour suppressor protein
RECIST	Response Evaluation Criteria In Solid Tumours
Ren	Renilla luciferase
RGD	Arginine-Glycine-Aspartic acid amino acid motif
RGG	Arginine-Glycine rich area
RID	receptor internalisation & degradation complex α/β
RNA	ribonucleic acid
RRM	RNA recognition motif
RT	reverse transcriptase
RT-PCR	reverse-transcriptase polymerase chain reaction
s	seconds
SBT	serous borderline ovarian tumour
SCARB	human scavenger receptor type B class I
SCCHN	squamous cell cancer of head and neck
SDS-PAGE	sodium dodecyl sulphate polyacrylamide gel electrophoresis

SOC	super optimal broth
ssDNA	single-stranded deoxyribonucleic acid
ssRNA	single-stranded ribonucleic acid
SV40	Simian vacuolating virus 40
TBE	Tris -borate EDTA
$TCID_{50}$	50% tissue culture infective dose
TEMED	N,N,N',N' – Tetramethylethylenediamine
TGF- βRI/II	TGF beta- serine/threonine kinase receptors I/II
TIC	tubal intraepithelial carcinomas
TK	thymidine kinase
TNFR-1	tumour necrosis factor receptor 1
TNF-α	tumour necrosis factor
TP	terminal protein
TPL	adenoviral tripartite leader
TP53	TP53 tumour suppressor gene encoding p53
TRAIL	TNF-related apoptosis-inducing ligand
tRNA	transfer ribonucleic acid
tRNAi	transfer ribonucleic acid initiator molecule
UKCCCR	United Kingdom Coordinating Committee for Cancer Research
VA RNA_1	virus-Associated RNA-1
VCAM	vascular cell adhesion protein-1
VEGF	vascular endothelial growth factor
VEGFR	vascular endothelial growth factor receptor
vs.	versus
WT	wild-type
γH2AX	histone H2 phosphorylated on serine 139
WHO	World Health Organisation

1. Introduction

Ovarian cancer is the second most common gynaecological malignancy (Li, Gayther et al. 2005) and is the 4th most common cause of death amongst women in the UK (CRUK 2011). The disease arises in the pelvis and symptoms are minimal until diffuse peritoneal dissemination causes abdominal distension, bloating and pain. As a result, more than 70% of patients present with advanced disease. Surgery remains the mainstay of treatment and aggressive surgical debulking, aimed at removing all visible disease within the peritoneal cavity, has been shown to improve prognosis (Piver, Lele et al. 1988). After this, platinum-based chemotherapy regimens have an initial response rate of approximately 70% but relapse and development of platinum resistance results in a 5-year survival rate of approximately 30%. Treatment developments in ovarian cancer since 1970s have increased survival rates by only 11% - half as much as those seen in most other common cancers (CRUK 2007). Ovarian cancer is unusual in that metastases are usually limited to a single area, the peritoneal cavity. This has led to the development of intraperitoneal therapy, with the potential advantage of bypassing systemic toxicities. The combination of refractory disease and its relative containment within the abdominal cavity makes ovarian cancer a viable target for novel therapies, such as gene therapy.

1.1. Ovarian cancer heterogeneity

A major hurdle to the development of new treatments for ovarian cancer has been the lack of an *in vivo* model for the disease and this, in turn, can be attributed to a relative lack of knowledge about the pathogenesis of the disease. The pathophysiology of ovarian cancer has remained a controversial subject for many years. 'Ovarian cancer' is a term which refers not to one single disease but to a diverse group of malignancies which affect the ovary. Ovarian tumours may develop from one of three cell types: epithelial cells, sex-cord stromal cells (including theca, granulosa and hilus cells) or germ cells (oocytes).

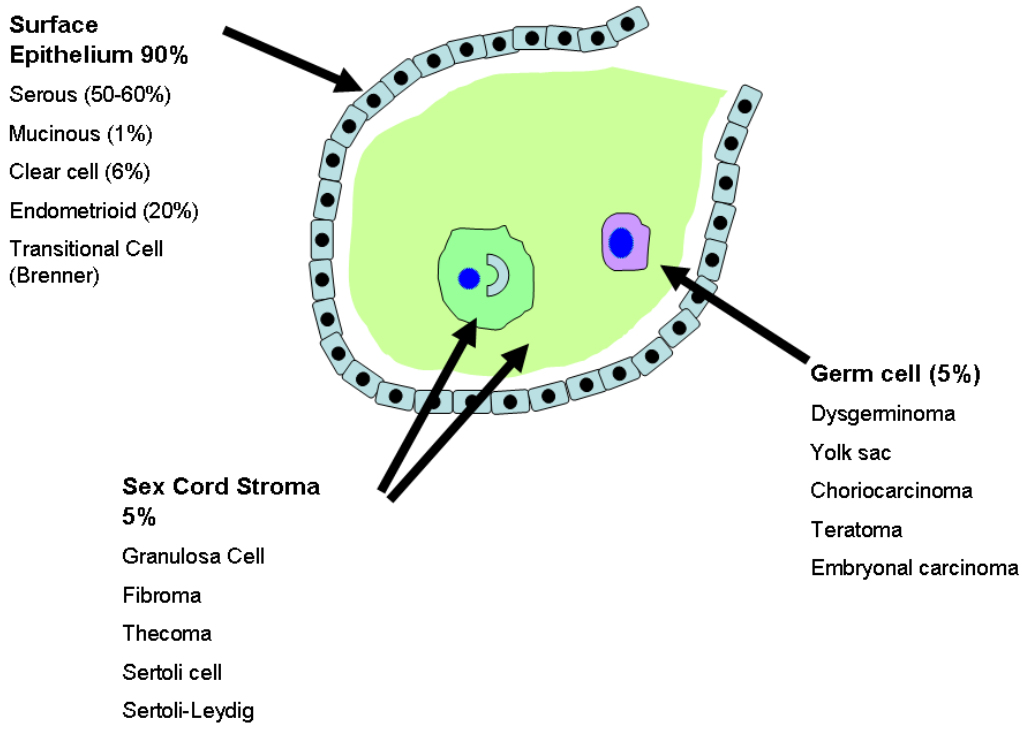

Figure 1 Ovarian Tumours: origins and cellular classification.

The majority of ovarian cancers were thought to originate from the flat-cuboidal epithelial cells covering the exterior surface of the ovary. Each of the ovarian surface epithelial (OSE) subtypes can be further divided into benign, intermediate (borderline) and malignant phenotypes.

Although 40% of all ovarian tumours are non-epithelial in origin, they account for only 10% of ovarian malignancies (Chen, Ruiz et al. 2003). 90% of ovarian malignancies arise in cells of epithelial origin and, even within this group, a wide range of tumour morphologies, clinical manifestations and genetic abnormalities are demonstrated. Current World Health Organisation (WHO) guidelines recognise eight histological tumour subtypes arising from the epithelial-derived tumours: serous, endometrioid, mucinous, clear cell, transitional cell, squamous cell, mixed epithelial and undifferentiated (Bocker 2002). Three tumour types, namely serous, mucinous and endometrioid are characterised by their morphological resemblance to mucosal tissues of the female genital tract and all derive from the Mullerian ducts. Serous tumours

resemble fallopian tube epithelium, endometrioid tumours resemble endometrial glands and mucinous tumours resemble endo-cervical epithelium (Dubeau 1999). Within each subtype, tumours can be low or high grade and are further categorised as benign, malignant or borderline. Generally borderline tumours are regarded as having low malignant potential. Each histological subtype exhibits differences in incidence, tumour behaviour, clinical outcome and chemosensitivity (Sugiyama, Kamura et al. 2000; Itamochi, Kigawa et al. 2002; Chen, Ruiz et al. 2003; Shih Ie and Kurman 2004; Landen, Birrer et al. 2008; Karst and Drapkin 2010).

As part of the work to understand the heterogeneity of ovarian cancer, genetic and biomarker profiling has been undertaken. This has demonstrated that each tumour subtype is associated with particular molecular signatures (Schwartz, Kardia et al. 2002; Zorn, Bonome et al. 2005; Iorio, Visone et al. 2007; Kobel, Kalloger et al. 2008). Further tumour heterogeneity has been demonstrated by examination of the genetic mutations underpinning the development of ovarian malignancies. Endometrioid, mucinous and low-grade tumours typically acquire mutations in signalling pathways controlling cell growth and proliferation such as KRAS, BRAF, PTEN, β-catenin and TFG- βRII (Shih Ie and Kurman 2004). High grade serous tumours exhibit mutations of tumour suppressor genes whose products play a part in DNA damage signalling and repair and include *TP53* (Ahmed, Etemadmoghadam et al. 2010) , *BRCA1&2* (TCGA 2011), *MLH1* and *MSH2* (Cannistra 2004; Singer, Stohr et al. 2005; South, Vance et al. 2009).

Historically, the hypothesis was that all ovarian tumours originated from the surface epithelial cells, themselves a monolayer of poorly differentiated mesothelial cells. The research of recent years is completely counter-intuitive to this and, as a result, more recent studies have questioned the validity of these models of pathogenesis.

1.2. Aetiology of ovarian cancer: models of pathogenesis

Until relatively recently the model for the pathogenesis of ovarian cancer was based on the premise that all tumour subtypes shared a common origin in the ovarian surface epithelium (OSE) and that ovarian cancer arose from malignant transformation of these cells. During ovulation, follicular rupture and oocyte release is known to inflict physical trauma on the OSE, which requires repair. In order to facilitate this, OSE cells must demonstrate a level of plasticity that allows tissue remodelling and can express both epithelial and mesenchymal phenotypes. (Czernobilsky, Moll et al. 1985; Siemens and Auersperg 1988; Auersperg, Maines-Bandiera et al. 1994). This repetitive process is also associated with inflammatory cytokines and reactive oxygen species that can damage DNA and result in transformation of epithelial cells (Murdoch and Martinchick 2004; Karst and Drapkin 2010).

It was hypothesised that repeated damage to OSE cells as part of this process contributed to malignant transformation. Cortical inclusion cysts (CICs) were also believed to be important to the OSE model of pathogenesis. Throughout a woman's reproductive time course, invaginations into the cortical stroma develop on the ovarian epithelium. These frequently pinch off to form separate entities known as cortical inclusion cysts (CICs) and the epithelial cell lining comes under the influence of hormones and homeobox (*Hox*) genes. These are thought to induce a form of differentiation or metaplasia leading to the emergence of a complex epithelium with a closer resemblance to that seen in Mullerian derived organs (Drapkin, Crum et al. 2004; Cheng, Liu et al. 2005; Karst and Drapkin 2010). In the presence of pre-existing DNA damage in the CIC, growth-promoting gonadotrophins and oestrogens may also facilitate a malignant transformation that ultimately leads to ovarian cancer. It has also been suggested that abnormal shedding of endometrial or tubal mucosa into the pelvis, such as is seen in endometriosis, may result in the incorporation of Mullerian-derived epithelial cells in the CICs (Dubeau 1999). This OSE- CIC model for the pathogenesis

of ovarian cancer appears to address the phenotypic features that are evident in some ovarian cancers e.g. cystic malignant tumours, ovarian cancers with Mullerian characteristics and also the presence of low grade and borderline tumours within the ovarian cortical stroma (Karst and Drapkin 2010). However it does not address the extra-ovarian peritoneal carcinomas which are histologically identical to ovarian carcinomas but do not involve the ovary.

Dissatisfaction with the OSE-CIC model led Shih and Kurman to examine ovarian pathogenesis from a different angle (Shih Ie and Kurman 2004). They examined the different morphological and molecular signatures of ovarian tumours and focussed on the differences seen in these between low grade serous borderline ovarian tumours (SBTs) and high-grade serous carcinomas. SBTs are a subset of ovarian tumours which are characterised by the fact that they are non-invasive, appear to derive from benign cystadenomas, and progress very slowly towards low grade serous carcinoma (Seidman and Kurman 1996; Smith Sehdev, Sehdev et al. 2003). Their main observation was the fact that the low grade borderline tumours did not have *TP53* mutations that are characteristic of high grade serous tumours. They proposed a new model which classified ovarian tumours as either a Type I or Type II tumour (see Figure 2).

In this model, type I tumours included all major histopathological subtypes but exhibited low grade nuclear and architectural features, slower growth and could be linked to benign pre-cursor lesions. These tumours commonly exhibited *BRAF* and *KRAS* mutations, which result in activation of the MAPK signalling pathway and cell growth and proliferation, and these were present in ~ 65% of SBTs but rarely in high grade tumours (Singer, Oldt et al. 2003). Other data indicated mutations in *PTEN, β-catenin* and *TGF- βRII* as more frequent in Type I endometrioid tumours (Obata, Morland et al. 1998; Janda, Lehmann et al. 2002; Shih Ie and Kurman 2004; Sabbah, Emami et al.

2008).

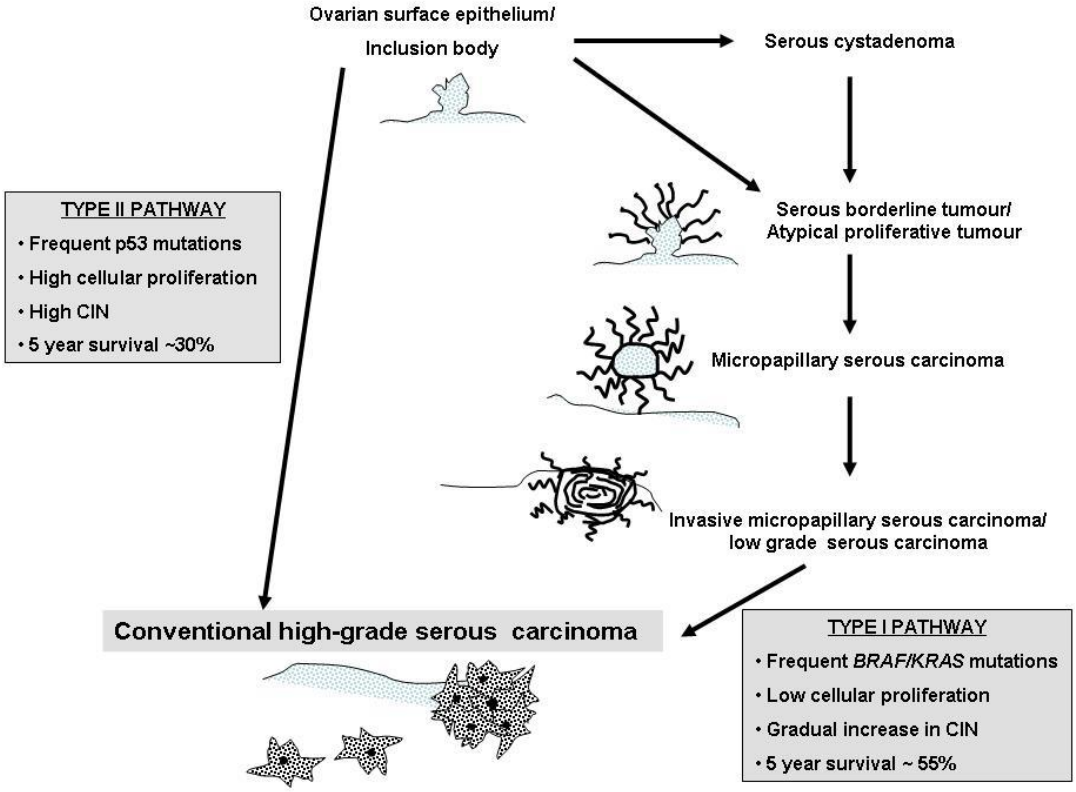

Figure 2 Two pathway model for the development of serous ovarian carcinomas.

Low-grade serous carcinoma is the prototype of Type I tumours and develops in a stepwise fashion from atypical proliferative tumours through to the non-invasive stage of micropapillary serous carcinoma before becoming high-grade invasive tumours. The Type I pathway is frequently associated with *BRAF* and *KRAS* mutations. High-grade serous carcinomas are the prototype of Type II tumours and develop from OSE or CICs without any identifiable precursors. In this pathway p53 mutations are more commonly found. (CIN=chromosomal instability). Adapted from Shih and Kurman 2004 (Shih Ie and Kurman 2004).

All of these genes encode molecules involved in the process of epithelial to mesenchymal transition (EMT). EMT is associated with early stages of carcinogenesis, cancer invasion and recurrence. During EMT a reduction of epithelial cell-cell adhesion via the transcriptional repression of cadherins occurs in combination with the acquisition of mesenchymal properties. Many of the signalling pathways which are the

focus of new anti-cancer drugs are key components in the intracellular signalling pathways which bring about EMT (De Wever, Pauwels et al. 2008; Sabbah, Emami et al. 2008).

Type II tumours mainly consist of high-grade serous carcinomas and less frequently undifferentiated carcinomas and malignant mixed mesodermal tumours. Unlike Type I tumours, they have almost universal p53 mutations (Ahmed, Etemadmoghadam et al. 2010), generally progress rapidly and are not commonly associated with a precursor lesion. They can also be associated with *AKT2* oncogenes and HER2 over-expression (Karst and Drapkin 2010).

Whilst logical, this model fails to explain how type II tumours develop and this has been the subject of much debate over the last 10 years. The histopathology found in samples from prophylactic hysterectomies and salpingo-oophorectomies performed in *BRCA* positive females may have gone a long way to explain this. Piek *et al.* (Piek, van Diest et al. 2001) published data in which the fallopian tubes of 12 *BRCA* positive patients demonstrated a high incidence of epithelial dysplasia (50%). They noticed that the fallopian tube epithelium (FTE), which normally contains both secretory and ciliated cells, demonstrated a higher number or secretory cells in areas of dysplasia. This was often accompanied by a loss of ciliated cells and greater proliferative activity.

Latterly Medeiros *et al.* conducted a similar study but this time examined the tubal fimbria rather than the distal end of the fallopian tube for early serous tumours (Medeiros, Muto et al. 2006). Examination of specimens from 13 *BRCA* positive women discovered serous tubal intraepithelial carcinomas (TIC) in 38% of patients without any evidence of serous tumours within the ovaries. 80% of these carcinomas were found exclusively in the fimbriated end of the fallopian tube suggesting that, in

BRCA positive women, the fimbria is the likely site of serous carcinogenesis and not the ovary.

Further work has demonstrated a very high incidence of TICs in patients with serous cancers of the ovary, fallopian tubes and peritoneum in patients not selected for *BRCA* status (Kindelberger, Lee et al. 2007). Of 42 cases designated “serous ovarian carcinoma”, 71% involved the fallopian tube and 48% of these contained a TIC. 93% of these TICs were found in the fimbrial region. This therefore suggests that high grade serous “ovarian” cancers may actually originate in the fallopian tubes but spread to the nearby ovary relatively early on. There are also data that corroborate this model for ovarian pathogenesis at a molecular level. Medeiros *et al*. had noted stretches of secretory-like cells which exhibited strong p53 immunoreactivity but were non-proliferative and were histologically benign (Medeiros, Muto et al. 2006). They termed these regions “p53 signatures” and further work established that they were found in the fimbria of both *BRCA* positive and negative women suggesting that this was a “normal” phenomenon (Lee, Miron et al. 2007). Furthermore, they also demonstrated that the p53 signatures stained strongly for γH2AX, the phosphorylated form of the *H2AX* gene that is a marker of DNA damage because DNA damage-sensing kinases ATM and ATR phosphorylate H2A at serine 139 at sites of double strand DNA damage. Its presence in the p53 signature patches of fimbrial cells demonstrated that DNA damage was present in these areas even under normal physiological conditions, and that a DNA repair response occurs. This work also demonstrated that p53 signatures were more frequent in fimbriae where synchronous TICs were present and that p53 signatures were composed exclusively of secretory cells like TICs. Even more compelling was the discovery that when TICs and p53 signatures were concurrent, identical *TP53* mutations were demonstrated in both suggesting a common origin and that TICs can be distinguished from p53 signatures by their increased proliferative capacity. Lee *et al.* therefore postulated that the p53 signatures were the precursor to

ovarian serous carcinoma. Interestingly, Folkins *et al.* detected very few p53 signatures in OSE and none in CICs when examining the tubal and ovarian tissue of 75 *BRCA* positive females (Folkins, Jarboe et al. 2008). It would therefore appear that p53 signatures arise preferentially in fimbrial tissue rather than ovarian.

Lee *et al.* concluded by incorporating all of the current evidence for ovarian pathogenesis into a single model for ovarian cancer which asserts that there are two distinct pathways which result in ovarian tumorigenesis (see Figure 3).

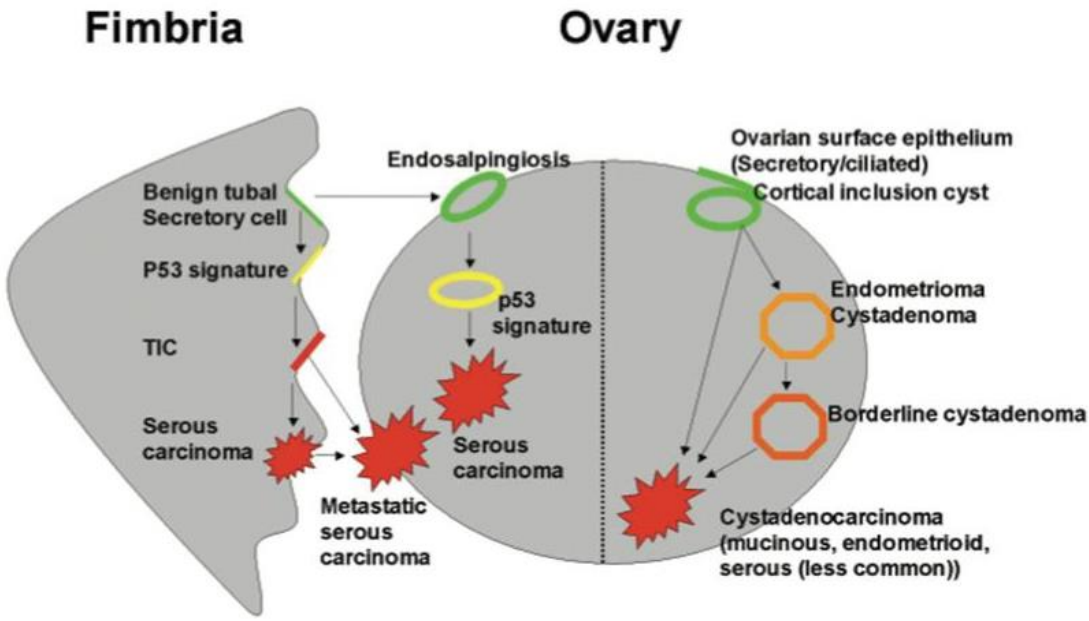

Figure 3 Fimbrial origins of ovarian cancer.

The pathway on the right originates from CICs that give rise to most Type I tumours by step-wise mutations (signified by the colour transitions from green to red) and includes endometriosis, benign and borderline cystadenomas. The pathway on the left could arise from either fimbrial mucosa that invaginates the ovarian cortex (endosalpingiosis) or TIC that develop in the fimbriae and have the potential to invade other peritoneal surfaces. This pathway consists of a p53 mutation arising as a result of genotoxic injury which results in the development of type II tumours. Adapted from Crum *et al.* 2007 (Crum, Drapkin et al. 2007).

The first is the OSE-CIC pathway in which OSE, fimbrial, endometrial or peritoneal tissue is entrapped within the CIC and undergoes Mullerian metaplasia via a series of stepwise mutations and results in Type I tumours. The second pathway evolves in the tubal fimbria where a combination of *TP53* mutation and genotoxic stress results in the clonal expansion of secretory cells and the emergence of the precursor p53 signatures. It is proposed that these regions then undergo additional genetic stresses which lend these cells a proliferative capacity and ultimately progression to TIC.

Quite what the genotoxic stresses are remains to be elucidated and is the subject of further research efforts, but they may be related to inflammatory cytokines and the reactive oxygen species present during ovulation. This would also explain why low parity is associated with an increased risk of developing ovarian cancer. Recent advances in molecular profiling are already expanding our knowledge of ovarian cancer pathogenesis as exemplified by the *BRCA* data and appear to support the histopathological models as discussed above. However, whilst molecular profiling goes some way to explaining the clinical heterogeneity of ovarian cancers, its clinical utility is not yet fully understood.

1.2.1. Ovarian cancer pathogenesis in the molecular era: *BRCA* mutation and PARP inhibition

One of the most significant contributions molecular pathology has made is to cancer therapeutics and, specifically, the identification of new signaling pathways which are amenable to pharmacological manipulation with a resultant therapeutic effect. Molecular profiling has led to the recognition of “synthetic lethality” as a mechanism which may be exploited to improve clinical outcomes. Synthetic lethality is the term used to describe a situation whereby two pathway defects acting individually have little effect, but when combined together become lethal (Ashworth 2008). In the cancer setting, the potential implication is that the targeting of one gene in a synthetic lethal

pair, where the other is defective, should be selectively lethal to the tumour cells, but not toxic to the normal cells (Kaelin 2005). The prime example of this is the synthetic lethal interaction between *BRCA1* or *BRCA2* mutations and poly (ADP-ribose) polymerase (PARP), an enzyme crucial for successful homologous recombination (HR), a key mode of DNA damage repair. *BRCA* genes encode proteins important for DNA damage repair. Patients with these germline mutations have abnormal DNA damage repair pathways which render them very prone to tumorigenesis. Inhibition of the PARP enzyme, another molecule required for DNA repair, precludes effective DNA repair and ultimately results in cell death. The development of a new class of drug , PARP inhibitors, has the potential to revolutionise the treatment of *BRCA* mutant ovarian cancer with response rates of over 40% in early clinical trials (Fong, Boss et al. 2009; Audeh, Carmichael et al. 2010; Fong, Yap et al. 2010; Gelmon, Tischkowitz et al. 2011; Ledermann J.A 2011). Indeed, PARP inhibitors are an early example of personalised treatment for ovarian cancer based on molecular profiling. *BRCA* status appears to correlate with responsiveness to chemotherapy in high grade ovarian cancers, adding to a growing body of evidence that type II tumours are linked to abnormalities of the HR pathway and predict response to platinum based chemotherapy and PARP inhibitors (Konstantinopoulos, Spentzos et al. 2010; Mukhopadhyay, Elattar et al. 2010; Kang, D'Andrea et al. 2012).

However, care must be taken not to assign patients to treatment groups based solely on the molecular profiling of a small tumour biopsy. Intratumoral heterogeneity should not be underestimated and one biopsy may not represent all the malignant phenotypes present within a tumour (Gerlinger, Rowan et al. 2012). Additionally, gene mutations do not necessarily predict abrogation of downstream events. Work with *BRCA* mutant and WT ovarian cancer is testament to this. 'BRCAness' is a term which has been used to describe disease wherein there is an abnormality of homologous recombination and thus DNA damage-repair in the absence of a *BRCA1* or *2* germline mutation (Turner,

Tutt et al. 2004). Up to 15% of sporadic ovarian cancers harbour *BRCA1* gene promoter methylation and BRCA1 protein is undetectable in many of these tumours, suggesting silencing of this gene (Baldwin, Nemeth et al. 2000). However, data suggest that up to 50% of high grade serous spontaneous ovarian carcinomas may have defects (including somatic *BRCA* mutations, *BRCA* methylation and dysfunction of other genes involved with HR) which confer sensitivity to PARP inhibition and mean that PARP inhibition may benefit many more than originally thought (Press, De Luca et al. 2008; Banerjee, Kaye et al. 2010; Hennessy, Timms et al. 2010). Furthermore, expensive molecular profiling may not be required for the identification of patients who may benefit from this new class of drugs. In the PARP arena, *in vitro* and *in vivo* work suggest that cheaper, more accessible markers predictive of PARP response can be considered. Immunohistochemistry for molecules expressed within the HR pathway such as γH2AX and Rad1 show promise as biomarkers of sensitivity to PARP inhibitors but these are yet to be ratified within the context of clinical trials (Konstantinopoulos, Spentzos et al. 2010; Mukhopadhyay, Elattar et al. 2010). Therefore, whilst *BRCA* mutational status is a useful tool which has undoubtedly contributed both to our understanding of ovarian pathogenesis and the developments of new therapeutic agents, cheaper, more accessible and more clinically relevant biomarkers predictive of treatment response such as immunohistochemistry (IHC) and tumour morphology may ultimately still be used to guide treatment decisions rather than molecular techniques.

1.3. Models of Ovarian Cancer

Against this background of confusion about the aetiology of the heterogenous groups of cancers termed “ovarian cancer”, research has continued into alternative therapies but with limited success. One of the problems hounding the development of new therapies for ovarian cancer has been the difficulty in creating an experimental model of the disease. Experimental models to date have been primarily murine models and historically have used the traditional OSE-CIC model of ovarian tumorigenesis as their

basis and have therefore sought to transform murine ovarian surface epithelial cells (MOSEC). MOSE cells were transformed by introduction of SV40 – large and small T antigen under the control of a Mullerian inhibitory substance II receptor (MIS*I*IR) to produce the MOSEC cell line (Connolly, Bao et al. 2003). Tumour suppressor genes *TP53* and *Rb* have been knocked out using the Cre-Lox system (Flesken-Nikitin, Choi et al. 2003) and resulted in a spectrum of ovarian tumours with differentiated serous ovarian tumours in 39% of mice. Median time to tumour development was a lengthy 227 days. Other models have used a combination of transgenic mice and avian retroviruses to introduce oncogenes, however such models required harvesting of ovarian cells from transgenic mice, transfection with retroviral vectors and also propagation of the primary cells *in vitro* before re-introducing them orthoptically into an immunocompetent mouse (Orsulic, Li et al. 2002). As such, these models are time consuming, expensive and potentially permit multiple *in vitro* genetic mutations that are not representative of the origins of epithelial ovarian cancer (EOC).

Some progress has been made in the field of mouse modelling of endometrioid ovarian adenocarcinomas. Dinulescu *et al.* investigated possible links between endometrioid ovarian adenocarcinomas and endometriosis as the latter is thought to contribute to the development of this type of ovarian cancer (Swiersz 2002). They were particularly interested in *PTEN* and *K-Ras* mutations, both of which are abnormalities associated with endometrioid ovarian adenocarcinomas (Cuatrecasas, Erill et al. 1998; Obata, Morland et al. 1998; Sato, Tsunoda et al. 2000; Gemignani, Schlaerth et al. 2003; Hogdall, Hogdall et al. 2003). They injected a recombinant adenoviral vector expressing Cre recombinase (AdCre) into the bursal cavity of transgenic mice harbouring a transcriptionally silenced oncogenic allele of *K-Ras* which was activated by Cre recombinase expression. After a period of 8 months, expression of oncogenic K-Ras in the OSE cells resulted in the development of benign epithelial lesions similar to the epithelial component of endometriosis which the authors termed “endometriosis-

like” (because of the absence of surrounding endometrial-like stroma). These lesions were not present in the control animals. In addition, nearly half the animals (7 of 15) developed widespread peritoneal endometriosis which was confirmed by morphological, and immunohistochemical studies. Interestingly, injection of the AdCre recombinase directly into the peritoneal cavity did not result in peritoneal dissemination of these lesions. This finding appears to correlate with the “implantation theory” of endometriosis pathogenesis that suggests a reflux of endometrial tissue through the fallopian tubes to the peritoneum is necessary for its development. Of note, long-term follow up of these lesions did not demonstrate progression to endometrioid ovarian cancer. However, in transgenic mice bearing both *K-Ras* and *PTEN* mutations, AdCre administration into the bursa resulted in invasive endometrioid ovarian adenocarcinomas in OSE as early as 7 weeks after injection. It was therefore postulated that Ras pathway activation may play an important part in the development of endometriosis. Indeed, the combination of *PTEN* mutation and Ras pathway activation comprises a plausible model of endometrioid ovarian adenocarcinoma evolution that merits further investigation (Dinulescu, Ince et al. 2005). In the relative absence of mouse models for ovarian cancer, models of disease based on mutational analyses are clearly of use. However, the work published by Clarke-Knowles *et al.* may curb some of our enthusiasm for them. In this work inactivation of *BRCA1*, *TP53* and *Rb* in knockout transgenic mice was undertaken by intrabursal injection of AdCre in a variety of combinations. Inactivation of *TP53* resulted in tumours in 100% of mice. Concomitant inactivation of *TP53* and *BRCA1* resulted in accelerated tumour progression. However this effect was not duplicated with the concomitant inactivation of both *TP53* and *Rb*. Curiously, histological examination of the tumours that developed did not demonstrate ovarian adenocarcinoma but unexpected leiomyosarcoma suggesting that additional factors must be involved (Clark-Knowles, Senterman et al. 2009).

It is clear that without a better knowledge of the mechanisms involved in ovarian pathogenesis researchers have struggled to develop a practicable *in vivo* model for this disease. Now that fallopian tube cells have been identified as the possible cell of origins for EOC we may hope that the development of animal models may progress. However experience of FTE cell culture *in vitro* is limited and it has been noted that the dual ciliated/ secretory phenotype found *in vivo* is often lost and rapid de-differentiation with a loss of the ciliated phenotype often occurs in culture (Henriksen, Tanbo et al. 1990; Comer, Leese et al. 1998; Fotheringham, Levanon et al. 2011). Indeed, to date, there are no readily available human FTE cell lines for experimental work.

1.4. Treatment of Ovarian Cancer

Notwithstanding the fundamental issues with current models of ovarian cancer pathogenesis, work into new treatments for this disease has continued. To date the accepted treatment protocol for ovarian cancer combines maximal surgical debulking followed by platinum based chemotherapy. The trials pertaining to chemotherapy are shown in table Table 1. In recent years the addition of taxane based chemotherapy to cisplatinum has become commonplace and the substitution of carboplatin for cisplatinum has also increased based on its equivalence in progression free survival (PFS) and its more favourable toxicity profile.

More recent data has looked at adding additional agents to platinum/ taxane combinations. The ICON5/ GOG-182 study looked at the addition of a third cytotoxic agent to this regime and examined several different drug types. None demonstrated any benefit in terms of PFS or overall survival (OS) when compared to carboplatin and paclitaxel (Bookman, Brady et al. 2009).

Trial	Regime	Evaluable patients	FIGO Stage	Result
GOG-111 (Bookman, McGuire et al. 1996)	Cis/Tax vs. Cis/Cyclo	386	III (suboptimal) & IV	PFS: 18 mo. vs. 13mo (p<0.001) OS: 38 mo. vs. 24 mo. (p<0.001)
OV10 (Piccart, Bertelsen et al. 2000)	Cis/Tax vs. Cis/Cyclo	680	IIb-c, III & IV with optimal or suboptimal residual disease	PFS: 16 mo. vs. 12 mo. (p<0.001) OS: 35 mo. vs. 25 mo. (p<0.001)
GOG-132 (Muggia, Braly et al. 2000)	Cis/Tax vs. Cis	424	III (suboptimal) & IV	PFS: 14.1 mo. vs. 16.4 mo. (n.s) OS: 26 mo vs. 30.2 mo (n.s)
ICON-3 (ICON 2002)	Carbo/Tax vs. Carbo or CAP	2,074	I-IV (any residual disease)	PFS: 17.3 mo. vs. 16.1 mo. (n.s) OS: 36.1 mo vs. 35.4 mo (n.s)
AGO study (Neijt, Engelholm et al. 2000)	Cis/Tax vs. Carbo/Tax	208	IIb-IV	PFS:16 mo. vs. 16 mo. (n.s) OS: 31 mo vs. 31 mo (n.s)
GOG 158 (Ozols, Bundy et al. 2003)	Cis/Tax vs. Carbo/Tax	792	III (optimal)	PFS: 19.4 mo. vs. 20.7 mo. (n.s) OS: 48.7 mo vs. 57.4 mo (n.s)
SCOTROC (Vasey, 2002)	Carbo/Tax vs. Carbo/Doc	1,077	Ic-IV	PFS: 15.4 mo. vs. 15.1 mo. (n.s)

Table 1 Platinum and taxane chemotherapy trials.

n.s. not significant; PFS, progression free survival; mo. months. Cis/Tax, Cisplatin and Paclitaxel; Cis/Cyclo, Cisplatin and Cyclophosphamide; Carbo/Tax, Carboplatin and Paclitaxel; Carbo-CAP, Cyclophosphamide/Doxorubicin/Cisplatin (CAP) or single agent Carboplatin; Carbo/Doc, Carboplatin and Docetaxel.

Patients who relapse more than 6 months after completing platinum based chemotherapy can be re-challenged with platinum based regimen and are deemed

"platinum sensitive". Recent work by Pujol *et al*. has suggested that re-challenge with a combination of carboplatin and pegylated liposomal doxorubicin may be preferable to the carboplatin/paclitaxel combination as it demonstrated a better PFS but data for OS are not yet available (Pujade-Lauraine, Wagner et al.). Ultimately, ovarian cancer patients develop platinum resistant disease at which point they are often treated with single agent regimes.

Phase II trial data for a number of agents is available and include paclitaxel, liposomal peygylated doxorubicin (Caelyx™), gemcitabine, etoposide, docetaxel, topotecan and vinorelbine (Gore, Levy et al. 1995; Kaye, Piccart et al. 1997; Bookman, Malmstrom et al. 1998; Rose, Blessing et al. 1998; Burger, DiSaia et al. 1999; von Minckwitz, Bauknecht et al. 1999; Gordon, Granai et al. 2000; Markman, Kennedy et al. 2000). These demonstrate response rates of up to only 20% and illustrate the severe limitations of treatments for platinum resistant disease in this setting.

As the search for innovative approaches to the treatment of ovarian cancer have continued, alternative delivery methods for chemotherapy have also been explored. Ovarian cancer has a propensity to spread within the peritoneal cavity over the peritoneal surfaces rather than metastasising to distant organs. As such, delivery of intraperitoneal chemotherapy has been evaluated as a treatment option. There have been three major trials published which are outlined in table Table 2. These studies provide level 1 evidence that demonstrate the benefits of adjuvant postoperative IP chemotherapy in improving disease-free and overall survival. Notwithstanding this, IP chemotherapy administration has not been adopted as standard practice. This is primarily because of poor treatment tolerance and because of the complications associated with indwelling intraperitoneal catheters. Aletti *et al.* attempted to translate research data from these randomized trials into routine clinical practice in accordance with best-practice evidence (Aletti, Nordquist et al. 2010). However, in their single

institution study, the investigators encountered challenges similar to those present in GOG-172, namely, the poor tolerability of IP chemotherapy that resulted in only 36% of patients completing the planned treatment. Their reasons for discontinuing treatment included catheter-related complications (38%), nephrotoxicity (14%), and sepsis (14%). Hence, although potential survival benefits may be obtained with IP chemotherapy, the morbidity of IP complications, the inability to complete planned treatment, and the possible effect on survival outcomes of the failure to complete treatment have limited clinicians' willingness to embrace IP chemotherapy as the standard chemotherapy delivery route.

Study	Intravenous Regimen	Intraperitoneal Regimen	PFS (Hazard Ratio)	OS (Hazard Ratio)	Outcome (IP vs. IV)
SWOG 8501/ GOG 104 (Alberts, Liu et al. 1996)	Cisplatin 100mg/m^2 IV Cyclophosphamide 600 mg/m^2 IV Q3 weeks x 6	Cisplatin 100mg/m^2 IP Cyclophosphamide 600 mg/m^2 IV Q3 weeks x 6	–	0.76	OS: 49 mo vs. 41 mo
GOG 114/ SWOG 9227 (Markman, Bundy et al. 2001)	Cisplatin 75mg/m^2 IV Paclitaxel 135 mg/m^2 IV Q3 weeks x 6	Carboplatin (AUC 9) IV q28 days x 2 Cisplatin 100mg/m^2 IP Paclitaxel 135 mg/m^2 IV Q3 weeks x 6	0.78	0.81	PFS: 28 mo vs. 22 mo (p=0.1) OS: 63 mo vs. 52 mo (p=0.5)
GOG 172 (Armstrong, Bundy et al. 2006)	Cisplatin 75mg/m^2 IV Paclitaxel 135 mg/m^2 IV Q3 weeks x 6	Paclitaxel 135 mg/m^2 IV Cisplatin 100mg/m^2 IP Paclitaxel 60 mg/m^2 IP on day 8 Q3 weeks x 6	0.8	0.75	PFS: 23.8 mo vs. 18.3 mo (p=0.05) OS: 65.6 mo vs. 49.7 mo (p=0.03)

Table 2 Trials evaluating intraperitoneal chemotherapy in ovarian cancer

Disappointing advances in improving outcomes in ovarian cancer has resulted in the evaluation of other potential therapeutic technologies. Increasingly therapies for cancer

are aimed at exploiting specific biological characteristics of an individual cancer. This has led to the emergence of the concept of individualised cancer treatments. An early example of this was the exploitation of the over-expression of oestrogen receptors seen in breast cancer and their blockade with tamoxifen (Jordan 1976). As a result, breast tumour hormone receptor profiling is now a routine feature of diagnosis and plays a key part in therapeutic decisions. Latterly, identification of the human epidermal growth factor family of receptors and, in breast cancer, the over-expression of HER2 has allowed us to exploit this tumour feature to arrest tumour growth using the HER2 monoclonal antibody trastuzumab. Blockade of the HER2 receptor results in arrest of the cell cycle in the G1 phase and, when used in combination with chemotherapy, trastuzumab has been very effective in the treatment of a subset of this disease which had previously been chemorefractory (Burstein 2005; Sumikawa, Shigeoka et al. 2008). This pattern has been repeated in a variety of tumour types and identification of novel biomarkers has allowed for the development of more tailored and hence less toxic therapies which have proven effective, often in tumour subgroups which had previously been treatment refractory.

To date, the biological agents most extensively studied in EOC are those which target vascular endothelial growth factor (VEGF) and the epidermal growth factor receptor (EGFR). Both of these factors play an important role in tumour microenvironment as they facilitate tumour neovascularisation. They are of particular interest in EOC as VEGF is expressed in high concentrations in ascitic and pleural fluid (Kraft, Weindel et al. 1999). VEGF levels also correlate with more extensive disease, increased microvessel density and worse prognosis (Paley, Staskus et al. 1997; Kraft, Weindel et al. 1999; Kassim, El-Salahy et al. 2004). This feature has been identified as a therapeutic target and the humanised monoclonal antibody to VEGFR, bevacizumab, has shown promise. Response rates of up to 20% and reduced rates of ascitic re-accumulation have been reported (Burger, Sill et al. 2007) although some of the side

effects, noticeably gastro-intestinal perforation, have been life-threatening. The combination of bevacizumab with chemotherapeutic agents has demonstrated synergy, with response rates of up to 80% in the first line setting and 40% in as a second line agent (Wright, Hagemann et al. 2006; Chura, Van Iseghem et al. 2007; Micha, Goldstein et al. 2007). The GOG-218 and ICON7 trials are examining how the addition of bevacizumab to the carboplatin/ paclitaxel combination might affect outcomes. The ICON7 phase III trial included 1528 women with high-risk early or advanced stage epithelial ovarian cancer, primary peritoneal cancer or Fallopian tube cancer. Investigators demonstrated that at 12 months the risk of developing further progression of ovarian cancer was reduced by 15% when compared to the risk of progression seen with chemotherapy alone. Of note, the major benefit is obtained in sub-optimally de-bulked and advanced-stage patients. Data are not yet fully mature but suggest that in higher risk patients the addition of the new agent improves PFS and may improve overall survival as preliminary data show an encouraging early trend with fewer deaths seen in patients treated with bevacizumab (Perren T 2010; Kristensen, Perren et al. 2011). As a result, combination treatment incorporating bevacizumab is now being proposed as the gold standard of care in the first line treatment of high risk ovarian cancer. However, there remains a failure of consensus that it should be added to first line adjuvant chemotherapy because clinicians feel that its addition does not result in either a statistically significant increase in overall survival and/or improved quality of life (Burger, Brady et al. 2011; Perren, Swart et al. 2011; Morgan, Alvarez et al. 2012).

Olaparib, an inhibitor of the DNA damage repair enzyme poly ADP ribose polymerase (PARP), has also shown promise in patients who have mutations in *BRCA1/2* genes in phase I trials (Fong, Boss et al. 2009). Fong *et al.* examined an expanded cohort of 50 patients with advanced *BRCA1/2* mutation associated ovarian, primary peritoneal and fallopian tube cancers. The clinical benefit rate (RECIST and/or CA125 response) was 46% and the median duration of response was 28 weeks (range 10−86 weeks).

Importantly, the overall clinical benefit rate decreased significantly with platinum insensitivity (platinum-sensitive: 69%, platinum-resistant: 46%; platinum-refractory 23%). Furthermore, there was a positive association between the overall platinum free interval and response to olaparib (P = 0.002). Although the clinical efficacy of olaparib was shown to diminish with decreasing platinum-free interval, it is noteworthy that the anti-tumour activity was still substantial, particularly in platinum-resistant disease compared with other known agents (Banerjee and Kaye 2011). These promising results led to a phase II multi-centre single-arm, open-label sequential dosing cohort study of *BRCA1/2* mutation carriers with recurrent ovarian cancer (Audeh, Carmichael et al. 2010). In this trial, women received 400 mg twice daily (33 patients) or 100 mg twice daily (24 patients). Efficacy was confirmed in both dosing cohorts, but was higher in those receiving the higher dose level (33% vs. 12.5%). Toxicities were mild (grades 1, 2) and consisted of nausea, vomiting, fatigue and anaemia.

A phase II study evaluating both PFS and OS has also been undertaken (Ledermann, Harter et al. 2012). Olaparib was given as maintenance therapy in women with relapsed high-grade serous ovarian cancer (either sporadic or associated with germline *BRCA1/2* mutations) that had responded to platinum-based chemotherapy in the relapsed setting. Patients were randomly assigned to receive olaparib, at a dose of 400 mg twice daily, or placebo. Of 265 patients who underwent randomization, 136 were assigned to the olaparib group and 129 to the placebo group. Progression-free survival was significantly longer with olaparib than with placebo (median, 8.4 months vs. 4.8 months from randomization on completion of chemotherapy; hazard ratio for progression or death, 0.35; 95% confidence interval [CI], 0.25 to 0.49; P<0.001). Subgroup analyses of progression-free survival showed that, regardless of subgroup, patients in the olaparib group had a lower risk of progression. However an interim analysis of OS has been disappointing. At 38% maturity (meaning that 38% of the patients had died), OS showed no significant difference between groups (hazard ratio

with olaparib, 0.94; 95% CI, 0.63 to 1.39; P=0.75). Whilst this immature data does not preclude possible adjuvant use of Olaparib as a monotherapy or in combination with cytotoxic chemotherapy, it has definitely dealt a blow to the prospects of this drug being taken forward into larger clinical trials.

1.5. Viral Gene Therapy

Our improved understanding of the molecular mechanisms which may result in disease has revealed a significant genetic component to the pathogenesis of many illnesses including cancer. As a result, attempts have been made to correct certain genetic abnormalities – so called gene therapy. The term “gene therapy” describes the use of DNA as a pharmaceutical agent to treat disease. It derives its name from the idea that DNA can be used to supplement or alter genes within an individual’s cells as a therapy to treat disease. In its simplest form, gene therapy involves using DNA that encodes a functional therapeutic gene to replace a mutated, dysfunctional gene. The DNA encoding the therapeutic protein must be introduced into the host cell using a vector. This packages the therapeutic DNA and ensures its delivery to the host cell nucleus. Once inside, the DNA is expressed by the host cell machinery and the therapeutic protein is produced which in turn treats the patient’s disease. There are two main classes of vector; those that use recombinant viruses and those that use naked DNA or DNA complexes (non-viral methods). Viruses are an obvious candidate for gene therapy vectors as they routinely introduce DNA into cells by exploiting normal biological processes. Viruses are obligate parasites and, after infection of a cell, must make their way to the cell’s nucleus in order to exploit the host cell replication machinery to ensure their own replication. As such, they are naturally designed to deliver DNA to a cell’s nucleus and override the host cell cycling to ensure their own preferential viral DNA replication and protein synthesis. Initially the use of viruses in gene therapy was limited to non-replicating viruses which aimed to deliver transgenes for hereditary diseases caused by single gene mutations. For example, the fatal

neurodegenerative disease x-linked adrenoleukodystrophy (ALD) carries a germline mutation of the *ABCD1* gene that codes for a transporter protein responsible for the transfer of fatty acids into peroxisomes. Mutations result in a loss of this protein and, as a result, saturated long-chain fatty acids accumulate in the tissues resulting in the progressive neuronal demyelination and adrenal failure. Gene therapy was used to correct this mutation and heralded the arrival of the new treatment modality of gene therapy. Hematopoietic cells were transfected *ex vivo* with a lentiviral vector containing the wild type *ABCD1* gene and these were re-introduced into two patients with a view to correcting the underlying genetic abnormality. As a result of successful recombination, progression of the disease was successfully halted (Cartier, Hacein-Bey-Abina et al. 2009).

The increased knowledge of viral biology that has facilitated gene therapy has also allowed us to investigate the use of viral vectors to deliver anti-cancer therapies (virotherapy). A link between cancer and viruses, either as an aetiological or therapeutic agent, is longstanding. Early last century, significant cervical carcinoma regression was noted following rabies vaccination and reports of remissions of haematological malignancies following natural infection with measles viruses are also documented (De Pace 1912; Bluming and Ziegler 1971; Taqi, Abdurrahman et al. 1981). The cell-cycle pathways that are deregulated in malignant cells are often the very same pathways that viruses interfere with in order to hijack the host cell's replication machinery. Thus, in the field of cancer, efforts have been made to combine our knowledge of viral biology and gene delivery systems to create a series of virally delivered anti-cancer therapies. Viral vectors have been used to deliver a variety of anti-cancer transgenes, including "suicide genes", tumour-suppressor genes and immunostimulatory genes with an increasing emphasis on vector design in order to maximise both target specificity and anti-cancer effect (Vorburger and Hunt 2002; Relph, Harrington et al. 2005). Suicide gene therapy refers to the delivery into tumour

cells of transgenes encoding enzymes that metabolize systemically delivered non-toxic pro-drugs to locally active therapeutic agents. Treatment efficacy is enhanced by the death of neighbouring, non-transduced cells (the so-called “bystander effect”) (Chen, Shine et al. 1994; Perez-Cruet, Trask et al. 1994; Colak, Goodman et al. 1995; Mizuno, Yoshida et al. 1998; Lanuti, Gao et al. 1999). However development has been limited by the toxic side effects which appear to be triggered by the immune responses witnessed in Phase I studies using higher levels of vector particles (Trask, Trask et al. 2000).

Immunotherapy has utilised gene-based strategies to harness the immune response to tumour-associated antigens. Dendritic cells, the key cell type responsible for initiating and controlling cellular immune responses, have also been manipulated to stimulate an anti-cancer effect. In tumour-lysate pulsing, the dendritic cells are collected from the peripheral blood stream and fed with whole tumour antigen proteins from lysates. The dendritic cells take up and process the proteins, then present their antigenic epitopes through the exogenous MHC class II pathway and in MHC class I molecules resulting in immune-mediated cytotoxicity. Again, phase I studies have shown some promise with up to 40% of patients deriving clinical benefit (Linette, Zhang et al. 2005). Another immunostimulatory technique is autologous vaccination. In a phase I study, autologous melanoma tumour cells were transduced *ex vivo* with adenoviral vectors encoding granulocyte-macrophage colony-stimulating factor (GM-CSF). Vaccination with these cells resulted in one complete, one partial and one mixed response. Of note in this study, 29% of the patients were alive at 3 years follow-up (Soiffer, Lynch et al. 1998). However although promising, immunostimulatory therapies pose particular problems; the production of autologous dendritic cells under contamination-free, good manufacturing conditions is expensive and the techniques required for tumour antigen preparation and loading have yet to be established. Furthermore, optimal immunization strategies have yet to be defined and are important, especially because

dendritic cells can induce immune tolerance which is clearly undesirable in this setting (Rissoan, Soumelis et al. 1999).

In the field of cancer, gene replacement therapies have focused primarily on the transduction of tumour suppressor genes such as *p53*. The role of *p53* as a central mediator of the damage and cellular stress responses in the cell is well documented (Fridman and Lowe 2003). One of the most important functions of p53 is its ability to activate apoptosis on encountering DNA damage. Therefore, disruption of this function promotes tumour progression and desensitizes the tumour to both chemotherapy and radiotherapy (El-Deiry 2003). The *p53* gene is mutated in most human cancers and in >90% of ovarian cancers and thus represents an ideal candidate for gene replacement therapy (Ahmed, Etemadmoghadam et al. 2010; TCGA 2011). It has been observed that the p53 pathway is altered in many ovarian cancers and that the development of cisplatin resistance can be associated with apparent loss of p53 function without a gene mutation (Yaginuma and Westphal 1992; Eliopoulos, Kerr et al. 1995; Righetti, Della Torre et al. 1996). Consequently a non-replicating recombinant adenoviral vector encoding wild type p53 under the control of the human CMV immediate early promoter was developed with a view to replacing aberrant p53 expression in the cancer setting (Buller, Runnebaum et al. 2002a; Buller, Shahin et al. 2002b; Wen, Mahavni et al. 2003). This virus, SCH58500, underwent phase I and II trials and was given intraperitoneally (IP) in normal saline. Some patients received it in conjunction with conventional intravenous chemotherapy. Adverse events were frequent, the most common being fever, hypotension, abdominal pain, nausea and vomiting, but dose-limiting toxicities did not occur. Notwithstanding dramatic increases in serum anti-adenoviral antibodies, reverse transcriptase polymerase chain reaction (RT-PCR) demonstrated vector-encoded p53 in 85% of tumour biopsies and ascitic fluid samples for up to 7 days post virus administration. However, attempts to assess the extent of p53 activity in tumour deposits were hindered by the inability to obtain biopsies.

Quantitative RT-PCR analyses of samples post 1 cycle of SCH58500 were performed in 5 subjects. These demonstrated increased expression of p53 targets such as BAX and p21, although copy number varied as much as 1000 fold between patients. Investigators were hopeful that these results suggested that viral gene transfer could result in p53 effects in infected tumour tissues. In reality, the absence of a control group meant that non-specific vector-induced effect could not be excluded as an explanation for their findings. Nonetheless, follow-up data on these patients demonstrated a median survival of 12-13 months (Buller, Shahin et al. 2002b) and on this basis a large phase III trial was commenced combining surgery and conventional chemotherapy with or without IP gene therapy (Zeimet and Marth 2003). As the trial has never been published, full details are not available, but the trial was stopped early due to inadequate therapeutic benefit and increased toxicity in the gene therapy arm. The conclusion was that single gene replacement therapy was unlikely to cause regression of tumours with multiple genetic abnormalities and that replication deficient viruses were not able to access sufficient numbers of tumour cells.

In response to the relatively disappointing results obtained with single gene replacement strategies in cancer therapy, work focused on harnessing the intrinsic cytotoxic effects of viral delivery agents and ultimately led to work on replication competent viruses. The hope was that successful viral transduction of malignant cells would result in increased tumour lysis as a result of intracellular viral replication. This offshoot of gene replacement strategy was termed oncolytic viral therapy. In oncolytic viral therapy the hypothesis is that completion of viral replication and mature virion release, which is accompanied by cell death, is intrinsically therapeutic. Clearly this requires the virus to replicate *selectively* in tumour cells. Such viruses should not be able to replicate in normal cells, and tumour-selective replication would maximize the therapeutic index and minimise toxicity to normal tissues (Figure 4). In addition,

transgenes may be added to the oncolytic virus to increase cytotoxicity – termed "oncolytic viral gene therapy".

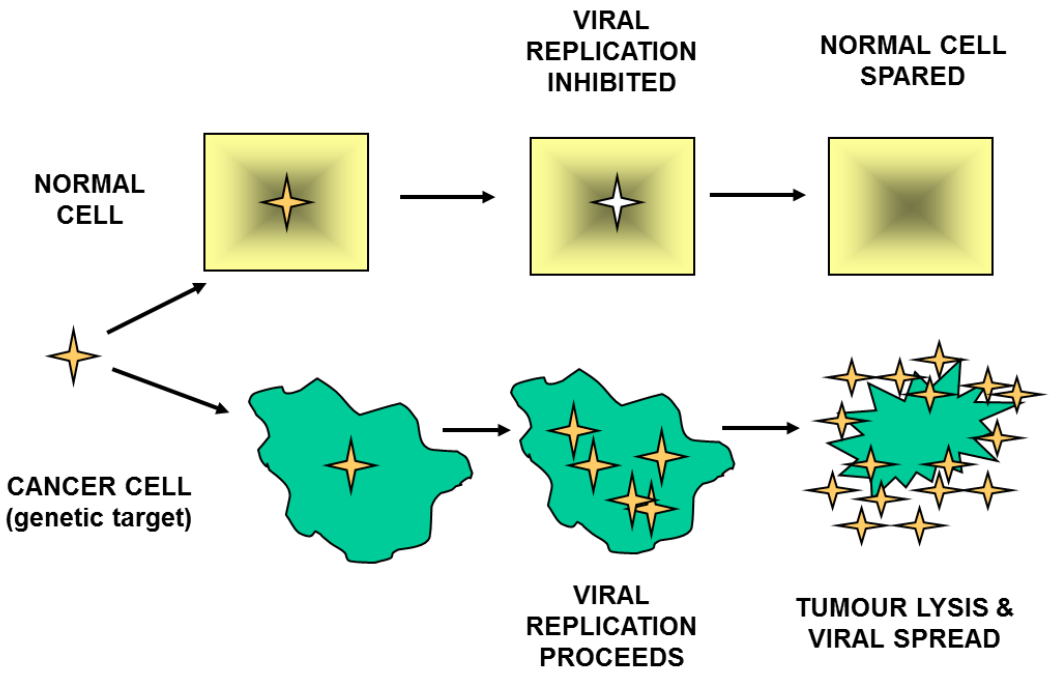

Figure 4 Schematic representation of the action of a replication selective oncolytic virus. The genetically altered virus is transfected into cells. In the cancer cell, the pathway in which the viral deletion occurs is already dysregulated as part of the pathological process. Therefore, the viral deletion in this area does not act as an obstacle to viral replication. The mutant virus is able to replicate and generates further virions using the host cell machinery. These are released from the cell resulting in host cell lysis and death of a selective population of cells. In the normal cell with intact cell cycle pathways, the viral deletion renders virus replication impossible. Viral replication is inhibited and the normal cell is spared.

1.6. Oncolytic Viruses

Several viruses are known to possess natural oncolytic activity (Roberts, Lorence et al. 2006). Adeno-associated virus-2 (AAV2) is a small non-pathogenic single stranded DNA virus which does not illicit a strong immune response in the host (Coura Rdos and Nardi 2007). It is dependent on the machinery of a helper virus, such as human papilloma virus or adenovirus for successful gene expression. However, even in the absence of such viruses it is able to infect cells where it integrates into the host cell DNA and lies dormant until secondary infection of that cell by a helper virus (Kotin, Linden et al. 1992). Its potential as an anti-cancer agent lies in its ability to disrupt cell cycle progression in the infected cell which in turn induces the DNA damage response and arrests the cell in G2. Cells which are p53 deficient are unable to maintain this state and undergo prolonged, incomplete mitosis. This leads to over-duplication of centromeres and the cell finally succumbs to mitotic catastrophe (Jurvansuu, Raj et al. 2005). As the majority of tumours have defective p53 pathways, AAV2 is a potential therapeutic agent (Bullock and Fersht 2001) and in serous ovarian cancer the incidence of p53 mutations is high in the region of 97% (Ahmed, Etemadmoghadam et al. 2010). However, to date, AAV2 has been used as a vector construct for gene replacement in chronic disorders rather than as an anti-cancer therapy predominantly due to the fact that its oncolytic effect requires secondary infection with a helper virus. (Carter 2005; Kaplitt, Feigin et al. 2007).

Newcastle disease virus (NDV) is a single stranded RNA avian virus which may be harmful to birds but in humans causes conjunctivitis and influenza-like symptoms. NDV has been shown to infect human cells successfully (Sinkovics and Horvath 2000) (Krishnamurthy, Takimoto et al. 2006). NDV appears to exert an oncolytic effect due to its intrinsic lytic activity (Polos and Gallaher 1981), its interaction with toll-like receptors which results in the activation of the innate immune system and its further activation of

innate and acquired immunomodulatory molecules through induction of cytokine release (Janke, Peeters et al. 2007). *In vitro* work suggests that its effect may be mediated by its interaction with Livin a member of the inhibitor of apoptosis (IAP) family. Not only does it appear to overcome the apoptotic resistance of Livin over-expressing cells but it also stimulates caspase cleavage of the Livin, endowing it with an additional pro-apoptotic effect (Lazar, Yaacov et al. 2010). NDV has been used to generate anti-cancer vaccines (Schirrmacher 1999) following its first recorded use as an anticancer agent in 1965 (Cassel and Garrett 1965). In recent years recombinant viruses have been used in a more formal setting. Of note, live attenuated virus MTH-68/H was used to treat high grade glioblastoma (Csatary, Gosztonyi et al. 2004) and reported improved patient quality of life and extended survival rates. PV701, a replication competent strain of NDV was given as part of a phase I trial for solid tumours and achieved some response (Pecora, Rizvi et al. 2002). NDV variant NDV-HUJ demonstrated some activity in glioblastoma patients (Freeman, Zakay-Rones et al. 2006) with a transient complete remission demonstrated in one patient. .

Reovirus is a double stranded RNA virus. It has also been identified as a possible agent for oncolytic viral therapy due to its apparent propensity for targeting cancer cells because its replication is restricted to cells with abnormal Ras signalling pathways - a feature of many malignancies (Coffey, Strong et al. 1998; Strong, Coffey et al. 1998) (Bos 1989). Early trials work has suggested that reovirus-based treatment is safe (Comins, Heinemann et al. 2008). Work combining it with chemotherapy had raised concerns about the attenuation of neutralising antibody responses and its possible impact on therapeutic efficacy and patient safety but more recent studies have been encouraging (Harrington, Bonner et al. 2010; Lolkema, Arkenau et al. 2010) and it is currently being evaluated in the phase III setting for the treatment of head and neck cancer (http://www.clinicaltrials.gov/Oncolytics Biotech NCT01166542).

1.7. Clinical trials of oncolytic viruses for cancer therapy

To date there have been multiple clinical trials investigating oncolytic viral therapy in the cancer setting. Although not exhaustive, many of these are outlined in Table 3 below. Whilst the work with reovirus uses wild-type virus, many of the viral agents mentioned in Table 3 have undergone modification in order to improve tumour tropism, infectivity and cytotoxicity. Differing types of modifications are discussed in greater detail later in this chapter with reference to human adenovirus thus are not dwelt on here.

Table 3 Clinical trials of oncolytic viruses adapted from (Bourke, Salwa et al. 2011)

Cancer Type	Viral Agent	Methodology	No. Pts	Patient Characteristics	Results	Reference
Miscellaneous advanced or metastatic solid cancers	PV701 (NDV)	Patients were administered PV701 **intravenously** via one of four different dosage regimens	79	All patients had an advanced or metastatic solid malignancy unresponsive to established therapies	Of 62 patients eligible for response assessment, 14 were free from tumour progression for 4-30 months and two had radiographic evidence of major responses	(Pecora, Rizvi et al. 2002)
	PV701 (NDV)	A desensitisation regimen was used. 6 cycles of PV701 were given **intravenously**. Six doses were given over 2 weeks followed by a 1-week rest. Doses 1 & 2 were 1 and 12 x 10(9) plaque-forming units (pfu)/m(2), respectively, whereas doses 3 to 6 were escalated by cohort from 24 to 120 x 10(9) pfu/m(2).	16	Pathologically confirmed advanced, incurable solid tumours. At study entry, at least 30 days had elapsed since any prior surgery, systemic therapy (6 weeks for mitomycin or nitrosourea), radiotherapy, or systemic corticosteroid use.	Mild flu-like symptoms were common following the first infusion, diminished with repeated dosing, and were less pronounced than those seen previously. Tumour regression was observed in a patient with anal carcinoma who enrolled with stable disease following palliative radiotherapy. 4 patients with clearly progressing cancer before enrolment had disease stabilization of >/=6 months.	(Laurie, Bell et al. 2006)
	Reovirus	Patients were divided into 8 cohorts and received Reovirus **intravenously** at increasing dosages	33	All patients had histologically or cytologically confirmed advanced-stage primary or metastatic solid tumours that were refractory to standard therapy	Both radiologic and tumour marker anti-tumour activity was seen	(Vidal, Pandha et al. 2008)
	ONYX-015 (Ad5)	Patients received intravenous ONYX-015 at a variety of dosages	10	All patients had advanced or metastatic solid tumours which had failed standard therapy	Although no objective responses were demonstrated with ONYX-015, tumour stabilization of 6.5+ months was demonstrated in two patients with ONYX-015 and carboplatin/paclitaxel-one of whom had previously failed prior carboplatin/taxol treatment	(Nemunaitis, Cunningham et al. 2001)
	Reovirus	Reovirus administered **intravenously** on D1-5 in dose escalation study with concomitant carboplatin (AUC5) and paclitaxel (175mg/m^2) on D1 every 21 days. Subsequent Phase II study examined response using viral titre of 3 x 10^{10} TCID50 dose.	31	Patients with histologically proven, incurable relapsed/ metastatic solid tumours for whom combined carboplatin/ paclitaxel or palliative chemotherapy were appropriate	1 patient had a complete response (3.8%), 6 patients (23.1%) had partial response, 2 patients (7.6%) had major clinical responses clinically evaluated in radiation pre-treated lesions which are not evaluable by RECIST. 9 patients (34.6%) had stable disease, and 8 patients (30.8%) had disease progression. Viral shedding was minimal and antiviral immune responses were attenuated compared with previous single-agent data.	(Karapanagiotou, Roulstone et al. 2012)

Cancer Type	Viral Agent	Methodology	No. Pts	Patient Characteristics	Results	Reference
Miscellaneous advanced or metastatic solid cancers	JX594 (Vaccinia)	Patients received a single intravenous infusion of JX-594 at one of six dose levels. Biopsies were obtained from all subjects 8–10 days after treatment, and sections were subjected to haemotoxylin and eosin and immunohistochemical staining for JX-594 proteins, and PCR for JX-594 genomes.	23	Patients with treatment-refractory, histologically con- firmed, advanced, metastatic solid tumours.	JX-594 was shown to selectively infect, replicate and express transgene products in cancer tissue after intravenous infusion, in a dose-related fashion. Normal tissues were not affected clinically. New tumour out- growth in the time after treatment was less frequent in patients treated with high doses than low dose. Two out of five high-dose patients had antitumour activity by FDG-PET	(Breitbach, Burke et al. 2011)
	OncoVEX GM-CSF (HSV)	Virus was administered by intratumoral injection in a dose escalation study. 13 patients were in a single-dose group, and 17 patients were in a multidose group testing a number of dose regimens	30	Treatment refractory solid tumours with cutaneous or subcutaneous deposits	Biological activity (virus replication, local reactions, GM-CSF expression & HSV antigen-associated tumour necrosis), was observed. 3 patients had stable disease, 6 patients had tumours flattened (injected and/or uninjected lesions). 4 patients showed inflammation of uninjected as well as injected tumour	(Hu, Coffin et al. 2006)
Malignant glioma	G207 (HSV)	Two doses of G207 were administered, the first preoperatively via a catheter placed into the tumour, the second into brain surrounding the resection cavity	6	Inclusion criteria were histologically proven recurrent malignant glioma, Karnofsky score ≥70, and ability to resect the tumour without ventricular system breach	Radiographic and neuropathologic evidence suggestive of anti-tumour activity reported. Evidence of viral replication was demonstrated	(Markert, Liechty et al. 2009)
	HSV-1716	HSV-1716 was injected into the tumour cavity post maximal resection. Patients proceeded to further treatment as clinically indicated.	12	All patients had recurrent or newly diagnosed high-grade glioma	Results compared favourably with historical controls. Two patients had stable disease at 18/12	(Harrow, Papanastassiou et al. 2004)
	NDV -HUJ	Designed to determine the safety and tumour response of repetitive IV administration. There were two parts to the study; The initial part utilized a six-step intrapatient accelerated dose escalation scheme. The second part of the study utilized a constant dosing step, which was one lower than the highest step reached in the first part of the study.	11	All patients had been diagnosed with GBM based on histology	Toxicity was minimal with Grade I/II constitutional fever being seen in 5 patients. Maximum tolerated dose was not achieved. One patient achieved a complete response.	(Freeman, Zakay-Rones et al. 2006)

Cancer Type	Viral Agent	Methodology	No. Pts	Patient Characteristics	Results	Reference
Malignant glioma	Reovirus	Patients received a single intratumoural administration of escalating doses of reovirus	12	Patients were adults with histologically confirmed recurrent glioma, had Karnofsky Performance score ≥60, had received prior radiotherapy with or without chemotherapy, and had up to the third recurrence.	No clinical evidence HSV-1716 toxicity.IT administration of reovirus well tolerated	(Forsyth, Roldan et al. 2008)
Primary pancreatic carcinoma	ONYX-015 (Ad5)	ONYX-015 was administered via CT-guided injection or intraoperative injection into pancreatic primary tumours every 4 weeks until tumour prog2ression	23	Eight patients had locally advanced disease and 15 had distant metastases at enrolment. Previous treatment for pancreatic carcinoma included chemotherapy in 10 patients, radiotherapy in four patients and surgery in 12 patients.	6 patients had a 25-49% decrease in the cross-sectional area of the tumour as measured by CT. An additional 10 patients maintained stable disease within the injected tumour for at least 3 months	(Mulvihill, Warren et al. 2001)
HNSCC	ONYX-015 (Ad5)	ONYX-015 was administered by a single IT injection to patients with recurrent HNSCC	22	histologically confirmed recurrent HNSCC refractory to radiotherapy and/or chemotherapy and with abnormal p53 status	Treatment was well tolerated. Biological activity demonstrated	(Ganly, Kirn et al. 2000)
	ONYX-015 (Ad5)	Patients were enrolled into one or two protocols, receiving either 5 consecutive IT injections of ONYX-015 over 5 days or 10 consecutive twice-a-day IT injections of over 5 days for 2 weeks	37	Patients had histologically confirmed HNSCC (excluding nasopharyngeal) that had recurred after surgery and/or radiotherapy for the primary tumour	Of 24 patients evaluable for response, 8 showed significant tumour regression. Both time to progression and treatment response correlated with p53 status.	(Nemunaitis, Ganly et al. 2000)
	Reovirus	Phase III study to evaluate OS and PFS after **intravenous** administration of carboplatin (AUC5) and paclitaxel(175mg/m^2) on D1 every 21 days +/- reovirus (3 x 10^{10} TCID50) administered iv on D1-5 of each cycle.	n/a	Recurrent/ metastatic histologically confirmed HNSCC or squamous cell nasopharynx who have completed first line chemotherapy which progressed on or within 190 days following the completion of platinum or platinum-based chemotherapy	Trial on-going. Final data collection date for primary outcome measure due January 2013	(Harrington, Bonner et al. 2010)
	HF-10 (HSV)	A single metastatic skin nodule in refractory HNSCC was injected with HF10 once a day for 3 days. Injected nodules were excised day 13 or day 15 after inoculation	2	Both patients had received systemic chemotherapy and radiotherapy +/- surgery	HF10 replicated, spread well in the tumour nodules, and caused cell death in a considerable population of tumour cells without any significant adverse effects	(Fujimoto, Mizuno et al. 2006)

Cancer Type	Viral Agent	Methodology	No. Pts	Patient Characteristics	Results	Reference
HNSCC	OncoVEX GM-CSF (HSV)	Dose-escalations study of OncoVEX GM-CSF when given with chemoradiotherapy (70 Gy/35 fractions with concomitant cisplatin 100 mg/m(2) on days 1, 22, and 43) and OncoVEX GM-CSF by intratumoural injection on days 1, 22, 43, and 64. Patients underwent neck dissection 6 -10 weeks later.	17	Stage III/IVA/IVB squamous cell carcinoma patients receiving chemoradiotherapy	14 patients (82.3%) showed tumour response by RECIST, and pathologic complete remission was confirmed in 93% of patients at neck dissection. No patient developed locoregional recurrence, and disease-specific survival was 82.4% at a median follow-up of 29 months (range, 19-40 months). HSV was detected in injected and adjacent uninjected tumours at levels higher than the input dose, indicating viral replication.	(Harrington, Hingorani et al. 2010)
Colorectal cancer metastatic to the liver	NV1020 (NDV)	In this dose-escalation study patients were randomly separated into 4 cohorts, with each patient received a single dose of NV1020 via hepatic artery infusion	12	All patients had at least three unresectable metastatic liver lesions from histologically confirmed primary colorectal carcinoma. Patients had also failed first-line chemotherapy with 5-FU plus either leucovorin or irinotecan	Anti-tumour activity was assessed 28 days after viral administration. One patient had 39% reduction in tumour size, while a second had a 20% reduction. Seven patients demonstrated stable disease	(Kemeny, Brown et al. 2006; Fong, Kim et al. 2009)
	ONYX-015 (Ad5)	Patients with metastatic colorectal cancer who were receiving 5FU/leucovorin were administered four cycles of ONYX-015 by hepatic artery infusion	24	All patients had histologically- or cytologically confirmed unresectable liver metastases from colorectal cancer and had failed first-line therapy with 5FU/leucovorin	Tumour response was determined 3 weeks after the last planned treatment with Onyx-015. Two patients had significant tumour volume reductions of 66% and 72% respectively. 11 patients had stable disease. Median survival for the 24 patients was 10.7 months and 46% were alive at 1 year	(Reid, Freeman et al. 2005)
	Reovirus	Window-of-opportunity clinical trial in colorectal cancer patients. A single cycle of **intravenous** reovirus monotherapy was given to patients before a planned resection of colorectal cancer liver metastases. Sequential blood samples were taken for assessment of viral distribution and resected tissue was analysed for the presence of virus by immunohistochemistry. Samples were also evaluated for the presence of replicating virus using viral plaque assays	10	All patients had histologically or cytologically confirmed resectable hepatic metastases form colorectal cancer.	Analysis of surgical specimens demonstrated greater, preferential expression of reovirus protein in malignant cells compared to either tumour stroma or surrounding normal liver tissue. Evidence of viral factories within tumour, and recovery of replicating virus from tumour (but not normal liver) was achieved in all 4 patients from whom fresh tissue was available. Tracking the viral genome in the circulation showed that reovirus could be detected in plasma and blood mononuclear, granulocyte, and platelet cell compartments after infusion. Reovirus was thought to be protected from neutralizing antibodies after systemic administration by immune cell carriage, which delivered reovirus to tumour.	(Adair, Roulstone et al. 2012)

Cancer Type	Viral Agent	Methodology	No. Pts	Patient Characteristics	Results	Reference
Colorectal cancer metastatic to the liver	ONYX-015 (Ad5)	Patients received hepatic artery infusion of ONYX-015 at escalating doses in combination with 5FU/Leucovorin	11	All patients had histologically or cytologically confirmed unresectable hepatic metastases from carcinoma of gastrointestinal origin	Antitumoural activity was demonstrated with high dose ONYX-015 in combination with 5-FU and LV. Two patients had stable disease on lasting from 7 to 17 months. In addition, one patient with 5-FU refractory colorectal carcinoma had a partial response following combination therapy	(Nemunaitis, Cunningham et al. 2001)
Bladder cancer	Vaccinia	Patients received 3 increasing doses of intravesical vaccinia virus.	4	All patients had high grade, muscle-invasive transitional cell carcinoma. One patient had received prior systemic chemotherapy	Demonstrated that vaccinia can be administered safely and repeatedly. A cellular infiltrate conducive to the development of an anti-tumour immunity was induced.	(Gomella, Mastrangelo et al. 2001)
Ovarian cancer	Measles Virus (MV) -CEA	MV was engineered to express CEA (MV-CEA virus) to permit real-time monitoring of viral gene expression in tumours. Patients were treated with IP MV-CEA every 4 weeks for up to 6 cycles	21	Patients with Taxol and platinum-refractory recurrent ovarian cancer and normal pre-treatment CEA levels were eligible for inclusion	Fourteen of 21 patients had dose-dependent disease stabilization for a median duration of 92.5 days. Five patients had significant decreases in CA-125. Dose-dependent CEA elevation in peritoneal fluid and serum was observed	(Galanis, Hartmann et al. 2010)
	ONYX-015 (Ad5)	ONYX-015 was infused via intraperitoneal catheter daily for 5 days	16	Eligible patients had histologically or cytologically confirmed primary epithelial ovarian cancer, with recurrent disease suspected either radiologically or by rising CA125 levels. All patients had received previous chemotherapy with platinum containing regimens and had relapsed within the previous 6 months	The primary aim of defining safety and evaluating dose-related toxicity associated with intraperitoneal delivery of ONYX-015 was achieved.	(Vasey 2005)
	Ad5-Δ24-RGD	Phase 1 dose escalation study evaluating tolerability of intraperitoneal delivery of adenoviral mutant given daily for 3 days	21	Patients with epithelial ovarian or primary peritoneal adenocarcinoma and then expanded to include fallopian tube and endometrial carcinoma. All patients were required to have had previous treatment with conventional surgery and chemotherapy and have evidence of intra-abdominal disease.	Adverse effects included G1/2 fever, fatigue, or abdominal pain. No vector related grade 3/4 toxicities. The MTD was not reached. Over 1 month, 15 (71%) of patients had stable disease and six (29%) had PD. No partial or complete responses were noted.7 patients had a decrease in CA-125; 4 had a >20% drop. RGD-specific-PCR demonstrated the presence of study vector in ascites of 16 patients. Seven revealed an increase in virus after day 3, suggesting replication of Ad5-Δ24-RGD.	(Kimball, Preuss et al. 2010)

Cancer Type	Viral Agent	Methodology	No. Pts	Patient Characteristics	Results	Reference
Prostate cancer	CV706 (Ad5)	Patients were treated viral particles injected by a real-time, transrectal ultrasound-guided transperineal technique	20	All pts had biopsy-proven, locally recurrent prostate cancer following radiotherapy	Intra-prostatic CV706 administration demonstrated to be safe. Conclusive evidence of CV706 infection of prostate cancer cells. Thirteen patients had a PSA reduction of at least 30% from the pre-treatment level	(DeWeese, van der Poel et al. 2001)
	CG7870 (Ad5)	CG7870 was administered as a single intravenous infusion	23	All patients had hormone-refractory metastatic prostate cancer	Five patients had a serum PSA decrease of 25-49%.All patients developed antibodies to CG7870. 16 patients had evidence of active viral replication.	(Small, Carducci et al. 2006)
	Reovirus	A single intraprostatic injection of reovirus was delivered transrectally	6	All patients had localized prostate carcinoma, had consented to a prostatectomy as their definitive cancer treatment and received intratumoural injection of reovirus 3 weeks before the planned surgery	Reovirus treatment was well tolerated. Both necrosis and apoptosis were in evidence in pathologic specimens that stained positive for reovirus infection	(Thirukkumaran, Nodwell et al. 2010)
Primary hepatobiliary cancer	ONYX-015 (Ad5)	Patients received intralesional injections of ONYX-015, apart from those with malignant ascites who received IP injections	19	All patients had biopsy-proven, unresectable tumours of the liver, gall bladder, or bile ducts	Patients were evaluated for response every 6 week, by CT scan and tumour markers. One patient had a radiographic partial response lasting 13.5 weeks. 8 patients had declines of at least 50% in at least one serum tumour marker	(Makower, Rozenblit et al. 2003)
Cutaneous metastases from breast cancer	HF10 (HSV)	HF10 was injected directly into the lesions. Control lesions were injected with saline	6	All patients had undergone mastectomy and had biopsy proven cutaneous or subcutaneous recurrences in spite of chemotherapy, endocrine therapy, surgical therapy, and/or radiotherapy	Intralesional HF10 was well tolerated. In 5 patients cancer cell death was observed after HF10 injection, whereas no cancer cell death was seen in saline-injected nodules	(Kimata, Imai et al. 2006)

Ad5, Human adenovirus serotype 5; CEA, carcinoembryonic antigen; FDG-PET, Fluorodeoxyglucose (18F) Positron Emission Tomography ; 5FU, 5,fluorouracil ;GM-CSF, granulocyte-macrophage colony-stimulating factor; HNSCC, head and neck squamous cell carcinoma; HSV, Herpes Simplex Virus; IP, intraperitoneal; IV, intravenous; MTD, maximum tolerated dose ; NDV, Newcastle Disease Virus; OS, overall survival; PFS, progression free survival; PSA, prostate sensitive antigen; RECIST, Response Evaluation Criteria In Solid Tumours

;

A couple of recent studies are worthy of further discussion as they demonstrate the problems and pitfalls of clinical studies using oncolytic viruses. JX-594 is a targeted oncolytic vaccinia virus designed to selectively replicate in and destroy cancer cells with cell-cycle abnormalities and epidermal growth factor receptor (EGFR)-Ras pathway activation. Vaccinia is an attractive vehicle for transformation into an anti-cancer agent due to several innate characteristics. It has the ability to infect efficiently a wide range of host cells, a genome that can accommodate large DNA inserts and express multiple genes, high immunogenicity and cytoplasmic replication without the possibility of chromosomal integration. As a result, vaccinia virus has been used as both a delivery vehicle for anti-cancer transgenes, a vaccine carrier for tumour-associated antigens and immunoregulatory molecules in cancer immunotherapy, and also as an oncolytic agent that selectively replicates in and lyses cancer cells (Shen and Nemunaitis 2005). JX594 has a transgene inserted which results in granulocyte-macrophage colony-stimulating factor (GM-CSF) expression. Thus, not only does it result in cell death through direct oncolysis, it also stimulates shutdown of tumour vasculature and enhances antitumor immunity (Park, Hwang et al. 2008). Intratumoral injection of vaccinia in cutaneous melanoma lesions provided promising results (Mastrangelo, Maguire et al. 1999) and work in primary and metastatic liver cancer also demonstrated promising phase I data (Park, Hwang et al. 2008). Excitingly, recent phase I data has reported the safe intravenous delivery of JX-594 in 23 patients with solid tumours. Patients with chemo-resistant solid tumours were given a single dose of JX594 in this dose escalation study. Importantly, tumour biopsies demonstrated dose-related delivery, replication and transgene expression in metastatic tumours in humans (Breitbach, Burke et al.). However, successful viral replication within the tumours was not proven (rising antibody response and transgene expression were used as surrogate markers) and there was no attempt to demonstrate the presence of virion progeny production. Therefore, as a proof of concept study demonstrating that JX594 can be delivered safely intravenously and reach tumour tissue with resultant transgene

expression, this was a success. However, it did not confirm successful replication of the oncolytic virus within the target cells and, of note, only one patient had neutralising antibodies present in the circulation prior to JX594 administration which may have minimised potential adverse events.

Adair et al. designed a "window of opportunity" study to evaluate the intravenous administration of reovirus (Adair, Roulstone et al. 2012). 1×10^{10} $TCID_{50}$ of intravenous reovirus monotherapy was given over 60 minutes on days 1-5 immediately prior to a planned resection of colorectal cancer metastatic to the liver. Reovirus was administered in this way to ten patients. Analysis of sequential blood samples, resected tumour and normal tissue was undertaken. Colorectal cancer is an appropriate target for reovirus oncolysis, with a reported *ras* mutation rate of 37% (Brink, de Goeij et al. 2003). Within this current study, 5 of the 10 patients' tumours were *ras* mutant. More reovirus protein was seen using immunohistochemistry at the time of surgery in malignant cells compared to tumour stroma or normal cells in 9 of 10 patients, irrespective of ras mutational status. The presence of reovirus was associated with cellular degeneration and apoptosis. Although these data demonstrate targeted viral delivery to, and/or replication in, malignant versus normal cells, it did not prove causation between the presence of reovirus and tumour cell apoptosis. The investigators deduced that the higher reovirus levels detected in tumour cells were due to selective replication in malignant cells rather than greater infection, firstly because reovirus receptors are ubiquitously expressed, and secondly because *in vitro* primary human hepatocytes are resistant to reovirus replication and killing. Electron microscope findings and the co-localisation of reovirus and tubulin were deemed consistent with viral reproduction "factories". Most importantly, however, replication competent reovirus (demonstrated using viral plaque assays) could be retrieved from the tumour in four of four patients tested. Virus could not be similarly retrieved from the corresponding normal liver samples demonstrating selective replication of an oncolytic

virus in malignant versus normal tissue. Neutralising antibodies were present in all patients prior to dosing, thus pre-existing immunity did not preclude viral replication. Interestingly, successful replication within the tumour appeared to depend on a 'threshold effect', requiring a minimal dose of virus delivery to the tumour before viral replication could proceed. Investigators concluded that successful delivery to the tumour had occurred because the virus had circumnavigated the immune system. Data suggested that virus had done so by "hitchhiking" onto a selection of circulating cells such as peripheral blood monocytes, granulocytes and platelets to evade detection/neutralization by the immune system. This again was encouraging, suggesting that the presence of neutralising antibodies did not preclude viral circulation or replication and suggested that evasion techniques could be exploited in future viral constructs. However, due to the nature of the study design no therapeutic effect could be demonstrated and this will require evaluation within the neo-adjuvant setting.

In summary there have been a number of early trials evaluating the use of replicating oncolytic viruses, some of which incorporate transgenes which are designed to increase their therapeutic effects. Most trials have examined intratumoural delivery but some have evaluated IP and IV administration. Trials of intravenous delivery to date have not reliably or consistently demonstrated effective viral targeting or virion progeny release although recent studies have been more encouraging. Of note, viruses have been well tolerated with no serious side effects noted and anti-tumour activity has been demonstrated across several tumour types.

1.8. Adenovirus life cycle

Over time adenoviridae have emerged as particularly appropriate vectors for cancer therapy for several reasons. They have a well-described entry pathway and are known to infect cycling and non-cycling cells efficiently (Barnes, Coolidge et al. 2002; Hawkins, Lemoine et al. 2002). The latter is important as most solid human tumours

have relatively low growth fractions (Tubiana and Malaise 1976). The parental wild-type causes a mild, well-characterised disease in humans. Its biology is well understood (Shenk 2001), which is important for engineering the virus, and it can be readily produced at high titres (Hawkins, Lemoine et al. 2002). To date, the majority of viral gene therapy work has been carried out using adenoviral vectors and this is also true of oncolytic viral agents.

1.8.1. Adenovirus classification & virion structure

The Adenoviridae family is divided into five genera: the most important are the genus Aviadenovirus, which causes disease in birds and the genus Mastadenovirus, which infects a wide range of species including humans. Human adenoviruses have been divided into 49 serotypes and these have been organised into six subgroups according to their ability to agglutinate red blood cells (Table 4).

Subgroup	Haemaglutination Group	Serotype
A	IV: little agglutination	12, 18, 31
B	I: complete agglutination of monkey erythrocytes	3, 7, 11, 14, 16, 21, 34, 35
C	III: partial agglutination of rat erythrocytes	1, 2, 5, 6
D	II: complete agglutination of rat erythrocytes	8, 9, 10, 13, 15, 17, 19, 20, 22-30, 32, 33, 36-39, 42-49
E	III	4
F	III	40, 41

Table 4 Classification of Adenoviruses.

Oncolytic viral therapy mainly used group C adenoviruses, primarily Ad2 and Ad5. Latterly, there has been increasing interest in the use of Group B adenoviruses because of their utilization of the CD46 molecule for cellular transduction which is abundantly expressed on most human cells and is upregulated in carcinoma cells (Kim, Sumerel et al. 2003; Anderson, Nakamura et al. 2004). This is in contrast to the coxsackie and adenoviral receptor (CAR) which is used by serotypes 2 and 5 and is expressed at lower levels in tumour cells (Hemmi, Geertsen et al. 1998; Miller, Buchsbaum et al. 1998; Asaoka, Tada et al. 2000; Luckey, Hernandez et al. 2000).

The adenovirus genome is contained within a capsid comprising 12 penton and 240 hexon subunits, plus minor structural proteins as illustrated in Figure 5. The icosahedral capsid structure is composed of seven polypeptides; the trimeric hexon (II), which is complexed with three minor hexon polyproteins (VI, VIII and IX) which provide stabilisation, the pentameric penton (III) protein which binds non-covalently to the N-terminus of the fibre protein (IV) (Mautner and Pereira 1971), the penton associated protein (IIIa) which cements the hexon-penton complex, and the receptor binding fibre (IV) protein (Everitt, Sundquist et al. 1973; Everitt, Lutter et al. 1975). The fibre protein (IV) is composed of three domains; the tail at the N-terminus, the rod-like shaft and the globular knob domain at the C-terminus.

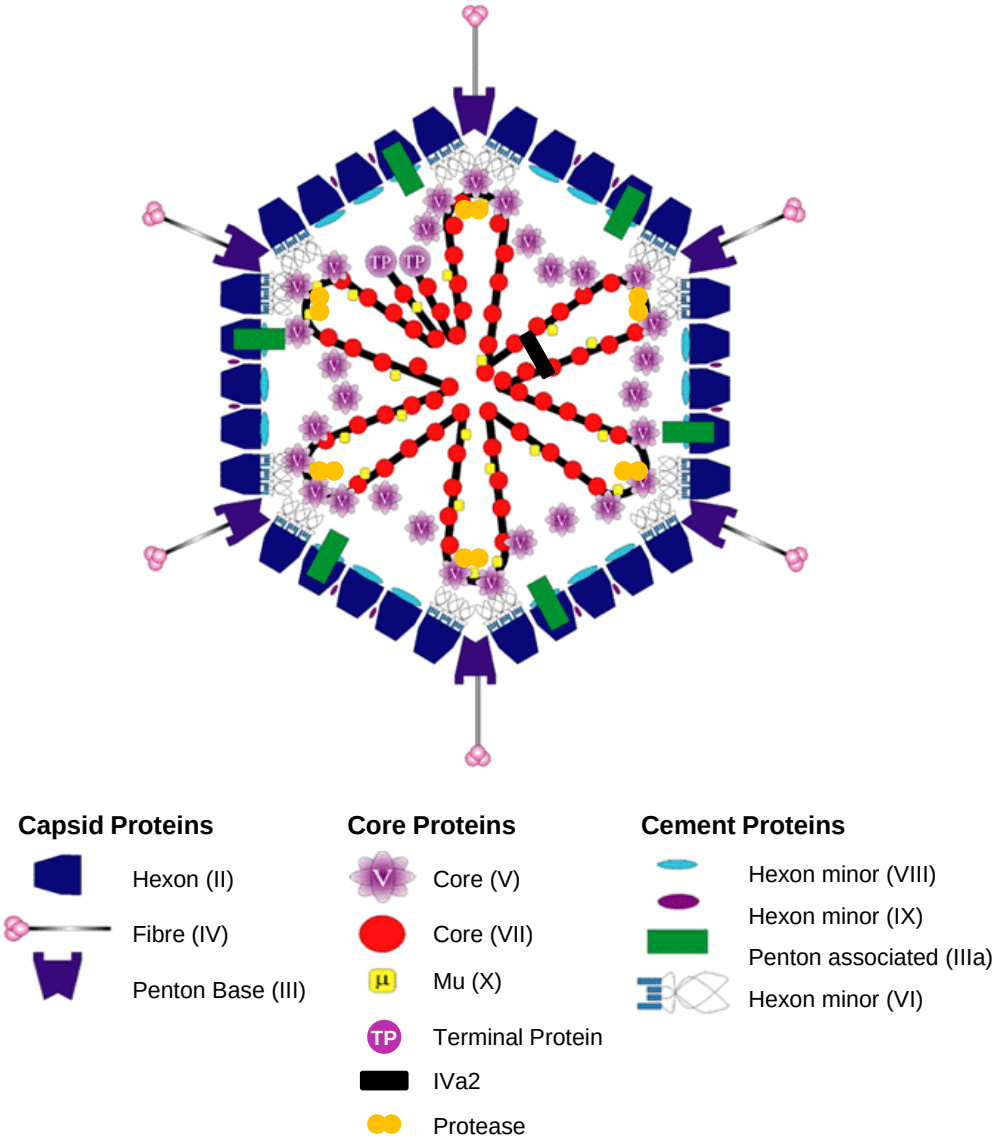

Figure 5 Adenoviral Structure.

Schematic representation of the major and minor structural proteins of adenovirus and the nucleoprotein core with terminal protein (TP) covalently attached at each end of the double stranded DNA (dsDNA) genome. Figure adapted from Russell (Russell 2009).

1.8.2. Adenoviral Entry

Human adenovirus type 5 (Ad5) enters the epithelial cells in a two-step process (Figure 6 below). Initially it docks with the cell via the distal knob of the viral fibre. This binds to the target cell via the 46kDa, transmembrane Coxsackie and Adenovirus Receptor (CAR) (Bergelson, Cunningham et al. 1997; Tomko, Xu et al. 1997; Roelvink, Lizonova

et al. 1998; Bergelson 1999; Roelvink, Mi Lee et al. 1999; Santis, Legrand et al. 1999; Tomko, Johansson et al. 2000). CAR is a member of the immunoglobulin (Ig) superfamily and has two extracellular Ig-like domains (D1 and D2). CAR functions as a cell adhesion protein within the tight junctions. It forms homodimeric adhesions between polarised epithelial cells and the cardiac intercalated disc (van Raaij, Chouin et al. 2000; Cohen, Gaetz et al. 2001; Shaw, Holland et al. 2004). Fibre-CAR binding is followed by the interaction of an Arg-Gly-Asp (RGD) motif in the penton base with αvβ3/αvβ5 integrins, which subsequently triggers viral internalisation (Wickham, Mathias et al. 1993). It is thought that the Ad5 penton-integrin interaction results in integrin clustering which activates signalling pathways, such as phosphoinositide-3-OH kinase (PI3K), p38 MAPK, p44/42 MAPK and ERK1/2, inducing downstream effects resulting in the polymerisation and reorganisation of actin filaments (Li, Stupack et al. 1998a; Li, Stupack et al. 1998b; Suomalainen, Nakano et al. 2001; Bhat and Fan 2002; Tibbles, Spurrell et al. 2002; Shayakhmetov, Gaggar et al. 2005; Farmer, Morton et al. 2009). Whilst the classical two-step pathway of adenoviral infection is still valid, it is now clear that the process of infection by Ad5 is more complex than previously assumed. Receptors and co-receptors other than CAR and αvβ3/αvβ5 integrins are now known to mediate adenoviral cell entry. Heparan sulphate proteoglycans (HSPGs) have been shown to permit binding of Ad5 in the absence of CAR in A549 and CHO-K1 cells (Dechecchi, Tamanini et al. 2000; Dechecchi, Melotti et al. 2001). Additionally, vascular cell adhesion molecule 1 (VCAM-1) or MHC class I have also been proposed to facilitate low affinity Ad5 interactions, although evidence which supports the latter interaction has been challenged (Hong, Karayan et al. 1997; Davison, Kirby et al. 1999; McDonald, Stockwin et al. 1999; Chu, Heistad et al. 2001). Additional integrins, αvβ1, α3β1, α5β1 and αMβ2 have also been shown to permit the internalisation of adenoviruses (Huang, Kamata et al. 1996; Davison, Diaz et al. 1997; Davison, Kirby et al. 2001; Li, Brown et al. 2001; Salone, Martina et al. 2003).

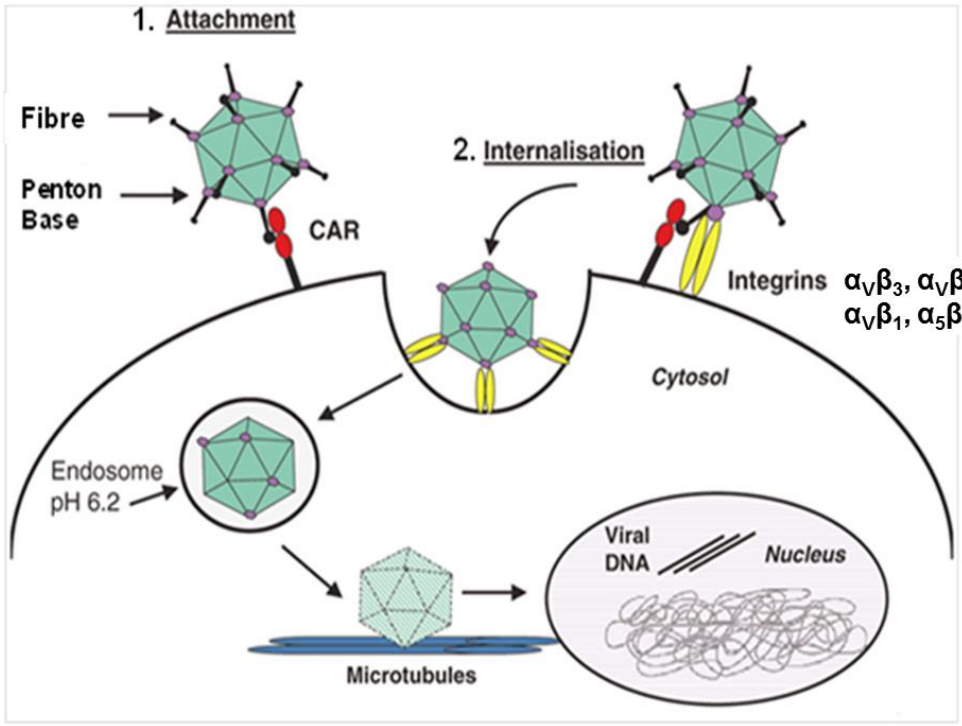

Figure 6Classical two-step adenoviral entry.

(1) Adenovirus attachment is mediated by the distal knob domain of the fibre. The flexible fibre binds to the 46kDa transmembrane protein, the Coxsackie and Adenovirus Receptor, CAR. **(2)** The RGD motif in the penton base of the Ad particle triggers internalisation via αvβ3/αvβ5 integrins. Partial disassembly of the capsid is induced by acidification of the endosome following clathrin-mediated endocytosis. Endosomal escape is modulated through the action of protein VI, after which the nucleocapsid core is translocated to the nucleus along the microtubule network. Further capsid dissociation permits the viral DNA to enter the nucleus for subsequent transcription and replication. Figure adapted from (Horwood, Smith et al. 2002).

Recent *in vivo* work has highlighted the importance of “bridging interactions” following systemic delivery of Ad5 in mice. It has now been shown by several groups that direct interactions between the Ad5 capsid and vitamin K-dependent coagulation factors, including FX, FIX, FVII, Protein C, in addition to Complement 4-Binding protein, can modulate viral entry through HSPGs or low-density lipoprotein receptor-related protein, LRP (Shayakhmetov, Gaggar et al. 2005; Waddington, Parker et al. 2007; Kalyuzhniy,

Di Paolo et al. 2008; Vigant, Descamps et al. 2008; Waddington, McVey et al. 2008; Alba, Bradshaw et al. 2009).These interactions appear to play a critical role in mediating hepatocyte transduction *in vivo* and are thus central to virus mediated hepatotoxicity. Additionally, coagulation factor “bridging” has been shown to be involved in the enhanced infection of various tumour cells both *in vitro* and *in vivo* (Shayakhmetov, Gaggar et al. 2005; Parker, Waddington et al. 2006; Parker, McVey et al. 2007; Gimenez-Alejandre, Cascallo et al. 2008; Coughlan, Vallath et al. 2009; Liu, Wang et al. 2009). However, Ad5 has also been shown to interact with various other components within the circulation, such as natural IgM and complement, platelets and erythrocytes. Opsonisation of Ad5 by IgM and complement, or binding to platelets to promote the formation of Ad5-platelet-leukocyte aggregates, are mechanisms proposed to play a role in Kupffer cell scavenging (Stone, Liu et al. 2007; Xu, Tian et al. 2008). Moreover, Ad5 interactions with CAR-expressing erythrocytes in mice have been shown to prevent efficient tumour transduction *in vivo* by trapping virus in the circulation (Carlisle, Di et al. 2009).

Viral internalisation is mediated via clathrin-mediated endocytosis (Wang, Huang et al. 1998; Meier, Boucke et al. 2002), followed by partial capsid disassembly upon acidification of the endosome (Greber, Willetts et al. 1993). The lytic action of protein VI facilitates endosomal escape, after which the nucleocapsid is translocated to the perinuclear envelope along the microtubule network (Dales and Chardonnet 1973; Suomalainen, Nakano et al. 1999; Wiethoff, Wodrich et al. 2005).

Transport to the nuclear pore complex is achieved using the microtubule-dependent motor. This is mediated by cytoplasmic dynein which permits adenoviral attachment to microtubules (Leopold, Kreitzer et al. 2000; Kelkar, Pfister et al. 2004). The capsid undergoes its final dissociation event at the nuclear pore complex (Greber,

Suomalainen et al. 1997), allowing the core DNA to extrude into the nucleus for subsequent transcription and replication.

1.8.3. Structure & Function of the Adenoviral Genome

Linear adenoviral DNA is 35-36kb long and is tightly wrapped around viral proteins V and VII in the adenoviral core. It contains 5 early transcription units named E1A, E1B, E2, E3 and E4, two delayed early units IX and IVa_2 and the major late transcription unit, which produces 5 species of mRNA designated L1-L5 (Figure 7). Transcription occurs from both the leftward and rightward strands of the adenoviral chromosome. With the exception of the E4 region, each transcription unit encodes proteins with similar functions.

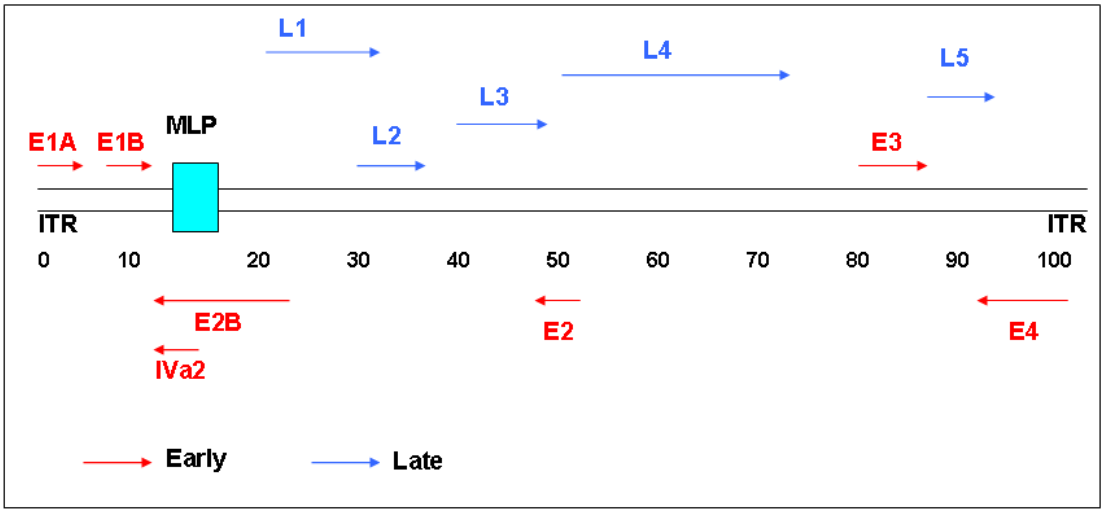

Figure 7 Schematic diagram of the adenoviral genome.

Red arrows represent early and delayed early genes. Blue arrows represent late genes. Numbers represent MAP units. **MLP**= Major Late Promoter. **ITR**= Inverted Terminal Repeats

Early regions are concerned with viral replication and late regions encode for viral structural proteins (Evans 2002). Once inside the cell, the only adenoviral gene that can be expressed independently of the host is E1A. E1A contains three regions; CR1, CR2 and CR3. It is predominantly through these domains that E1A binds to cellular

proteins, many of which regulate gene transcription and cell cycle control (Shenk 2001; Evans 2002; Berk 2005).

pRb is a tumour suppressor protein and is part of the Retinoblastoma family of proteins that regulate transition into S phase (Felsani, Mileo et al. 2006). In quiescent cells, un or hypo-phosphorylated pRb binds to and inhibits the E2F family of transcription factors, holding the cell in G1 phase of the cell cycle. In the early stages of adenoviral infection, E1A CR1 and CR2 bind to pRb. CR2 binds with high affinity to the B-domain of the pRb pocket (Felsani, Mileo et al. 2006) and subsequently E1A CR1 displaces E2F from the E1A CR2/pRb complex by low affinity binding with pRb directly at the E2F binding site. The released free E2F transactivates genes necessary for DNA replication and S phase entry.

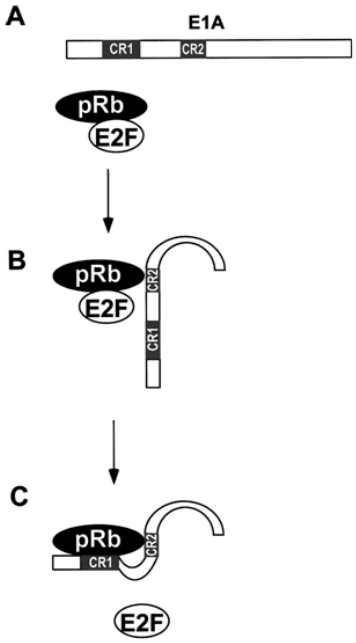

Figure 8 Disruption of pRb/E2F complexes by E1A.

E1A binds to the pRb via the LxCxE motif in CR2 (A & B). This allows for CR1 to contact a site on pRb that overlaps with the E2F-binding site (C) which results in dissociation of the E2F from pRb. Adapted from Helt and Galloway (Helt and Galloway 2003).

E2F also transactivates the E2 region of the adenovirus, which is how E2F was first described. The E2 region encodes proteins required for viral genome replication (de Jong, van der Vliet et al. 2003). Thus, normal control of the cell cycle is bypassed by the adenoviral early coding regions in order to facilitate preferential replication of the viral genome. In addition to orchestrating viral genome replication, E1A expression promotes apoptosis by sensitizing host cells to death receptor-mediated apoptotic pathways (Shao, Hu et al. 1999; Routes, Ryan et al. 2000).

In response to the unscheduled induction of cellular proliferation brought about by E1A, the innate cellular tumour suppressor mechanisms (p53) respond by activating pro-apoptotic pathways (Debbas and White 1993; Lowe and Ruley 1993). However, adenoviral E1B products work to counteract the downstream sequelae of pRb inhibition (Figure 8). Increased levels of free E2F upregulate $p19^{ARF}$, which in turn blocks the p53 inhibitor Mdm2 (White 2001) and this leads to the stabilisation and accumulation of p53. Under normal circumstances, increased levels of p53 lead to transcriptional activation of the cdk inhibitor $p21^{Cip1}$ (Sherr and McCormick 2002) and arrest of the host cell cycle in G1 phase. p53 stabilisation also triggers death of the normal cell via the intrinsic apoptotic pathway through its activation of the cellular pro-apoptotic genes Bax and Bak (White 2001). However, adenoviral E1B products inhibit the induction of these apoptotic pathways and work together with E1A products to prevent p53 mediated cell cycle arrest in G1.

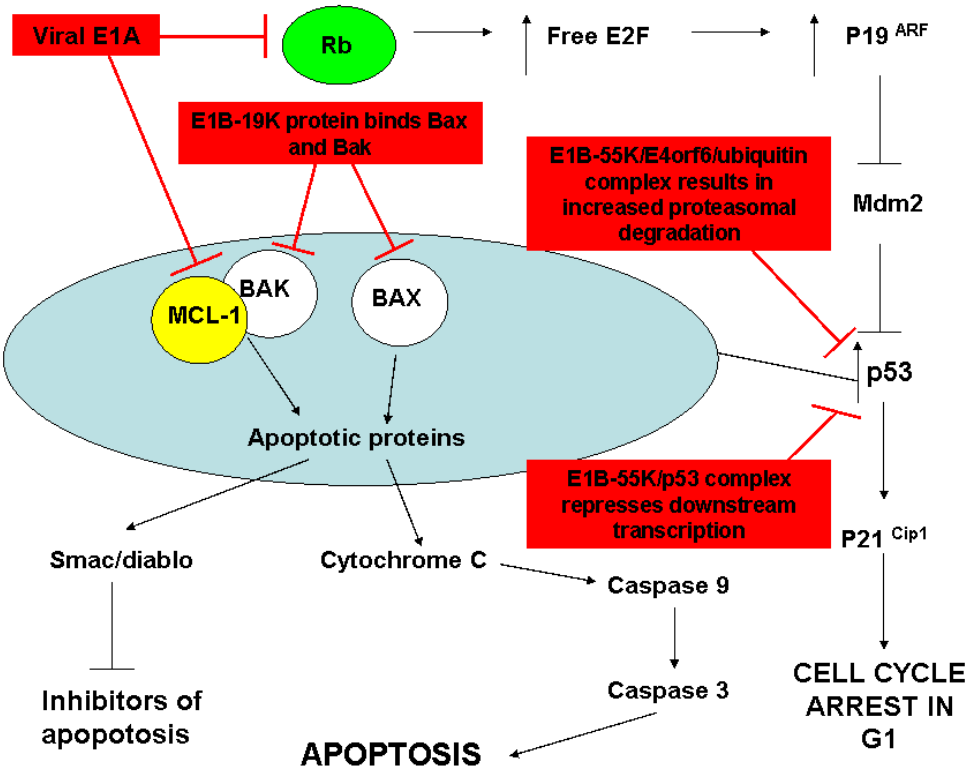

Figure 9 Inhibition of intrinsic apoptotic pathway after viral infection.

The anti-apoptotic action of E1A and E1B adenoviral early gene products is shown in red.

E1B encodes two proteins that act to prevent p53-mediated apoptosis and hence promote viral replication. E1B-19K is a Bcl-2 homologue that binds to and inhibits BAX and BAK, thus inhibiting p53-mediated apoptosis (Berk 2005). E1B-55K stabilises p53 by binding to its Mdm2 binding site, thus increasing the concentration and binding affinity of p53 (Martin and Berk 1998). The E1B-55K/p53 complex then acts as a repressor of p53 target genes and prevents cell cycle arrest and apoptosis (Shenk 2001; Berk 2005).

E1B-55K also forms an important complex with E4orf6 and ubiquitin ligases. This E1B-55K/E4orf6/ubiquitin complex binds to p53 and targets it for proteasomal degradation (Evans 2002; Berk 2005). In addition, this complex targets the DNA damage recognition/repair complex MRN and DNA ligase IV, a protein essential for DNA repair

by non-homologous end joining. By targeting these for proteosomal degradation, the complex switches off defences designed to prevent viral DNA replication. E1B-55K is also important in the transport of mRNA from the nucleus to the cytoplasm (Dosch, Horn et al. 2001). Originally believed to be a function of its interaction with E4orf6 protein, it is now known that E1B-55K contains a specific nuclear export signal (NES) between amino acids 83-93, which effects this function and has been observed in other viruses (Dobbelstein, Roth et al. 1997). More recently the E1B55K/E4orf6/ubiquitin ligase complex has been implicated as a factor promoting viral release via interaction with α-integrin (Dallaire, Blanchette et al. 2009).

As is the case with most DNA viruses, adenoviral replication takes place in the nucleus. Both strands of DNA are transcribed by 5'-3' directional reading. The E2 region encodes for proteins which are required for viral genome replication (de Jong, van der Vliet et al. 2003). E2 proteins which facilitate viral replication include the terminal protein (TP), a precursor of which primes synthesis of the viral genome, the DNA polymerase, which possesses an intrinsic 3'-5' exonuclease activity, and finally the DNA-binding protein (DBP), which permits elongation. These proteins act in concert with various cellular factors, such as nuclear factors NFI/NFIII which provide stabilisation, to enhance viral DNA replication, and NFII which facilitates successful DNA elongation (Nagata, Guggenheimer et al. 1983; Bosher, Robinson et al. 1990; Chen, Mermod et al. 1990; Mul, Verrijzer et al. 1990).

The E3 region encodes proteins that subvert the host immune response and allow persistence of the infected cell. These act by preventing viral antigen presentation by MHC Class I molecules (Hermiston, Hellwig et al. 1993; Hermiston, Tripp et al. 1993a) and inhibiting apoptosis mediated by the chemokines TNFα, Fas-ligand and TRAIL (Krajcsi, Dimitrov et al. 1996; Shisler, Yang et al. 1997; Li, Kang et al. 1998; Benedict, Norris et al. 2001; Lichtenstein, Doronin et al. 2004; Carmody, Maguschak et al. 2006).

Upon adenoviral infection, the host cell mounts a multi-faceted response to try to repel viral entry and replication. Generation of an acute inflammatory response marked by TNF-α production leads to immune cell recruitment and activation of humoral immunity (Janeway C. 2005). Direct lysis occurs following activation of the extrinsic apoptotic pathway which is mediated by death receptor binding (Park, Schickel et al. 2005) (White 2001). Adenovirus acts to neutralise these threats with inactivation of apoptotic receptors TNFR-1/ TRAIL/Fas ligand (FasL) via the death receptor internalisation complex (RID) (Benedict, Norris et al. 2001; Evans 2002; Lichtenstein, Toth et al. 2004; Schneider-Brachert, Tchikov et al. 2006) and anti-inflammatory effects mediated by prevention of phospholipid cleavage of arachidonic acid and NFκB-mediated cytokine transcription (Shenk 2001; Carmody, Maguschak et al. 2006).

E3 Region	**Protein**	**Protein Function**
E3A	6.7K	Aids internalisation of TRAIL receptor in conjunction with RID-α and RID-β
	gp19K	Complexes with MHC class I antigens and holds them in the endoplasmic reticulum to prevent presentation to cytotoxic T lymphocytes (CTLs)
E3A&B	11.6 K Adenoviral Death Protein (ADP)	Major contributor to cell lysis resulting in host cell's death and mature virion propagation
E3B	10.4Kd RID-α	Binds and internalises FAS death receptor to inhibit lyzosomal destruction
	14.5K RID-β	Binds TNFR-1 death receptor and internalises receptor to inhibit lyzosomal destruction Complexes with the 6.7K protein of E1A to downregulate TRAIL receptor binding
	14.7K	Inhibits TNFR-1 Modulates TNFα activity via inhibition of the phospholipase A2 and NFκB pathways

Table 5 Major proteins encoded by adenoviral E3 region.

RID = Receptor Internalisation and Degradation complex. For references please refer to the text.

The function of the E4 transcription products was not well characterised but recent work suggests that this previously overlooked part of the genome is just as important as its 5' counterpart. It encodes proteins with diverse functions that are involved in avoiding intracellular obstacles to viral DNA replication and late gene expression (Weitzman 2005a; Weitzman and Ornelles 2005b). In the last few years there has been a growing understanding of their important role in combination with early protein E1B-55K (Blackford and Grand 2009). E4 deleted viruses produce large concatemers of viral DNA which are recognised by the host cells as DNA damage and are thus targeted for repair via the action of the MRN complex and DNA ligase IV. In E4 intact adenoviruses, this genome concatenation is prevented by E4orf3 and E4orf6 proteins together with the E1B-55K/E4orf6 ubiqitin ligase complex as discussed above.

E4orf3 plays an important role in the orchestration of the elements required to effect disarmament of the DNA damage response. Firstly it disrupts the localisation of Promyelocytic leukaemia (PML) bodies (Leppard and Everett 1999). These are hypothesised to be highly sensitive DNA damage sensors and each normal human cell contains 5-30 of them. The result of their re-positioning by E4orf3 protein is to facilitate their interaction with E1B55-K/E4orf6 and ultimately their ubiquitination. E4orf3 proteins also act independently of E1B-55K to mislocalize MRN complexes and thus foil DNA repair (Stracker, Carson et al. 2002; Evans and Hearing 2005).

E4 proteins have been shown to be important for late events in the adenoviral life cycle; E4orf3 and E4orf6 affect alternate splicing of the tripartite leader mRNA, with E4orf3 favouring inclusion of the i-leader exon earlier on in infection and E4orf6 causing i-leader exon skipping in later mRNA transcripts (Nordqvist 1994). Infection with E4-deleted adenoviruses result in the intranuclear accumulation of late viral mRNAs as late viral mRNA is exported from the nucleus under the control of the E1B-55K/E4orf6 complex (Blanchette, Cheng et al. 2004). E4orf4 mutants have been

shown to exhibit defective host protein translation due to a defect in the assembly of the eIF4-E/eIF4-G translation complex (Huang and Schneider 1991; O'Shea, Johnson et al. 2004; O'Shea, Klupsch et al. 2005). In contrast, E4orf4 and E4orf1 both act to maintain the host cell protein production machinery to ensure successful viral protein production by their independent stimulation of the mTor pathway (O'Shea, Choi et al. 2005).

The late phase of an adenovirus infection begins with the onset of viral DNA replication. Almost all of the proteins produced late in infection are the products of translation of 'late mRNAs' derived from the major late transcriptional unit (MLTU); the MLTU extends rightward from the major late promoter (MLP), located at genome position 16.6 almost to the end of the genome. The nearly exclusive expression of MLTU products late in infection is the result of profound changes in patterns of both viral and host gene expression that coincide with the beginning of viral DNA replication. The adenoviral MLP is activated by a combination of early and late viral proteins and is expressed at a low level in the early stages of viral genome replication. Later in the cycle, it is markedly up-regulated, allowing efficient transcription of the entire late transcription unit from regions L1-L5. Post transcriptionally, splicing and polyadenylation site utilization in the primary transcriptional product of the MLTU changes, as do rates of transport and stability of viral RNAs. Transport and translation of most host mRNAs are concomitantly inhibited. Transcription of most of the viral early genes is gradually reduced.

The MLTU expresses a ~ 28,000 nucleotide long pre-mRNA, which is polyadenylated at 5 possible sites and generates a family of 5 mRNAs with co-terminal 3’ ends. After the selection of the polyadenylation sites, the primary transcript is spliced so that each mature mRNA receives a common set of three short 5’ leader segments termed the tripartite leader sequence (TPL). This leader is then spliced to one of several

alternative 3' splice sites generating over 20 cytoplasmic mRNAs (Figure 10). This process is subject to temporal control at the levels of transcription elongation, polyadenylation site choice and alternative 3' splice site selection (Imperiale, Akusjnarvi et al. 1995).

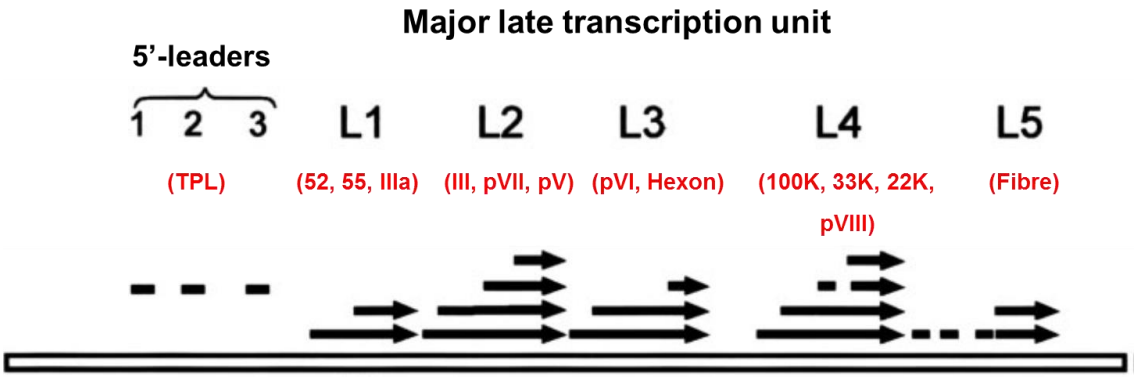

Figure 10 Schematic representation of the Major Late Transcription Unit.

Gene products are shown in red. TPL=Tripartite Leader. Adapted from (Tormanen, Backstrom et al. 2006).

It has been demonstrated that at a transient stage following initiation of DNA replication, mRNAs from both the L1 and L4 region are selectively overexpressed compared to L2, L3 and L5 mRNAs (Larsson, Svensson et al. 1992). Whilst L1 52,55K appears to have a role in viral capsid formation and possibly DNA packaging (Ostapchuk and Hearing 2005; Perez-Romero, Gustin et al. 2006), work has shown that a product of the L4 gene, protein 33K, acts as a virally-encoded alternative RNA splicing factor. L4 33K and E4orf4 act together to switch L1 gene expression from production of L1 52,55K to L1 IIIa mRNA. Initially E4orf4 protein dephosphorylates the SR proteins which repress the IIIa splice site (Kanopka, Muhlemann et al. 1996; Kanopka, Muhlemann et al. 1998). L4 33K then acts as a pyrimidine binding factor at the IIIa splice site and facilitates binding of the spliceosome to it. Using this "switch", L4 33K appears to orchestrate the upregulation of late viral gene expression post-translationally in preparation for virion capsid assembly and release (Farley, Brown et

al. 2004; Tormanen, Backstrom et al. 2006). Protein IIIa, unlike L1 52,55K, is only expressed late in viral infection and is a capsid structural protein that holds together the penton base from within (Saban, Silvestry et al. 2006). However, it is also noted to contain multiple phosphorylation sites and a number of protein kinase sites towards the C terminus (Russell and Blair 1977; Russell 2009). This suggests that protein IIIa may itself have an additional regulatory function in the control of late viral protein production.

Recently, another L4 product protein 22K has been of interest. Like the other non-structural L4 proteins, it appears to act as both an MLTU transcriptional activating and splicing factor. It has been shown to bind to protein IVa_2 and downstream elements 1 and 2 (DE1, DE2) to form the DEF A complex which stimulates activation of the MLP and hence late viral protein production. Studies with 22K mutant virus show no reduction in genome replication or viral gene expression but do result in the failure to produce infectious virus. It has been postulated that protein 22K in conjunction with protein IVa_2 is central to viral DNA encapsidation (Ostapchuk, Anderson et al. 2006). Further work using a 22K deleted mutant has suggested that this protein may also have a role as a splicing factor for late structural proteins penton (III) and V (Morris and Leppard 2009).

1.8.4. Viral Protein Translation

In order to ensure preferential translation of viral mRNA, adenovirus has developed several mechanisms to ensure the preferential production of viral proteins. These are outlined in Figure 11 below.

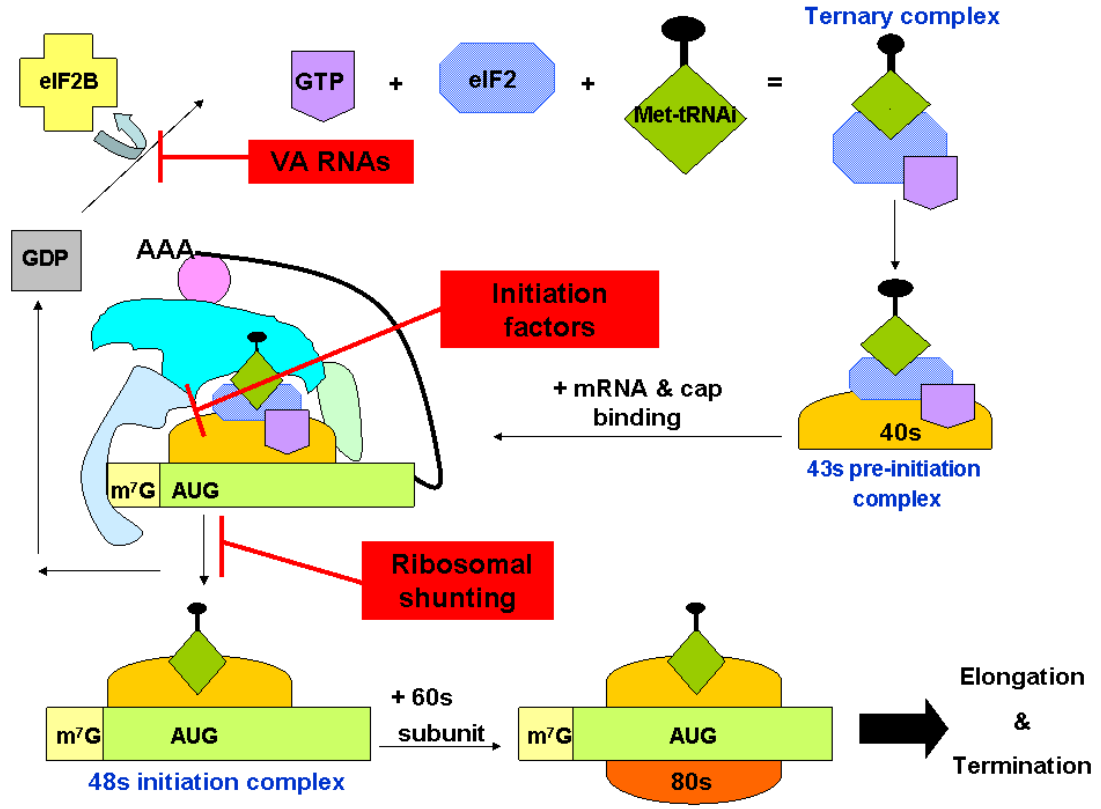

Figure 11 Schematic illustration of eukaryotic mRNA translation.

Sites of adenovirus translational regulation are shown in red. Please refer to text for details. Adapted from Gale *(*Gale, Tan et al. 2000).

Translation initiation is a complex process in which initiator tRNA (tRNAi), the 40s and 60s ribosomal subunits are assembled by eukaryotic initiation factors (eIFs) into a 80s ribosome at the initiation codon of mRNA. This comprises several stages:

i) Eukaryotic initiation factor 2 (eIF2) selects the tRNAi from the pool of tRNAs and these are bound into an eIF2/GTP/Met- tRNAi ternary complex. Other eIFs such as eIF3 are also recruited to form the 43S pre-initiation complex.

ii) The eIF4E (cap-binding) subunit of the eIF4F cap-binding complex recognizes the m^7G cap at the mRNA 5' terminus and initiates binding of the mRNA to the 43S complex.

iii) The mRNA bound ribosomal complex moves along the 5' non-translated region (5' NTR) from its initial binding site to the initiation codon to form a 48S initiation complex. In this, the mRNA initiation codon is base paired to the anti-codon of initiator tRNA

iv) Factors are displaced from the 48S complex and the 60s sub-unit joins to form the 80S ribosome. The Met-tRNAi is left positioned in the ribosomal P site at the initiation codon and mRNA translation and protein elongation can continue.

1.7.3.1. Disruption of eIF2α phosphorylation by Virus-Associated RNA-1 (VA RNA_1)

Under normal circumstances, the presence of linear double stranded RNA (dsRNA) within the host cell cytoplasm would initiate the production of cellular protein kinase R (PKR). PKR prevents phosphorylation of eukaryotic initiation factor-2 alpha subunit (eIF-2α) and thus prevents formation of the ternary complex which binds with the ribosomal 40s subunit to initiate protein translation. In this way, a global shut-down of protein synthesis is brought about as an anti-viral response. However, the adenoviral molecule VA RNA_1 prevents PKR activation and thus ensures that the host translational machinery continues to function in order to permit viral mRNA translation as illustrated in Figure 12. In this way, a phased shut-down of protein synthesis is brought about as an anti-viral response (Mathews 1980).

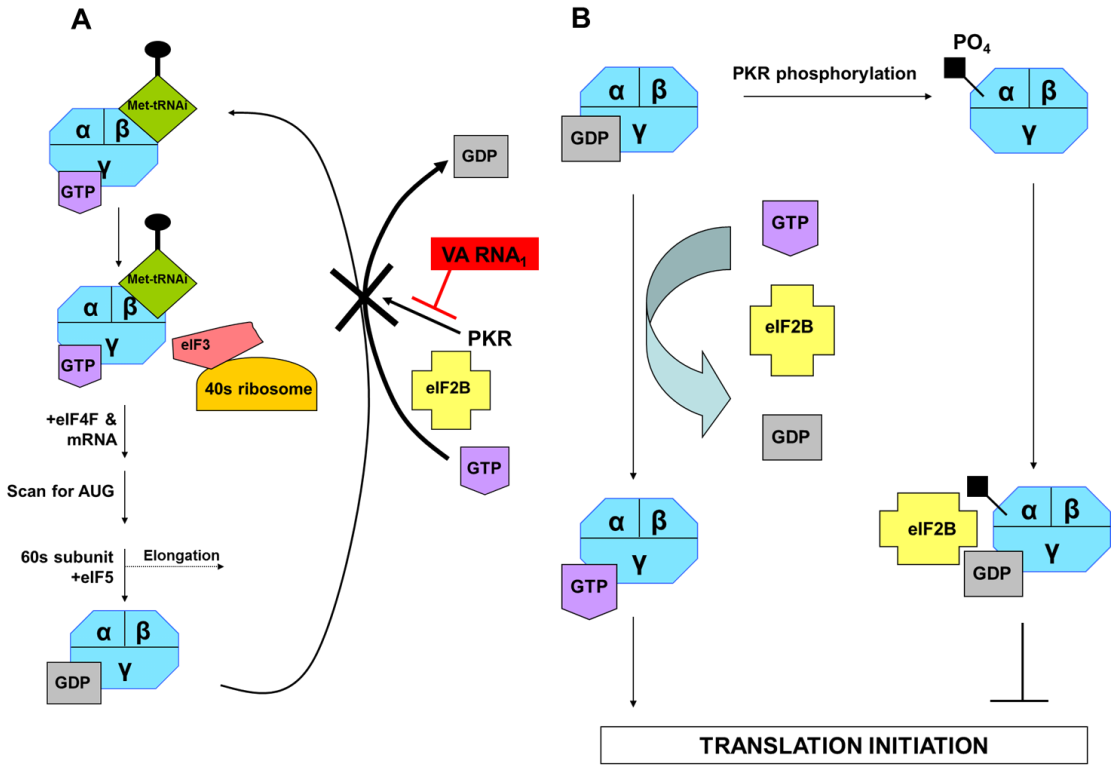

Figure 12 PKR inactivation of GDP-GTP recycling.

Translation is regulated by phosphorylation of eIF2 which is composed of α, β and γ subunits. eIF2 forms a ternary complex with GTP and the initiator RNA (tRNAi). This complex associates with the 40S ribosomal subunit bound to eIF3 and recognizes the 5' end of the mRNA through its association with eIF4F (**A**). Once the AUG codon in the mRNA has been identified during scanning, eIF5 stimulates GTP hydrolysis and the eIF2-GDP complex is released. This facilitates the joining of the 60s ribosomal subunit and translation elongation commences. The GTP bound to eIF2 is exchanged for a GDP molecule with the aid of the guanine nucleotide exchange factor eIF2B thus the eIF2 is recycled to its active form in preparation for further translation initiation.VA RNA_1 inhibits the action of PKR ensuring continued protein translation. In the presence of dsRNA, dimerisation and activation of PKR occurs (**B**). PKR phosphorylates Ser51 of the α subunit of eIF2. As a result of which eIF2B remains tightly bound to both the eIF2 and GDP molecules. This prevents GDP-GTP recycling and results in global inhibition of host cell translation unless PKR is inactivated.

1.7.3.2. Un-coupling of host cell mRNA cap binding

In the normal cells, eukaryotic initiation factor eIF4F functions as a cap-dependent RNA helicase that promotes the association of mRNA with the 40S subunit. The eIF4F complex consists of 3 initiation factors: eIF4G and eIF4E (cap binding protein associated with the N terminus of eIF4G), eIF4A (an RNA helicase) together with MAP kinase activating enzyme-1 (Mnk-1) as shown below. Mnk-1 phosphorylates eIF4E at Ser209/Thr210, which results in increased initiation of translation, the mechanism of which is not well understood.

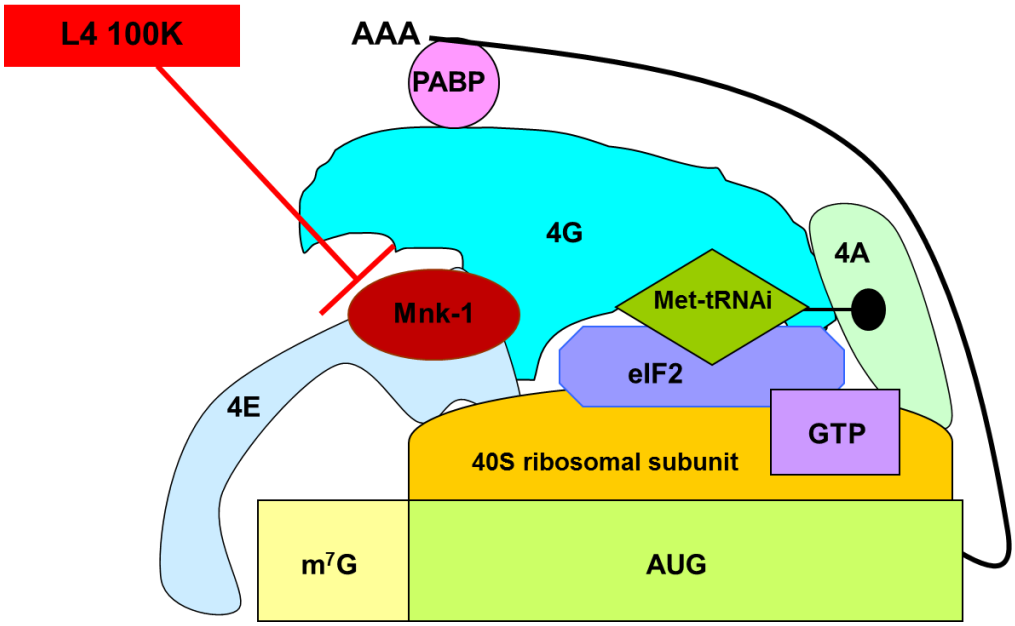

Figure 13 Inhibition of cap binding by L4 100K.

L4 100K competes with Mnk-1 for binding to the C terminus of eIF4G and interferes with the phosphorylation of eIF4E. This brings about a conformational change in the cap and prevents cap binding and host cell mRNA translation and protein synthesis. 4G, 4A and 4E represent eukaryotic translation initiation factors eIF4G, eIF4A and eIF4E. Adapted from (Cuesta, Xi et al. 2000)

1.7.3.3. Ribosomal Shunting

Ribosome shunting is a poorly understood form of initiation in which 40S ribosome subunits are loaded onto mRNA through interactions with the m^7GTP cap, but then

bypass large segments of the mRNA as directed by *cis*-acting RNA shunting elements and *trans*-acting proteins (Futterer, Kiss-Laszlo et al. 1993). Mutational and biochemical studies demonstrate that the ability of 100K protein to bind both the tripartite leader and eIF4G are critical to promote a high level of ribosome shunting. A molecular mechanism for ribosome shunting is described by which enhanced binding of eIF4G and possibly PABP with 100K protein, and simultaneous interaction with the tripartite leader 5'NCR, drive 40S ribosome recruitment and translation initiation on mRNAs (Yueh and Schneider 1996; Xi, Cuesta et al. 2004). Further work suggests that it is the complementarity of the TPL sequence to that of 18S RNA which may allow the ribosome to bypass large segments of RNA and jump to the initiation codon (Yueh and Schneider 2000). 100K protein has been shown to promote ribosomal shunting and selective translation of viral mRNAs by binding specifically to the adenovirus tripartite leader in a phosphotyrosine-dependent manner (Xi, Cuesta et al. 2005). Successful expression of the L1-L5 gene products is therefore a complicated process depending on the co-ordination of temporal and geographical factors.

1.9. Genome encapsidation, virion release and host cell death

Virion construction and viral DNA encapsidation mechanisms are poorly understood but late viral gene products are of central importance. The late genes predominantly encode structural and scaffolding proteins, and virion assembly is initiated by the formation of an empty capsid, after which a viral DNA molecule enters mediated by the *cis*-acting packaging sequence (Hearing *et al.*, 1987; Sundquist *et al.*, 1973). Structural proteins accumulate in the nucleus where they are incorporated into the virus capsid structure. Monomeric hexon proteins polymerise into trimeric capsomers, assisted by the L4 100K chaperone protein (Cepko & Sharp, 1982; Hong *et al.*, 2005). Penton-fibre capsomers are joined following their independent assembly (Horwitz *et al.*, 1969). Encapsidation of the genome is polar and is facilitated by the L1-52/55 kDa protein,

IVa_2 and pVII (Ewing *et al.*, 2007; Gustin & Imperiale, 1998; Hasson *et al.*, 1989; proteinase, which requires a fragment of a viral polypeptide and DNA as co-factors, then cleaves the last few virion constituents to generate the proteins VI, VII, VIII and the terminal proteins (Chen, Ornelles et al. 1993). This stabilises the particle and renders it infectious. The L3 proteins act to cleave the cytoskeleton further and the virus also releases the E3 11.6kd protein, known as the Adenovirus Death Protein (ADP), which is thought to promote cell lysis by an unknown mechanism (Tollefson AE 1996). Furthermore, Ad5 is able to exploit its affinity for CAR to promote efficient lateral spread. Ad5 fibre is produced in excess quantities during the viral lifecycle and it has been shown that fibre can competitively disrupt CAR:CAR homodimer formation because of a superior affinity of the knob domain for CAR (Walters *et al.*, 2002, Freimuth *et al.*, 1999; van Raaij *et al.*, 2000). Ad5 can therefore disrupt CAR mediated tight junction adhesions to facilitate infectious virion spread to neighbouring cells.

As with encapsidation and cell lysis, the mechanisms of adenovirus-mediated cell death remain poorly understood and it is unclear whether classical apoptotic pathways are activated. Historically cell lysis with virion release was thought to be the mechanism of cell cytotoxicity (Fields, Knipe et al. 2007) but investigation of replicating virus-mediated cell death suggested a much smaller role for the classical apoptotic pathway than previously thought (Abou El Hassan, van der Meulen-Muileman et al. 2004). Evaluation of oncolytic adenoviral cell death has failed to demonstrate convincing evidence of the activation of classical apoptosis (Baird, Aerts et al. 2008). As a result, other modes of cell death have been proposed including “necrosis-like programmed cell death” (Abou El Hassan, van der Meulen-Muileman et al. 2004) and autophagy (Ito, Aoki et al. 2006; Jiang, White et al. 2011). Autophagy is a cellular response to stresses such as pathogen infection and is characterised by the development of acidic vesicular organelles. *In vitro* evaluation of this process in ovarian cancer cell lines treated with adenoviral mutant *dl*922-947 suggested that

autophagy has a protective effect and contributes to cell survival rather than cell death (Baird, Aerts et al. 2008). Recent work suggests that autophagy may have a dual action, promoting cell survival initially post adenoviral infection and then orchestrating cell death in a temporal fashion, once viral replication is complete (Jiang, White et al. 2011). Jiang *et al.* have examined how oncolytic adenoviral mutant Δ-24-RGD effects cell lysis in glioma cells. Data demonstrated that a combination of autophagy and classical apoptotic pathway activation (as evidenced by increased caspase 8 levels) may combine to effect cell lysis and death. These conflict with our group's data which failed to detect apoptotic activity in ovarian cell lines but only evaluated caspase 3 activation rather than caspase 8. Latterly DNA over replication and inhibition of homologous repair (HR) mechanisms have been implicated in work published by our group investigating the relative susceptibility of cell lines to *dl*922-947-mediated death (Connell, Wheatley et al. 2008; Connell, Shibata et al. 2011). Following infection, viral DNA replication triggers DNA damage signalling pathways which then initiate cell death. However, the virus must maintain host cell protein synthesis long enough to allow successful viral replication. How this is achieved is not fully understood but it is thought to be through viral manipulation of the host cell DNA damage/ repair mechanisms. Viral proteins act to evade host cell defences by inhibiting the activity of ATM and ATR - the cellular kinases which mediate the host cell DNA damage response. E4orf3 immobilises the MRN complex thus abrogating ATR signalling (Carson, Orazio et al. 2009) and E1B55K/E4orf6 complexes act to block signalling downstream of ATM (Karen, Hoey et al. 2009). However, ultimately cell death and consequent viral progeny release are still required for maximal viral propagation. In her paper Dr. Connell suggests that increased cytotoxic activity of the oncolytic adenovirus *dl*922-947 in ovarian cancer cells results from cell cycle deregulation, accelerated cell cycle progression and abrogation of homologous repair pathways, mediated by viral inhibition of Chk-1 kinase (Connell, Shibata et al. 2011). Downregulation of Chk-1 activity results in the stabilisation of Cdc25A leading to deregulated DNA synthesis and

marked over replication with an accompanying rise in the generation of double-stranded DNA breaks (Sorensen, Syljuasen et al. 2003). She also demonstrates that Chk-1 abrogation of host cell DNA damage responses corresponds with reduced formation of DNA damage repair complexes with Rad51 resulting in decreased DNA damage repair by HR and ultimately cell death. The applicability of this mechanism to Ad5 WT virus remains unknown as the paper primarily examined the reasons for increased cytotoxic susceptibility to the adenoviral oncolytic mutant *dl*922-947. There were data in the paper to suggest that similar mechanisms maybe relevant to WT virus cytotoxicity. However, to date, the mechanisms of adenoviral cell death and viral cell lysis remain unclear.

1.10. Clinical Trials of Viral Gene Therapy in Ovarian Cancer

Published studies in ovarian cancer reflect the overall progress made in the field of gene therapy and cancer over the last 20 years. An early approach was the use of oncolysates. Malignant cells were exposed to virus *ex vivo*, which induced oncolysis. In this way, they acquired antigenicity, which was used for vaccination. Influenza viral oncolysates were observed to induce greater anti-tumour activity *in vivo* than either tumour alone or unmodified tumour cell extracts. One trial used this approach in advanced ovarian cancer. Two patients demonstrated durable responses that appeared to be enhanced following treatment with interleukin-2 (IL-2) (Ioannides, Platsoucas et al. 1990). Following the disappointing results seen with the *p53* gene replacement strategy in ovarian cancer (discussed earlier in section 1.5), a more targeted approach was clearly required. *dl*1520 (Onyx-015 or H101) was a conditionally replicating adenovirus, which appeared to target cells with non-functional p53 (Bischoff, Kirn et al. 1996). Made from human group C adenovirus (serotypes 2 and 5), it contained several deletions within the serotype 5 portion of the virus. It had been attenuated by deletion of the E1B 55K gene region, the protein product of which binds and inactivates p53 to allow continued DNA synthesis and viral replication.

Mutants lacking the E1B 55K gene were unable to replicate in normal cells (Kao, Yew et al. 1990; Yew, Kao et al. 1990). Thus, in cells with an intact p53 pathway, the deletion of the gene appeared to prevent viral replication. Theoretically, in cells whose p53 pathway was not functional, as is the case with the majority of tumour cells, *dl*1520 would continue to replicate (Sherr and McCormick 2002). In vitro studies supported this and showed that *dl*1520 was capable of efficient, selective replication and cytopathogenicity in p53-deficient human tumour cells, whilst replication was abrogated in cells containing wild-type p53 (Bischoff, Kirn et al. 1996). *In vivo* data in nude mouse-human ovarian xenograft models supported this (Heise, Hermiston et al. 2000a). Anti-tumour efficacy was demonstrated in the mice carrying p53 mutant xenografts unlike those with wild-type p53 xenografts. Some misgivings about the p53 hypothesis were expressed: *in vitro*, it emerged that p53 gene sequence alone did not predict for the efficacy of *dl*1520 (Goodrum and Ornelles 1998; Hall, Dix et al. 1998; Harada and Berk 1999). However, phase I data in head and neck cancer, another tumour type with a high rate of p53 mutations, had shown significant activity following intra-tumoural (IT) injection of *dl*1520 (Ganly, Kirn et al. 2000). *In vivo* correlation of p53 function and *dl*1520 efficacy was also seen in nude mice carrying mutant p53 xenografts of human ovarian cancer (Heise, Ganly et al. 2000b).

On the basis of these results, a phase I trial of *dl*1520 was performed (Vasey, Shulman et al. 2002). Sixteen women with recurrent ovarian cancer were given *dl*1520 IP at doses escalating from $1x10^9$ to $1x10^{11}$ plaque forming units (pfu) on days 1-5 of a 21-day cycle. The virus was well tolerated, the most common toxicities being mild “flu-like” symptoms shortly after viral administration. One patient, with high volume disease in the abdomen, experienced dose limiting abdominal pain and diarrhoea. No grade 4 toxicity was reported. Assessment of pre-treatment samples showed p53 mutations in 71% of the tumours. PCR of peritoneal washings for adenoviral E1A indicated that viral DNA could be detected up to 10 days after the final day of infusion. However, 62% of

cytology samples prepared from peritoneal washings were not assessable due to low cellularity and/or no evidence of malignancy. Of 10 remaining cytology samples, in-situ hybridization (ISH) detected adenoviral DNA in only one specimen. Five blood samples were taken from each of 8 patients within 24 hours following the first infusion of *dl*1520. Quantitative PCR for adenovirus E1A DNA in these samples were negative although antibody titres did rise acutely in all patients. There was no evidence of clinical or radiological response in any patient and median overall survival was 165 days.

The primary conclusion drawn from the study was that viral oncolytic gene therapy delivered via an IP route was safe and non-toxic for the patient. It also proved that attenuated adenovirus could be produced in large enough quantities and administrated safely via the IP route. The lack of therapeutic gain was a disappointment, but in many ways this was a seminal study for oncolytic viral gene therapy in ovarian cancer. It highlighted several important points for future work: most importantly, the difficulty of virus delivery to the tumour. The trials in head and neck cancer (Ganly, Kirn et al. 2000; Nemunaitis, Ganly et al. 2000; Nemunaitis, Khuri et al. 2001) used direct intra-tumoural injection, guaranteeing delivery of a known quantity of virus. In this study, the virus was administered in 500 ml of normal saline, which, in an abdomen distorted by adhesions and scarring, might be insufficient to allow delivery to the tumour. In addition, CAR and integrin expression on ovarian cancer cells has been demonstrated to be low which may detrimentally affect viral transduction of the malignant cells (Hemmi, Geertsen et al. 1998; Bruning, Kohler et al. 2001; You, Fischer et al. 2001). Assessment of viral uptake by the tumour was also likely to be difficult. Access to intraperitoneal tumours for biopsy can be technically difficult. Peritoneal washings provided unsatisfactory samples, possibly due to a dilutional effect or limited shedding of tumour cells. PCR of early gene products are not indicative of viral replication and, as the authors pointed out, PCR for late protein mRNA expression such as hexon

would have been preferable. Furthermore, serum antibody responses are not indicative of new virion production and thus cannot be used as surrogate markers of virion release and cell lysis. However, one of the most far-reaching outcomes of the study was its failure to show any therapeutic effect. This renewed earlier doubts about the proposed p53-mediated action of *dl*1520 and called into question not only its replicative target but also the ability to achieve selective replication in these agents as a whole. This resulted in an unprecedented surge of interest in adenoviral biology and its relevance to oncolytic viral gene therapy. Following the perceived failure of the *dl*1520 ovarian trial, much work has been undertaken to address the problems it raised. The remainder of this introduction will outline some of the advances that have been made since its publication.

1.11. Mechanisms to Improve Selectivity – Rb pathway targeting & the development of Ad5 *dl*922-947

In order to maximise therapeutic benefit, the ideal oncolytic virus needs to replicate in and destroy only tumours cells, leaving normal tissues unharmed. Re-examination of *dl*1520 in normal primary cells revealed its selectivity was dependent upon viral mRNA transport mechanisms not p53 (O'Shea, Johnson et al. 2004). The E1B-55K/E4orf6 complex regulates the nuclear export of viral mRNA allowing cytoplasmic translation of the viral proteins (DobbelsteinM., J. Roth et al. 1997). The E1B-55K deletion in *dl*1520 meant that, in order to achieve successful viral replication, the tumour cells needed to provide a complementary nuclear mRNA export mechanism. It is very possible that the tumours of those enrolled in the phase I trial lacked such an export mechanism and hence viral replication was not supported. Second-generation oncolytic adenoviruses emerged that targeted the pRb pathway such as adenovirus 5 mutants *dl*922-947 and Δ24. These viruses contain a 24 base pair deletion in E1A CR2 portion of the viral

genome, between amino acids 122 and 129.

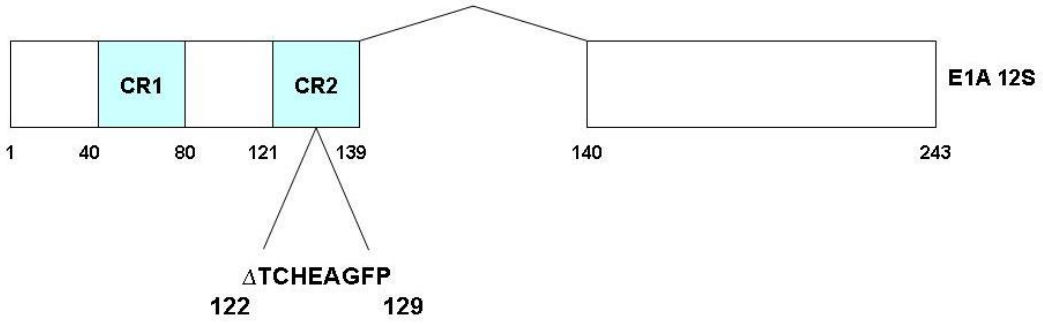

Figure 14 Diagram of deletion within the E1A CR2 region of *dl*922-947.

E1A CR2 contains an LxCxE motif that is present in a number of cellular proteins that bind to pRb with high affinity and weaken the pRb/E2F complex. Binding of E1A CR2 allows E1A CR1 to bind to pRb at a site that overlaps with E2F resulting in displacement of the latter (Helt and Galloway 2003). Deletion of this binding region renders the virus unable to replicate in cells with an intact pRb pathway. In contrast, tumour cells are permissive to viral replication because the normal G1/S transition is lost and high levels of free E2F allow uncontrolled cell division. Pre-clinical models compared *dl*922-947 to adenovirus type 5 wild-type (Ad5 WT) and a range of adenoviral mutants including *dl*1520 (Heise, Hermiston et al. 2000a). The potency of *dl*922-947 in cancer cell lines was found to be greater than that of Ad5 WT and *dl*1520. Its ability to lyse tumour cells was 2-8 times more effective than Ad5WT and 10-1000 times more effective than *dl*1520. This was attributable to the selectivity of *dl*922-947 for malignant cells as *dl*922-947 was seen to replicate 20 to 100 times less effectively than Ad5 WT in the growth-arrested normal cells with an intact Rb pathway. It remains unclear why *dl*922-947 replicates more effectively in malignant cells than wild type. *In vivo*, both intravenous (IV) and IT administration showed promising potency as *dl*922-947 exhibited a survival advantage comparable to that of Ad5 WT. Both *dl*922-947 and Ad5 WT increased median survival and complete response rates over those of *dl*1520. Mice bearing the breast cancer xenograft SC MDA-MB-231 were treated with IV *dl*922-

947. After 56 days, mice injected with *dl*922-947 showed no evidence of metastases at the time of sacrifice, compared to 57% in those treated with *dl*1520, 37% with Ad5 WT and 62% seen in vehicle control (Heise, Hermiston et al. 2000a). Work from our group has investigated *dl*922-947 activity in a range of human ovarian cell lines (Lockley, Fernandez et al. 2006). *In vitro* data showed that *dl*922-947 induced S phase more rapidly than Ad5 WT and hence more rapid viral replication as S-phase entry is a pre-requisite for effective viral genome replication. It was also shown to be able to induce S phase in G_0-arrested human ovarian cancer cells. Increased viral genome replication was demonstrated by greater production of infectious viral particles compared to Ad5 WT in one of two ovarian cell lines assessed. *dl*922-947 also exhibited a greater cytopathic effect than Ad5 WT or *dl*1520. This superiority was shown to be selective for human ovarian cells known to have an abnormal Rb pathway. *In vivo* data showed a significantly prolonged median survival for mice treated with *dl*922-947. At a 10 fold lower dose than the control virus, *dl*922-947 prolonged median survival from 26.5 to 49.5 days ($P< 0.001$). At the higher dose, the survival advantage was such that median survival was not reached and 18 mice were still alive at day 125. At post mortem, mice treated with *dl*922-947 showed the lowest tumour mass, especially those treated at a higher dose ($P< 0.001$) compared with control virus. At the time of sacrifice due to clinical deterioration, 2 mice had no evidence of any disease, which suggested that their clinical state was caused by a factor other than tumour progression. When repeated to compare *dl*922-947 and Ad5 WT, 4 of 6 mice treated with *dl*922-947 had no residual tumour at time of sacrifice due to clinical deterioration. Macroscopically *dl*922-947 and Ad5 WT treated mice had more thickening of the liver capsule compared with viral control. This was often accompanied by liver necrosis and diffuse eosinophilic degeneration. This suggested that liver toxicity may have contributed to their clinical deterioration. Mice treated with Ad5 WT and *dl*922-947 alive at the end of the experiment had grossly normal livers.

1.12. Viral Targeting

The effectiveness of any oncolytic virus depends on the ability to deliver it to the target cells efficiently. Any attempts to modify the tropism of adenovirus must retain the three functions of attachment, internalization and transfer to the nucleus. In order to improve oncolytic viral delivery and therapeutic effectiveness, several strategies have been used to optimize viral activity. These include strategies to increase both viral entry into cells and their replication therein (transductional and transcriptional targeting), strategies to minimalise virus entry into and damage of normal cells such as hepatocytes (de-targeting), modulation of the immune response to virus and constructs aimed at increasing viral cytotoxicity. An extensive review of adenoviral targeting approaches for gene therapy is beyond the remit of this thesis but is discussed in Young *et.al*. (Young and McNeish 2009).

1.13. De-targeting: adenoviral hepatotoxicity

It is important to consider potentially toxic side effects associated with the systemic delivery of high doses of viral particles. The death of Jesse Gelsinger in 1999 resulted from induction of an overwhelming innate immune response following the administration of high dose adenovirus type 5 viral gene therapy delivered directly into the hepatic artery (Raper, Yudkoff et al. 2002). Clinical trials of IV adenovirus have reported grade 2 and 3 transaminitis (Small, Carducci et al. 2006) and IT injection has also resulted in systemic viral leakage (Lohr, Huang et al. 2001; Sauthoff, Hu et al. 2003; Wang, Hu et al. 2003). Nude mice, with no previous human adenovirus exposure, have also shown apparently fatal hepatotoxicity with replicating adenovirus and hepatic necrosis is a major dose limiting toxicity (Heise, Williams et al. 1999; Johnson, Shen et al. 2002). The aetiology of this hepatic necrosis remains unclear. Adenovirus has not evolved as a blood borne pathogen and thus has not developed mechanisms to survive when delivered intravascularly. After IV delivery, it is cleared

rapidly and sequestered in the liver (Alemany, Suzuki et al. 2000; Muruve 2004). Animal studies indicate that hepatic macrophages or Kupffer cells (KCs) play a major role in the trapping of viral particles within the liver (Lieber, He et al. 1997; Wolff, Worgall et al. 1997; Tao, Gao et al. 2001; Manickan, Smith et al. 2006). Hepatic necrosis may result from direct infection of hepatocytes and subsequent cell lysis after the completion of viral replication. Alternatively, an immune-mediated response, orchestrated by the Kupffer cells, may be responsible.

1.14. Fibre-detargeting

In the absence of a clear understanding of the mechanism of adenoviral hepatotoxicity, much work in this area has focussed on the prevention of viral uptake into the KCs and hepatocytes by fibre detargeting. Although it was presumed that adenoviral uptake into cells was predominantly mediated by CAR, it was noted that adenoviral vectors mutated to lack CAR binding produced equivalent liver transduction compared to their CAR-binding counterparts following intravascular injection in rodents and non-human primates (Alemany and Curiel 2001; Smith, Idamakanti et al. 2003). This suggested a CAR-independent mechanism of hepatocyte infection *in vivo*. Deletion of the heparan sulphate proteoglycan binding site on the fibre shaft displayed reduced binding, infection and toxicity in hepatocytes and KCs (Koizumi, Kawabata et al. 2006). Further work has suggested that plasma proteins factor IX (FIX) and complement binding protein-4 (CBP-4) acted as a bridge, binding the Ad fibre knob to alternative receptors in the hepatocytes and KCs, thus bypassing CAR (Shayakhmetov, Gaggar et al. 2005). Platelets have also been implicated in KC uptake of adenovirus (Stone, Liu et al. 2007). Latterly it has been shown that Ad5 binds directly to coagulation factor X (FX) via an interaction between the hypervariable regions (HVR) of the hexon surface and the FX Gla domain (Parker, McVey et al. 2007; Waddington, Parker et al. 2007; Waddington, McVey et al. 2008). Ablation of functional levels of FX by warfarin in mice treated with intravenous adenovirus resulted in a significant reduction of transgene

expression in hepatocytes by both CAR-binding and CAR-nonbinding adenoviral vectors. This was reversed when physiological levels of FX were injected into mice previously treated with warfarin. Blocking of the interaction between Ad5 hexon and the Gla domain of FX by injection of mice with a snake venom protein X-binding protein resulted in a 150-fold reduction in hepatocyte transduction. Group D adenoviruses (including Ad48) were found to have no binding affinity for FX. A chimeric Ad5 vector bearing the HVR of Ad48 (Ad5HVR4) lacked hepatocyte tropism. Whilst attractive, pseudotyping as a tool to detarget the virus must be approached carefully. Subsequent work by this group has shown that, despite apparent lack of liver tropism for the Group D viruses, hexon in pseudotyped viruses still has the ability to bind FX and infect hepatocytes. Whilst FX is important, other blood factors also require further evaluation, especially as potential mediators of uptake into KC cells. To date no work has established the mechanism of uptake into KC cells, which has important implications for immune-mediated hepatotoxicity.

1.15. Immune-mediated hepatoxicity

Another approach to adenoviral-mediated hepatotoxicity has centered on immune reactions. The occurrence of hepatic necrosis in nude mouse xenograft models with no previous human adenoviral exposure suggests that hepatotoxicity is not antibody-mediated. Adenovirus naïve mouse models have illustrated that KC uptake of systemically-delivered adenovirus is very efficient and the half-life of Ad5 in mice in one study was less than 2 minutes (Alemany, Suzuki et al. 2000). E1-deleted adenoviruses induce pro-inflammatory cytokines (IL-6, IL-1β, TNF-α) via KCs (Lieber, He et al. 1997; Ben-Gary, McKinney et al. 2002; Miller, Lahrs et al. 2002). In the absence of viral genome replication, it appears that this immune response is triggered by the intrahepatic presence of adenovirus itself and/or inactive virions and capsid components. Work with a recombinant adenovirus encoding for human interferon β demonstrated that viral sequestration by KCs has a saturation level of approximately

$3x10^6$ viral particles. Once this biological filter effect is exceeded, a non-linear dose-response occurs in hepatocytes as evidenced by high levels of transgene expression in these cells (Tao, Gao et al. 2001). Subsequently, with replicating viruses, E1A expression within the hepatocytes is recognised as DNA damage and triggers the intrinsic, pro-apoptotic host cell responses of the innate immune system, resulting in hepatocyte death and liver necrosis (Chen, Holskin et al. 1987) (Cook, May et al. 1989). Engler *et al.* examined the complex relationship between replicating oncolytic adenoviruses, hepatotoxicity and the immune system (Engler, Machemer et al. 2004). They observed that replicating oncolytic adenoviruses demonstrate greater hepatotoxicity than their E1-deleted, non-replicating counterparts and that the relative immunocompetence of the mice used attenuated viral hepatotoxicity. Beige/Scid mice, which are deficient in B-cells and T-cells, showed **high** levels of transgene expression in hepatocytes at **lower** dose levels than more immunocompetent mice. Hepatotoxicity correlated with the expression of E1A in the liver and increases of viral DNA within hepatocytes correlated with a rapid induction of TNF-α and a concomitant rise in serum alanine transaminase (ALT). This work supports the theory of Tao *et al.* of a bimodal action of TNF-α and the immune system in mediating hepatotoxicity. An immunomodulated, “tolerable” threshold of hepatic viral infection is supported by the fact that, in severely immunocompromised mice, a lower viral dosage was required to trigger high hepatocyte transgene expression. Once exceeded, fuller activation of the innate immune system occurs (evidenced by rising TNF-α levels), which is accompanied by hepatic necrosis and raised liver transaminases. Repeated dosing did not alter pharmacokinetics, which supports an innate rather than humoral mechanism. A recent study aimed to detarget both hepatocytes and KCs. Pre-treatment with warfarin (to prevent vitamin K blood factor-dependent uptake by hepatocytes) was combined with Kupffer cell depletion (by saturation with $3x10^{10}$ viral particle dose of a non-replicating adenovirus Ad5-DsRed-RD) 4 hours before administering Ad-EGFP-RD (Shashkova, Doronin et al. 2008). Ad-EGFP-RD is a replication deficient adenovirus

that has an expression cassette in the place of E1 to express EGFP-1- a fusion protein of enhanced GFP and firefly luciferase under the control of the CMV immediate early promoter. In nude mice with subcutaneous hepatocellular carcinoma xenografts, Kupffer cell depletion resulted in a 40-fold increase in hepatocyte transgene delivery with associated transaminitis. Pre-treatment with warfarin alone or in combination with KC depletion markedly reduced liver transduction and damage. Results from this study confirmed the role of KCs as protective against viral hepatocyte infection. The possible therapeutic role for warfarin to mitigate hepatic toxicity in this setting is clearly important. However, replication incompetent adenoviruses were used and only one dose was given. Although liver detargeting with warfarin was seen in immunocompetent mice, it is important to assess the effects *active* viral replication and multiple dosing might have.

There is now no doubt that the complex relationship between viral hepatotoxicity and the damaging effects of an immune response are central to oncolytic adenoviral gene therapy toxicity. As a result research emphasis is turning towards immunomodulation of the interaction of adenoviral gene therapy agents with the host immune system.

1.16. Increasing Cytotoxicity

There is much speculation about the untapped potential of the proteins encoded by the E3 region of the viral genome. These include the adenoviral death protein (ADP), which is an 11.6Kd protein that falls between the E3A and E3B regions and is expressed at the end of the infectious cycle (Evans 2002). E3 positive and E3 negative mutants of Δ24 adenovirus have been assessed using *in vitro* and *in vivo* human cancer models (Suzuki, Alemany et al. 2002). E3 positive virus was shown to spread much more quickly and cause more rapid and potent oncolysis compared to the E3 negative strain. The advantage was attributed to the presence of ADP in the E3 positive virus although the E3 positive virus also had RGD re-targeting. ADP

overexpressing adenovirus has also demonstrated an enhanced cytopathic effect (Yun, Kim et al. 2005). Work examining this in ovarian cancer has shown that the presence of ADP does not affect either the mode or the extent of viral cytotoxicity in ovarian cancer (Baird, Aerts et al. 2008).

Combinations of oncolytic adenoviral gene therapy with conventional cytotoxic chemotherapy have also been encouraging. A combination of *dl*1520 with cisplatin given IT and IP in nude mice xenografts showed superior anti-tumoural efficacy compared with either vehicle alone and interestingly, sequencing of treatment was important. Administration of the virus *before* the chemotherapy or concurrently *with* chemotherapy significantly prolonged survival versus after chemotherapy (P=0.02). Complete responses in these groups were 33% and 20% versus none in the chemotherapy first group (Heise, Lemmon et al. 2000). More recent work combining a selectively replicating oncolytic adenovirus with gemcitabine and epirubicin given IP also demonstrated increased survival in a nude mouse xenograft model of human ovarian cancer. Combination treatments were shown to significantly increase survival over each agent alone. Multiple doses made no difference to survival over a single injection and dose de-escalation was feasible without compromising treatment efficacy (Raki, Sarkioja et al. 2008).

1.17. Immunocompetent models

The data presented above illustrates the vital need for assessment of adenoviral gene therapy within the context of an immunocompetent host. The risks of adenoviral hepatotoxicity cannot be truly evaluated in nude mouse xenograft models lacking an intact host immune response. As already mentioned, relative immunocompetence attenuates viral hepatotoxicity in murine models (Engler, Machemer et al. 2004). It is important to recall that *dl*922-947 has partial deletion of the E3 region and therefore does not encode for RID-α, RID-β or the 14.7K protein (Table 5). These regions are

important for attenuation of the virus interaction with apoptotic receptors TNFR-1, TRAIL and Fas-Ligand and the cytokine responses initiated by TNF-α and NFκB pathways. However, work undertaken on murine tumours in immunocompetent murine models using both E3 intact and E3 deleted oncolytic agents suggests that an intact immune system could improve the therapeutic efficacy of viral agents such as *dl*922-947 (Hallden, Hill et al. 2003; Wang, Hallden et al. 2003). Such data serve to emphasise the importance of evaluation of *dl*922-947 as an anti-cancer agent within the context of an immunocompetent model.

The absence of relevant animal models in oncolytic viral gene therapy generally, and ovarian cancer specifically, has served to complicate the situation further. Unfortunately, female mice do not develop spontaneous ovarian tumours and thus work to date has used human carcinoma xenografts in nude mice. In addition, human adenovirus is highly species specific and infection of murine cells results in reduced viral replication and anti-tumour efficacy when compared to human counterparts (Blair, Dixon et al. 1989; Ganly, Mautner et al. 2000; Hallden, Hill et al. 2003). Porcine and canine cell lines have been shown to support adenoviral replication but the cost of larger animal models is likely to be prohibitive (Hemminki, Kanerva et al. 2003; Jogler, Hoffmann et al. 2006). Recently, permissiveness to adenoviral replication and effective viral progeny production has been demonstrated in Syrian hamster and cotton rat models (Toth, Spencer et al. 2005; Thomas, Spencer et al. 2006; Steel, Morrison et al. 2007; Toth, Spencer et al. 2007; Ying, Toth et al. 2009). This work has been undertaken using replication competent oncolytic Ad5 vectors but unlike *dl*922-947, the viruses used have not been engineered to replicate selectively in malignant cells. In the Syrian hamster model, the adenovirus used (VRX-007/ INGN007) is identical to Ad5 and does contain similar deletions in the E3 region but of note it is designed to overexpress the E3 11.6K adenoviral death protein (ADP) which is important for cell death and virion release (Tollefson AE 1996). Whilst attractive as possible models,

relatively little animal modelling has been done using Syrian hamsters and cotton rats to date and we have no experience of their use in a transgenic setting.

1.18. Murine adenovirus (MAV-1)

In view of the species specificity of adenovirus, where possible we have evaluated the cells lines using both human adenovirus and murine adenovirus type-1 (MAV-1). MAV-1 was first isolated in 1960 when it was recognised as a natural pathogen of suckling mice (Hartley and Rowe 1960). It has been shown to cause disease in certain strains of adult in-bred and out-bred mice but its clinical course is different from human adenovirus. Rather than being limited to the respiratory tract, it shows a preference for the central nervous system and can result in a wide range of clinical phenotypes, from an asymptomatic subclinical viraemia to florid and lethal haemorrhagic pan encephalitis (Kring, King et al. 1995) (Guida, Fejer et al. 1995). This difference was originally ascribed to the fact that MAV-1 did not exhibit tropism for CAR receptors (Lenaerts, Daelemans et al. 2006). However, like its human counterpart, MAV-1 has now been shown to use integrin and heparan sulphate as receptors for cell entry (Raman, Hsu et al. 2009). Despite this similar tropism, MAV-1 exhibits less hepatic uptake than Ad5 WT when delivered intravenously in SCID mice (Lenaerts, McVey et al. 2009).

The MAV-1 genome is 30,946 nucleotides long and thus is smaller than its human counterparts, such as Ad5 (35,935) (Meissner, Hirsch et al. 1997). Analysis of dinucleotide frequency, genome organisation, open reading frame preservation and amino acid identity of structural proteins suggest that MAV-1 is more closely related to human adenoviruses than to any animal adenoviruses for which complete sequence data are available. Mapping has shown that in the early gene regions E1-E4 nucleotide differences do affect restriction sites (Ball, Beard et al. 1989; Beard, Ball et al. 1990; Kring, Ball et al. 1992). MAV-1 sequences equivalent to those of E2B, L1 and L2 in human Ad2/5 demonstrate that VA RNA coding regions are absent and ORF for

proteins V and IIIa are truncated. Overall, genes encoding for late viral proteins exhibit a 50-70% similarity to their human counterparts (Meissner, Hirsch et al. 1997) (Cauthen and Spindler 1996). A notable exception to this is the region of the MAV-1 genome that is positionally equivalent to the L4 100K ribosomal recognition sequence. Here the similarity of sequence is minimal (Cauthen and Spindler 1996). Functional assays of the MAV-1 MLP have also commented on the longer leader regions of MAV-1 late mRNAs, ascribing the failure of predicted MAV-1 5' PCR oligonucleotide probes for late mRNAs to this disparity (Song and Young 1997). Functional assays have also highlighted transcriptional differences between MAV-1 and human adenovirus. In the MAV-1 MLP, there is an apparent lack of initiator element (INR) around the transcription start site, the USF binding site is replaced by a potential Sp-1 binding site and the second downstream element DE2 is absent. The functional sequelae of these differences remain subject to conjecture, but it is hypothesised that they may contribute to the weaker promoter action seen in MAV-1 renilla luciferase reporter gene assays and contribute to the virus' slower growth, reduced cytotoxicity and low viral yields when compared to its human counterpart (Song and Young 1997).

1.19. Study rationale

Work discussed in this chapter has shown that a plethora of research into viral biology, molecular genetics and gene therapy have resulted in the development of viruses designed to replicated selectively within cancer cells that are armed with transgenes which enhance cytotoxicity and maximise cancer cell death but minimise toxicity to normal cells. Despite multiple phase I trials of these agents, very few compounds have progressed to Phase II or III clinical trials. The reasons for this are multiple. Certainly there has been nervousness within the medical profession about the use of viruses in this setting. Much of this dates back to early work when a gene replacement strategy using an adenoviral vector demonstrated little therapeutic effect but, disastrously, one patient died as a result of a cytokine storm triggered by the viral vector (Raper, Yudkoff

et al. 2002). This event called into question the overall safety of gene therapy using viral vectors and led researchers to try and minimise any risk of adverse side effects. Work in the intervening 10 years has shown clinical tolerability and safety of viral vectors and latterly conditionally replicating oncolytic viruses. However, despite numerous early clinical trials, we remain in doubt as to their true clinical effect either as a monotherapy or in combination with chemotherapy and/or radiation. There is no doubt that the field of oncolytic viral therapy has suffered from a lack of immunocompetent animal models which has contributed to the disappointing clinical trial data. Animal modelling would allow better examination of repeated dosing and increasing viral dose concentrations, immunological responses, post mortem analysis of virus biodistribution and evaluation of the presence of replicating virus within tumour cells and other tissues. Current animal models are often inadequate because they lack an immune system or are not susceptible to the virus in question. Viruses such as vaccinia and reovirus are the exception in that they will replicate in animal models but trial data shows that a “one-size-fits-all” approach will not suffice and that different tumour groups will require different viruses. Therefore, if we are to take this complex technology forward we must devise strategies to overcome viral species selectivity and allow evaluation of conditionally replicating oncolytic viral constructs within immunocompetent animal models. We acknowledge that animal models are not perfect and may not reflect viral behaviour in humans, but for safety reasons and in order to encourage investor confidence in this technology we must make every effort to improve the animal modelling for virotherapy. As a forward step in this process, the aim of this project is to try to create an immunocompetent mouse model of ovarian cancer in order to evaluate the complex interaction of oncolytic adenoviral agents with an intact host immune system in an orthoptic model of the disease. As such I have set out firstly to identify the obstacle(s) to *dl*922-947 replication in murine cells. Attempts have then been made to devise a strategy to overcome this/these that can be incorporated into either an oncolytic viral or transgenic mouse construct.

2. Materials & Methods

2.1. Viruses & Cancer Cell Lines

2.1.1. Cancer Cell Lines

OVCAR4 cells were obtained from Dr. R. Camalier, National Cancer Institute, Frederick, MD, USA. IGROV1, CMT-93, CMT-64 cells were obtained from the Cancer Research UK Central Cell Service (Clare Hall, Herts, UK). MOSEC cells were obtained from Dr Katherine Roby (University of Kansas Medical Center, Kansas City, KS USA). MOVCAR7 and MOVCAR 12 were obtained from Dr. Denise Connolly (Fox Chase Cancer Center, Philadelphia, PA, USA). All cell lines except MOSEC, MOVCAR7 and MOVCAR12, were maintained in DMEM plus 10% heat inactivated foetal calf serum (FCS). MOSEC, MOVCAR7 and MOVCAR12 were maintained in DMEM plus 4% FCS together with 1% supplemental insulin, transferrin and selenium (Invitrogen, UK)

2.1.2. Viruses

Human Adenovirus 5 *dl*922-947 was provided by Dr. D Kirn (Kirn Oncolytic Consulting, Mill Valley, USA) and is deleted in the region encoding amino acids 122-129 of the E1A CR2 domain as well as in E3B (Heise, Hermiston et al. 2000a). Ad CMV GFP was kindly provided by V. Stoll (Cancer Research UK, Charterhouse Square, London UK) and is deleted in the E1 and E3 regions and has green fluorescent protein (GFP) in the E1 position under the control of the cytomegalovirus (CMV) immediate early promoter. Ad Control is an E1 deleted Ad5 vector that lacks any transgene in the E1 region. It does not contain an E1 deletion (McNeish, Tenev et al. 2001). MAV-1 was kindly provided by Dr K. Spindler (University of Michigan, Ann Arbor. MI, USA).

2.1.3. Other Cell Lines

JH293 and NIH 3T3 cells were obtained from the Cancer Research UK Central Cell Service (Clare Hall, Herts, UK). HEK 293 cells were obtained from the America Type Culture Collection (ATCC Reference CRL-1573). All three cell lines were maintained in DMEM plus 10% FCS.

2.2. *In vitro* evaluation of human and murine carcinoma cell line panel for permissiveness to infection with Ad5 type 5

$5x10^5$ cells were plated onto 6cm plates. 24 hours later, they were infected with Ad CMV GFP at a multiplicity of infection (MOI) of 5 and 50 plaque forming units (PFU) per cell. Uninfected cells were used as a negative control. 24 hours post infection (pi), cells were trypsinised, washed once in phosphate buffered saline (PBS) and re-suspended in 500µl PBS. Samples were processed in a FACS Caliber (Beckton Dickinson, CA, USA) and analysed using CellQuest Software (Beckton Dickinson, CA, USA). Infectivity was determined after 10,000 total events were recorded. The percentage of GFP positive cells was determined from the total event count. All experiments were carried out in triplicate.

2.3. Evaluation of viral cytotoxicity using MTT assay

Cell survival following viral infection was estimated using MTT (3-2,5-diphenyltetrazolium bromide) assay. When MTT (Sigma Chemical Co., Poole, Dorset, UK) is in solution, its tetrazolium ring can be cleaved to form an insoluble purple formazan crystal by dehydrogenase enzymes such as those found in the mitochondria of living cells (Mosmann 1983). This converted formazan dye can be solubilised with DMSO (dimethyl sulfoxide: Fisher Scientific UK Ltd. Leics, UK) and the absorbance of the purple solution measured on plate reader gives an estimate of cell survival. Cells were plated into 24 well plates (10^4 cells/well) and infected in triplicate 24 hours later

with either *dl*922-947 or MAV-1 (MOI 0.01 – 1000 pfu/cell). MTT assays were performed up to 144 hours pi (*dl*922-947) or 192 hours pi (MAV-1). At the appropriate time point, 100 µl of a 5 mg/ml solution of MTT in PBS was added to each well. After 3 hours incubation at 37 ºC, the medium was discarded and the crystals dissolved in 1ml of DMSO per well. The absorbance was measured at 560nm with a Perkin Elmer Victor^3 spectrophotometer (Beaconsfield, UK) and analysed using Wallac® Oy software (Turku, Finland). The inhibitory concentration required for a 50% reduction in cell survival (IC_{50}) was calculated using GraphPad Prism version 5 (GraphPad Software, San Diego, California, USA).

2.4. Infectious virion quantification ($TCID_{50}$ Assay) – Evaluation of viral replication

Infectious virions were quantified by the limiting dilution titration assay ($TCID_{50}$, tissue culture inhibitory dose 50%). 10^5 cells were seeded onto 6 well plates and 24 hours later were infected with *dl*922-947 (MOI 10 pfu/cell). Cells were harvested at 24, 48 and 72 hours pi. Medium was removed, cells washed twice with cold PBS and scraped into 500µl ice cold 10mM Tris pH 8.0 and then freeze-thawed three times (liquid nitrogen/ 37ºC). At the time of assay, $1x10^4$ JH293 cells in 200µl of medium were seeded into each well of a 96 well plate. Plates were prepared in triplicate for each cell line and each time point assessed. 24 hours after plating the cells, 22µl of the diluted lysates from the virally-infected cells was added to the second row of each plate. Serial 1:10 dilutions were then made by the transfer of 22µl from one row to the next. The top row of each plate was left uninfected. The JH293 cells were scored for cytopathic effect (CPE) 11 days pi. The observed number of wells displaying CPE at each dilution were counted and the $TCID_{50}$ calculated with an established formula (O'Reilly D 1994):

$TCID_{50} = 10^{1-d(s-0.5)}$

where d= Log10 of the dilution at which CPE is first seen and S = the ratio of the number of wells per row with CPE: number without CPE

This gives a value for 22 µl virus and is divided by 0.022 to give the $TCID_{50}$/ml. $TCID_{50}$ overestimates the viral titre by 0.7 log compared to plaque assay, so the $TCID_{50}$/ml is converted to pfu/ml using the following formula:

$PFU/ml = 10^{n-0.7}$

where n = log $TCID_{50}$/ml

The titration is only valid if the lowest dilution gives greater than 50% CPE, the highest dilution gives less than 50% CPE and the negative controls show none.

2.5. Adenovirus DNA transcription in infected cells – DNA harvest

5×10^5 cells were seeded on 6cm plates and infected 24 hours later with *dl*922-947 (MOI 10). Mock-infected cells were used as controls. Up to 72 hours pi, cells were scraped into 500µl ice-cold 0.1M Tris pH 8.0 and subjected to 3 rounds of freeze/thaw as above. DNA was extracted using a Qiagen, QIAamp DNA blood minikit (Crawley, West Sussex, UK), and the concentration measured with a NanoDrop©, ND 1000 spectrophotometer (Wilmington, DE, USA). DNA samples were stored at -80ºC.

2.6. Quantitative PCR of viral DNA

A standard curve for genomic DNA was created from a sample of *dl*922-947 DNA according to the instructions provided by Applied Biosystems (Cheshire, UK). To summarise:-

The mass per haploid genome

$$m = n \times 1.096 \times 10^{-21}$$

Where m = mass of haploid DNA

n = genome size in base pairs

The concentration of genomic DNA needed to achieve the copy number of interest was calculated as follows:

$$\text{Concentration required } (C_2) = \frac{\text{copy number of interest x mass of haploid DNA}}{\text{volume to be used per sample}}$$

From the initial measured DNA concentration (C_1) and the required DNA concentration (C_2) and assuming a final volume (V_2) of 100 µl, the volume of stock required to obtain the highest concentration of DNA for the standard curve was calculated according to the following formula:

$$C_1 \times V_1 = C_2 \times V_2$$

Serial dilutions of this stock were prepared by 1:10 dilutions in nuclease free water (Ambion, Cambridgeshire, UK). Primers and probes were purchased from Applied Biosystems (Cheshire, UK) and Sigma–Aldrich (Poole, Dorset, UK). Primers and probes are listed in Table 6 below.

	Manufacturer	5' Primer Sequence	3' Sequence	Probe Dye	Probe sequence
E1A	Applied Biosystems Cheshire UK	CCACCTACCCTT CACGAACTG	GCCTCCTCGTTG GGATCTTC	VIC	ATGATTTAGACG TGACGGCC
E1A	Sigma-Aldrich Poole, Dorset, UK	CCACCTACCCTT CACGAACTG	GCGTCCTCGTTG GGATCTTC	HEX	ATGATTTAGACG TGACGCCC
Hexon	Applied Biosystems Cheshire UK	AGCGCGCGAATA AACTGCT	AGGAGACCACTG CCATGTTGT	6-FAM	CCGCCGCTCCGT CCTGCA
L4 100K	Applied Biosystems Cheshire UK	TGGAGTGTGTCA CTGTCGGCTGC	CTGCGAATTGCA AACCAGG	6-FAM	ACCTATGCACCC CGCACCGCT
L4 33K	Applied Biosystems Cheshire UK	TGCCTGTATCAC AAAAGCGAA	CTGAAGAGAGCC TCCGCGT	HEX	AGCTTCGGCGCA CGCTGGAA
L4 22K	Applied Biosystems Cheshire UK	AGAGCAACAACA GCGCCAA	CAACTATGGCGT TCTTGTGCC	HEX	CCGCTCATGG CGC
Fibre	Applied Biosystems Cheshire UK	AATGGCATGCTT GCGCTC	GGTAAGGTTGCC GGCCTC	HEX	ATGGGCAACGGC CTCTCTCTGGA

Table 6 q-PCR Probes & Primers

Inter-sample pipetting errors were minimised by quantifying E1A and hexon simultaneously in each sample. 2µl (100ng) template (DNA standard or DNA sample) and non-template control (NTC) were mixed with 2X reaction buffer (TaqMan Universal PCR Master Mix, Applied Biosystems, Cheshire, UK) and 10µM each of forward primers, reverse primers and probes for both E1A and hexon. Samples for standard curve, NTC and DNA were plated in triplicate in a 96 well plate (Applied Biosystems, Cheshire, UK). The plate was then covered with an optical adhesive lid and samples were briefly centrifuged to remove air bubbles. The qPCR reaction was carried out on a 7500 Real Time System (Applied Biosystems, Cheshire, UK) using the following programme:-

50 ^{o}C for 2 minutes

95^{o}C for 10 minutes followed by:

95^{o}C for 15 seconds

60^{o}C for 60 seconds for 40 cycles

Light emission from the fluorophore was analysed using 7500 System SDS Software (Applied Biosystems, Cheshire, UK). This is quantified as the cycle threshold (C_T), or the number of PCR cycles needed for the emission to reach a predetermined level. The software then constructs a curve for the DNA standards in which C_T is plotted against log DNA copy number. A slope of -3.3 indicates 100% PCR efficiency, in which there is a 10 fold increase in PCR product every three cycles. Slopes within the range -3.1 to- -3.6, representing PCR efficiency of greater than 90%, were deemed acceptable. From this standard curve the software quantifies a DNA copy number for each sample.

2.7. Analysis of gene transcription

2.7.1. RNA Harvest

5 x 10^5 cells were seeded in 6 cm plates. 24 hours later, cells were infected with *dl*922-947 (MOI 10 pfu/cell) and one plate per cell line was mock infected. Up to 48 hours later, cells were trypsinised, washed twice in cold PBS and resuspended in 1ml TRIzol® (Invitrogen, Paisley, UK) and lysed by pipetting up and down. All samples were incubated for 5 minutes at room temperature. 0.2ml chloroform was added to each sample per ml of TRIzol® used. Tubes were shaken vigorously by hand for 15 seconds and then incubated again at room temperature for 3 further minutes. Samples were then centrifuged at 12,000xg for 10 minutes at 4 ºC. The colourless aqueous upper phase, containing the RNA, was transferred to a fresh tube. 500µl of isopropanol per 1ml TRIzol® used was added and incubated at room temperature for 10 minutes.

Samples were then centrifuged for 10 minutes at 12,000xg at 4 ºC. The supernatant was discarded. 1ml 75% ethanol was added to each sample and vortexed briefly. Samples were centrifuged for 5 minutes at 7,000xg, 4°C. The RNA pellets were left briefly to air-dry before being redissolved in 30 µl of RNAse free water. Samples were then incubated for 10 minutes at 55-60°C.

2.7.2. Reverse Transcription and Quantitative PCR analysis of cDNA

RNA was converted to complementary 1st strand DNA (cDNA) by reverse transcription and subsequently assessed by quantitative PCR. 1µg of RNA was made up to 20µl with the following components of a 1st strand cDNA synthesis kit for RT- PCR (Roche, Welwyn Garden City, UK): 10x reaction buffer, 5mM magnesium chloride, 1mM deoxynucleotide mix, 3.2µg random primer, 50 units of RNase inhibitor, 20 units of reverse transcriptase and RNase-free water. Reverse transcription conditions were as follows: 25°C for 10 minutes, 42°C for 60 minutes, 99°C for 5 minutes and 4°C for at least 5 minutes. cDNA was stored at -20°C until required. Q-PCR was undertaken using the 7500 Real Time System and software (Applied Biosystems, Cheshire, UK) as described in section 2.7.2 above. In the case of cDNA, the corresponding RNA samples initially also underwent q-PCR in order to ensure their purity by demonstrating C_T values comparable to those seen in the non-template control wells.

2.8. Nuclear/Cytoplasmic Subcellular Fractionation of RNA

5 x10^5 cells were plated onto 6 cm plates. 24 hours later they were infected with *dl*922-947 (MOI 10), harvested 48 hours later and fractionated into nuclear and cytoplasmic compartments using a Protein And RNA Isolation System (PARIS™ [Ambion, Cambridgeshire, UK]). RNA was extracted from nuclear and cytoplasmic compartments, cleaned and DNase treated as before. cDNA was generated as per

section 2.7.2 and analysed for the presence of viral transcripts by q-PCR. Purity of nuclear and cytoplasmic fractions was evaluated by western blotting for lamin and β-tubulin, as described in section 2.11.

2.9. L4 Alternate Splicing Analysis

5 x 10^5 OVCAR4, CMT64 and MOSEC cells were seeded onto a 6cm plates and infected 24 hours later with *dl*922-947 (MOI 10). RNA was extracted up to 72 hours later and reverse transcribed using random hexanucleotide primers. Samples then underwent PCR amplification using the communal TPL sequence (5'-forward) and a sequence in the L4 transcript communal to the L4 products 100K, 22K and 33K (3' – reverse) see below 2.16.1. The PCR cycle was as described in section 2.6 above.

2.10. DNA Analysis by Gel Electrophoresis

Samples were electrophoresed on a 0.8-1% (w/v) agarose gel [1-2g agarose in 1X Tris-Borate- EDTA (TBE) buffer with 5µl ethidium bromide (EtBr) at 0.5µg/ml] for 30-60 mins @ 80-100mV. Samples were run alongside a 1kb DNA ladder (Invitrogen™). Bands were visualised under UV light.

2.11. Viral Protein Evaluation by Western Blot

2.11.1. Whole Cell Extract Preparation

Cells were washed twice with ice-cold PBS and scraped into 300 µl lysis buffer (150mM NaCl, 50mM tris Base, 0.05% SDS and 1% Triton X 100) and lysed for 10 minutes on ice. They were then sonicated for 10-15 seconds and centrifuged at 4 ^oC for 5 minutes at 8,000 rpm. The supernatant was retained and stored at -20 ^oC.

2.11.2. Protein Concentration Calculation

The protein concentration of cell lysates were established using the Dc protein assay (Bio-Rad, CA, USA). Bovine serum albumin (BSA) acted as positive protein standards control. Reagent A' was prepared by adding 20 µl of Bio-Rad reagent S to 1ml of Bio-Rad reagent A. 5µl sample or protein standards were added to 96 well plates in duplicate. To each well, 25 µl A' mix and 200µl Bio-Rad reagent S were added. The plate was incubated at room temperature for 15-30 minutes and then the absorbance was measured at 630nm on a Perkin Elmer Victor^3 spectrophotometer (Beaconsfield, UK) and analysed using Wallac® Oy software (Turku, Finland).

2.11.3. SDS Polyacrylamide Gel Electrophoresis (SDS PAGE)

Resolving gels were poured as shown in table 6 below. Once set, a stacking gel was poured on top. 25µg/lane protein lysates were mixed with 10µl/lane of loading buffer (50mM Tris, 4% SDS, 10% Glycerol, 5% Mercaptoethanol and 0.01% Bromophenol Blue) made up to a total volume of 20µl/lane with dH_2O. Samples were boiled at 100 ^oC for 5 minutes and were then transferred to ice and centrifuged briefly before loading into the gels.

Gels were electrophoresed at 110V for 90-120 minutes (Hoeffer SE-245 western blot system, Fisher Scientific UK Ltd, Leics, UK) in 1x running buffer diluted from a 10x stock (30.2g Tris Base, 94g Glycine, 100ml SDS in 1 litre). Molecular weight rainbow markers (Amersham Biosciences, Bucks, UK) were loaded alongside the protein samples to allow size comparison of bands. Proteins were transferred onto nitrocellulose membranes (Amersham Biosciences, Bucks, UK) using a semi-dry transfer system (Trans-Blot, Bio-Rad, CA, USA) at 20V for 45-60 minutes in the presence of transfer buffer (39mM Glycine, 48mM Tris Base, 20% Methanol). All membranes except those to be probed with anti-Flag antibody were blocked with a 4%

solution of non-fat milk in a solution of 0.1% Tween (Sigma Chemical, Poole, Dorset, UK) in PBS (0.1% PBS/Tween) for at least 1 hour at room temperature.

Reagent	**8%**	**10%**	**12%**	**Stacking Gel**
Water	4.6 ml	4.0ml	3.3 ml	3.4ml
30% Proto-Gel (Kimberley Research Hull UK)	2.7 ml	3.3ml	4.0 ml	0.83ml
1.5M Tris (pH 8.8) (Cancer Research UK, Clare Hall, UK)	2.5 ml	2.5ml	2.5 ml	
1M Tris (pH 6.8) (Cancer Research UK, Clare Hall, UK)	-	-	-	0.63ml
10% SDS (Bio-Rad, CA, USA)	0.1 ml	0.1ml	0.1 ml	0.05ml
10% Ammonium persulphate (Sigma Chemicals Co., Poole, Dorset, UK)	0.1 ml	0.1ml	0.1 ml	0.05ml
TEMED (N,N,N',N' – Tetramethylethylenediamine) (Sigma Chemicals Co., Poole, Dorset, UK)	0.006ml	0.004ml	0.004ml	0.005ml

Table 7 SDS-Page gel reagents

Primary antibody was diluted in 1.5% BSA (Sigma Chemical, Poole, Dorset, UK) in 0.1% PBS/Tween and incubated with membrane overnight at 4 ^{o}C with the exception of phosphor antibodies which were diluted in 5% BSA in 0.1% TBS/Tween. Primary antibody was removed by 3 sequential washes in 0.1% PBS/Tween for 5, 10 and 15 minutes. Secondary horseradish peroxidise-conjugated antibody was diluted in 1.5% BSA in 0.1% PBS/ Tween and incubated with the membrane for 1 hour at room temperature. The three wash steps were repeated to remove the secondary antibody. Details of the antibodies used are listed below in Table 7.

Antibody	Primary/ Secondary	Species	Conditions	Supplier
E1A	primary	Mouse	1:1000 4ºC overnight	Oncogene Research Products, CA, USA
Human Ad5 structural proteins	primary	Goat	1:2000 4ºC overnight	Abcam, Cambridge, UK
Human adenovirus L4 100K	primary	Rabbit	1:100 4ºC overnight	Dr W Russell, St Andrews University, Scotland, UK
ANTI-FLAG M2	primary	Mouse	1:800 4ºC overnight	Sigma-Aldrich, Poole, Dorset, UK
Alpha tubulin	primary	Rabbit	1:800 4ºC overnight	Abcam, Cambridge, UK
Beta Tubulin	primary	Mouse	1:1000 4ºC overnight	Sigma-Aldrich, Poole, Dorset, UK
p21	primary	Mouse	1:300 4ºC overnight	Santa Cruz Biotechnology, CA, USA
PCNA	primary	Mouse	1:1000 4ºC overnight	Santa Cruz Biotechnology, CA, USA
Beta actin	primary	Mouse	1:1000 4ºC overnight	Santa Cruz Biotechnology, CA, USA
Ku70	primary	Goat	1:1000 4ºC overnight	Santa Cruz Biotechnology, CA, USA
eIF2-alpha/ Phospho-eIF2-alpha [Ser ^{51}]	primary	Rabbit	1:1000 4ºC overnight	Cell Signaling, Beverly, MA, USA
eIF4E/ phospho-eIF4E [Ser ^{209}]	primary	Rabbit	1:1000 4ºC overnight	Cell Signaling, Beverly, MA, USA
Lamin A/C	primary	Mouse	1:1000 4ºC overnight	Santa Cruz Biotechnology, CA, USA
Anti- mouse HRP	secondary	Rabbit	1:1000 1 hour room Tº	Dakocytomation, Denmark
Anti-goat HRP	secondary	Rabbit	1:1000 1 hour room Tº	Dakocytomation, Denmark
Anti-rabbit HRP	secondary	Goat	1:1000 1 hour room Tº	Dakocytomation, Denmark

Table 8 Western blot primary & secondary antibodies

Antibody binding was detected by enhanced chemiluminescence (ECL Plus detection reagent, Amersham Biosciences, Bucks, UK) according to the manufacturer's instructions. Visualisation of signal was achieved with Amersham Hyperfilm® (GE Healthcare, Buckinghamshire, UK). Protein intensity was quantified either directly from nitrocellulose membranes using a Typhoon 8160 Phosphorimager and ImageQuant®

TL 1D gel analysis software (GE Healthcare, Buckinghamshire, UK), or from Hyperfilm, using ImageJ software (v1.40g, NIH, MD, USA).

2.11.4. Anti-Flag Antibody Protocol

M2 monoclonal antibody to Flag was obtained from Sigma Chemicals (Poole, Dorset, UK) and antibody was utilised as follows: After protein transfer to a nitrocellulose membrane, the blot was washed in Milli-Q® water for 2-3 minutes with mild agitation. It was then blocked in TBS with 3% non-fat milk (50mM Tris, 0.138M NaCl, 2.7mM KCL, pH8.0 containing 30mg/ml non-fat dry milk) for 30 minutes at room temperature with agitation at 50-60 rpm. After removal of the blocking agent, the membrane was washed once with TBS (50mM Tris, 0.138M NaCl, 2.7mM KCL, pH8.0). Anti-Flag M2 antibody was diluted 1:800 in TBS with 3% milk. The membrane was incubated in the anti-Flag M2 antibody overnight at 4^{o}C. The next day, it was washed once with TBS for 5 minutes. Rabbit anti-mouse HRP was diluted 1:1000 in TBS with 3% milk and the membrane was incubated in this with agitation at room temperature for 1 hour. The membrane was then washed eight times for a total of 20 minutes in TBS/Tween (50mM Tris, 0.138M NaCl, 2.7mM KCL, pH8.0, 0.05% Tween). The chemiluminescent detection of horseradish peroxidise-conjugated secondary antibodies was performed by ECL Plus detection reagent (Amersham Biosciences, Bucks, UK) according to the manufacturer's instructions. Visualisation of signal was achieved with Amersham Hyperfilm® (GE Healthcare, Buckinghamshire, UK).

2.12. Virus Preparation

2.12.1. Human adenovirus production

293 cells were grown in DMEM supplemented with 10% FCS in thirty 15cm plates. Viral seed stock was added once cells were 80% confluent. Once full cytopathic effect was seen (approximately 48-72 hours later), cells were harvested and centrifuged at

5000 rpm for 10 minutes after which the supernatant was discarded and the pellet resuspended in 2ml of ice-cold 0.1M Tris pH 8.0 per 15cm plate. After three cycles of freeze/thaw (liquid nitrogen/37ºC), the virus suspension was centrifuged for 10 minutes at 6000 rpm prior to separation on caesium chloride (CsCl) gradients. The CsCl gradient was prepared by placing 11.4ml of a 1.25g/ml CsCl solution into a 25 x 98mm ultraclear centrifuge tube (Beckman Coulter Ltd, Bucks, UK) and carefully underlaying 7.6ml of a 1.4g/ml CsCl solution. The virus solution was then layered onto the gradient and centrifuged at 25,000 rpm for 2 hours at 15 ºC using a Beckman SW28 swing out rotor in an Optima LE-80K ultracentrifuge (Beckman Coulter Ltd, Bucks, UK).

After the centrifugation, 3 bands were visible: an upper band of cellular debris, a central band of empty virus particles and a lower band of packaged, viable adenoviral particles. The ultracentrifuge tube was placed in a clamp and pierced using a sterile 19-gauge needle attached to a 10ml syringe. The band of adenoviral particles was aspirated and layered onto 3ml of a 1.35g/ml CsCl solution in a 31 x 51mm ultraclear centrifuge tube (Beckman Coulter Ltd, Bucks, U.K). The tubes were centrifuged at 40,000 rpm for 15 hours at 15 ºC using a Beckman SW55 swing out rotor in an Optima LE-80K ultracentrifuge (Beckman Coulter Ltd, Bucks, UK). Again the virus band was removed using sterile 19-gauge needle attached to a 10ml syringe as above and was made up to a total volume of 5ml with TSG (90ml Solution A [150M NaCl, 1mM Na_2HPO_4, 5mM KCL, 30mM Tris Base], 450 µl Solution B [200mM $MgCl_2$, 180mM $CaCl_2$ and 38.5ml Glycerol]. This was then injected into a 3-12ml Slide-a-Lyzer cassette (molecular weight cut-off 3500Da [Pierce Biotechnology Inc., IL, USA]). This cassette was then placed in the float provided and placed in a 5 litre beaker containing 2 litres of dialysis solution (10mM Tris pH 7.4, 1mM $MgCl_2$, 150mM NaCl, 10 Glycerol in distilled water). The beaker was then placed on a magnetic stirrer in a cold room and the virus left to dialyse for 24 hours. Following dialysis, the virus was removed using a

syringe, aliquoted and stored at -80ºC. Viral particle counts was estimated using OD_{260} (see section 2.12.3) and titre measured by $TCID_{50}$ assay (section 2.4).

2.12.2. MAV-1 Preparation

In view of the much lower yields seen with MAV-1 production *in vitro*, production of this virus was slightly different. Firstly stock virus was produced in bulk. 4 X T175 flasks were seeded with NIH3T3 cells, which were grown in DMEM supplemented with 10% FCS. When these were 80% confluent they were infected with stock MAV-1. When full CPE was evident in the T175 flasks (72-96 hours post infection) the cells and media were harvested, subjected to three rounds of freeze/thaw and centrifuged at 5000 rpm for 10 minutes. The supernatant was added to two 10-layer HYPERflasks® (Corning Life Sciences, MA, USA) already seeded with 3T3 cells. The HYPERflasks® were topped up with DMEM supplemented with 10% FCS. When full CPE was evident in the hyperflasks (approximately 96 hours post infection) this viral stock was harvested and centrifuged at 5000 rpm for 10 minutes after which the supernatant was discarded and the pellet re-suspended in 20ml/hyperflask of ice-cold 0.1M Tris pH 8.0. After this step, virus production proceeded as outlined in section 2.12.1 above. As the particle count of MAV-1 is too low to quantify by OD_{260}, viral titre was calculated only using the $TCID_{50}$ assay as outlined in section 2.4 above.

2.12.3. Viral Particle Count

Viral lysis buffer (0.1% SDS, 10mM tris pH7.4, 1 mM EDTA) was used for the particle count. 100µl of virus stock was added to 100µl lysis buffer in duplicate and incubated for 10 minutes at 55 ºC. 300µl dH_2O was added. Absorbance at 260nm was measured using a spectrophotometer. A mixture of 200µl of lysis buffer and 300µl of distilled water was used to measure background absorbance.

The number of viral particles was calculated using the following formula:

$$\text{Particles/ml} = \frac{OD_{260} \times \text{dilution factor (in this case 5)}}{9.09 \times 10^{-13}}$$

The co-efficient factor was calculated from measurements of virion total protein and OD_{260} (assuming a molecular mass of Ad5 DNA of 2.3×10^7 D and also that 87% of the dry weight of Ad5 is protein (Mittereder, March et al. 1996).

2.13. Proteasome Inhibition

10^5 cells were seeded onto 6cm plates and 24 hours later were infected with *dl*922-947 (MOI 10). 24 hours pi, medium was aspirated and the proteasome inhibitor MG132 (Sigma-Aldrich, Poole, Dorset, UK) was added in 5ml of medium at concentrations of 10µM and 1µM. 24 hours later (48 hours post infection with *dl*922-947) cells were harvested for western blotting (see section 2.11.1). Membranes were probed for E1A and Ad5 structural proteins (see Table 8 above). Membranes were also probed for p21 expression as positive control for proteasome inhibition.

2.14. Rapid Coomassie Blue Staining

5×10^5 cells were seeded in 6 well plates. After 24 hours, they were infected with *dl*922-947 (MOI 10). Protein was harvested for western blot up to 72h post-infection (see section 2.11.1 above). Protein concentrations were calculated (section 2.11.2 above) and 20 µg run on an 8% SDS-PAGE gel (section 2.11.3 above). The gel was covered with isopropanol fix (250ml isopropanol, 100ml acetic acid, 650ml purified water) and placed on a rocker at room temperature for 30-60 minutes. Rapid Coomassie blue solution was prepared (10% acetic acid, 0.006% Coomassie Brilliant Blue R-250 [Bio-Rad, CA, USA]). The isopropanol fix was discarded and the gel covered with the Rapid Coomassie blue stain and left overnight at room temperature with mild agitation. The staining solution was then discarded and the gel was covered

with a 10% acetic acid solution and left for 2 hours at room temperature on the shaker to allow de-staining.

2.15. Cloning

2.15.1. Plasmid Amplification and purification

Plasmids pCMV 22K Flag, pCMV 33K Flag, pCMV 100K Flag and pCMV 22/33K Flag were kindly donated by Dr Keith Leppard (Dept. of Biological Sciences, University of Warwick, UK). Their construction has been described previously (Farley, Brown et al. 2004; Morris and Leppard 2009). Each was made into a working stock of 1µg DNA in 20µl of 10mM Tris. 2µl working stock added to chemically competent TOP10 *E. Coli* (Invitrogen) and mixed gently. The samples were placed back on ice for 5 minutes to allow adsorption to take place. The cells were heat shocked (42 ºC for 45 seconds). They were then placed back on ice for 10 minutes. 250 µl of pre-warmed SOC medium was then added. The reactions were then incubated at 37 ºC for 1 hour with vigorous shaking. 50µl aliquots of the transformed bacteria were spread onto pre-prepared agar plates containing kanamycin 25µg/ml. These were placed in an incubator at 37 ºC overnight. The following day, two colonies per plasmid were picked and transferred to sterile flasks containing 200ml of LB plus 25µg/ml kanamycin. Flasks were covered and incubated overnight at 37 ºC with agitation at 200-250 rpm. The next day the samples were transferred to sterile centrifuge tubes (Beckman Coulter Ltd, Bucks, UK) and centrifuged at 6000 rpm for 15 minutes at 4 ºC.

Plasmid DNA was purified using the QIagen Maxi Prep® kit (QIAgen Crawley, West Sussex, UK). DNA extraction using this kit exploits the unique property of plasmid DNA that it is able to anneal rapidly following denaturation. Cells are suspended in EDTA, which chelates divalent metals and thus destabilises the cell membrane. Alkaline lysis using sodium hydroxide (NaOH) and SDS breaks the cells open. SDS is a detergent that permeabilises the cell membrane. NaOH loosens the cell walls leading to the

release of the plasmid DNA and the sheared cellular DNA. Cellular DNA is denatured and becomes linearised and the strands are separated. Plasmid DNA is circular and is topologically constrained. Addition of potassium acetate allows circular plasmid DNA to renature. Sheared cellular DNA remains denatured as single-stranded DNA (ssDNA). The ssDNA is then precipitated out in a high salt solution. SDS forms insoluble KDS with the potassium and thus the SDS and debris contained therein are easily separated from the plasmid DNA which remains in the supernatant. Alcohol precipitation is then used to form a DNA pellet. After precipitation with isopropanol the plasmid DNA underwent further DNA purification. The DNA pellet was re-dissolved in 0.1 volume of 3M sodium acetate. One volume of phenol/chloroform was added and mixed. The sample was spun at 3500 rpm for 10 minutes on a benchtop centrifuge. The supernatant was put in a fresh sterile tube and 1 volume of chloroform added. The sample was centrifuged again at 3500 rpm for a further 5 minutes. The supernatant was removed and placed in a fresh Sorvall® tube (GMI Inc., Minnesota, MI, USA) and 2-3 volumes of ice-cold 100% ethanol were added. The samples were incubated at -20 ºC for 30 minutes. They were then spun in the centrifuge for 20 minutes at 13,000 rpm. The pellet was re-dissolved in 200µl 10 mM Tris pH 8.0 and concentration measured using a Nanodrop spectrophotometer.

2.15.2. Plasmid Transfection

Transfections were carried out using FuGene® 6 transfection reagent (Roche, Welwyn Garden City, UK). 5 x 10^5 cells were seeded in 6 well plates with 2 ml of the appropriate medium. 24 hours later, 2µg plasmid DNA was prepared for transfection as per the manufacturer's protocol as detailed in table Table 9. A FuGene® 6: DNA plasmid ratio of 3:1 was utilised.

FuGene® 6 was added to an appropriate volume of pre-warmed serum-free medium. This mixture was vortexed briefly and left to incubate for 5 minutes. The volume required for 2µg of plasmid DNA was added to this mixture, vortexed briefly and left to incubate for 15 minutes. The transfection mixture was then added to the 6cm plate. Samples were harvested for western blotting 48 hours post transfection and membranes were probed for anti-Flag M2 antibodies (Sigma-Aldrich, Poole, Dorset, UK) as per the protocol in section 2.11.4 above.

Reagent volume	Plasmids			
	pCMV 22K Flag	pCMV 33K Flag	pCMV 100K Flag	pCMV22/33K Flag
Serum Free Medium (µl)	193.1	189.7	192.93	192.4
FuGene® 6 (µl)	6	6	6	6
Plasmid DNA [volume req'd for 2µg DNA] (µl)	0.95	4.3	1.1	1.6
Total volume (µl)	200	200	200	200

Table 9 Plasmid transfection reagents

2.16. Luciferase reporter assays: Overview

The aim of the luciferase reporter assays was to assess the relative contribution of the Major Late Promoter and Tripartite Leader Sequence to overall expression late viral genes. pGL4.11 Reporter constructs were generated in which expression of Firefly luciferase lay under the transcriptional control of either hAd5 or MAV-1 MLP, with either hAd5 or MAV-1 TPL sequence controlling translation. Thus, reporter construct generated in separate steps as outlined below in Figure 15.

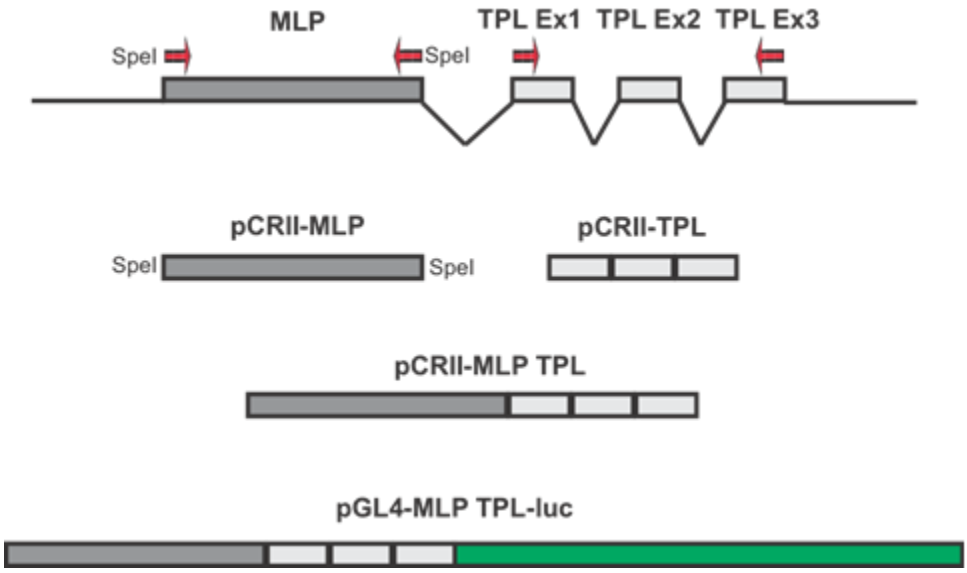

Figure 15 Schematic outline of cloning strategy for luciferase reporter gene constructs. Major late promoter sequences were amplified by PCR directly from whole adenovirus (*dl*922-947 and MAV-1). TPL was amplified from cDNA derived from RNA extracted from OVCAR4 cells infected with *dl*922-947 and MOVCAR7 cells infected with MAV-1. Both pairs of MPL and TPL sequences were ligated into pCRII Blunt TOPO. MLP constructs were ligated as SpeI fragments into pCRII TPL to create pCRII MLP TPL. The entire MLP TPL cassette was then ligated into pGL4.11 as either KpnI/XhoI or KpnI/EcoRV fragments.

Vector plasmid pCRII-Blunt-Topo® was supplied by Invitrogen (Paisley, Scotland, UK). The firefly luciferase reporter plasmid pGL4.11[luc2p] and the renilla expressing transfection control plasmid pRL-TK were obtained from Promega Corporation (WI, USA). Four pGL4-MLP TPL-luciferase reporter constructs were generated, called pGL4 AA luc, pGL4 AM luc, pGL4 MA luc and pGL5 MM luc, where the A = hAd5 and M = MAV-1. Thus, AA = hAd5 MLP and hAd5 TPL and AM = hAd5 MLP and MAV-1 TPL.

2.16.1. PCR Primer Design

Primers were designed using Primer Express™ software using sequences from the NCBI GenBank database for human adenovirus C serotype 5 (AC_000008) and Murine adenovirus type 1 (AC_000019), apart from the MAV-1 TLP primers, which

were designed using nucleotide sequences obtained from Dr K. Spindler, Michigan, USA, which were the result of work done by J. Boeke and C. Coombes of Johns Hopkins, Baltimore, MD, USA using MAV-1 RNA and rapid amplification of cDNA ends (RACE) technology.

PCR Primer	Forward primer (5' – 3')	Reverse primer (5' – 3')
Ad5 TPL Sense	ACTCTCTTCCGCATCGCTG	CTTGCGACTGTGTGACTGGTTAGACGCC
MAV-1 TPL	GTGATAGTTCGGCGGAATCTGCG	CTGTAAATTCGCAAAACTGG
Ad5 MLP SpeI	GAGACAAAGGCTCGCGTCCAGG	ACTAGTGAGGACGAACGCCCCCAC
MAV-1 MLP SpeI	TGAAGACCTCGGTCACTTTCG	ACTAGTGAGGACGAACGCCCCCAC

Table 10 Primers used for MLP and TPL cloning. Underlined sequence corresponds to an inserted SpeI restriction site.

2.16.2. PCR Amplification of TPL Sequences of *dl*922-947 and MAV-1

Tripartite leader sequence from *dl*922-947 and MAV-1 was amplified from cDNA extracted from OVCAR4 and MOVCAR7 cells infected with *dl*922-947 and MAV-1 respectively at MOI 10 for 48h. 1µg of RNA was reverse transcribed as per protocol described in section 2.7.2.

2.16.3. PCR Amplification of MLP Sequences of *dl*922-947 and MAV-1

MLP sequences were expanded directly from virus using PCR and Phusion™ DNA polymerase (New England BioLabs). For *dl*922-947, 10^6 and 10^5 particles were used as template. For MAV-1, 10, 1 and 0.1 µl of a viral stock (4.18 pfu/ml) was used. Reactions utilised Phusion™ DNA polymerase (New England BioLabs) and were performed in a PTC-200 Peltier Thermal Cycler (ML Research).

2.16.4. Insertion of PCR Fragments into pCR Blunt II-Topo

The PCR products obtained were ligated into the plasmid pCR® Blunt II-TOPO® (Invitrogen, CA, USA) as per manufacturer's instructions. Thereafter, 1 µl ligation product was transformed into OneShot® TOP10 Chemically Competent E.coli (See section 2.15.1). 50 µl from each transformation were spread onto prewarmed kanamycin selective plates and were incubated overnight at 37 ºC. Colonies were picked from overnight selective medium plates, inoculated into 2-3 ml of antibiotic selective LB broth, and were incubated in a shaking 37°C incubator overnight. Bacterial cultures were harvested by centrifugation at 13,000rpm and plasmid DNA purified using QIAprep® Spin Miniprep Kit 250 (Qiagen®). Correct insertion of PCR products was confirmed by restriction enzyme digestion.

2.16.5. Sequencing and Analysis using Bioedit Software

pCRII minipreps containing ligation products of the correct size and orientation were sequenced at the Genome Centre (William Harvey Institute, Barts and The London School of Medicine). Reactions were set up in 12µl volumes and sequencing PCR carried out on a Peltier Thermal Cycler DNA Engine PTC-225 (MJ Research) using BigDye® Terminator v3.1 Cycle Sequencing reaction reagent (Applied Biosystems) in 1X sequencing buffer (Applied Biosystems), with 10pmol primer and ~ 400ng template DNA. Each clone was sequenced with a minimum of two different primers to generate overlapping readings. The cycling reaction was: denaturation at 96°C for 30sec followed by 25 cycles of 30s denaturing at 96°C, 15s annealing at 50°C followed by 1 min elongation at 60°C for a final time of ~1.5hours. The PCR products were cleaned up, the plate was sealed and PCR products sequenced on an ABI Prism 3700 DNA Analyzer by capillary electrophoresis (performed by staff at the Genome Centre). Chromatograms were analysed using Bioedit software, and 100% identity confirmed by BLAST analysis comparing against plasmid sequences created and stored in the

VectorNTI database by the licence holder (VectorNTI Advance 10, Invitrogen). One miniprep per construct containing the correct insert in the correct orientation was amplified and DNA extracted as per section 2.15.1.

2.16.6. DNA Analysis and Manipulation

2.16.6.1. DNA Gel Extraction & De-phosphorylation

Digested fragments, or PCR bands required for further cloning and ligation steps underwent gel purification. 5 µg of digested DNA was loaded onto a 0.8% agarose gel and run at 20mv over 13 hours. Bands were then excised from the gel under UV light using a sterile blade and DNA purified using QIAquick® Gel Extraction Kit 50 (Qiagen®). Vector backbones underwent de-phosphorylation using Antarctic Phosphatase (New England Biolabs® Inc.) and reactions were performed as recommended by the manufacturer.

2.16.6.2. DNA Ligation

The molarities of the linearised backbone and desired insertion were calculated according to molecular weight. A molar ratio of 1:1 was used for all ligations. Roche Rapid DNA Ligation Kit® was utlilised according to manufacturers' specification. Briefly, reactions were set up in 20µl volumes using 1µl T4 DNA Ligase, 2 µl T4 Ligase buffer. Control consisted unmodified backbone with no insert. Standard ligation reactions were incubated overnight at 16°C in a PTC-200 Peltier Thermal Cycler (MJ Research), prior to transformation into competent E.coli bacteria as outlined in section 2.15.1 above.

Digest of all constructs was performed to confirm insertion of the genes of interest. All 4 constructs underwent digest with SpeI to confirm presence of MLP. Directional digest of the pCRII AA and AM constructs with KpnI/ XhoI was performed following

transformation to ensure correct presence of MLP/TPL insert. Directional digest of the pCRII MA and MM constructs was performed using KpnI and EcoRV.

2.16.7. Firefly Luciferase Assay

2.16.7.1. Construction of pGL4.11 Firefly Luciferase Expressing Constructs

5 µg pGL4.11 luc was digested with KpnI/XhoI (for the AA and AM MLP-TPL constructs) and KpnI/ EcoRV (for the MA and MM constructs) and underwent dephosphorylation as per the protocol described in materials and methods section 2.16.6.1, and gel purified. The MLP-TPL inserts were ligated into linearised pGL4-luc at a backbone:insert molar ratio of 1:3. Ligations were transformed into TOP10 electrocompetent *E.coli*. After overnight growth under ampicillin selection, minipreps were grown. One clone per ligation, proven to contain the appropriate construct, was amplified as described in section 2.15.1.

2.16.7.2. Luciferase Assay

Firefly and Renilla luciferase expression were measured contemporaneously using the Dual Luciferase® Reporter Assay (Promega Corporation , USA). 5 x 10^5 OVCAR4 cells and 2 x 10^5 CMT64 and MOVCAR7 cells were plated onto a 6 well plate. 24 hours later each well was transfected with 2µg of one firefly luciferase reporter gene construct and the control renilla luciferase vector pRL-TK (Promega Corporation, USA) using Fugene 6 at a transfection ratio of 3:1. One well was mock transfected. The other control well was transfected with the promoterless parental pGL4.11 vector together with pRL-TK.

Cells were harvested 48 hours post transfection. Briefly, growth medium was aspirated. Cells were washed gently with 1ml of phosphate buffered saline (PBS). 500 µl of 1 x passive lysis buffer (PLB) was added to each well and the plate placed on a rocking

platform shaking gently for 15 minutes to ensure even coverage of the cell monolayer. Luciferase Assay Reagent II substrate was resuspended in Luciferase Assay Buffer II to prepare LAR II. 1 x Stop and Glo® Substrate was prepared by dilution of 50x solution in 50 volumes Stop and Glo® Buffer as per manufacturers' guidelines. 20 µl of cell lysate was loaded in triplicate into a 96-well opaque plate in order to prevent cross-contamination between samples. 5 non-template control samples were used to calculate a reading for background luminescence that was subsequently subtracted from sample readings.

Dual Luciferase® Reporter Assay was undertaken using a Perkin Elmer Victor^3 spectrophotometer (Beaconsfield, UK). The luminometer was programmed to dispense 100 µl of each luciferase reagent to each sample. A 2s pre-measurement delay followed by a 10s measurement period was programmed for each reporter assay. The ratio of mean firefly:renilla luciferase expression was calculated for each cell line and plotted using GraphPad Prism 5® software, normalised to luminescence ratio from cells transfected with parental pGL4.11 vector and pRL-TK alone.

2.17. Construction of Ad100K: Overview

L4 100K sequence was amplified from the pCMV100K plasmid kindly donated by Dr. Keith Leppard of the Univeristy of Warwick, using PCR primers designed using Primer Express software and with the addition of a Sal I restriction site at both the 5' and 3' ends. These were incorporated into pCRII Blunt TOPO vector as per the manufacturer's instructions and were then subsequently transformed into TOP10 chemically competent E. Coli. Cells were incubated overnight on antibiotic selective agar plates. Plasmid DNA from bacterial colonies was extracted using the QIAprep® Spin Miniprep Kit. Presence of the 100K fragment in the plasmid was confirmed by Sal

I restriction enzyme digest and agarose gel analysis. Constructs confirmed by gel analysis were amplified by QIAprep® Maxiprep Kit.

The pAdEasy system was used to construct the non-replicating virus. L4 100K DNA was digested out of the pCRII100K using the Sal I restriction enzyme and underwent gel purification. pShuttle CMV was linearised using Sal I, and the L4 100K DNA ligated into this using Roche Rapid DNA Ligation Kit® to form pShuttle CMV100K . Successful ligation was confirmed by with Sal I digest. pShuttle CMV 100K was linearised using Pme I and DNA extracted using the phenol/chloroform method. pAdEasy1 and pShuttleCMV100K DNA were then simultaneously transformed into electrocompetent BJ5183 cells using the electroporation method. Cells were plated onto antibiotic selective agar and smaller colonies screened for recombinant plasmid DNA on a cracking gel. Colonies of appropriate clones were incubated overnight and DNA extracted using the QIAprep® Spin Miniprep Kit. To prevent further recombination, recombinant miniprep DNA was transformed into Top10 E. coli and a single colony amplified to yield the recombinant construct pAd100K. Virus production was then undertaken as described in Material and Methods section 2.12 to generate a working stock of Ad100K virus.

2.18. Construction of Ad CMV 100K

2.18.1. PCR Amplification of L4 100K Sequence and ligation into pCRII TOPO

Initially, I attempted to digest out the 100K sequence from the pCMV100K FLAG provide by Professor Keith Leppard (Dept. Biochemistry, University of Warwick, UK). Unfortunately, I was unable to identify appropriate restriction sites that would permit ligation into the adenovirus shuttle vector pShuttle CMV. Therefore PCR primers were designed using Primer Express Software®. The Flag tag sequence was omitted from

the construct and instead a Sal I restriction site sequence inserted in order to facilitate subsequent ligation into pCMV Shuttle.

The primers used were as follows:

L4 100K Sal I forward: 5'-gtcgacatggagtcagtcgagaagaaggacagcc

L4 100K Sal I reverse: 5'-gtcgacctacggttgggtcggcgaacgggc

Underlined sequence corresponds to the Sal I restriction enzyme site

PCR reactions were set up in 50µl volumes containing 10 ng and 100 ng of pCMV 100K plasmid DNA, primers (sense and anti-sense) using the primer at a concentration of 1.0µM and the proof-reading taq polymerase enzyme pfx50™ (Invitrogen, USA). PCR was performed in a PTC-200 Peltier Thermal Cycler (MJ Research) under the following conditions; denaturation at 95°C for 5mins followed by 35 cycles of 40 seconds denaturing at 95°C, 1 minute annealing at 60°C and 1.5mins elongation at 72°C, followed by a final extension step at 72°C for 9 mins. Samples were then run on a 0.8% agarose gel to ascertain PCR product size.

1 µl PCR product was mixed with pCRII Blunt-TOPO according to the manufacturer's instructions. After adsorption at room temperature for 5 minutes the reaction was placed on ice. The cloning reaction complete, 5µl ligation reaction was transformed into TOP10 chemically competent E.coli as previously described using the heat shock method. After incubation overnight on LB plates containing 50 µg/ml kanamycin, only one colony was identified. Plasmid DNA was extracted using the QIAprep® Spin Miniprep Kit as described previously. Presence of the 100K fragment in the plasmid was confirmed by Sal I restriction enzyme digest and agarose gel analysis. Constructs confirmed by gel analysis were amplified by QIAprep® Maxiprep Kit.

2.18.2. Construction of pShuttle CMV 100K

The pAdEasy system was used to construct Ad CMV 100K according to manufacturer's protocol. 10 µg pCRII L4 100K was digested with Sal I and the 100K fragment was gel purified as described in section 2.16.6.1. pShuttle CMV was also linearised using Sal I, dephosphorylated and gel purified as previously described. Ligation of pShuttleCMV and the Sal I digested L4 100K fragment was executed using Roche Rapid DNA Ligation Kit® to form pShuttle CMV 100K. Successful ligation was confirmed by SalI digestion.

2.18.3. Generation of Recombinant Adenovirus pAd100K

10 µg of pShuttle CMV 100K was linearised with Pme I, purified by phenol/chloroform extraction as described in section 2.15.1. 200ng of pAdEasy-1 and 100ng of linearised pShuttle CMV100K were made up to a final volume of 10µl with distilled water. BJ5183 electrocompetent cells (Stratagene, UK) were defrosted on ice and 30µl added to the plasmid mix. All 40µl was placed in a cuvette and electroporated using a BioRad GenePulser® II (1.8kV, 200Ω, 25µF). After recovery on ice for 5 minutes, bacteria were resuscitated in 250µl SOC (Invitrogen™) medium [0.5% (w/v) Yeast extract, 2.0%(w/v) tryptone, 10mM NaCl, 2.5mM KCl, 10mM $MgCl_2$, 20mM $MgSO_4$ and 20mM glucose]. Samples were place in a mixing incubator at 37°C with aeration for 30 minutes. 100µl of this suspension was plated onto prewarmed kanamycin selective agar plates and were incubated upside-down overnight at 37°C. The following day the smaller colonies were picked and screened by cracking gel.

2.18.4. Cracking Gel

Colonies growing on the kanamycin plates were picked and inoculated in 2-3 ml of LB + kanamycin, and incubated in a shaking 37°C incubator overnight. 1ml of overnight bacterial cultures was transferred to a sterile eppendorf tube. The sample was spun at

13,000rpm for 1 minute and the supernatant was discarded. The sample was spun again for a further 15 seconds and further supernatant removed by pipetting. 40µl of double distilled H_2O was added to the remaining pellet and left for 5 minutes to allow absorption. The eppendorf tube was vortexed until the bacterial pellet dissolved. 40µl of phenol/chloroform was added to the pellet and vortexed for 10 seconds. The sample was then spun at 13,000 rpm for 2 minutes. 30µl of the top aqueous phase containing the dissolved DNA was removed and placed in a fresh sterile eppendorf tube. 6µl of RNase loading dye was added and the sample left for 5 minutes to allow RNA digestion. 10µl of the digested sample was loaded onto a 0.8% agarose gel together with empty plasmid vectors pCMVshuttle and pAdEasy as control to screen for colonies which may contain the recombined plasmid DNA.

Colonies which were likely to contain recombinant plasmid DNA were identified using a cracking gel. These were then amplified overnight and DNA extracted using the QIAprep® Spin Miniprep Kit. In the final step, 2 x 25µl water at a temperature of 55ºC was use to elute the DNA after being left on the column for 1 minute prior to centrifugation.

To prevent further recombination, recombinant miniprep DNA was transformed into TOP10 E.coli, and a single colony amplified to yield the final adenovirus plasmid pAd CMV 100K.

2.18.5. Initial viral production

24 hours before transfection 293 cells were plated onto 6cm plates. Confluency at the time of transfection was 60-80%. 10 µg recombined pAd CMV 100K was linearised overnight with PacI, purified by phenol/chlorform extraction and dissolved in 20µl dH_2O. Linearised pAd CMV 100K DNA was transfected into 293 cells using Effectene®

Transfection reagents (QIAgen®, Crawley, West Sussex, UK) according to manufacturer's instructions. Briefly, DNA was made up to a volume of 150µl using DNA condensation buffer EC. 8µl of enhancer was added and the mixture vortexed for 1 second. The sample was then incubated at room temperature to 2-5 minutes and centrifuged at 5,000 rpm for 5 seconds. 25 µl of Effectene® transfection reagent was added to the DNA-Enhancer mix. After pipetting up and down 5 times, the sample was incubated at room temperature for a further 10 minutes to allow transfection-complex formation. 293 cells were washed in warm PBS and re-fed with 4ml medium. 1ml medium was added to transfection complexes and mixed. The transfection complex mixture was immediately added dropwise to the 293 cells.

7-10 days post transfection, cells were scraped into 500 µl 0.1M Tris pH 8.0, and subjected to three rounds of freeze/thawing (liquid nitrogen/37^{o}C). After centrifugation, 100 µl supernatant was added to subconfluent 293 cells growing on 6 cm plates. Once cytopathic effect (CPE) was evident (usually 4 – 6 days), cells were again scraped in 500 µl 0.1M Tris pH 8.0 and subjected to three rounds of freeze/thawing. 250 µl supernatant was added to subconfluent 293 cells growing on a 15 plate. At full CPE, cells were dislodged by pipetting and the cell suspension (approximately 25 ml – the viral seed stock) was subjected to three rounds of freeze/thawing and added to 80% confluent 293 cells growing on a 10-layer Hyperflask. Purification of virus is described further in section 2.12.

2.19. *In vivo* experiments

All experiments were performed under suitable Home Office Personal and Project licence authority. Experiments were devised and analysed by Iain McNeish. The efficacy experiment was performed at Cancer Research UK Biological Services Unit (London Research Institute Clare Hall laboratories). All other experiments were

undertaken at Biological Services Unit, Barts and the London School of Medicine, Charterhouse Square.

2.19.1. Efficacy of *dl*922-947 in murine carcinoma models

5 x 10^6 CMT64 cells were injected IP in 4-6 week old female C57Bl/6 mice in 200 µl PBS (day 1). On days 4-8 inclusive, *dl*922-947 was injected IP (5 x 10^9 particles in 400 µl 20% icodextrin per day). Mice were monitored daily and killed when they reached Home Office limits according to UKCCCR guidelines (Workman, Balmain et al. 1988).

2.19.2. Expression of human adenovirus proteins in intraperitoneal human and murine ovarian tumours

5 x 10^6 IGROV1, MOSEC or CMT64 cells were injected IP into 6 week old female ICRF nu/nu mice. Once intraperitoneal tumours were evident (approximately day 30 for IGROV1, day 65 for MOSEC and day 24 for CMT64), mice received a single intraperitoneal injection of *dl*922-947 (1 x 10^{10} particles in 400 µl 20% icodextrin). 24 hours later, mice were killed and all visible tumour dissected out – tumours were divided in two and either fixed in 4% paraformaldehyde or snap frozen on dry ice. Paraformaldehyde samples were transferred to 70% ethanol after 24 hours, and processed in the Molecular Pathology laboratory (Barts Cancer Institute). Adenovirus structural protein expression was assessed by immunohistochemistry by Dr. Mohammed Ikram using rabbit anti-adenovirus antibody (Abcam, Cambridge, UK). RNA was extracted from frozen tumours by Ms. Katrina Pirlo. 1 µg total RNA was reverse transcribed using random hexanucleotide primers. Transcription of Hexon was assessed by RT-PCR using 100 ng cDNA as template.

2.19.3. Co-infection of murine intraperitoneal tumours with *dl*922-947 and Ad CMV 100K

5 x 10^6 MOSEC cells were injected s/c into the left flank of 6 week old female ICRF nu/nu mice. On days 90 – 93, when tumours were approximately 8mm in diameter, mice were treated with *dl*922-947 (3 x 10^9 particles/day in 50 µl PBS). On day 65, mice

received a single intraperitoneal dose of Ad CMV 100K (5×10^9 particles in 50 µl PBS). Mice were killed on day 68. Tumours were dissected out, cut in half and either snap frozen on dry ice or fixed in 4% paraformaldehyde.

Frozen and paraformaldehyde-fixed tumour samples were analysed as described above.

3. Results: Activity of human adenoviruses in malignant murine cell lines

3.1. Introduction

The aim of this thesis is to assess the activity of human adenoviruses in murine cells, to aid development of a murine model of intraperitoneal carcinoma that is sensitive to human oncolytic adenovirus, and thus allow the evaluation of adenovirus gene therapy in an immunocompetent animal. I first examined a panel of malignant murine cell lines *in vitro* for human adenovirus infectivity and cytotoxicity. Subsequently, I assessed murine cells for their ability to support viral protein expression, genome replication and infective virion production, predominantly using MOVCAR7 and CMT64 cells. Data from murine cells were compared to those derived from the human ovarian cancer cell line OVCAR4 *in vitro* as well as IGROV1 xenografts *in vivo*.

3.2. Infectivity of malignant murine cells

Permissiveness to adenovirus type 5 infection was evaluated by infecting cells at two multiplicities of infection (MOI) with an E1-deleted Ad5 vector encoding green fluorescent protein (GFP) under the control of the cytomegalovirus (CMV) immediate early promoter. GFP expression in these cells was then quantified by flow cytometry. At MOI 50 plaque forming units (pfu)/cell, infection rates exceeded 90% in all cell lines, both murine and human. At MOI 5, four of the five murine cell lines demonstrated infection rates >80% and exceeded that of the human line OVCAR4. Only MOVCAR12 cells exhibited a reduced permissiveness compared to the positive human control at the lower MOI, but GFP positivity was detected in over 65% of cells. Therefore, the murine cell lines tested were readily infected with human Ad5 vectors.

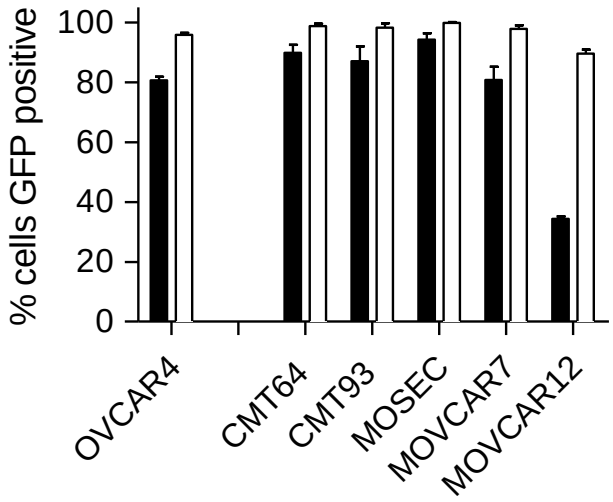

Figure 16 Infectivity of human and murine cell lines.

Cell line infectivity was assessed using AdGFP. 5 x 10^5 cells were infected with Ad CMV-GFP at MOI 5 (black bars) and 50 (white bars) pfu/cell. Infectivity was assessed 24 hours post infection by flow cytometry. Mean percentages of GFP- positive cells after infection are shown. Error bars represent mean +/- standard deviation.

3.3. Viral toxicity on malignant murine cell lines

3.3.1. Susceptibility of murine cell lines to human adenovirus cytotoxicity

Susceptibility of the cell lines to death induced by the adenovirus type 5 E1A CR2 deletion mutant *dl*922-947 was assessed 144 hours post-infection (pi) by MTT assay (Figure 17). The human OVCAR4 cells were significantly more sensitive to *dl*922-947 (IC_{50} 0.23 pfu/cell) than any of the murine cells. Of the murine cell lines, three (MOSEC, MOVCAR12 and CMT93) were largely resistant to *dl*922-947. MOVCAR7 (IC_{50} = 19 pfu/cell) and CMT64 (IC_{50} = 65 pfu/cell) could be killed by *dl*922-947, but were still significantly less sensitive than OVCAR4.

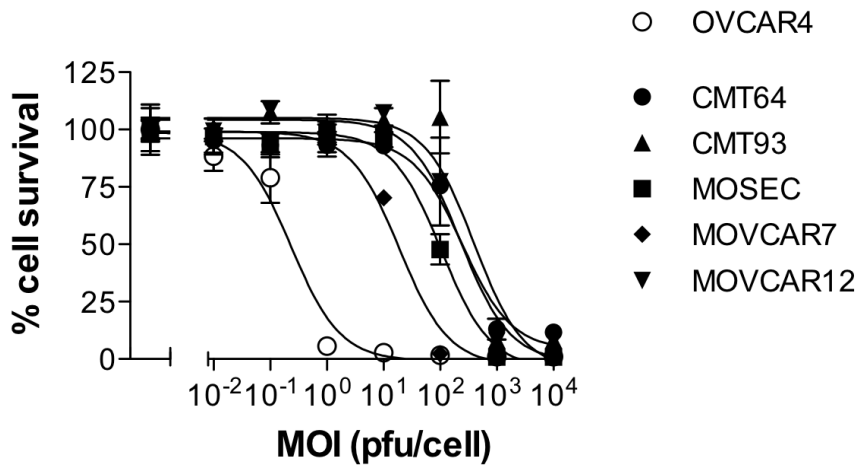

Cell line	*dl*922-947 IC_{50} (pfu/cell)	Comparison with OVCAR4
MOSEC	105	***
MOVCAR 12	219	***
MOVCAR 7	**19**	***
CMT 93	615	***
CMT 64	**65**	***
OVCAR 4	0.23	-

Figure 17 Cytotoxicity of *dl*922-947 in murine cell lines.

2 x 10^4 cells were infected with *dl*922-947 (MOI 0.01 – 10,000) in triplicate. Cell survival was assessed 144 hours pi by MTT assay. Error bars represent mean +/- standard deviation. IC_{50} values 144 hours p.i. are presented in table. Analysis by Sum-of-squares F test, ***; $p < 0.0001$.

MTT assay in malignant murine cells was also undertaken using the wild type (WT) human adenovirus serotype 5 in order to ensure that the reduction in cell cytotoxicity was not attributable to the deletion of E1A CR2 in the human adenoviral mutant *dl*922-947 (Figure 18). Infection with the wild type virus did not result in lower IC_{50} values in the murine cell lines and, in fact, demonstrated less cell death compared to that seen in the mutant virus.

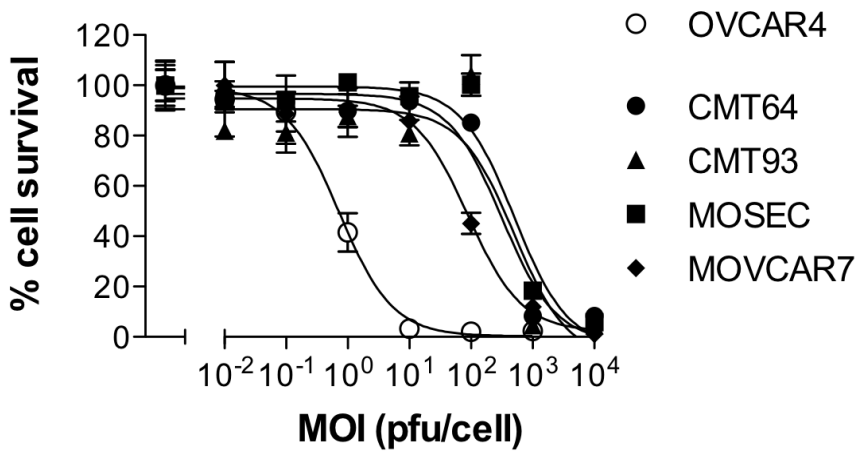

Cell line	hAd5 WT IC_{50} (pfu/cell)
MOSEC	505
MOVCAR7	89
CMT93	501
CMT64	317
OVCAR4	0.7

Figure 18 Cytotoxicity of WT hAd5 in human and murine malignant cell lines.

2 x 10^4 cells were infected with human adenovirus type 5 wild type virus (MOI 0.01 – 10,000) in triplicate. Cell survival was assessed 144 hours pi by MTT assay. Error bars represent mean +/- s.d., n = 3.

3.3.2. Susceptibility of murine cells to human adenovirus cytotoxicity *in vivo*

To evaluate whether human oncolytic adenoviruses had efficacy against murine carcinoma cells in vivo, CMT64 cells were injected intraperitoneally (ip) into C57Bl/6 mice by Professor Iain McNeish. CMT64 cells were used not only because of their known susceptibility to infection with *dl*922-947 but also because, after peritoneal injection into mice, they grow within the abdominal cavity in a similar way to ovarian malignancies in humans. On days 4-8 inclusive, *dl*922-947 was injected ip in 400 µl

20% icodextrin, a regime that our group has previously shown to induce anti-tumour effects in mice bearing ip human IGROV1 (Lockley, Fernandez et al. 2006) and A2780CP (Ingemarsdotter, Baird et al.) xenografts. Control mice received either vehicle or a non-replicating E1-deleted Ad5 vector with no transgene (Ad Control) (McNeish, Tenev et al. 2001). Results indicated that the median survival was the same in all three groups (26 days for vehicle, 21 days for Ad Control and 23 days for *dl*922-947. Thus, *dl*922-947 has no anti-tumour activity in mice bearing CMT64 tumours.

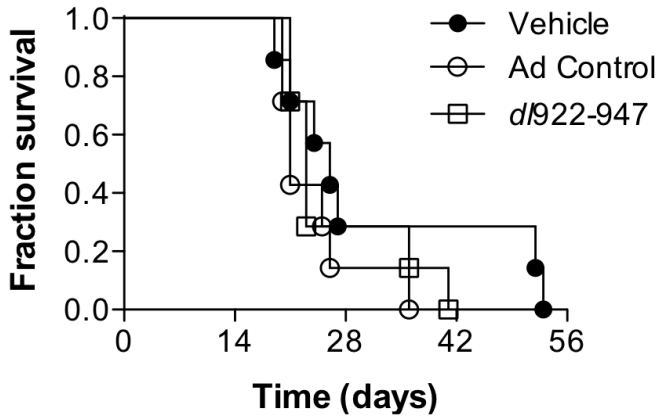

Figure 19 In vivo activity of *dl*922-947 in mice bearing intraperitoneal CMT64 tumours. On day 1, C57Bl/6 mice received intraperitoneal (ip) injections of 5 x 10^6 CMT64 cells in 200 µl PBS. On days 4-8 inclusive, mice were injected ip with vehicle (400 µl 20% icodextrin), Ad Control or *dl*922-947 (both 5 x 10^9 particles/day). Mice were monitored daily and killed when they reached UK Home Office limits.

3.4. Viral genome replication

Having demonstrated that murine cell lines could be infected with human adenovirus but that they were all significantly less sensitive to killing induced by *dl*922-947, genome replication was assessed using quantitative PCR (qPCR) in the two most sensitive murine cell lines (MOVCAR7 and CMT64) and the human positive control OVCAR4. Cells were infected at MOI 10 and 100 pfu/cell and DNA was extracted up to 96 hours later. Two separate sets of oligonucleotide primers and probes (E1A and

Hexon region) were used. At both MOI 10 and 100, the copy numbers of early and late region DNA were equal within each cell line at each time point, implying that replication occurred evenly throughout the viral genome.

Twenty-four hours following infection at MOI 10, the genome copy number was significantly higher in CMT64 cells than seen in human control cells (1.1×10^8 vs. 3.3×10^7 E1A transcript copies/µg cDNA; p= 0.0002), whereas it was significantly lower in MOVCAR7 (9×10^5 vs. 3.3×10^7 copies/µg; p = 0.0023 – Fig. 20). By 48 hours after infection at MOI 10, there was no significant difference in genome copy number between murine and human cells (CMT64 1.1×10^8 vs. OVCAR4 2.2×10^8 copies/µg; p = 0.26. MOVCAR7 4.1×10^7 vs. OVCAR4 $^{2.2} \times 10^8$; p = 0.11). Beyond 48 hours, genome copy number reached a plateau in all three cell lines, although OVCAR4 cells consistently produced the greatest number. At 96 hours pi, cell death precluded extraction of sufficient DNA from OVCAR4 cells.

At MOI 100, differences between the murine and human cells were less marked. Twenty-four hours post-infection, the genome copy number in CMT64 cells was again greater than in human control (7.6×10^8 vs. 4.8×10^8 E1A transcript copies/µg cDNA respectively; p = 0.04) and MOVCAR7 cells were again slower to replicate the viral genome than OVCAR4 (2.7×10^8 vs. 4.8×10^8 copies/µg; p = 0.036). By 48 hours post infection, genome production in OVCAR4 and CMT64 cells was the same (1.0×10^9 vs. 1.1×10^9 copies/µg respectively: p = 0.12), whilst in MOVCAR7 cells, genome copy number exceeded that seen in human control (1.7×10^9 vs. 1.0×10^9 copies/µg; p=0.0008). Beyond 48 hours, cell death precluded any further analysis in OVCAR4 cells. There was on-going genome replication in CMT64 cells up to 96 hours pi, whereas replication fell in the MOVCAR7 cells after 48 hours, which may have reflected early cell death at the higher MOI - MOVCAR7 cells were three times more susceptible to cell death than CMT64 cells at MOI 10 (Figure 17). Of note, at MOI 100,

the maximum number of genome copies produced in both murine cells was approximately equal to that produced in the OVCAR4 cells at MOI 10 (1.0×10^9 transcript copies/µg cDNA).

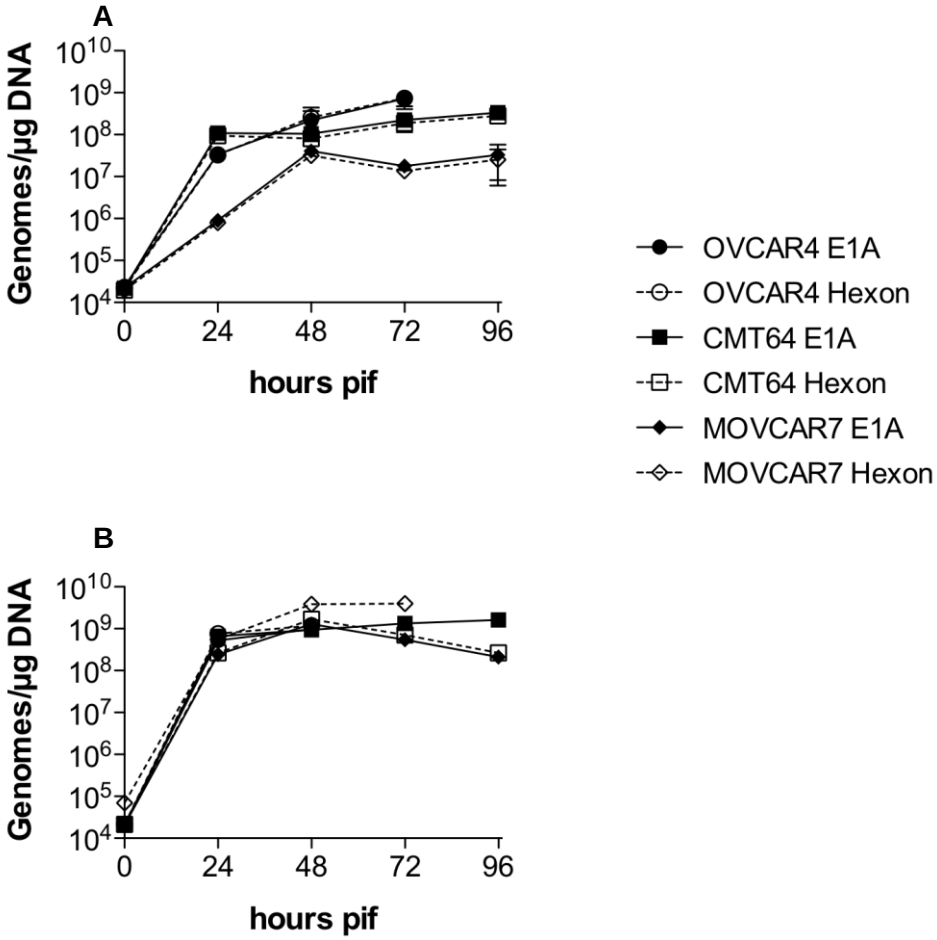

Figure 20 Viral genome copy number following infection with *dl*922-947.

5×10^5 cells were infected with *dl*922-947 (MOI 10 or 100). DNA was extracted up to 96 hours pi and genome copy number assessed using quantitative PCR. Points represent mean ± s.d., n = 3

3.5. Infectious virion production

Having demonstrated that viral genome replication occurred in murine cells following infection with a human adenovirus, CMT64, MOVCAR7, MOSEC and OVCAR4 cells were then evaluated for their capacity to support infectious virion production using $TCID_{50}$ assays (Figure 21). At all time points and at two different multiplicities of

infection, the level of infectious virion production in human cells was at least 2 log scales greater than that demonstrated in the murine cell lines. At MOI 10, virion production in OVCAR4 cells had increased from 22 pfu/cell to approximately 10^4 pfu/cell by 72 hours post-infection. By contrast, in the murine cell lines, virion production failed to exceed the input dose at any time and, in MOVCAR7 cells, was below the limit of quantification at 24 hours. At MOI 100, the pattern was similar. Production in OVCAR4 cells peaked at 48 hours, after which there was significant cell death. In the murine cells, although the number of virions produced at MOI 100 exceeded that at MOI 10 and production in CMT64 and MOSEC cells was greater than in MOVCAR7, the absolute numbers were still negligible compared to OVCAR4.

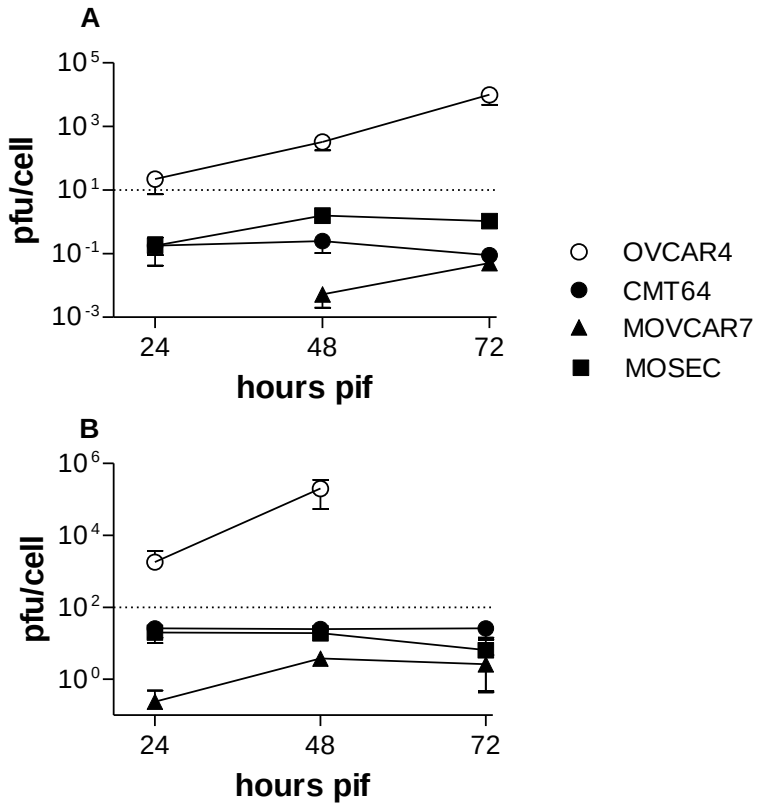

Figure 21 Infectious virion production following infection with *dl*922-947.

5 x 10^5 cells were infected with *dl*922-947 at MOI 10 (**A**) or MOI 100 (**B**). Cells were harvested up to 72 hours pi. Intracellular infectious virion production was assessed by $TCID_{50}$ assay. Dotted line indicates input dose of virus. Error bars indicate mean +/- standard deviation, n = 3.

3.6. Viral protein expression *in vitro*

I then evaluated whether murine cells could support expression of human adenovirus proteins. Cells were infected with either *dl*922-947 or the E1A wild-type adenovirus *dl*309 at MOI 10. Protein was harvested up to 96 hours post infection and expression of E1A and adenovirus capsid proteins was assessed by immunoblot (Figure 22). Early and late viral proteins were expressed at higher levels in all cell lines when infected with *dl*922-947 compared to *dl*309, in keeping with previous data from our group (Lockley 2007).

The human control cell line OVCAR4 demonstrated greater early and late viral protein expression following infection with both *dl*922-947 and *dl*309 adenoviruses when compared to the murine cell lines. Both murine cell lines expressed readily detectable levels of E1A but these were at a lower level than those seen in the human control. In the human control OVCAR4, such was the extent of late viral protein expression that film exposure time was a matter of seconds compared to minutes in their murine counterparts. In OVCAR4 cells hexon, penton and fibre were detected 24 hours post infection. Expression of the smaller capsid proteins was also readily detectable. Again, expression was greater in human cells infected with *dl*922-947 compared to those infected with *dl*309.

In the murine cell lines, expression of late viral capsid proteins was lower than E1A expression in the same cell lines. In the CMT64 cell line hexon, penton and fibre proteins were detectable although expressed at a lower level than seen in OVCAR4 cells. In the MOVCAR7 cell line, fibre was not detected.

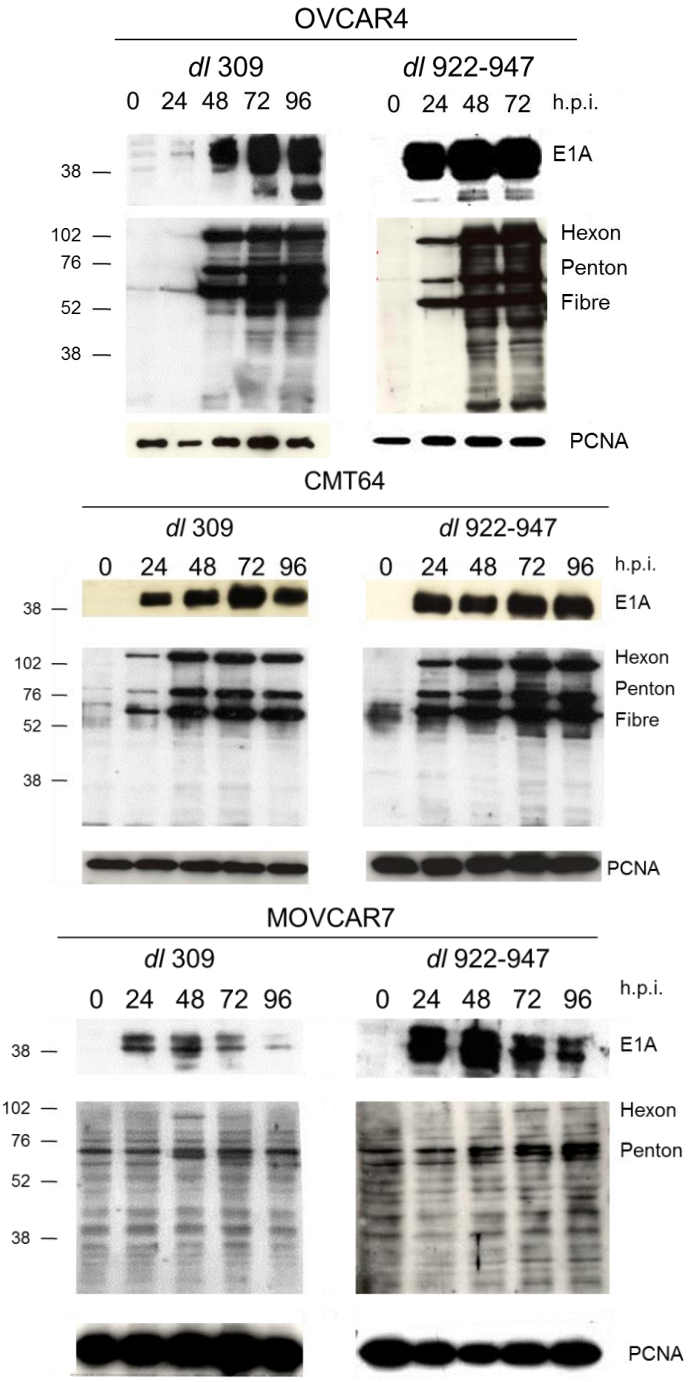

Figure 22 Western blots of cell lines OVCAR4, CMT64 and MOVCAR7 infected with *dl*922-947 and E1A wild type control virus *dl*309. 5 x 10^5 cells from each cell line were infected with *dl*922-947 (MOI 10). All cells were infected at MOI 10 and harvested up to 96 hours post infection. 24µg protein was loaded per well. Membranes were probed for human adenoviral type 5: E1A, capsid proteins and PCNA as described in section 2.11.3**.** Capsid protein molecular weights in kDa: Hexon=107,996; Penton=63,642; Fibre=62,000: h.p.i = hours post infection. Numbers represent molecular weight in kilodaltons (kDa)**.**

In the MOVCAR7 cell lines, hexon and fibre were detected but were expressed at a much lower level than seen in the CMT64 cells. In addition, viral capsid proteins in this cell line were detectable in lysates 24 hours later than in the CMT64 and OVCAR4 cell lines. In both murine cell lines, overall viral protein expression was greater in cells infected with *dl*922-947 when compared to the wild type control *dl*309.

Due to the technical difficulties presented by the considerable variation in viral protein expression between the human and murine cell lines, a further western blot was performed to examine more closely the relative expression of viral proteins between cell lines. In addition, protein expression in the MOSEC cell line was evaluated.

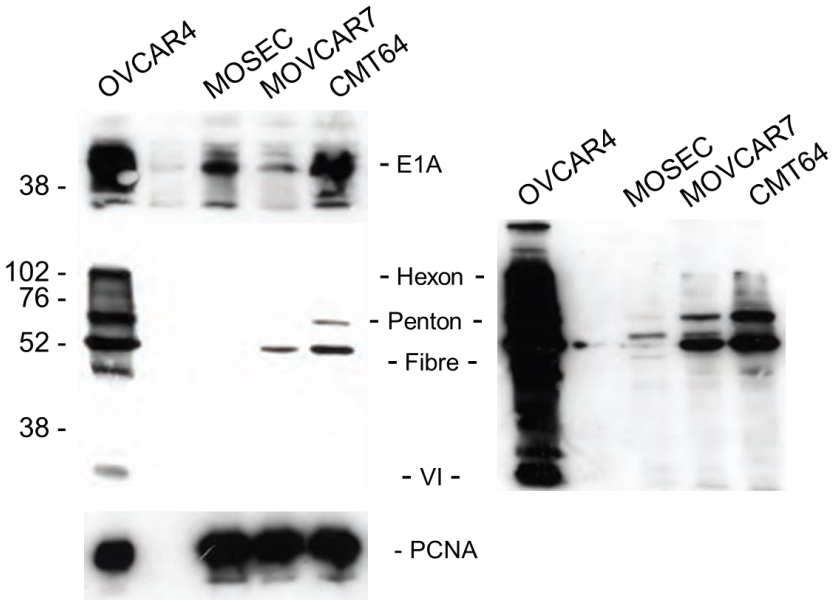

Figure 23 Western blot to examine viral protein expression.

5 x 10^5 cells from each cell line were infected with *dl*922-947 (MOI 10). Lysates were harvested 48 hours later and 20 µg protein from each lysate was run on the same 10% SDS page gel and blotted for with antibodies to E1A, adenovirus capsid proteins and PCNA. Capsid protein molecular weights in kDa: Hexon=107,996; Penton=63,642; Fibre=62,000; VI=22,000. Short (left) and long exposure (right) images of the structural protein blot are presented.

Further immunoblot demonstrated a clear abrogation of late viral protein expression in all the murine cell lines analysed to varying degrees. In the case of CMT64 and MOSEC cell lines, reduced capsid protein expression was demonstrated despite detectable levels of E1A. Of note, in the MOSEC cell line, no capsid proteins were detected by immunoblot despite detectable E1A. Of the murine cell lines, CMT64 cells exhibited the highest levels of protein expression. In these cells E1A, hexon, penton and fibre were all detected but at a much lower level than that seen in the human control OVCAR4. Furthermore none of the smaller capsid proteins was detectable in CMT64 cell lysates. The MOVCAR7 cell line demonstrated reduced expression of both E1A and late viral proteins, with only one capsid protein, fibre, detectable at 48 hours pi.

3.7. Viral protein expression *in vivo*

Expression of viral protein was also analysed *in vivo* by Dr. Kyra Archibald and Professor Iain McNeish. A single dose of *dl*922-947 was administered to female ICRF nude mice bearing intraperitoneal CMT64, MOSEC and IGROV1 tumours. Mice were killed 24 hours after infection and expression of hexon was analysed both by qRT-PCR and immunohistochemistry.

As with the *in vitro* experiments, there was evidence of hexon transcription in murine tumours, with no statistically significant difference in transcript copy number between IGROV1 and either CMT64 or MOSEC tumours. However, there was a marked difference in protein expression by IHC. In the two murine tumours, only very occasional cells demonstrated hexon, in sharp contrast to the IGROV1 tumours.

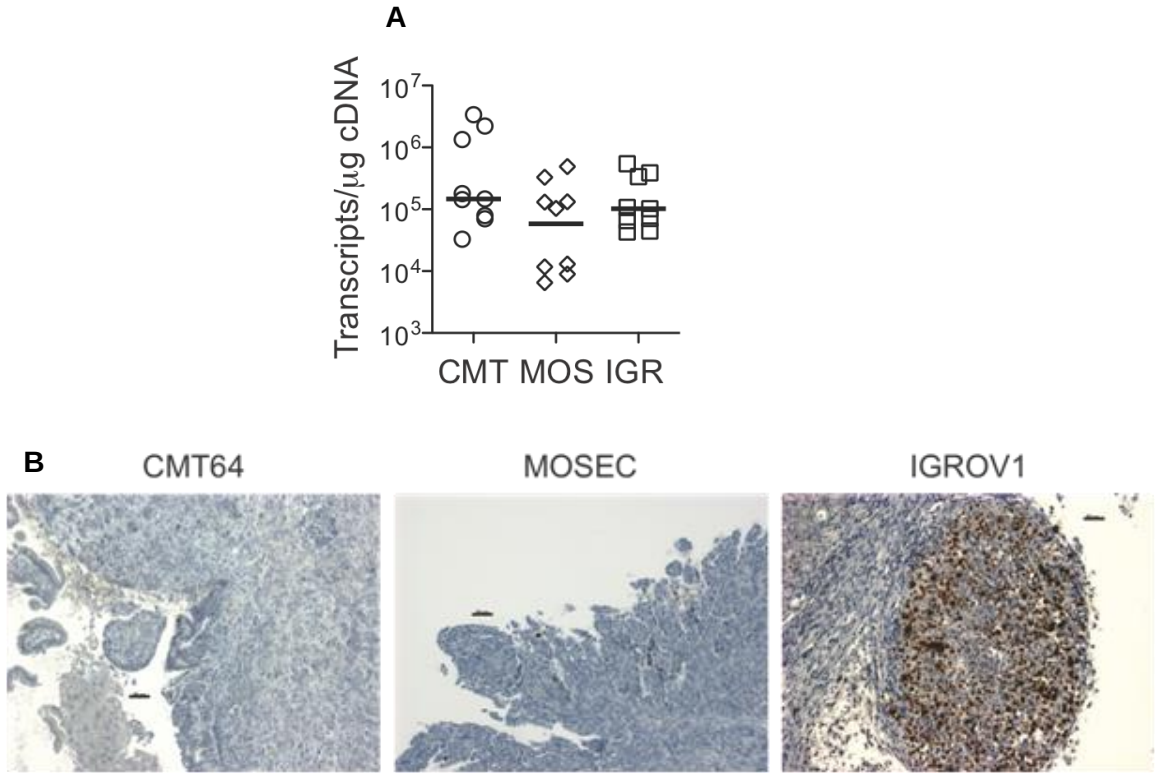

Figure 24 Hexon transcription rate in human and murine xenograft tumours.

5x10^6 cells were injected ip into ICRF nude female mice in 200 µl PBS. When ascites was clinically evident, mice received a single ip injection of *dl*922-947 (10^{10} particles in 400 µl 20% icodextrin). Mice were killed 48 hours later and all tumour dissected out. Half was snap frozen in dry ice, whilst half was fixed in 4% paraformaldehyde. RNA was extracted from the snap frozen specimens, DNAse I treated and reverse transcribed using random hexanucleotide primers. 50ng cDNA was then subjected to quantitative PCR using Hexon region primers and probes as described in Materials and Methods (**A**). Purified *dl*922-947 DNA was used to generate standard curves. Expression of adenovirus structural proteins was assessed in paraformaldehyde-fixed tissue by immunohistochemistry (**B**). Cells staining positive for hexon appear brown. Bar represents 50µm.

3.8. Summary & Discussion

The data presented in this chapter demonstrate that malignant murine cell lines were permissive to infection human adenovirus type 5 vectors but were significantly less sensitive to adenovirus cytotoxicity than human cells. Viral genome replication was seen in murine cells, but there was a dramatic reduction in infectious virion production. There was also a marked reduction in adenovirus protein expression in murine cells, in particular late viral structural proteins. This difference was seen both *in vitro* and *in vivo*.

In the majority of the cell lines examined, permissiveness of murine cells to infection was at least as great as that seen in the human control cell line OVCAR4. Although this contradicts some earlier reports in which murine cells were reported to be non-permissive to human adenoviral entry (Ganly, Mautner et al. 2000), there are multiple previous publications, including from our own department (Hallden, Hill et al. 2003; Wang, Hallden et al. 2003) (Hallden, Hill et al. 2003) indicating that murine cells can be infected with human adenovirus. The classical pathway of group C adenovirus entry to the cell is via the CAR receptor (Bergelson, Cunningham et al. 1997). Murine CAR (mCAR) and human CAR (hCAR) are 83% identical and share a >90% common amino acid identity in their extracellular domains (Tomko, Xu et al. 1997; Bergelson, Krithivas et al. 1998). Although I have not undertaken explicit study of the CAR expression of the murine cell lines used, similarities between mCAR and hCAR structure and expression are such that it is unsurprising that human adenovirus can infect murine epithelial cells. Data from our department have suggested that expression of CEACAM6 in pancreatic cancers can block adenovirus transport to the nucleus (Wang, Gangeswaran et al. 2009). However, the Ad CMV GFP infectivity assay measures not only adenovirus entry to the infected cell, but also exit from the endosome, transport to the nucleus and subsequent gene expression. The fact that over 80% of all murine cells were GFP positive at MOI 5 suggested that failure of trafficking of the viral DNA to the host cell

nucleus was not an obvious cause of the discrepant cytotoxicity and viral protein expression data seen. Repetition of the GFP infectivity assay at lower MOIs (1.0, 0.1) may have provided additional information about the relative susceptibility of the murine cell lines to AdGFP infection. In addition, formal evaluation of the CAR and p53 statuses of the cell lines used would have been of interest. OVCAR4 is known to carry a p53 mutation (Jia, Osada et al. 1997; O'Connor, Jackman et al. 1997) and work within our group has demonstrated that it expresses CAR on immunoblot. However, there is no available data for the Rb/p53 statuses of the murine cell lines. CMT 64 has demonstrated only low levels of CAR expression (Lindström 2005) and data has not been published regarding the CAR status of other murine cell lines.

The cause of the disparity between permissiveness to infection and subsequent cytotoxicity levels was then investigated. Previous data have suggested that the restriction to adenoviral replication in murine cells occurs at a post entry step (Duncan, Gordon et al. 1978; Eggerding and Pierce 1986; Silverstein and Strohl 1986; Blair, Dixon et al. 1989; Ginsberg, Moldawer et al. 1991; Jogler, Hoffmann et al. 2006). The qPCR data presented here demonstrate that the adenoviral genome does replicate within the CMT64, MOSEC and MOVCAR7 cell lines. Indeed, genomic DNA replication rates in CMT64 cells exceeded those seen in OVCAR4 cells 24 hours post infection at two separate MOIs and were not significantly reduced at 48 hours pi. In order to initiate viral genome replication, a series of complex interactions between viral proteins and the host cell replication machinery must occur (Jones, Rigby et al. 1988; Fang, Stevens et al. 2004; Berk 2005). Central to this is the activity of E1A, which drives the cell into S phase-like state by binding to pRb, thus dissociating it from the E2F family of transcription factors and allowing the transactivation of genes necessary for viral DNA replication. Although *dl*922-947 contains a 24bp deletion in the E1A CR2 region that is responsible for pRb binding, it replicates selectively in malignant cells due to the abnormalities in the Rb pathway and G1-S checkpoint seen in transformed cells

(Sherr and McCormick 2002), The fact that IC_{50} values for hAd5 WT virus were lower than those seen with *dl*922-947 demonstrate that the E1A CR2 deletion in the mutant virus did not affect viral activity in the murine cell lines. This was supported by the genomic DNA q-PCR data which demonstrated comparable rates of replication in the murine cell lines. Indeed, the temporal pattern of genome replication seen in the CMT64 cells suggests that there was no barrier to the activity of these early viral proteins in this murine cell line and, as a result, overall levels of viral genome copy number at $> 1 \times 10^9$ were on a par with the human control. Furthermore, the increased cytotoxicity of *dl*922-947 compared to WT seen in the murine malignant cell lines mirrors its effect on human carcinoma cell lines. Previous publications have demonstrated lower IC_{50} values for *dl*922-947 when compared to Ad5 WT (Heise, Hermiston et al. 2000a; Lockley, Fernandez et al. 2006). As discussed in section 1.9 the exact mechanisms of adenovirus-mediated cell death are yet to be fully elucidated and as such the reasons for increased *dl*922-947 cytotoxicity compared to WT are not clear. Host cell factors have been implicated. Flak *et. al.* suggest that host cell factors such as p21 expression may be important for successful oncolysis following adenoviral infection (Flak, Connell et al. 2010). Connell *et. al*. demonstrated that cells exhibiting profound over replication of viral genomic DNA via stabilisation of Cdc25A with evidence of associated DNA damage and inhibition of the ATR-Chk-1 pathway displayed high susceptibility to *dl*922-947 induced cell death (Connell, Shibata et al. 2011). The superior cytotoxic activity of *dl*922-947 was attributed to higher levels of DNA damage and over-replication when compared with Ad5 WT infection. The 24 base pair deletion in within E1A-CR2 was thought to contribute to this phenomenon. Deletion in this region reduces binding to host cell p107, pRb and cyclin A (section 1.8.3) and may result in reduced viral control of DNA replication leading to the over replication phenotype that is more susceptible to cell death (Wang, Draetta et al. 1991; Howe and Bayley 1992).

In MOVCAR7 cells, the rate of genome replication was slower in the first 24 hours than in either OVCAR4 or CMT64. The causes of this remain unclear, but may be due to relatively lower expression of early adenovirus proteins. Interestingly, whatever the cause, this hurdle was overcome at the higher MOI of 100. At this concentration, genome copy numbers were not significantly lower than the human control 24 hours after infection ($p=0.36$) and significantly exceeded those see in human control at 48 hours ($p=0.0008$). This may have occurred as a direct result of the increased MOI but the step up in genome replication rates at 24 hours raises the possibility that a threshold effect may be required to allow the viral replication cycle to proceed, a phenomenon that has been demonstrated in a recent clinical trial (Breitbach, Burke et al. 2011). Again evaluation of genome replication using different MOIs and at differing timepoints would have been useful to evaluate this further. Notwithstanding this, we can conclude that that in both MOVCAR7 and CMT64, there was adequate expression and activity of the early viral proteins resulting in effective viral genome replication.

The rates of viral DNA replication in murine cell lines, albeit variable, did not correlate with the striking absence of infectious virion production. None of the murine cells examined managed to produce enough infectious viral progeny to exceed the input dose. This confirms earlier data published by Ganly *et al*. (Ganly, Mautner et al. 2000) but contradicts that published by Hallden *et al*. (Hallden, Hill et al. 2003). Hallden *et. al.* demonstrated infectivity levels of only 15 and 25% in CMT64 cells at infection concentrations of 100 and 1000 particles per cell respectively but demonstrated infectious virion yields of 10^8 pfu/cell at 96 hours pi. Reasons for the disparity between my data and that published by Hallden *et al.* remain unclear. Another striking feature of these data is the discrepancy between virion production and cell cytotoxicity. Although all four murine cells generate essentially no productive virions, they can still be killed by human adenovirus mutant *dl*922-947 with IC_{50} values that are lower than those seen with many human ovarian cancer cells. Historically, adenovirally-mediated cell death

was thought to result from cell lysis and the release of infective virions from the host cell (Fields, Knipe et al. 2007)l. However, to date, the process of cell death has not been clearly documented. As discussed above, previous data from our group suggest that there is a disconnection between virion production and cell death, and the data here strongly support this (Flak, Connell et al. ; Connell, Shibata et al. 2011).

To explain the largely absent virion production, I examined viral protein expression. *In vitro* examination of lysates of murine cells infected with *dl*922-947 demonstrated detectable E1A expression. The level of expression was lower than that seen in the human control. However, E1A expression was greater in cells infected with *dl*922-947 than the E1A wild type control virus *dl*309 demonstrating that this effect was not ascribable to the deletion in E1A CR2 region of *dl*922-947. In addition, the presence of effective viral genome replication suggests that E1A expression was at least functionally adequate in these cells. The most striking feature in repeated immunoblots, however, was the marked reduction of late viral protein expression. This was seen with both *dl*922-947 and WT control virus *dl*309, which suggests that this is a generic problem with human adenoviruses type 5. Previous papers have demonstrated expression of the larger viral proteins (hexon, penton and fibre) after infection of some murine cell lines (Hallden, Hill et al. 2003). My data show that expression of these three main capsid proteins does occur in the murine cells but at reduced levels and that the level of expression varies between cell lines. Although the antibody used was not dedicated to the detection of small adenoviral structural proteins, they were clearly demonstrated in the human control lysate. These smaller structural proteins were not well visualised in the murine cell lysates. This low level of structural protein expression was hypothesised to be a major factor in the absence of virion production in the murine cell lines, as, without structural proteins, a viral capsid could not be created in order to package the viral DNA.

Further evaluation of *dl*922-947 infection, DNA transcription and protein expression were undertaken i*n vivo* using malignant murine cells in mouse xenografts models by Dr. Kyra Archibald and Professor Ian McNeish. The MOSEC cell line had demonstrated both a permissiveness to infection on a par with CMT64 and MOVCAR7 (Figure 16) and also lower levels of cytotoxicity than seen in the human cells (Figure 17). Successful viral DNA transcription was demonstrated *in vivo* and, of note, there was no statistical difference in the rate of hexon transcription seen in both human and murine tumour xenografts. This demonstrates that both *in vivo* and *in vitro*, murine malignant cell lines were permissive to infection with *dl*922-947 and the rates of viral genome transcription within the tumour lysates strongly suggest that all the steps required for viral DNA replication (cell entry, trafficking to and entry into the nucleus) were achieved with equal efficacy in the human and murine xenografts. However, despite this, tumour immunohistochemistry revealed an almost complete absence of viral hexon expression in the murine CMT64 and MOSEC xenografts. Therefore, although viral gene transcription was occurring in murine cell lines *in vivo* and *in vitro*, late viral protein expression was starkly absent both in murine xenograft lysates and on immunoblot analysis. The causes of this failure of late protein expression are investigated in the rest of this thesis.

In summary, results in this chapter have confirmed and expanded on previous preliminary findings; murine cell lines are permissive to infection with human Group C adenoviruses and support replication of the adenovirus genome. Despite this, murine cells fail to support the generation of infectious virions. Abrogation of late viral capsid protein expression in murine cell lines is evident *in vitro* and *in vivo* and requires further investigation. In addition, putative differences between early and late viral gene expression need to be explored in greater depth, commencing with analysis of early and late gene transcription in murine cells.

4. Results: Investigation of failed late viral protein expression

4.1. Introduction

Results in chapter three indicated that there was a marked failure of viral protein expression and virion production in murine cells upon infection with a human adenovirus, despite levels of genome replication that matched and occasionally exceeded those in human cells. This failure of protein expression was most marked in late adenoviral capsid proteins. Causes for this failure are explored in this chapter. Experiments were performed to evaluate the stages of late viral protein expression in a stepwise manner. Examination encompassed assessment of viral gene transcription, viral mRNA export and alternate splicing of late mRNA transcripts, as well as protein stability. An evaluation of the host cell translational machinery was also undertaken.

4.2. Successful transcription of early and late genes

Quantitative-RT-PCR was used to examine levels of early and late gene transcription. Primers and probes for E1A, hexon, fibre and the L4 genes 100K and 33K were designed using Primer Express™ software.

Q-RT-PCR demonstrated that both early and late genes of the oncolytic adenovirus *dl*922-947 were successfully transcribed in human (OVCAR4) and murine (CMT64 and MOVCAR7) carcinoma cell lines. Cells were infected at two different MOI of 10 and 100. In all murine cell lines, E1A transcription was maximal 48 hours post infection, rather than at 24 hours as was seen in the human control. E1A transcription 6 hours post infection at MOI 10 was at least one log scale greater in the OVCAR4 cell line than in CMT64 ($p=0.0003$) and MOVCAR7 ($p=0.0001$) cells. Twenty-four hours post infection, transcript copy numbers for E1A in the human cell line remained significantly higher than in murine cell lines ($p<0.0001$).

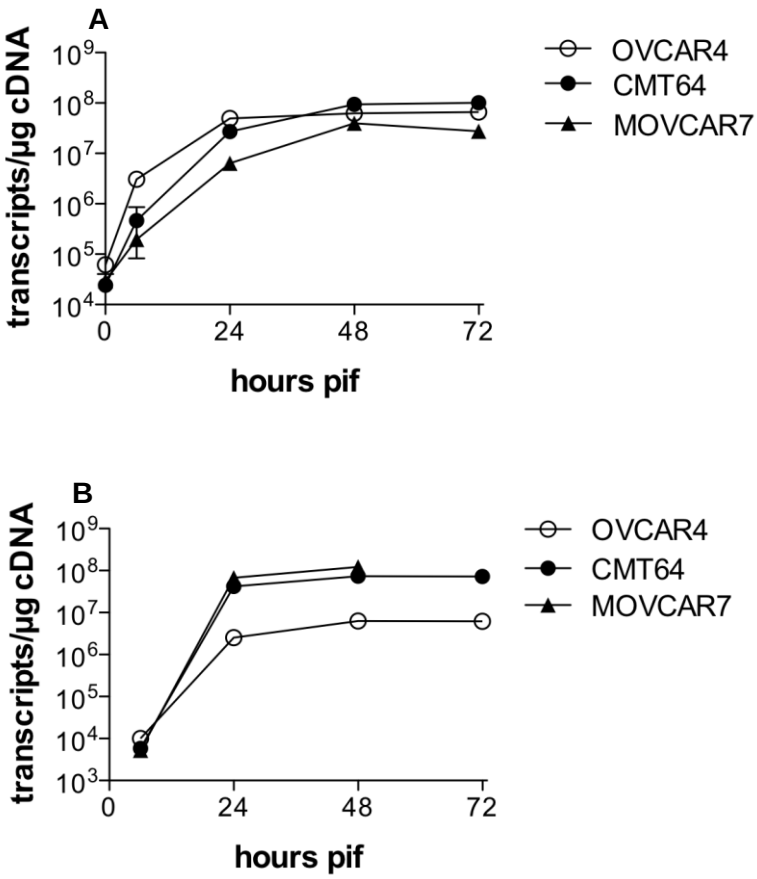

Figure 25 E1A transcription at MOI 10 and 100.

Transcription rates of early and late genes in OVCAR4, CMT64 and MOVCAR7 cell lines. 1 x 10^5 cells were infected with *dl*922-947 at MOI 10 (**A**) or MOI 100 (**B**). One plate was mock infected. Plates were seeded concurrently to assess transcription rates under the same experimental conditions. RNA was harvested at 6, 24, 48 and 72 hours post infection.

However, later in the infectious cycle this, disparity between human and murine E1A transcript copy numbers reduced and, at 48 and 72 hours p.i., E1A transcript copy numbers in CMT64 cells exceeded those seen in OVCAR4 ($p<0.0001$ at 48 hours p.i.; $p=0.0042$ at 72 hours p.i.). In MOVCAR7 cells E1A transcript copy numbers were lower than those seen in the human cell line at all time points.

Transcription rates in murine cell lines were also assessed at the higher MOI of 100. This evaluation was hampered in the human control cell line OVCAR4 by significant

toxicity and consequent insufficient RNA samples for analysis at the later time point. Infection of murine cells at MOI 100 increased the rate of early gene transcription at early time points and reduced the discrepancy between the numbers of E1A transcripts generated in murine cells compared to human control early on in infection. At 6 hours p.i. early transcript copy numbers in the murine cell lines did not exceed those produced by them at MOI 10 and were still half a log lower than those seen in the human control at the lower MOI. From 24 hours p.i., infection at the higher MOI increased the number of E1A transcript copies in a dose-dependent manner. At MOI 100, murine E1A transcript copy numbers in the CMT64 and MOVCAR7 cells consistently exceeded those produced by the human control ($>10^7$ compared to 2 $x10^6$ in OVCAR4) at later times after infection.

Transcription rates for the late structural viral genes were also examined. Transcript copy numbers for the late structural proteins at MOI 10 were lower in the murine than human cell lines at all time points post infection with *dl*922-947 ($p<0.0001$). Of note, CMT64 cells transcribed > 10^8 copies of fibre per µg cDNA consistently at the 24, 48 and 72 hour time points, which was closest to the transcription rates seen in OVCAR4 cells (3.4.x 10^8, 6.8 x 10^9 and 5.2 x 10^9 copies per µg cDNA respectively). MOVCAR7 transcription rates were lower than the human control throughout the course of the experiment, with a maximum number of 5.9 x 10^7 transcript copies per µg cDNA detected at 48 hours post infection.

At the higher MOI 100, transcription rates of the late gene hexon increased by 0.5-1 log from 24 hours p.i. in CMT64 and MOVCAR7 when cells compared to those demonstrated at MOI 10 and this increased rate was maintained.

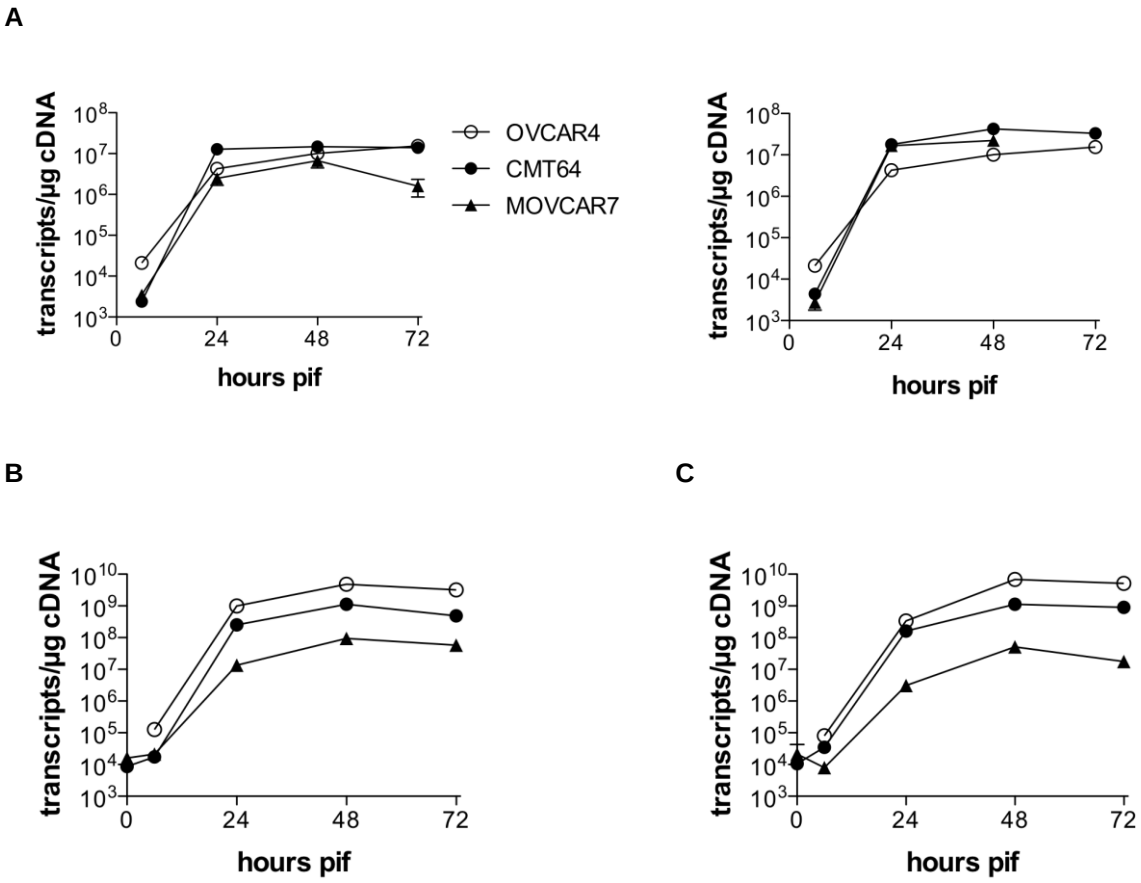

Figure 26 Transcription rates of late structural genes in human and murine malignant cell lines.

1 x 10^5 cells were infected with *dl*922-947 and harvested at 6, 24, 48 and 72 hours post infections. One plate was mock infected. **A**; transcription rates of Hexon at MOI 10 (left) and 100 (right), **B**; transcription rates of IIIa at MOI 10, **C**; transcription rates of fibre at MOI 10.

Transcript copy numbers for the non-structural L4 genes 100K, 33K and 22K were also evaluated. As previously discussed, L4 100K ensures the preferential translation of viral mRNA by disrupting cap binding to host cell mRNA (Cuesta, Xi et al. 2000). L4 22K and 33K are important for the promotion of late viral gene transcription at the MLP and for the alternate splicing of viral capsid mRNAs from the MLTU (Fessler and Young 1999; Farley, Brown et al. 2004; Morris and Leppard 2009; Backstrom, Kaufmann et al. 2010; Morris, Scott et al. 2010). It was therefore deemed important to evaluate these genes as well because they are required for successful late gene

transcription (22K), mRNA splicing (33K) and protein translation (100K), although not directly forming part of the viral capsid. Primers and probes were constructed for the 100K and 33K cDNA sequences, but an effective probe for the L4 22K could not be designed due to the extent of sequence overlap with L4 33K.

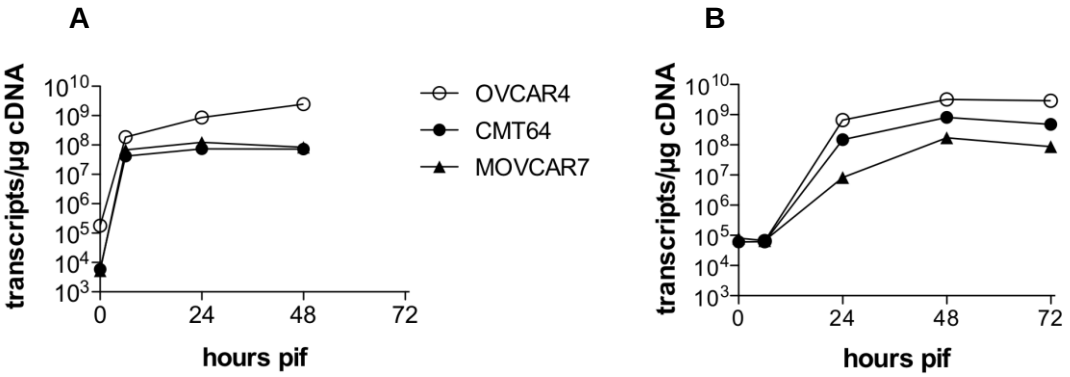

Figure 27 Transcription rates of non-structural late genes.

Transcription rates of the non-structural late genes L4 33K (**A**) and L4 100K (**B**) were evaluated in OVCAR4, CMT64, MOVCAR7 cell lines: 1 x 10^5 cells were infected with *dl*922-947 (MOI 10). One plate was mock infected. RNA was harvested at up to 72 hours post infection.

L4 100K copy number demonstrated a different temporal pattern of transcription to E1A, as would be expected for a later protein. At 6 hours p.i., both murine cell lines demonstrated L4 100K transcript copy numbers similar to those seen in the human control cell line (CMT64: 6.35 x 10^4 vs. 6.43 x 10^4 copies/µg cDNA; p = 0.82; MOVCAR7 6.71 x 10^4 vs. 6.43 x 10^4 copies/µg cDNA; p = 0.85). At 24 hours p.i., L4 100K transcription rates in the murine cell lines were reduced compared to the human control (CMT64 1.47 x 10^8 vs. 6.59 x 10^8 copies/µg cDNA; p = 0.0011; MOVCAR7 8.32 x 10^7 vs. 6.59 x 10^8 copies/µg cDNA; p = 0.0004). At 48 hours, the reduced rate of L4 100K transcription in the murine cell lines persisted (both p<0.0001 compared to OVCAR4). However, although reduced, copy numbers in the murine cells were not inconsiderable (48 hours p.i. CMT64 8.19 x 10^8, MOVCAR7 8.32 x 10^6 L4 100K

transcript copies/μg cDNA). Unlike the transcription rates of E1A, L4 100K transcript copy numbers in murine cells did not reach the levels seen in the human control cell line OVCAR4 at any time point.

The transcription rates of L4 33K demonstrated an early rise in transcription rates across all three cell lines 6 hours p.i. Even at this early time point, both murine cell lines demonstrated significantly lower rates of mRNA transcription compared to human control (6 hours p.i. CMT64 4.22×10^7 vs. 1.86×10^8 copies/μg cDNA; $p<0.0001$; MOVCAR7 6.81×10^7 vs. 1.86×10^8 copies/μg cDNA; $p<0.0001$). After this time point, the disparity between the L4 33K transcription rates between human and murine cell lines continued to increase. As previously noted, however, transcript copy numbers were $>10 \times 10^7$ across all cell lines.

4.3. Export of viral mRNA

In order to investigate whether the low level of protein expression in murine cells was attributable to defective mRNA export from the nucleus to the cytoplasm, subcellular fractionation of cell lysates was performed following infection with *dl*922-947. Q-RT PCR was used to quantify both early (E1A) and late (hexon) mRNA in nuclear and cytoplasmic fractions. Purity of the samples was ratified via western blot using antibodies to the nuclear protein lamin and cytoplasmic protein beta tubulin. Cytoplasmic:nuclear transcript copy ratios were calculated and values for murine cell lines normalised to those of the human E1A control.

Cytoplasmic levels of E1A mRNA were higher in murine cell lines compared to human control (CMT64 $p=0.0012$; MOVCAR7 $p=0.0002$). Hexon mRNA was also exported from the nucleus effectively but at reduced levels compared to the human control (CMT64 $p=0.0071$: MOVCAR7 $p=0.0037$). Therefore, a failure of viral mRNA export did not appear to underlie the failure of human adenovirus proteins in murine cells.

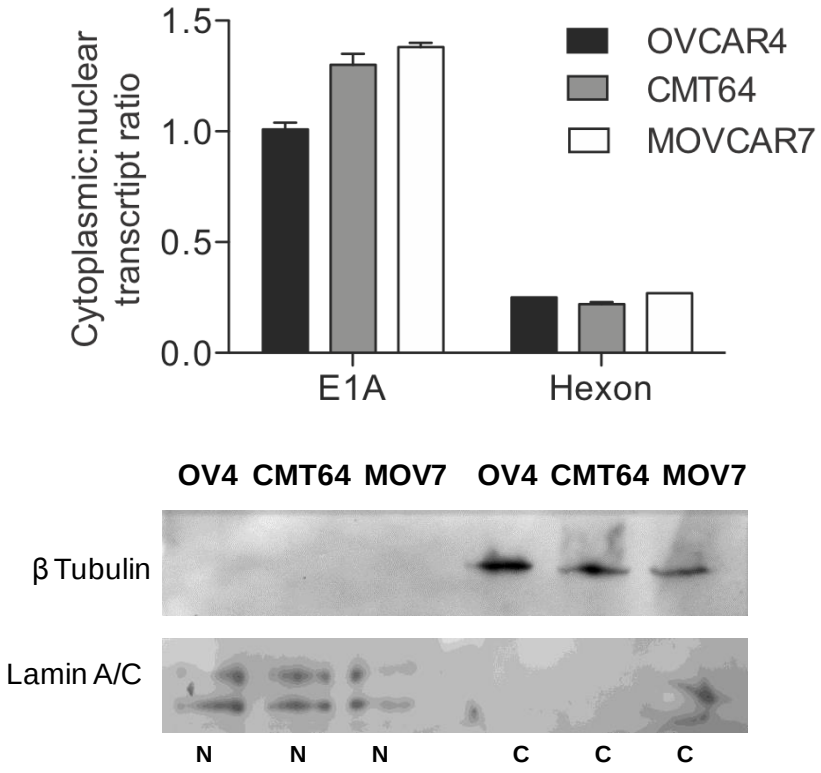

Figure 28 Cytoplasmic: Nuclear viral mRNA ratio.

5 x 10^5 cells were infected with *dl*922-947 at MOI10 and were harvested 48 hours p.i. Subcellular fractions of viral RNA were extracted. 1µg cDNA from nuclear (**N**) and cytoplasmic (**C**) fractions was assessed for early (E1A) and late (Hexon) mRNA copy numbers using qRT-PCR. Western blots probing for beta tubulin (cytoplasmic) and Lamin A/C (nuclear) proteins demonstrated the purity of fractionation.

4.4. Alternate splicing

Alternate splicing of mRNA is a major mechanism that allows a single gene to increase its coding diversity. In this way, post-transcriptional changes to the mRNA can control gene expression. Cellular and viral genes both utilise this process. The incongruity of the presence of numerous late viral gene RNA transcripts but a subsequent failure to demonstrate late viral proteins on immunoblot raised the possibility that a failure of effective RNA alternate splicing caused the failure of late protein expression. I undertook to evaluate the integrity of the alternate splicing pathway of the L4 gene products in human and murine cells.

4.4.1. L4 mRNA alternate splicing

Transcription of the MLTU produces a 28,000 base pair section of pre-mRNA that undergoes extensive polyadenylation and alternate splicing, which results in more than 20 species of transcript. Qualitative analysis of the L4 mRNA transcripts was undertaken. PCR primers were designed for both the TPL sequence (which is present at the 5' end of all MLTU mRNA transcripts) and a sequence at the 3' end that is common to the L4 cDNA transcripts (RP2). An additional 3' primer (RP1) was designed for the sequence at the beginning of the L4 100K unique open reading frame in order to facilitate evaluation of this larger molecule and distinguish it from the smaller 22K and 33K splice products. PCR products were then run on a 1% agarose gel to assess different spliceoforms between cell lines. Mock samples, which were processed without reverse transcriptase, confirmed that there was no contaminating DNA.

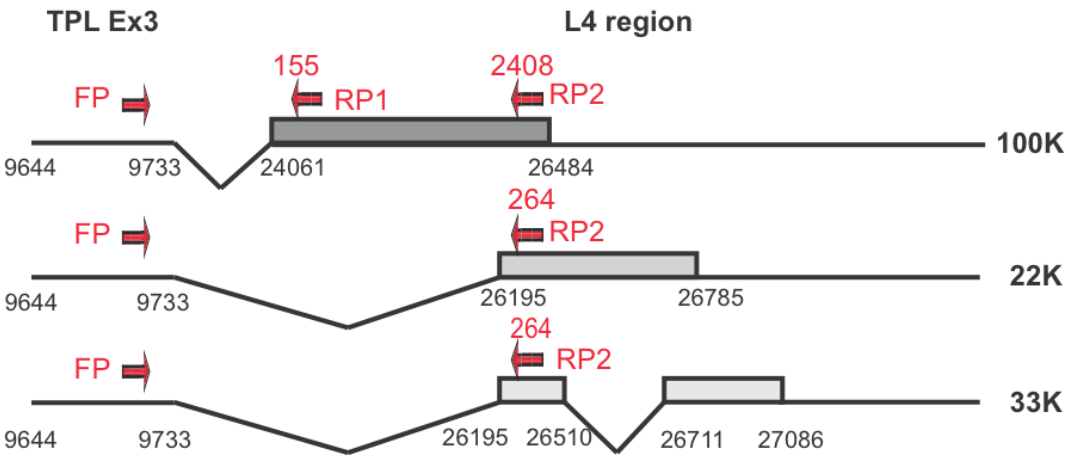

Figure 29 Organisation of the L4 100K, L4 33K and L4 22K open reading frames (ORFs) showing the pattern of mRNA alternate splicing.

Forward primer located in exon 3 of the Tripartite Leader Sequence: 5'- gcgtctaaccagtcacagtcg; Reverse Primer 1 (RP1) located in L4-100K unique open reading frame: 5'- tcacttcctcctcctcaagc; Reverse Primer 2 (RP2) located in the common open reading frame of L4-100K, L4-33K and L4-22K: 5'- gttgtagccatgctggaacc. Figures in red indicate expected band size on gel electrophoresis.

DNA bands were clearly visible and corresponded to the expected size for the primers. The most striking feature of the gel was that mRNA splice products were very similar across all the cell lines and both murine and human malignant cell lines demonstrated bands corresponding to the variably spliced mRNA transcripts 48 hours p.i. Qualitatively, PCR products corresponding to spliced mRNA for L4 100K and L4 22 and 33K were similar across all cells lines. This suggests that overall splicing of the late mRNA is functional in murine cells and qualitatively similar to that which occurs in human cells. Although not formally evaluated, there was no discernible difference in the quantity of the smaller splice products. The larger L4 100K splice product of 2408 base pairs was only detectable in the murine cell lines.

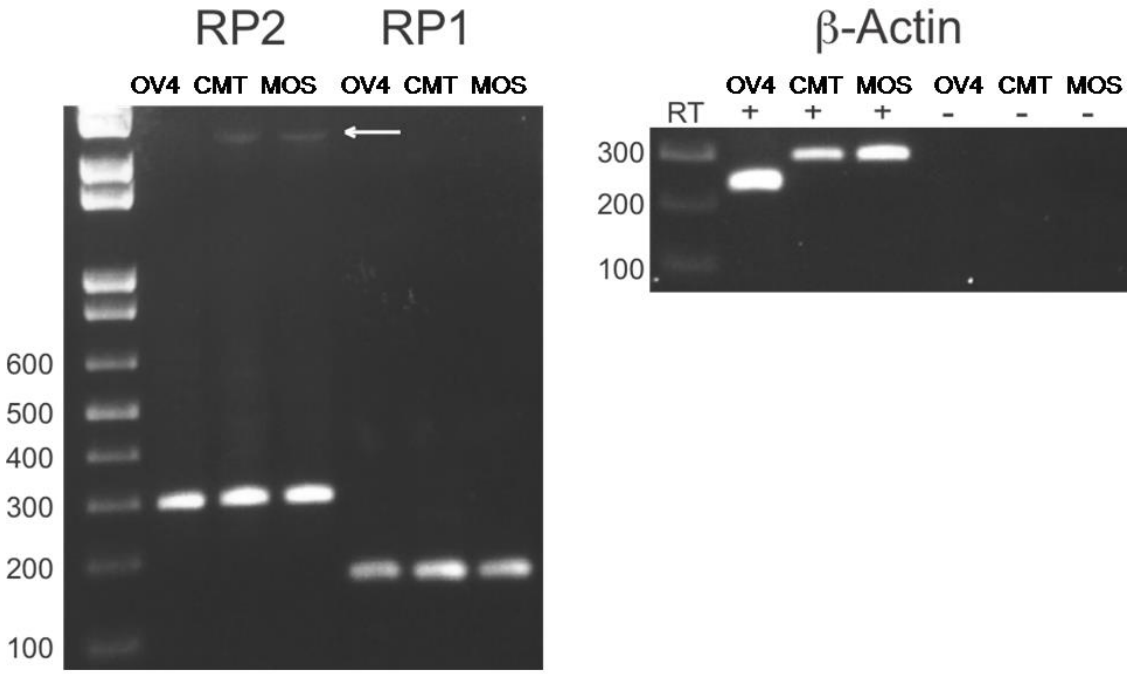

Figure 30 Qualitative analysis of post transcriptional L4 mRNA splice product.

RNA was extracted from OVCAR4, CMT64 and MOSEC cells 48h after infection with *dl*922-947 (MOI 10). After DNAse I treatment and reverse transcription, 50ng cDNA underwent PCR using TPL exon3 sense primer and either L4 reverse primer 1 or 2 as depicted. Expected band sizes were 155bp for RP1, and both 264bp and 2408bp (arrowed) for RP2. Samples were also analysed for β actin expression (right) +/- reverse transcriptase (RT).

4.5. Viral protein degradation

Cell lines infected with *dl*922-947 were also treated with the proteasome inhibitor MG132. The addition of the proteasome inhibitor 6 hours post infection did not result in an increased expression of late viral protein in the murine cell lines. Increased levels of p21 in the presence of MG132 demonstrated the effectiveness of this agent as p21, which is increased following adenovirus infection (Flak, Connell et al.), is subject to proteasomal degradation. Treatment with MG132 as described did not result in increased expression of late viral capsid proteins when murine cells were infected with *dl*922-947.

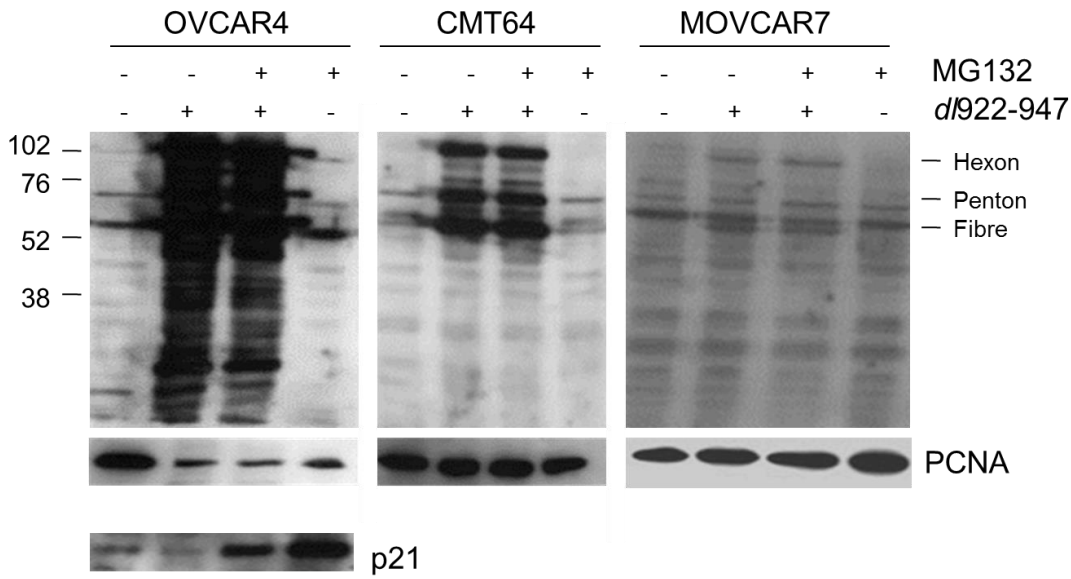

Figure 31 Effect of proteasomal inhibition on viral capsid protein expression.

5 x 10^5 cells were infected with *dl*922-947 (MOI 10) and treated with MG132 (10µM at 6 hours p.i.) prior to harvest 48 hours post-infection. Expression of viral capsid proteins was evaluated by immunoblot. Expression of p21 in human cells was also assessed to demonstrate effective proteasomal inhibition by MG132.

4.6. Integrity of host cell protein translation

To investigate whether the failure of viral protein expression resulted from global shut-off of protein translation in the infected cell, whole cell lysates from human and murine cells infected with *dl*922-947 (MOI 10) were run on a non-denaturing, 8% polyacrylamide gel and stained with Rapid Coomassie blue. In the human cell line OVCAR4, protein bands corresponding to the late viral protein hexon were visible at later time points, accompanied by visible attenuation of host protein bands. In the murine cell lines, there was no visible attenuation of host protein expression and hexon was not detected. This demonstrated that the failure of viral protein expression in murine cells could not be attributed to a global failure of protein synthesis initiated by the cell defence mechanisms.

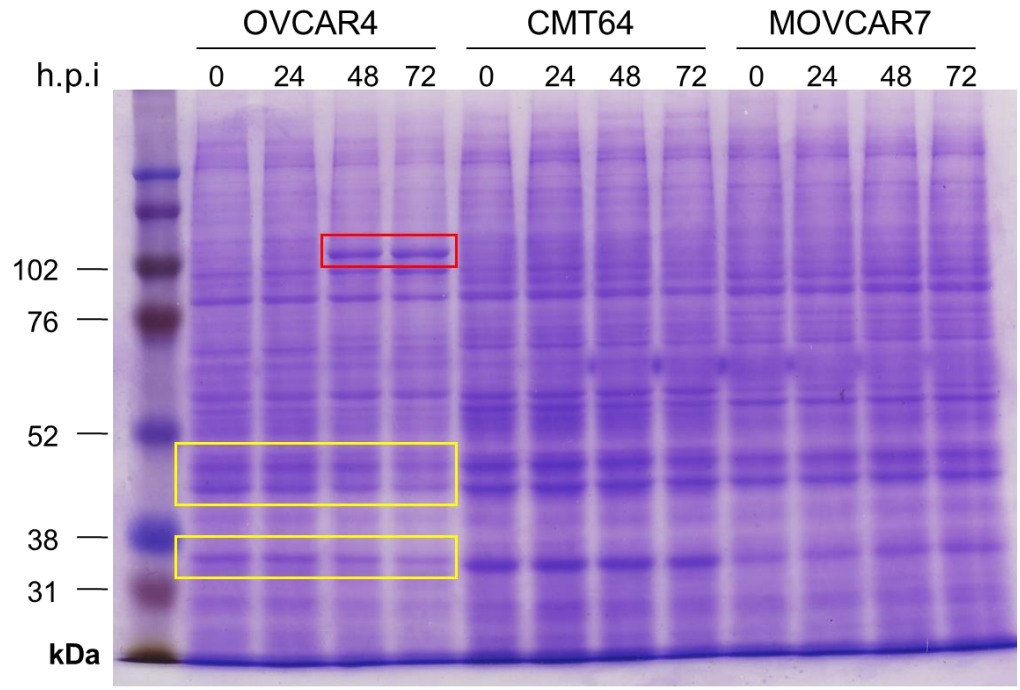

Figure 32 Assessment of host cell translational machinery.

The integrity of overall host cell translation was evaluated using Rapid Coomassie blue staining. Cell lysates were harvested up to 72 hours after infection with *dl*922-947 (MOI 10). The red rectangular box highlights the presence of viral protein hexon. The yellow rectangular box highlights the attenuation of other protein expression at later time points post infection in the human cell line OVCAR4.

4.7. Phosphorylation of eIF2α following adenovirus infection

In order to evaluate possible variations in the ability of murine and human cell lines to inhibit host cell protein synthesis post infection, phosphorylation of eIF2α by host cell PKR was evaluated by immunoblot by Dr. Kyra Archibald. As previously discussed in section 1.7.3.1, one of the host cell defences against adenoviral infection is to activate PKR. PKR phosphorylates Ser51 on the α-subunit of eIF2 and prevents the recycling of the guanine nucleotide exchange factor eIF2B. As a result, GDP-GTP exchange cannot take place and the tMetRNAi-eIF2-GTP initiator complex that binds to the 40s ribosomal subunit cannot be formed. Consequently, host cell translation is halted and viral replication is prevented. In view of the fact that Coomassie blue staining had

demonstrated an absence of protein expression attenuation in the murine cells, it was hypothesized that attenuation of PKR activation in the murine cell lines might be contributing to the failure to turn off host cell synthesis. 5 x 10^5 cells were infected with *dl*922-947 MOI 10 and lysates were harvested up to 72 hours p.i. Immunoblot assessment of eIF2α and Ser-51 phospho- eIF2α was undertaken. Extent of phosphorylation was assessed using ImageJ and was expressed a ratio of phosphorylated-eIF2α: total eIF2α normalized to uninfected cells.

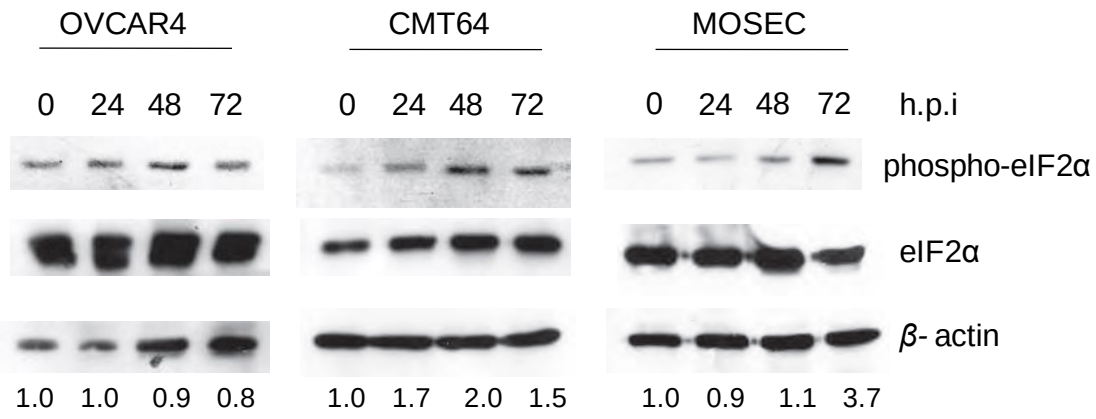

Figure 33 Phosphorylation of eIF2α following adenovirus infection.

5 x 10^5 cells were infected with *dl*922-947 (MOI 10). Protein was extracted up to 72h post-infection. Expression of eIF2α and Ser-51 phospho-eIF2α was assessed by immunoblot. Extent of phosphorylation was assessed using ImageJ – numbers below each blot represent phospho-eIF2α: total eIF2α ratio normalized to uninfected cells.

Phospho-eIF2α immunoblotting demonstrated no significant increase in eIF2α phosphorylation in OVCAR4 cells over 72h. Of note, there was detection of increased levels of the control protein β-actin in the human cell line. This was not thought to be secondary to increased protein loading and may have resulted from up-regulation of protein expression driven by viral factors. In CMT64 and MOSEC cells there was a discernible increase in the extent of eIF2a phosphorylation and no concomitant increase in the expression of β-actin. It is not known whether this was a downstream

effect of increased eIF2α phosphorylation. Again, re-evaluation of this phenomenon at lower MOIs may have given greater insight into the mechanisms linking PKR activity, eIF2α phosphorylation and viral control over host cell synthesis and whether the relationship was dose-dependent. The level of phosphorylation seen in the murine cells was counter-intuitive to the results of the Coomassie blot. Increased eIF2α phosphorylation should have resulted in a reduction of detectable protein in Figure 32.

4.8. Summary & Discussion

In this chapter, I sought to evaluate the point at which viral protein expression failed in murine cells following infection with a human adenovirus. Viral gene transcription, mRNA export and post transcriptional splicing, viral protein degradation and the activity of host cell translational mechanisms post infection were assessed.

4.8.1. Transcription

In general, the pattern of early and late gene transcription was similar across all cells lines evaluated and there was demonstrable transcription of all viral genes examined in murine cells. Overall, transcription of viral genes increased more slowly in the murine cells compared to human but, by 48 hours p.i. E1A transcript number in CMT64 cells actually exceeded that seen in human controls, whilst the number in MOVCAR7 was similar. Increase of the MOI to 100 resulted in a rise in transcription rates proportional to the higher dose of virus used. This suggested that transcription may be less efficient in murine cells, but that there was no fundamental transcriptional failure.

Reasons for this immediate delay in the transcription initiation of early viral genes in murine cell lines are likely to be due to host cell factors. Effective binding of crucial host cell molecules and interaction with host cell transcription factors are required to anchor the transcriptional machinery onto the E1A promoter/enhancer (Reach, Xu et al. 1991; Song, Hu et al. 1996; Song and Young 1997). The initially lower rates of viral

early gene transcription in murine cells seen in my work may be attributable to problems with binding of murine host cell transcription factors to the human Ad5 E1A promoter required for transactivation. BLAST analyses of amino acid and nucleotide sequences of human and murine transcription factors such as E2F, Sp1 and ATF-1 demonstrate sequence homology of >75% for DNA and >90% for amino acids. However, levels of nucleotide or amino acid sequence homology between human and murine species do not necessarily provide information on resultant functional changes.

Gene transactivation also relies heavily on the promiscuity of the E1A protein (Pelka, Ablack et al. 2008). This, in turn, is dependent on the conformational plasticity of E1A and its ability to bring together host and viral transcriptional elements within a 3-dimensional structure. Incompatibility of the human viral E1A binding motifs and the murine host cell factors could result in inefficient binding and a subsequent reduction in transcriptional efficiency (Webster and Ricciardi 1991; Strom, Ohlsson et al. 1998; Pelka, Ablack et al. 2008). However it is interesting to note that even a molecule as promiscuous as E1A demonstrates variable transcription rates across different hAd serotypes (Ablack, Pelka et al. 2010). Consequently, cross-species variations in host cell transcription rates may be expected but do not preclude successful viral replication.

Most importantly these data demonstrate that murine cells are indeed able to produce mRNA transcript of viral genes. The interspecies cross-reactivity of murine E1A has been demonstrated by Ball et al. using plasmid constructs and supports the results seen in my work. MAV-1 E1A was able to transactivate the human adenoviral E3 promoter when transfected into human and murine cell lines (Ball, Williams et al. 1988). Here too, gene expression was lower in the heterogeneous system but the ability of human cells to recognise murine adenoviral E1A and produce a functional gene product was demonstrated. However, this work utilised a plasmid construct and

the end point was not successful adenoviral replication. As such, the temporal aspects of gene expression and regulation were not addressed and these may be important for the switch from early to late viral gene expression.

The late adenoviral genes evaluated in my work demonstrated two contrasting patterns of transcription rates within cell lines. All cell lines, human and murine, demonstrated high transcript copy numbers of L4 33K 6 hours p.i. (10^7 -10^8 copies per µg cDNA). In contrast, transcripts of L4 100K and the late structural gene Fibre had not risen from baseline at 6 hours p.i. This is due to the fact that transcription of L4 33K and 22K is under the control of the separate L4 promoter (L4P) that has recently been identified (Morris, Scott et al. 2010). By contrast, L4 100K expression is controlled by the MLP, which is activated later than L4P, by viral gene products acting in *cis* and is thus very dependent upon earlier viral protein expression (Yang and Maluf ; Tribouley, Lutz et al. 1994; Lutz and Kedinger 1996; Fessler and Young 1999; Ali, LeRoy et al. 2007; Backstrom, Kaufmann et al. 2010). L4P transcription factors have yet to be fully identified but include E1A, IVa_2 and E4orf3 (Morris, Scott et al. 2010).

My work shows that murine cells are able to support the transcription of significant numbers of both early and late human adenoviral gene transcripts. Levels of transcription demonstrated in murine cells did not support the hypothesis that reduced gene transcription accounted for the failure to express late adenoviral structural proteins in these murine cell lines.

4.8.2. mRNA processing & translation

Although mRNA was present within cells, its mere presence does not guarantee protein expression. mRNA undergoes extensive post-transcriptional modification before it is able to engage with the ribosome and undergo successful translation and protein expression. Post-transcriptional modification of viral mRNAs is key to ensuring progression of the viral life cycle and the production of infectious virions. One such

modification, the alternate splicing of pre-mRNAs produced by E1A and the MLTU, allows the viral products to control gene expression in a temporal fashion (Akusjarvi 2008).

Like transcription, effective viral pre-mRNA splicing requires interaction with key host cell molecules, including the host cell spliceosome. Presentation of pre-mRNA to the spliceosome is controlled by multiple *trans* and *cis*-acting factors. Qualitative analysis of L4 late viral mRNA showed no demonstrable difference in the adenoviral mRNA species in murine cells compared to those seen in the human control. Although not exhaustive, the uniformity of the results suggests that post transcriptional processing of these late genes was similar despite the multitude of host and viral factors that control alternate splicing. Of note, the detection of the larger L4 100K splice product was seen only in the murine cell lines. In view of the lower transcription rates of L4 100K in murine cells (Figure 27) this seems unlikely to be due to increased rates of gene transcription and raises the possibility that transcript copies accumulate as a result of failed translational mechanisms in the murine cells. The work undertaken on viral RNA presented here is not exhaustive and further RNA analysis, both qualitative and quantitative, is required. Northern blotting would allow more extensive qualitative comparison of the viral RNA species produced in the murine and human cell lines. Gel extraction, purification and sequencing of cDNA bands would allow comparison with predicted sequences and thus identification of fully processed mRNA. Mass spectrometry of RNA species could also be used to identify RNA species variations and relative quantification across species could be undertaken. Direct measurement of mRNA integrity with *in vitro* translation assays could also be performed. I chose to evaluate L4 products because of my interest in molecules important for late viral protein translation, but other key mRNA species which might be evaluated in this way could include E1A isoforms, intermediate molecules such as IVa_2 and also the E4 species. In addition, assessment of the nuclear:cytoplasmic ratios of L4 100K mRNA

transcript copies should be undertaken to ascertain if there is a cytosolic accumulation of this important mRNA species in the murine cells.

Export of viral RNA to the cytosol is crucial for continued adenoviral replication as it is vital to ensure cytosolic ribosomal protein translation. This was clearly demonstrated by the work of O'Shea *et al.* (O'Shea, Johnson et al. 2004) on the oncolytic adenovirus *dl*1520. Originally this virus, deleted in the E1B 55K region, was assumed to replicate selectively in malignant cell lines because of their aberrant p53 pathways. In a normal cell, E1B 55K stabilizes p53 in order to prevent activation of cell apoptosis pathways. In malignant cells, p53 is frequently mutated and thus deletion of E1B 55K was assumed not to interfere with viral replication. However, it was noticed that the virus could replicate in cell lines with intact p53 pathways (Harada and Berk 1999). O'Shea *et al.* showed that *dl*1520 selectivity depended on whether the infected cells were able to replace the mRNA transport function of the E1B 55K protein, which facilitates the movement of mRNA from the nucleus to the cytoplasm (O'Shea, Johnson et al. 2004). My work has shown that reduced late viral protein expression does not arise from a failure of viral mRNA nuclear export. Cytoplasmic levels of early and late viral mRNAs demonstrated in the murine and human cell lines here may represent a combination of incomplete MLP activation and ineffective mRNA translation. Incomplete MLP activation has been shown to lead to increased levels of cytosolic mRNA for early viral products and translational failure of late viral proteins results in a deficit of late viral molecules acting *in trans* which are important for full activation of the MLP (Fessler and Young 1998).

Increased proteasomal degradation was also considered and excluded as a cause for the reduced expression of late viral proteins in murine cell lines. The proteasome inhibitor MG132 has been shown previously to function in murine cells (Yu and Lai 2005; Harris, Anderson et al. 2008). Inhibition of proteasomal degradation using

MG132 did not result in an increase in late viral protein levels in the CMT64 and MOVCAR7 murine cell lines.

In my work, rapid coomassie blue staining showed that host cell proteins were still expressed in murine cells following *dl*922-947 infection and thus a global failure of host cell translation was not the cause of low late viral protein expression. Upon viral infection, the host cell aims to halt protein translation via activation of the PKR pathway (Gale, Tan et al. 2000; Mohr 2005). Following activation by the binding of double-stranded RNA (dsRNA), PKR phosphorylates cellular targets, such as eukaryotic translation initiation factor 2 alpha (eIF2α). Phosphorylation of eIF2α results in shut down of host cell protein synthesis as cap-binding pre-initiation complexes are unable to form. To circumvent this defence mechanism, viral E1A blocks interferon-induced gene expression immediately after infection and viral VA-RNA_1 inhibits interferon-induced PKR activity (Burgert, Ruzsics et al. 2002). In addition, viral L4 100K uncouples ribosomal cap binding so that preferential viral protein translation can take place via ribosomal shunting (Cuesta, Xi et al. 2000). Thus the virus ensures that a global shut down of protein synthesis is not initiated and viral proteins are synthesised rather than host cell proteins. Therefore, there is a phased shift in protein production in human cells with the attenuation of some host cell proteins synthesis as viral protein expression increases. However, in my data, not only was there no visible hexon expression in murine cells, there was also no concomitant attenuation of other protein synthesis. This therefore raised the possibility of a problem with the shift from host cell protein expression to preferential viral protein expression. Evaluation of PKR activity by immunoblot of eIF2α showed increased levels of Ser51 phospho-eIF2α in the murine cell lines and demonstrated that there was no intrinsic malfunction of PKR activation in the murine cell lines. However, the results suggest that this rise in Ser51 phosphorylation was not functionally significant as the increased eIF2α phosphorylation seen on immunoblot was not accompanied by a concomitant abrogation of host cell

protein expression on Coomassie staining. Reasons for this are subject to conjecture and were not evaluated as part of this work but may be due to incomplete tyrosine phosphorylation of PKR. Work by Su *et al.* has examined the importance of tyrosine phosphorylation and its effects on functionality of the anti-viral response (Su, Wang et al. 2006). They demonstrated that full biological activity of PKR requires phosphorylation at three residues; Y101, Y162, and Y293. Their data demonstrated that tyrosine phosphorylation modulates PKR function independently of eIF2α phosphorylation. Importantly, Y101F mutation impaired the translational, antiproliferative and antiviral activities of PKR without affecting the ability of the PKR mutant to phosphorylate eIF2α. The exact mechanisms were not clear but it was proposed that phosphorylation of all three residues was required to achieve effective PKR signaling through interactions with downstream proteins (Su, Wang et al. 2006). As a result, incomplete tyrosine phosphorylation of PKR in the murine cell lines may fail to activate the PKR response fully, allowing host cell protein synthesis to continue at the expense of viral mRNA translation and in the presence of phosphorylated eIF2α.

In summary, although there were some delays in the initiation of transcription in one of the murine cell lines, this was not a phenomenon seen in both murine cell lines evaluated despite the fact that low levels of capsid protein expression have been demonstrated in both. No universal abnormality was detected in either the transcription levels or quality of the mRNA to account for the failure of protein expression. Viral mRNA export from the nucleus was demonstrated to occur and cytosolic concentrations of late viral mRNA species in the murine cells were comparable to the human control cell line. Increased protein degradation was also eliminated as a cause of decreased protein expression and, despite the apparent integrity of PKR activation in the murine cell lines, no global cessation of translation was demonstrated. Thus, failure of viral gene transcription and/or mRNA processing was excluded as a cause for failed late viral protein expression and a global cessation

of host cell protein synthesis secondary to PKR activation was not demonstrated. The focus of our investigation therefore changed to evaluation of the mechanisms and molecules involved in translational control.

5. Results: Overcoming failure of viral mRNA Translation

5.1. Introduction

Data presented in the previous chapter demonstrated that lack of viral gene transcription was not the main factor causing the failure of late viral protein expression in murine cell lines. Post transcriptional splicing variations in the L4 proteins, which are important for successful viral mRNA translation, also did not account for the failure of late gene expression. mRNA export and proteasomal degradation were also excluded as major causes for failure to express late viral proteins. Global shutdown of protein expression was not seen despite evidence of some increased phosphorylation of eIF2α, implying that the cellular PKR response was triggered but was either effectively inhibited by the virus (e.g. VA RNAs) or was not functionally active. It was therefore hypothesised that the major hurdle to successful virion production in murine cell lines was the inability to effect translation of viral mRNA by the host cell ribosomes.

Complete understanding of the mechanisms controlling preferential viral protein translation remains incomplete. Non-structural adenovirus proteins encoded in the L4 region are thought to have an important role. In particular, L4 100K protein has emerged in recent times as having a pivotal role in this process. L4 proteins are expressed early in infection (Larsson, Svensson et al. 1992). L4 100K acts to uncouple the cap-binding complex required for host cell protein translation via competitive antagonism of Mnk-1 (Cuesta, Xi et al. 2000) thus preventing eIF4E phosphorylation and halting cellular cap-dependent mRNA translation. Displacement of Mnk-1 is thought to be concentration dependent and thus, if insufficient amounts of viral L4 100K are produced, the switch to translation of late capsid proteins cannot take place (Cuesta, Xi et al. 2004). L4 100K then appears to co-ordinate the recruitment of many of the components necessary for viral mRNA translation into a translation complex. It

achieves this by utilising RNA binding sites located at fixed points along its length. Displacement of Mnk-1 results in the L4 100K C-terminal binding to eIF4G and facilitates recruitment of other components of the cap-binding complex such as eIF3 (Xi, Cuesta et al. 2004). Other RNA binding sites are used to recruit mRNAs from the cytoplasm (Adam and Dreyfuss 1987; Riley and Flint 1993). L4 100K demonstrates preferential binding of adenovirus late mRNAs via the TPL using a specific binding site in its middle region (Xi, Cuesta et al. 2004). Preferential TPL binding is mediated by the phosphorylation of tyrosine residues in the RNA binding site (Xi, Cuesta et al. 2005). In addition to drawing the viral mRNA physically into a translation complex with the ribosomes, the phosphorylation of tyrosine residues appears actively to promote ribosomal shunting, allowing the ribosomes to skip to the downstream AUG start codon of the viral mRNA which results in preferential viral mRNA translation (Hayes, Telling et al. 1990; Yueh and Schneider 1996; Yueh and Schneider 2000; Xi, Cuesta et al. 2005). L4 22K and 33K are also important for activation of the major late promoter in on-going viral infection. They up-regulate transcription of late viral genes by stimulating the major late promoter and controlling the splicing of late mRNA into its various spliceoforms (Tormanen, Backstrom et al. 2006; Morris and Leppard 2009; Backstrom, Kaufmann et al. 2010; Morris, Scott et al. 2010). Their effects are also thought to be concentration-dependent (Kanopka, Muhlemann et al. 1998; Tormanen, Backstrom et al. 2006).

Strategies were therefore devised to overcome translational problems, focussing on L4 non- structural protein expression and host cell interactions with the TPL.

The Tripartite Leader Sequence (TPL) is known to have a pivotal role in preferential viral protein translation (Logan and Shenk 1984; Berkner and Sharp 1985) and comprises a 200 nucleotide non-coding region that is found at the 5’ end of all late viral mRNAs (Chow, Gelinas et al. 1977) (Dolph, Racaniello et al. 1988; Zhang, Dolph et al.

1989). It is coded by 3 leader sequences (1, 2 and 3) and its first sequence encodes an essentially single stranded RNA sequence. This lends the RNA a plasticity that is permissive for ribosomal attachment. The other two leader exons encode sequences that are able to form a more rigid structure similar to the internal ribosomal entry site (IRES) structures first described in poliovirus (Pelletier and Sonenberg 1988). As such, the TPL eliminates the need for the host cell translation initiation factor eIF4F or the cap-binding complex (Zhang, Dolph et al. 1989). In addition to its role in translation initiation, the TPL acts to facilitate mRNA export (Huang and Flint 1998), mRNA stabilisation (Logan and Shenk 1984; Soloway and Shenk 1990) and may play a role in adenoviral cytotoxicity (van den Hengel, de Vrij et al. ; Subramanian, Vijayalingam et al. 2006).

The TPL consists of three exons 1, 2 and 3. An optional fourth exon, called the i-leader, is inserted between leaders 2 and 3 and is much larger than its counterparts as it consists of 400 base pairs. The role of the i-leader is not well understood. Work has centered upon its role in L1 mRNA transcripts. The i-leader exon is retained in the majority of L1 52/55K mRNA produced at early times, whereas it is mostly excluded from this and other MLTU mRNAs at late times (Chow, Broker et al. 1979). The inclusion or exclusion of the i-leader is regulated by E4orf3 and E4orf6, respectively (Ohman, Nordqvist et al. 1993; Nordqvist, Ohman et al. 1994) and its presence destabilizes the mRNA. A single base-pair mutation in the i-leader exon increases the L1 52,55K mRNA half- life from 3-4 hours to 26 hours (although such a dramatic extension has not been demonstrated in other i-leader containing mRNAs). It has therefore been postulated that the inclusion of the i-leader exon is another mechanism by which the virus can control late viral protein expression (Soloway and Shenk 1990). As my interest focussed on late viral transcripts, PCR primers were designed for the late mRNA TPL sequence and did not include the i-leader exon.

5.2. Susceptibility of cell lines to MAV-1 cytotoxicity

Susceptibility of the cell lines to death induced by the murine adenovirus type 1 (MAV-1) was assessed 120 hours post-infection (pi) by MTT assay Of the murine cell lines, CMT64 and MOVCAR7 were the most sensitive to cell death following MAV-1 infection with IC_{50} values of 0.4 and 0.2 pfu/cell. CMT93 cells (IC_{50} = 4.4 pfu/cell) and MOSEC (IC_{50}= 37 pfu/cell) demonstrated a greater susceptibility to MAV-1 induced cell death than the human cell line OVCAR4 (IC_{50} = 48 pfu/cell). MOVCAR 12 cells were resistant to MAV-1 induced cell death with an IC_{50} = 420 pfu/cell

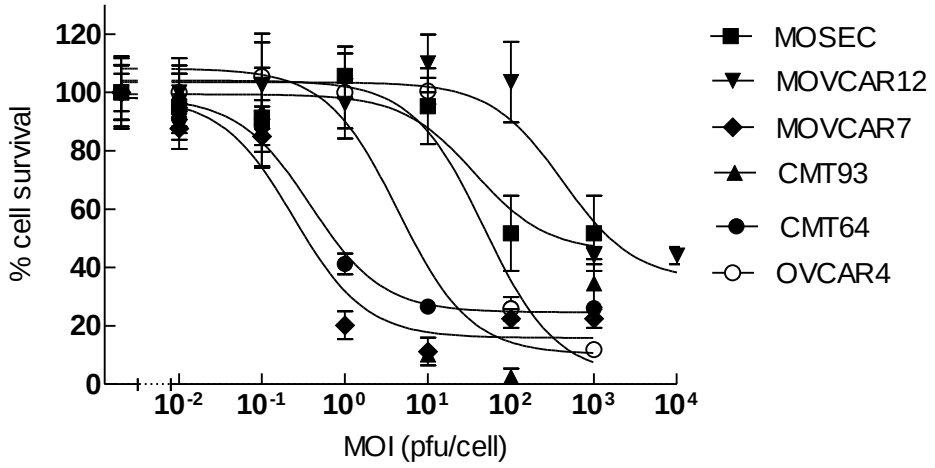

Figure 34 Cytotoxicity of MAV-1 in murine and human cell lines.

2 x 10^4 cells were infected with MAV-1 (MOI 0.01 – 10,000) in triplicate. Cell survival was assessed 120 hours pi by MTT assay. Error bars represent mean +/- standard deviation.

5.3. Co-infection with *dl*922-947 and MAV-1: MTT Assay

Because the two murine cells that I have investigated most are sensitive to cell killing by MAV-1, it was hypothesised that co-infection with MAV-1 might provide factors *in trans* necessary for late structural protein expression of the human virus *dl*922-947. On this basis, *dl*922-947 cytotoxicity assays were performed in the presence and absence of MAV-1. Twenty-four hours after plating, cells were infected with *dl*922-947

and MAV-1 at increasing titres as described in section 2.3 and cell survival assessed 120 hours post infection.

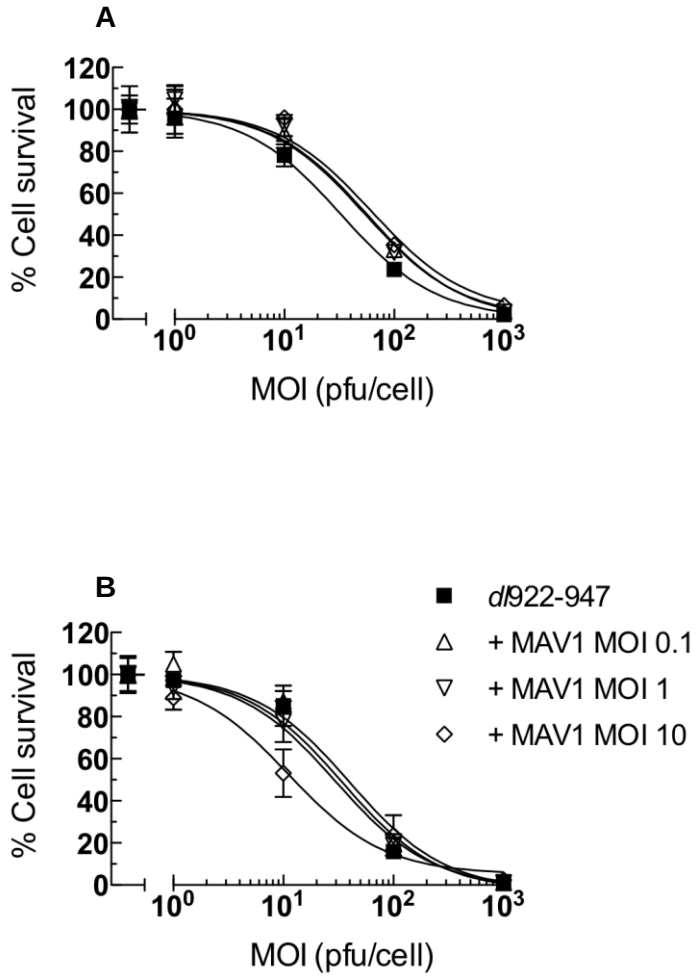

Figure 35 MTT assay following co- infection with *dl*922-947 and MAV-1.

2 x 10^4 CMT64 (**A**) and MOVCAR7 (**B**) cell lines were seeded in a 24-well plate. 24 hours later plates were infected with *dl*922-947 +/- MAV-1 at increasing titres. MTT assay was performed 120 hours p.i. Survival is normalised to remove the effect of MAV-1 alone and thus represents *dl*922-947-specific killing.

In MOVCAR7 cells, co-infection with MAV-1 at MOI 10 did result in increased *dl*922-947-mediated cell death; IC_{50} values in cells co-infected with *dl*922-947 and MAV-1 cells were lower than MAV-1 infected control; IC_{50} values (pfu/cell) control = 34.6; +MAV-1 MOI 0.1= 40.3; +MAV-1 MOI1.0= 29.6; +MAV-1 MOI 10= 11.2. Although possibly clinically relevant, the reduction in IC_{50} value was not statistically significant (p=0.75). This effect was not reproduced in the CMT64 cell line.

5.4. Co-infection with *dl*922-947 and MAV-1: Effect on the expression of human adenoviral late capsid proteins

The assays above suggested that co-infection of MOVCAR7 cells, if not CMT64, with *dl*922-947 and MAV-1 resulted in greater cytotoxicity. Further evaluation of this was undertaken using western blot to assess whether co-infection also resulted in an increased expression of human adenoviral late structural proteins.

MOVCAR7 cells were infected with *dl*922-947 and MAV-1 (both MOI 10) both individually and in combination. OVCAR4 cells were infected *dl*922-947 alone (MOI 10) as a positive control. Cells were harvested for western blotting 48 hours p.i. and viral structural protein expression assessed by immunoblot.

Immunoblotting with an anti-human Ad5 antibody demonstrated an increased expression of capsid proteins when MOVCAR7 cells were co-infected with *dl*922-947 and MAV-1. Increased expression of hAd5 hexon, penton and fibre was demonstrated in this cell line. Of note, viral capsid antibody minor cross-reactivity between the human and murine proteins was demonstrated, predominantly for hexon. Therefore, we concluded that the MOVCAR7 cell line could be forced to express greater levels of human adenovirus capsid proteins in the presence of MAV-1 co-infection. This implied

that molecule(s) supplied *in trans* by the murine adenovirus promoted human adenoviral gene expression.

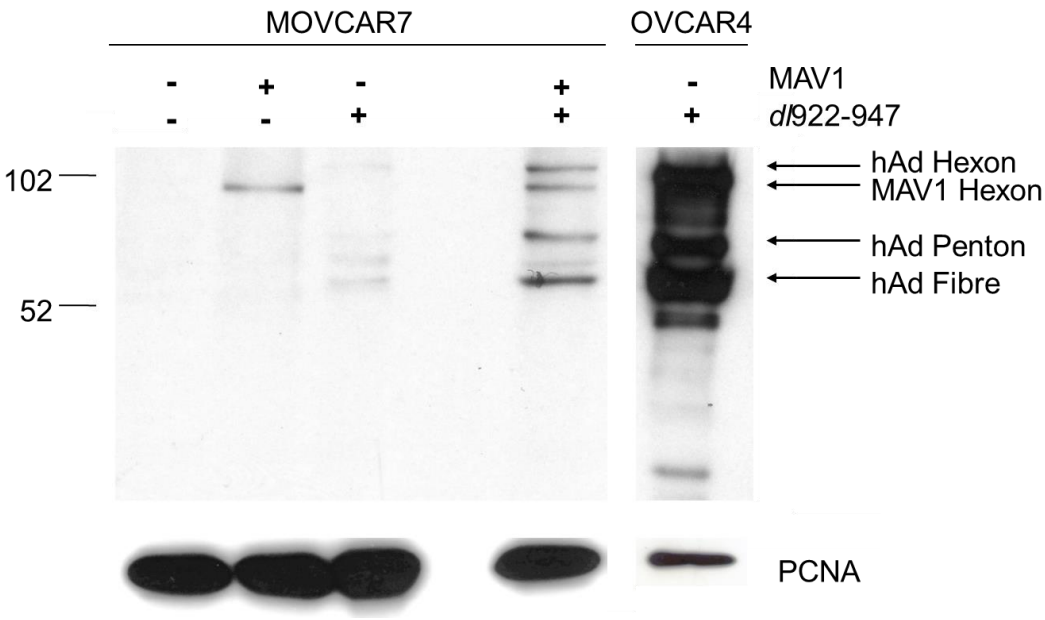

Figure 36 Expression of hAd5 capsid proteins following co-infection with *dl*922-947 and MAV-1.

5 x 10^5 MOVCAR7 cells were seeded onto 6cm plates. 24 hours later they were infected at an MOI of 10 with Ad5 *dl*922-947 and MAV-1 both individually and in combination. 5 x10^5 OVCAR4 cells were infected with *dl*922-947 (MOI 10) as a positive control. Cells were harvested for western blotting 48 hours p.i. and membranes were probed with goat polyclonal anti-Ad5 structural protein antibody at a concentration of 1:4000. Images shown are from the same membrane.

5.5. Evaluation of the role of the human adenoviral TPL in viral mRNA translation

The presence of the TPL at the 5' end of all late mRNA transcripts and its key interaction with the host cell ribosome at the initiation of translation earmarked the TPL as a molecule central to late viral protein expression and worthy of further evaluation. It was hypothesised that differences between the MAV-1 TPL and hAd5 TPL might account for the failure of murine cells preferentially to translate viral mRNA. There are

no published data delineating the DNA sequence for the MAV-1 TPL. However, proposed sequences for the MAV-1 TPL were obtained from Professors K. Spindler at the University of Michigan, USA and J. Boeke at Johns Hopkins University, Baltimore, USA. The Johns Hopkins group had extracted RNA from mouse brain microvascular endothelial cells (MBMEC). Using probes for the known sequences of MAV-1 hexon, fibre and pVII cDNA, the Boeke group used rapid amplification of cDNA ends (RACE) technology to obtain sufficient cDNA and 12 RACE clones were sequenced. Consensus sequences for the three exons comprising the TPL were identified but in 3 clones an additional leader exon was identified. Comparison of the known human Ad5 and proposed MAV-1 TPL sequences demonstrated divergence (Figure 37).

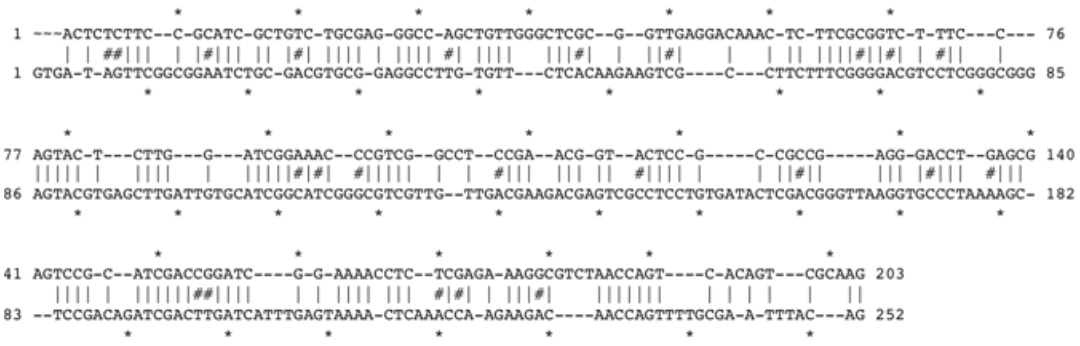

Figure 37 BLAST Analysis of hAD5 TPL sequence and proposed MAV-1 TPL sequence. Consensus sequence for MAV-1 TPL sequence was derived from late cDNA sequences using RACE technology (MAV-1 TPL sequences supplied by Professor J Boeke, Johns Hopkins University, Baltimore, USA). BLAST analysis demonstrated minimal sequence homogeneity between the hAd5 TPL sequence and the proposed MAV-1 TPL sequence.

To evaluate the importance of the murine TPL, firefly luciferase reporter gene constructs using the MAV-1 and hAd *dl*922-947 MLP and TPL sequences were cloned as illustrated below in Figure 38 .

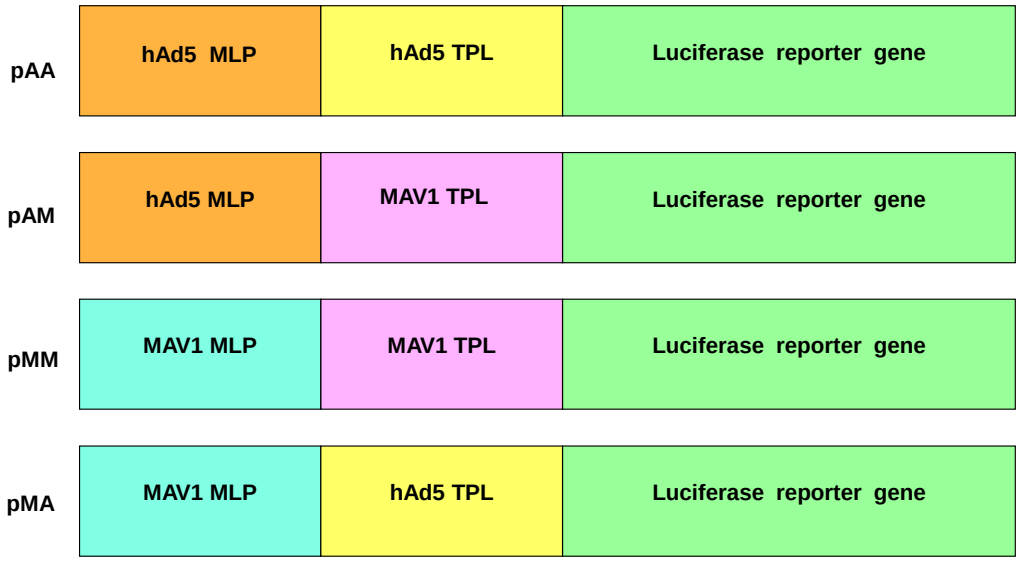

Figure 38 Schematic representation of the luciferase reporter gene constructs.

Luciferase expressing constructs pAA, pAM, pMM and pMA were used to assess effect of human and murine MLP and TPL on protein expression in human and murine cell lines. hAd5: human adenovirus serotype 5.

If central to successful adenoviral translation in murine cell lines, introduction of the MAV-1 TPL into the luciferase gene construct under the control of the hAd5 MLP (pAM) would result in increased luciferase activity when transfected into the murine cells compared to the purely human adenoviral construct pAA. The plasmid pTK Ren, which expresses Renilla luciferase under transcriptional control of the constitutive HSV TK promoter, was used as a transfection control.

The above constructs were transfected into human and murine cells lines as outlined in materials and methods. Luciferase activity was measured using Promega Stop & Glo Dual Luciferase Reporter Assay. Firstly, luciferase constructs were transfected into cells with a transfection agent:DNA ratio of 3:1 or 6:1 to ascertain optimal transfection ratios. In all cell lines human and murine, the ratio of 3:1 was chosen. Firefly luciferase activity for each construct was measured using a transfection reagent:DNA ratio of 3:1.

Reporter gene expression was normalised relative to the firefly:renilla ratio of the control plasmids pGL4.11 and pTK-Ren for each variant.

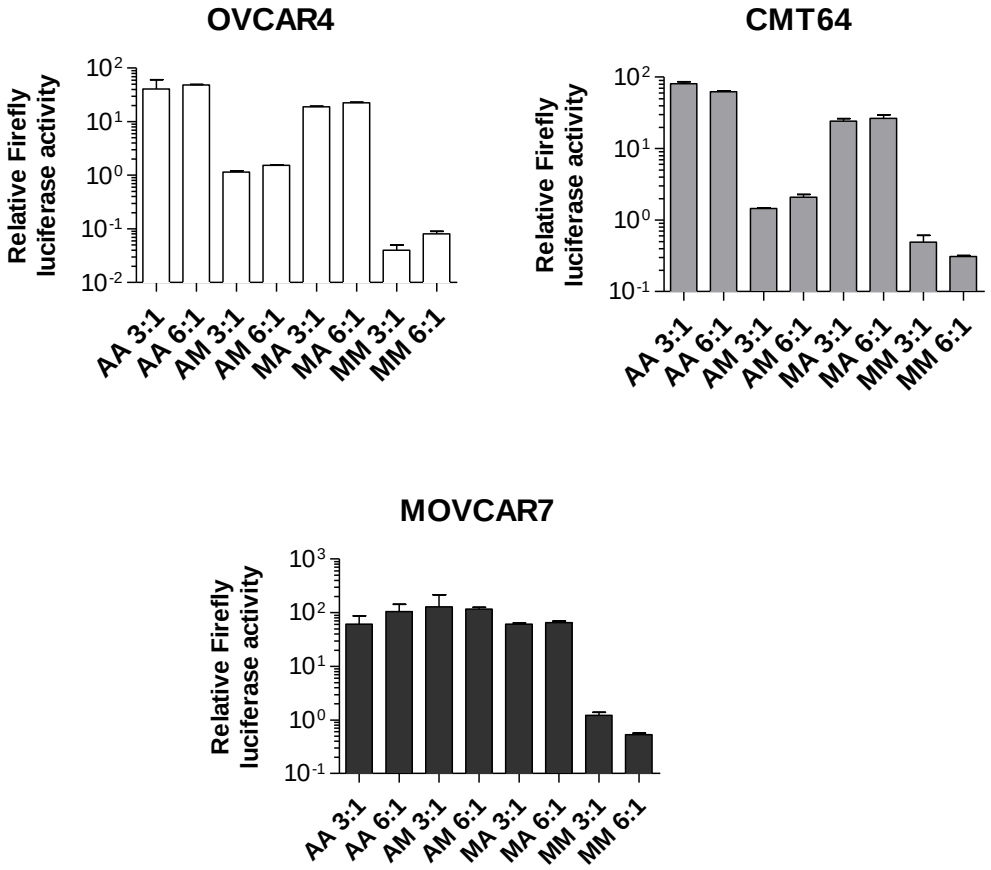

Figure 39 Evaluation of transfection ratios for luciferase reporter gene constructs.

5 x 10^5 OVCAR4 cells and 2 x 10^5 CMT64 and MOVCAR7 cells were plated onto a 6 well plate. 24 hours later each well was transfected with 2000ng of the firefly luciferase reporter gene construct using Fugene 6 at a transfection ratio of 3:1 and 6:1. Cells were harvested 48 hours post transfection. Firefly luciferase expression was measured using the Dual Luciferase Reporter Assay.

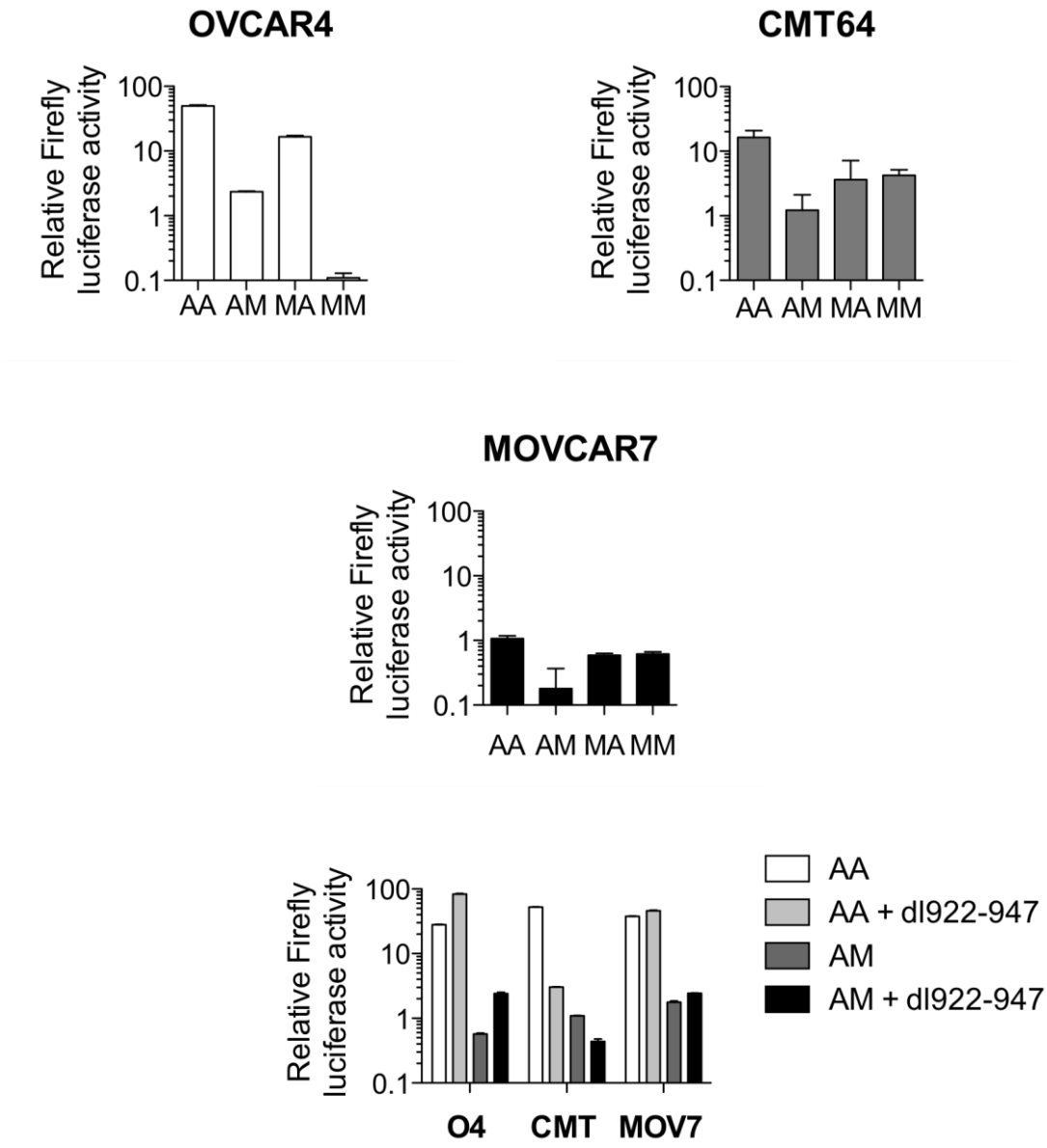

Figure 40 Relative Firefly luciferase gene expression in human and murine cell lines.
5 x 10^5 OVCAR4 cells and 2 x 10^5 CMT64 and MOVCAR7 cells were plated onto a 6 well plate. 24 hours later each well was transfected with 2000ng of the firefly luciferase reporter gene construct using Fugene 6 at a transfection ratio of 3:1. Cells were harvested 48 hours post transfection and firefly luciferase expression was measured using the Dual Luciferase Reporter Assay. Reporter gene expression was normalised relative to the Firefly:Renilla ratio of the control plasmids pGL4.11 and pTK-Ren for each variant. AA: hAd5MLP + hAd5TPL. AM: hAd5MLP + MAV-1TPL. MA: MAV-1MLP + hAD5TPL. MM: MAV-1MLP + MAV-1TPL. The effect of the addition of *dl*922-947 to luciferase expression for the AA and AM constructs in all cell lines was also assessed. Cells were infected with *dl*922-947 MOI 10 at 6 hours after transfection with luciferase gene construct.

The pattern of gene expression in the human control cell line OVCAR4 was in keeping with the hypothesis that inclusion of the murine TPL (mTPL) would reduce gene expression in human cells. Indeed higher levels of relative gene expression were seen in the constructs containing the human TPL (hTPL), pAA and pMA. Both constructs with the mTPL demonstrated reduced expression (pAM, pMM). Of note, the murine construct pMM demonstrated very low levels of gene expression in human cells; 20-fold less than the pAM construct and 500-fold less than the pAA construct.

In the murine cell lines greatest relative firefly luciferase activity was seen with the human pAA construct, albeit at lower levels than seen in the human control cells OVCAR4. Disappointingly, the inclusion of the mTPL in the pAM construct demonstrated lower levels of relative firefly luciferase activity than all the other constructs in the murine cells. pMA and pMM, the constructs containing the murine MLP (mMLP) had equivalent levels of firefly expression in both MOVCAR7 and CMT64 cell lines. In the CMT64 cells the ratio of pAM and pMM firefly luciferase activity was 3-4 times that of the transfection control. In the MOVCAR7 cells this ratio was lower at 0.6 of the transfection control.

Luciferase assays were also performed in the presence of *dl*922-947 infection, to assess whether the presence of other viral gene products could enhance the activity of chimeric promoter/TPL constructs. As shown in Figure 40, *dl*922-947 co-infection increased Firefly luciferase activity four to five-fold in OVCAR4 following transfection with both pAA and pAM. In MOVCAR7 cells, there was minimal increase in luciferase activity with the addition of virus (1.4 – 1.5-fold increase) and there was a marked decrease in reporter gene expression in CMT64 cells.

As a result of these largely negative data, further exploration of the role of TPL in promoting translation of viral mRNA in murine cells was abandoned.

5.6. Plasmids over-expressing L4 non-structural proteins as a strategy to increase late viral capsid protein production

Having established in the MOVCAR7 cell line that a molecule important for viral protein expression might be supplied *in trans* by MAV-1, it was hypothesised that this might be one of the L4 non-structural proteins. Confirmed sequences for the MAV-1 L4 proteins have not been published although amino acid homogeneity with human Ad5 has been demonstrated (Cauthen and Spindler 1996). Earlier data had suggested that late viral mRNA transcript copy numbers were comparable to human control and we hypothesized that inefficient late mRNA translation prevented effective late viral protein expression. Data has suggested that the L4 100K "switch" to cap-independent translation may be dependent on competitive displacement of the Mnk-1 molecule (Cuesta, Xi et al. 2000; Cuesta, Xi et al. 2004). We also postulated that a threshold concentration of transcript copy numbers might be required to trigger the switch to preferential late protein expression. We therefore hypothesized that increasing the amount of mRNA transcript copy numbers via exogenous plasmid expression of L4 proteins *in trans* might overcome such a hurdle if exstant. To explore this further, we used plasmids encoding Flag-tagged constructs of late non-structural adenoviral proteins L4 100K, 33K and 22/33K, which were kindly donated by Dr. Keith Leppard, Dept. of Biological Sciences, University of Warwick.

5.6.1. Plasmid transfection into murine cells

The plasmids pCMV 100K, 33K, 22K and 22/33K were transfected into CMT64 and MOVCAR7 cells using FuGene6 as described in Materials and Methods. 48 hours following transfection, cells were lysed and assessed for Flag expression by immunoblot. JH293 cells were infected with flag tagged pCMV100K as a positive control. The CMT64 cell line did not demonstrate detectable levels of plasmid gene expression. However, Flag-tagged 22K, 33K and 22/33K proteins were seen in the

MOVCAR7 cell lines. Flag-tagged 100K protein was not detected in either murine cell line.

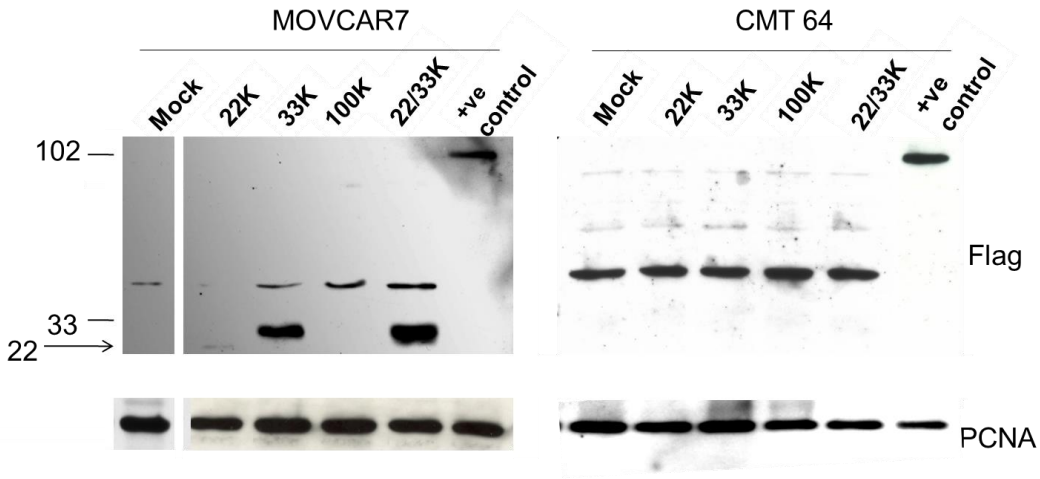

Figure 41 Plasmid transfection into murine cell lines.

Western blot of CMT64 and MOVCAR7 cell lysates harvested 48 hours after transfection with pCMV 22K, 33K, 100K & 22/33K. Cell lysates were run on an 8% SDS page gel. Membranes were probed with anti-Flag antibody 1: 800. Positive control was JH293 cells transfected with pCMV 100K.

5.7. Effect of pCMV L4 plasmids on the expression of late viral proteins following infection with *dl*922-947

Previous data has shown that co-infection with adenovirus can increase plasmid gene expression. This is thought to result from the virus' ability to upregulate transcription and facilitate translation of exogenous mRNA using viral molecules such as E1A, E2, E4, and VA RNA (Imperiale, Feldman et al. 1983; Kao and Nevins 1983; Kovesdi, Reichel et al. 1986; Nevins 1986; Reichel, Neill et al. 1989). Other viral molecules, such as VA RNA, have been shown to facilitate protein expression by stabilizing cytosolic mRNA (Strijker, Fritz et al. 1989). Therefore I examined whether co-infection of murine cells following L4 plasmid transfection could rescue expression of viral late structural proteins. MOVCAR7 cells were transfected with Flag-tagged pCMV 100K, 22K, 33K and 22/33K. 16 hours later cells were infected with *dl*922-947 at MOI 10. Cell

lysates were harvested 48 hours post infection with *dl*922-947 and were analysed both for Flag and adenoviral structural proteins expression by immunoblot.

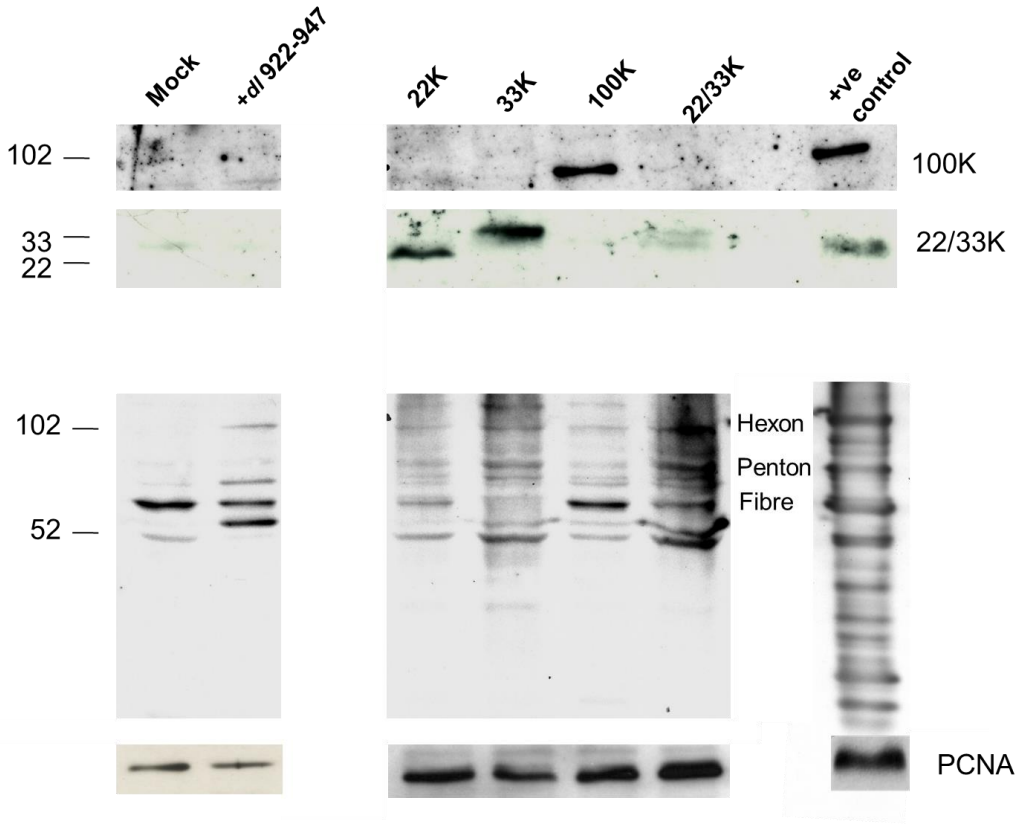

Figure 42 Effect of plasmids encoding L4 non-structural proteins on human Ad5 capsid protein expression in MOVCAR7 cells.

1 x 10^5 cells were plated and 24 hours later were infected with *dl*922-947 at MOI10. 16 hours post infection cells were transfected with pCMV 22K, 33K, 100K or 22/33K. Western blot of cell lysates harvested 48 hours after transfection is shown. JH293 cells transfected with pCMV100K served as a positive control. Cell lysates were run on 8% and 10% SDS page gel and were probed with anti-Flag antibody 1:800 and anti-Ad5 structural protein 1:2000 respectively.

In the presence of *dl*922-947 infection, successful transfection of all the L4 plasmids into MOVCAR7 cells was demonstrated by gene expression detected using immunoblot. However, increased viral capsid protein expression following infection with *dl*922-947 was not demonstrated despite L4 plasmid protein expression.

In summary, attempts to transfect CMT64 and MOVCAR7 cell lines with plasmids encoding L4 proteins met with variable success. The CMT64 cell lines failed to express any of the plasmid proteins. The MOVCAR7 cells did express the 22K, 33K and 22/33K plasmid products but failed to stably express the 100K protein. Interestingly, infection with *dl*922-947 16 hours post transfection did result in detectable expression of all the plasmid proteins in this cell line suggesting that adenoviral products were able to affect plasmid expression in this cell line.

5.8. L4 100K expression in murine cell lines

L4 100K was hypothesised to be a key molecule in effecting preferential late viral protein translation. Plasmids expressing flag-tagged L4 22K, 33K and 22/33K proteins could be successfully transfected into MOVCAR7 cells and did result in demonstrable gene expression. However, stable expression of the pivotal molecule L4 100K could not be demonstrated in the MOVCAR7 cells. This was thought to be due partly to technical problems with the Flag epitope. Therefore an antibody to human Ad5 L4 100K was obtained from Prof. W. Russell, University of St. Andrews (Scotland, UK). This allowed a more direct approach to the evaluation of this important molecule. As a first step in evaluating this candidate molecule, immunoblotting of all three murine cell lines and one human cell line was undertaken following infection with *dl*922-947. Lysates were harvested 48 hours p.i. and membranes were probed for hAd5 L4 100K.

Evaluation of L4 100K by western blot showed that it was produced by CMT64 and MOSEC cell lines at detectable levels although, like the other viral proteins, its expression was much lower than that seen in the human control cell line. L4 100K could not be detected in the MOVCAR7 cells following infection with *dl*922-947 at an MOI of 10 despite the fact that at 48 hours p.i. early and late viral mRNA transcript copy numbers for 100K ranged from 10^7 – 10^8 copies/mcg DNA loaded.

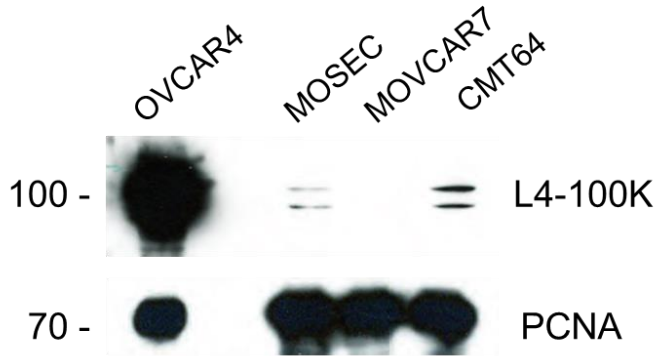

Figure 43 L4 100K expression in murine cell lines following infection with *dl*922-947.

5 x 10^5 cells from each cell line were infected with *dl*922-947 (MOI 10). Lysates were harvested 48 hours later and an equal amount of protein from each lysate was run on the same 10% SDS page gel and blotted for with antibodies to L4 100K at a concentration of 1:100 (courtesy of Professor W. Russell St. Andrew's University, Scotland, UK) and PCNA at a concentration of 1:1000.

5.9. Effect of co-infection with pCMV L4 100K plasmid on capsid protein expression

In view of previous problems transfecting CMT64 cells with pCMV- L4 plasmids, further evaluation of the effect of L4 100K over expression in viral capsid protein expression was undertaken in MOSEC cells. As discussed in section 5.6, we speculated that a failure of late viral protein translation might be overcome by exogenous plasmid expression of L4 100K by facilitating increased cap-independent mRNA translation. However, earlier evaluation of this was hampered by technical difficulties with antibody detection on immunoblot. Therefore, using the L4 100K antibody, I re-valuated the effect of exogenous plasmid expression on capsid protein expression.

Cells were transfected with pCMV-100K and 4 hours post transfection were infected with *dl*922-947 at MOI 10. Cell lysates were harvested 48 hours post infection and evaluated by immunoblot using antibodies to hAd5 L4 100K and Ad5 structural capsid proteins.

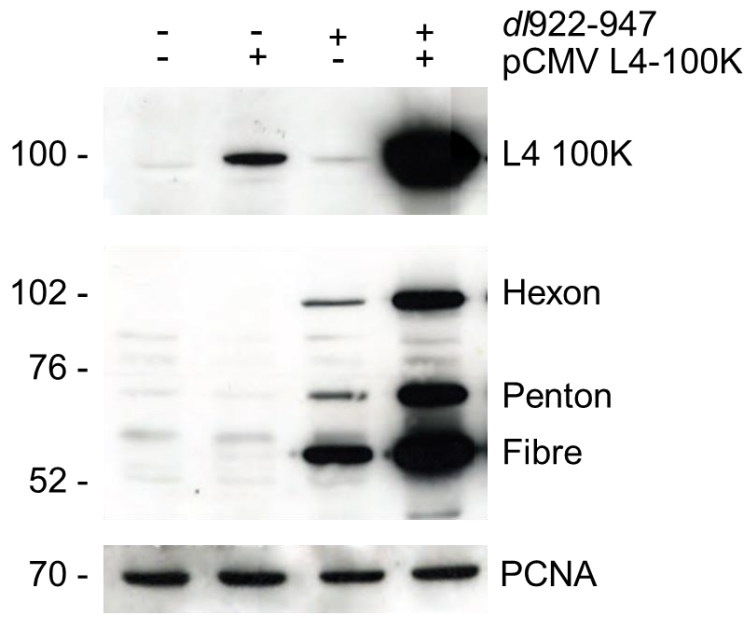

Figure 44 Transfection of MOSEC cells with pCMV-100K and effect on late viral capsid expression.

5 x 10^5 cells from each cell line were infected with *dl*922-947 (MOI 10). 2 hours p.i. cells were transfected with pCMVL4-100K. Lysates were harvested 42 hours later and were assessed by immunoblot with antibodies to L4-100K at a concentration of 1:100 (courtesy of Professor W. Russell St. Andrew's University, Scotland, UK) and PCNA at a concentration of 1:1000.

Western blotting demonstrated successful transfection with pCMV-100K plasmid as evidenced by visibly increased expression of L4 100K compared to untransfected control. This was accompanied by a marked increase in the expression of the viral capsid proteins. There was also greater expression of L4 100K in the presence of both plasmid and virus than with either alone, implying the existence of a positive feedback mechanism.

5.10. Construction of adenovirus Ad 100K

In view of these data, an E1-deleted, non-replicating adenovirus vector expressing L4 100K under the control of the CMV immediate early promoter in the E1 region was

generated (Ad100K). Construction of this vector is described in material and methods section 2.18.

5.11. Co-infection with adenoviridae Ad 100K and *dl*922-947

In order to assess the effect of concurrent Ad 100K on adenoviral late viral protein expression, co-infection assays were undertaken with *dl*922-947. 5 x 10^5 MOSEC cells were plated onto 6 cm plates. 24 hours later they were infected with *dl*922-947 at MOI 10 in the presence or absence of simultaneous Ad 100K co-infection at MOI 10. Expression of E1A, L4 100K and adenoviral structural proteins was assessed up to 72h post-infection by immunoblot.

Western blot demonstrated that simultaneous co-infection with *dl*922-947 and Ad 100K resulted in increased expression of L4 100K, which was maximal 48 hours p.i. Detectable L4 100K expression coincided with increased expression of the late viral capsid proteins hexon, penton and fibre at all time points post infection, strongly suggesting that the higher levels of L4 100K contributed to increased viral capsid protein production. Of note, at 48 hours p.i. when L4 100K and viral capsid protein expression were maximal, there was visible attenuation of E1A expression in the co-infected samples. This was not evident in the lysates infected with *dl*922-947 alone suggesting that L4 100K and/or increased expression of late viral capsid proteins affected E1A expression as part of a negative feedback mechanism. Also of interest was the fact that even after L4 100K expression appeared to wane at 72 hours p.i., late structural protein expression continued unabated.

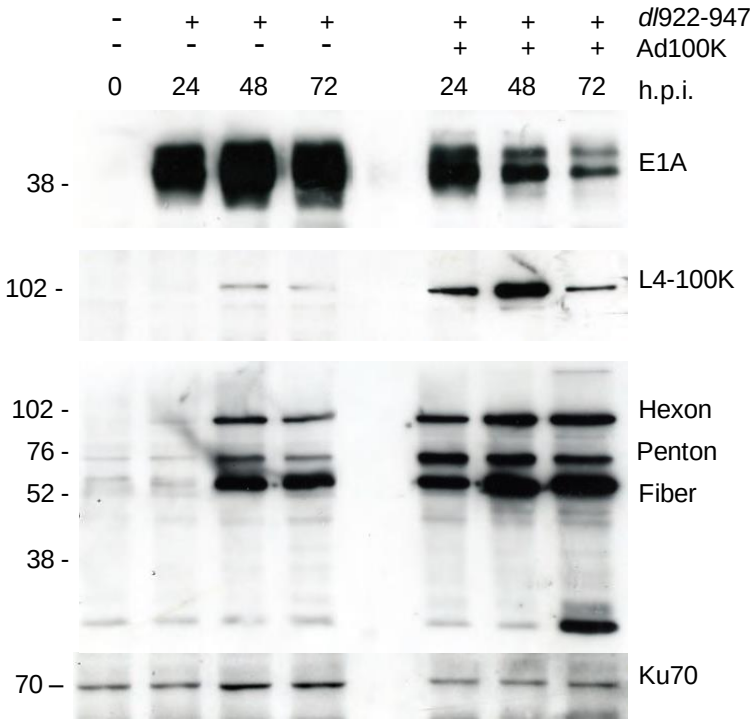

Figure 45 Effect of co-infection with *dl*922-947 and Ad 100K on E1A, L4 100K and adenoviral capsid expression.

5 x 10^5 MOSEC cells were plated onto 6 cm plates. 24 hours later they infected with *dl*922-947 at MOI 10 in the presence or absence of simultaneous Ad 100K co-infection at MOI 10. Expression of E1A, L4 100K and adenoviral structural proteins was assessed up to 72h post-infection by immunoblot.

5.12. Co-infection with *dl*922-947 and Ad 100K at staggered time points

In order to investigate further a possible relationship between L4 100K and late viral capsid expression and reduced E1A expression, co-infection assays were repeated but with the addition of the Ad 100K 0, 4 and 8 hours p.i. MOSEC cells were infected with *dl*922-947 at MOI10. Ad 100K (MOI 10) was added 0, 4 or 8 hours later. Expression of E1A, L4 100K and adenovirus structural proteins was assessed 48h after initial *dl*922-947 infection.

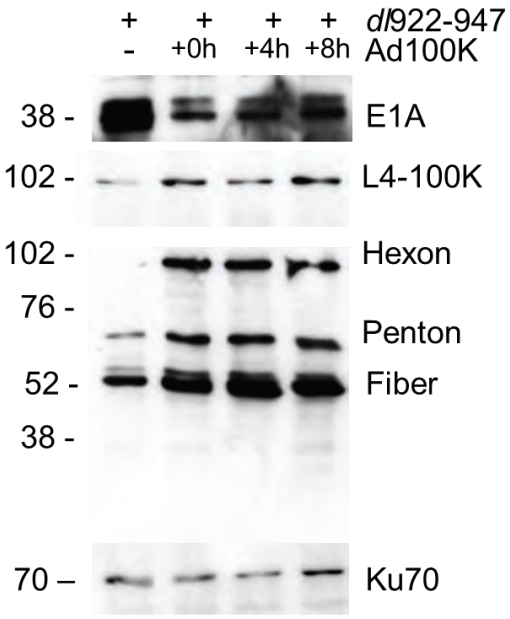

Figure 46 Infection with *dl*922-947 and co-infection with pAd 100K 0, 4 and 8 hours post primary infection.

5 x 10^5 MOSEC cells were plated onto 6 cm plates. 24 hours later they infected with *dl*922-947 at MOI 10. Co-infection with Ad 100K (MOI 10) was undertaken contemporaneously, 4 or 8 hours later. Expression of E1A, L4 100K and adenoviral structural proteins was assessed up to 72h post-infection by immunoblot.

Addition of Ad 100K at different time points resulted in similar levels of L4 100K and late adenoviral structural protein expression in lysates harvested 48 hours p.i. Co-infection with Ad 100K 8 hours after *dl*922-947 expression reduced E1A protein inhibition.

5.13. Effect of co-infection of *dl*922-947 and Ad 100K on early and late gene transcription rates

In order to ascertain whether increase late viral protein expression was attributable to increase gene transcription rate, MOSEC cells were infected with *dl*922-947 (MOI 10) and Ad 100K (MOI 10) either alone or together. Gene transcript copies for E1A, hexon and L4 100K were measured using qRT-PCR up to 48 hours post infection.

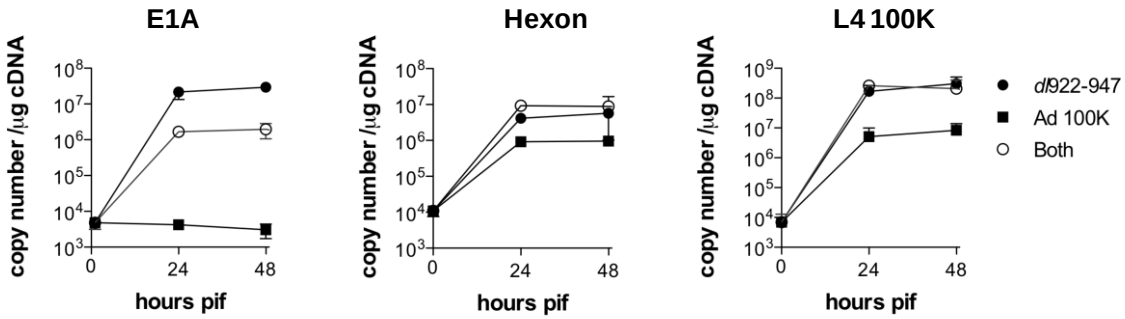

Figure 47 Early and late viral gene transcription rates in MOSEC cells following infection with *dl*922-947 and/or Ad 100K.

The number of E1A, hexon and L4 100K transcripts in MOSEC cells infected with *dl*922-947 (MOI 10), Ad 100K (MOI 10) either alone or together was measured using quantitative reverse-transcription PCR up to 48h post-infection. 1 x 10^5 cells were infected with *dl*922-947 and harvested up to 48 hours post infection.

Infection with Ad 100K alone did not generate E1A transcript copies as Ad 100K has no E1A gene. Co-infection with Ad100K and *dl*922-947 resulted in reduced E1A transcription rates than seen when MOSEC cells were infected with *dl*922-947 alone. L4 100K was transcribed after infection with Ad 100K alone but at lower levels than seen after infection with *dl*922-947 +/- Ad 100K. Of note, maximal L4 100K gene transcription was seen following infection with *dl*922-947 alone and this was not increased by co-infection with Ad 100K and copy numbers were 1.5 log scales greater than those seen after infection with Ad 100K alone. Overall, addition of Ad 100K

resulted in decreased transcription of the early viral gene E1A but did not significantly affect the rate of hexon or L4 100K transcription. It was also noted that there was demonstrable hexon transcription following infection with Ad100K alone, even though this virus does not express E1A, which is thought to be the prerequisite for transcription of all other viral genes.

5.14. Effect of co-infection of *dl*922-947 and Ad 100K on cell cytotoxicity in vitro

MTT assays were undertaken by Dr. Kyra Archibald to assess whether co-infection with *dl*922-947 and Ad100K resulted in increased cell cytotoxicity in vitro. MOSEC and MOVCAR7 cells were infected with *dl*922-947 MOI 10 alone and in combination with Ad 100K at MOI 10 and/or 100.

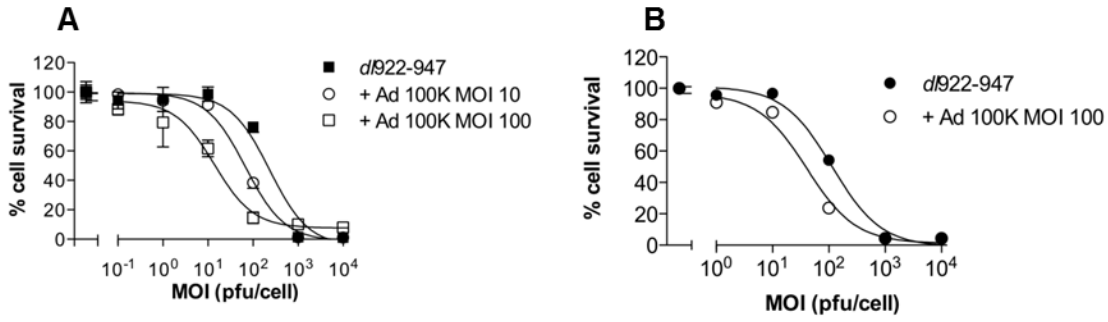

Figure 48 MTT assay following infection of murine cell lines with *dl*922-947 +/- Ad 100K. MOSEC (**A**) and MOVCAR7 (**B**) cells were infected with *dl*922-947 in the presence or absence of Ad 100K. Cell survival was assessed 120h later by MTT assay. Survival is normalised to remove the effects of Ad 100K alone and thus represent *dl*922-947-specific killing.

MTT assay demonstrated that co-expression of L4 100K resulted in increased cell cytotoxicity in both MOSEC and MOVCAR7 cell lines. Of note, the control arm in this experiment (infection with *dl*922-947) did not include an adenoviral control construct which would have been advisable.

5.15. Effect of co-infection with *dl*922-947 and Ad 100K on viral replication

Evaluation of whether co-infection with *dl*922-947 and Ad 100K increased the capacity of murine cells to support viral replication was undertaken using $TCID_{50}$ assay. MOSEC cells were infected with *dl*922-947 and/or Ad 100K at MOI10 and cells were harvested 48 hours post infection. Assessment using $TCID_{50}$ assay was undertaken as outlined in Material and Methods 2.4

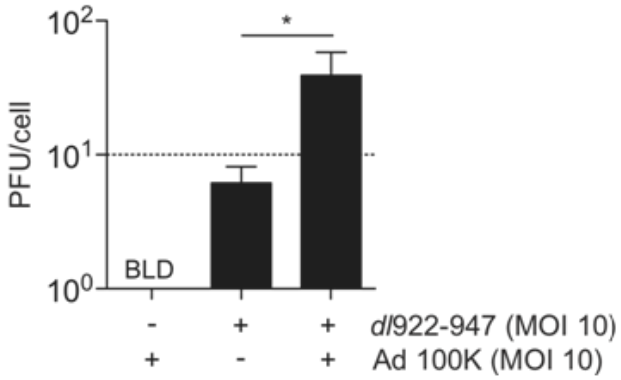

Figure 49 Infectious virion production following infection with *dl*922-947.

5 x 10^5 cells were infected with *dl*922-947 and/or Ad 100K both at MOI 10. Cells were harvested up to 72 hours pi. Intracellular infectious virion production was assessed by $TCID_{50}$ assay. Dotted line indicates input dose of virus. Error bars indicate mean +/- standard deviation, n = 3. BLD = below limit of detection.

Co-infection with Ad 100K resulted in increased virion production above that seen following infection of MOSEC cells with *dl*922-947 alone and, importantly, above the input dose of virus. However, virion production was still far below that seen in human cell lines when infected with *dl*922-947 (Figure 21).

5.16. Effect of co-infection with *dl*922-947 and Ad 100K on late protein expression in vivo

In order to assess the effect of co-infection of *dl*922-947 and Ad 100K in vivo, subcutaneous MOSEC tumours were grown on the left flank of ICRF nude female mice (experiments kindly undertaken by Professor Iain McNeish and Katrina Pirlo). Once tumours reached approximately 7 mm in diameter, *dl*922-947 was injected intra-tumourally on days 1-3 inclusive. Mice also received a single intratumoural dose of Ad 100K given alone on day 4. Tumours were excised on day 5 and expression of adenovirus structural proteins was assessed by IHC (bars represent 200 µm). In addition, the number of hexon transcripts was measured using quantitative reverse-transcription PCR.

Tumours co-infected with *dl*922-947 and Ad100K demonstrated increased expression of adenoviral structural proteins compared to those infected with *dl*922-947 alone and no significant increase in gene transcription rates was seen. However, concomitant expression of Ad100K did not result in the same levels or pattern of expression seen in human tumour xenografts (Figure 24).

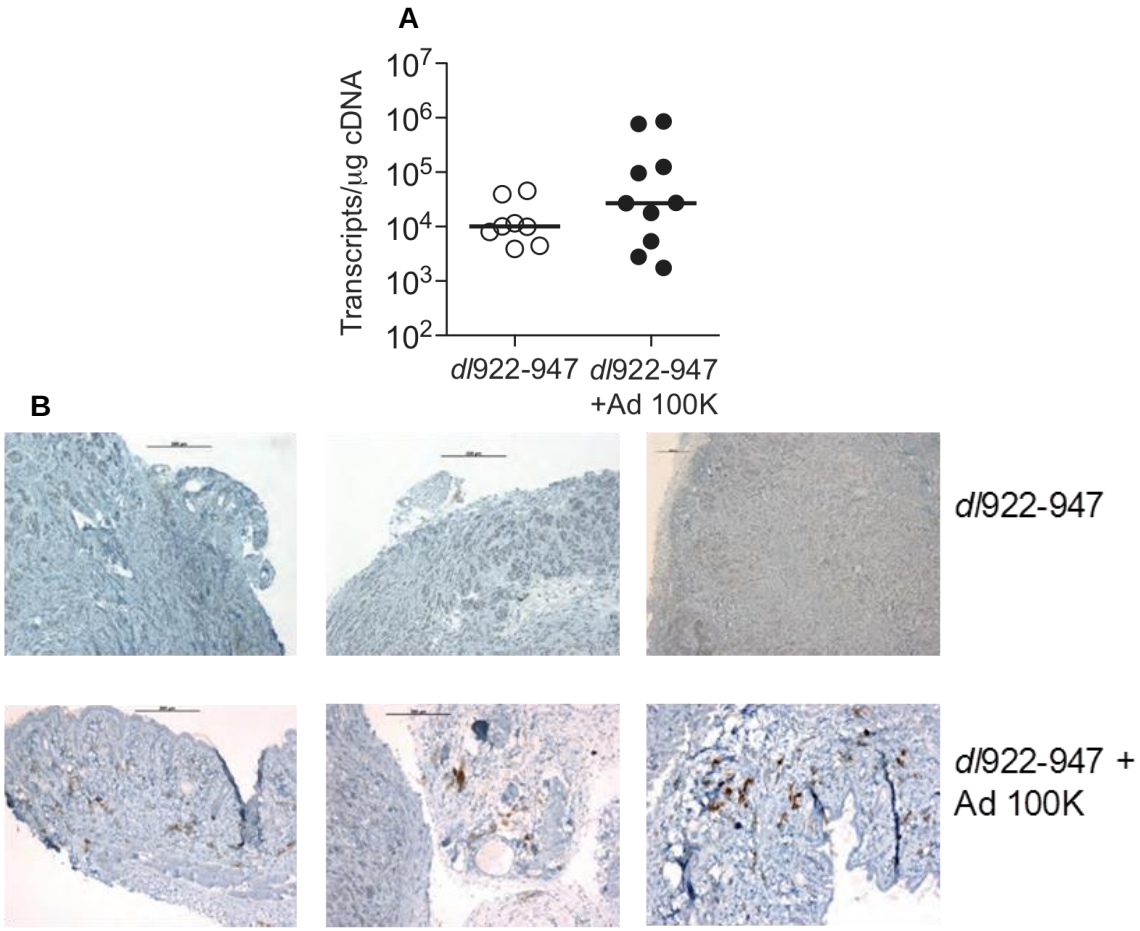

Figure 50 In vivo cytotoxicity of co-infection of MOSEC xenografts with *dl*922-947 +/-Ad 100K

Subcutaneous MOSEC tumours were grown on the left flank of ICRF nude female mice. Once tumours reached approximately 7 mm in diameter, *dl*922-947 was injected intra-tumourally ($5x10^9$ particles in 50 µl PBS on days 1-3 inclusive). Mice also received a single intratumoural dose of Ad 100K ($3x10^9$ particles in 50 µl PBS) or PBS alone on day 4. Tumours were excised on day 5, dissected in two and either snap frozen in dry ice or fixed in 4% paraformaldehyde. Expression of adenovirus structural proteins was assessed by IHC **(B)** (bars represent 200 µm). In addition, the number of hexon transcripts was measured using quantitative reverse-transcription PCR **(A)**.

5.17. Summary & Discussion

Data presented in this chapter established that murine cell lines are permissive to infection with MAV-1 and susceptible to cell death following this. We therefore explored the use of the murine adenovirus as a helper agent for *dl*922-947. MAV-1 has previously been demonstrated to be an effective helper virus for AAV-2 whose replication is most commonly effected by co-infection with hAd (Hoggan, Blacklow et al. 1966; Bhrigu and Trempe 2009). Co-infection with both murine and human adenoviruses was able to increase *dl*922-947-specific cytotoxicity in MOVCAR7 cells. Of much greater interest was the fact that this increase was accompanied by an increased expression of human adenoviral capsid proteins in these cells. This demonstrated that there was potential to increase capsid protein expression in the murine cell line using a helper molecule from the murine adenovirus. However, the mechanism of this increase in viral gene expression was not known. It is possible that co-infection with MAV-1 results either in increased hAd5 gene transcription or increased mRNA translation. The latter may be mediated by a MAV-1 molecule supplied *in trans* that exhibits sufficient homogeneity to its human adenoviral isoform that it can up-regulate human viral mRNA translation. Unfortunately, MAV-1 has not been the subject of much research and there is a dearth of tools, such as antibodies, available to investigate its function at a molecular level. As a result, we cannot draw conclusions from my data regarding MAV-1 late capsid expression levels or how increased expression of hAd5 capsid proteins may affect their expression. The absence of detectable MAV-1 fibre and penton expression is likely to be due to the failure of anti-hAd5 antibodies to bind to MAV-1 proteins.

Efforts therefore focussed on developing strategies to overcome a failure of adenoviral mRNA translation. The Tripartite Leader (TPL), the 5' untranslated region of viral mRNA that is thought to be important for preferential viral protein mRNA translation, was evaluated within a reporter gene construct. The TPL has been shown to enhance

translation at late but not early time points (Logan and Shenk 1984; Berkner and Sharp 1985; Dolph, Racaniello et al. 1988). The TPL is found at the 5' end of all late mRNA transcripts and thus was of interest because differences between human and murine adenoviral TPL sequences might account for the failure to translate the human viral proteins preferentially in the murine cells. Luciferase constructs combining human and murine MLP and TPL combinations were used to test the hypothesis that incorporation of the murine MLP and /or TPL would result in increased protein expression in murine cell lines. Results in the OVCAR4 cells confirmed the hypothesis with maximal luciferase expression with the homogenous construct of hAd5 MLP and TPL (pAA). Substitution of the hTPL with mTPL resulted in a greater attenuation of gene expression than substitution of the hAd5 MLP, corroborating work which has shown that the TPL is important for the preferential translation of late viral mRNA by the ribosome (Berkner and Sharp 1985; Dolph, Racaniello et al. 1988; Cuesta, Xi et al. 2001; Xi, Cuesta et al. 2004). As expected, the totally murine luciferase construct pMM resulted in very low levels of gene expression in OVCAR4 cells. Overall the OVCAR4 results correlated with our hypothesis with maximal gene expression with the wholly human construct and poor gene expression in the wholly murine construct.

Disappointingly, results in the murine cell lines were not as encouraging. The murine pMM construct generated a lower level of gene expression than that seen for the human pAA construct in both murine cell lines. The lowest rates of gene expression in murine cells were with the pAM construct, which were only 10% of that seen in the pAA plasmid despite incorporation of the mTPL. The reasons for this remain unclear. The apparent uniformity of pMA and pMM gene expression levels using the mMLP constructs in the murine cell may reflect the fact that mMLP activity is lower than its human counterpart (Song and Young 1997). Relatively low levels of gene expression seen in luciferase constructs containing mTPL even in the murine cell lines may reflect problems with the sequence for the MAV-1 TPL. The MAV-1 TPL sequence was

derived from PCR amplified cDNA using RACE technology. Whilst Professors Spindler and Boeke used recognised MAV-1 sequences as anchor primers during this process, the sequence for the TPL was a consensus sequence and was uncorroborated. The paucity of published data about MAV-1 and the absence of available molecular tools for its investigation meant that we were unable to undertake this. Therefore it is possible that errors occurred in the sequencing of the MAV-1 TPL and these, in turn, may have inhibited gene expression in the constructs containing the mTPL. During cloning, we excluded the i-leader sequence from the MAV-1 TPL reporter gene construct. The role of the i-leader remains unclear. It encodes a 13.6-kilodalton protein and is located between the second and third components of the tripartite leader sequence. It is produced from about 8 hours post infection until 35 hours post infection (Symington, Lucher et al. 1986) and its expression appears to destabilize late proteins and reduce their half life - in the case of L1 52,55K from 26 hours to 4 hours (Soloway and Shenk 1990). Its absence may interfere with the cycling of viral proteins, which seems to be important to push infection forward and achieve maximal rates of virion production. However, the i-leader sequence was also excluded in human adenoviral pAA and pMA constructs and therefore its omission is unlikely to be the major factor resulting in the contrasting results.

In order to try and identify possible helper molecules, work focussed on the L4 proteins. However, the lack of antibodies to the non-structural proteins 22K and 33K and initially L4 100K hampered direct evaluation. Attempts to express flag-tagged 22K and 33K plasmid constructs were not informative in CMT64 cells due to lack of successful transfection. MOVCAR7 cells supported expression of the 22K, 33K and 22/33K-encoding plasmids but did not demonstrate increased viral capsid expression. Expression of L4 100K was achieved following plasmid transfection in the presence of *dl*922-947 in the MOVCAR7 cells, but considerable cell death occurred, which prevented further evaluation. It is possible that L4 100K expression resulted in

inhibition of all host cell protein expression by the uncoupling of mRNA cap-binding by 100K product and that this, in turn, resulted in cell death. Unfortunately a balance between successful transfection and sustained plasmid expression could not be achieved and therefore robust data for L4 100K could not be obtained using the flag tagged-plasmids.

Latterly L4 100K expression was evaluated in three murine cell lines using a specific 100K antibody generously donated by Dr. W. Russell of St Andrews University, Scotland, UK. With this antibody, L4 100K was detectable in both the CMT64 and MOSEC cells following infection with *dl*922-947. However, L4 100K was expressed at much lower levels compared to human control. L4 100K expression was not detected in MOVCAR7 cells after infection with *dl*922-947 despite earlier data that demonstrated effective transcription in these cells. With the improved antibody, further work on the activity of L4 100K was continued by Dr. Kyra Archibald. The effect of pCMV100K co-transfection into MOSEC cells further supported the hypothesis that L4 100K was important for viral capsid gene expression with increased detection of hexon, penton and fibre proteins. However pCMV 100K co-infection only partially rescued the expression of the late capsid proteins and did not result in demonstrable expression of the numerous late viral proteins that are seen in human cell lysates.

Attenuation of both E1A and L4 100K expression was noted as late viral capsid expression increased. Other publications have commented upon E1A inhibition in the later stages of adenoviral infection. Late viral gene expression is thought to result in a negative feedback loop whereby late viral proteins inhibit early protein synthesis and allow host cell machinery to concentrate on late viral protein production and successful virion release (Fessler and Young 1998). The fact that delayed expression of L4 100K results in less E1A inhibition supports this theory of an inhibitory role for late viral proteins. Q-RT PR data presented here suggest that the mechanism for this effect is

an inhibition of E1A transcription however it remains unclear whether this is ascribable to a direct effect of L4 100K or another late viral protein whose expression is increased by L4 100K.

Co-infection of MOSEC cells with the *dl*922-947 and the recombinant virus Ad 100K demonstrated a similar pattern of partial recovery of late adenoviral gene expression. Increased L4 100K protein levels were demonstrated and were initially associated with greater expression of hexon, penton, fibre and latterly also with protein VI expression. The relationship between transcription rates of late viral proteins and protein expression requires further scrutiny. Infection with Ad 100K alone resulted in lower rates of L4 100K and Hexon mRNA transcription than seen with co-infection with *dl*922-947 as might be expected. Interestingly, concomitant infection with Ad100K and *dl*922-947 did not demonstrate increased late gene transcription rates over and above those seen with *dl*922-947 alone but did result in a marked increase in late protein expression. This suggests that our evaluation of mRNA transcription rates as being equivalent in murine and human cell lines may be somewhat simplistic. Co-infection of murine MOSEC cells may demonstrate late gene transcription rates equivalent to those seen following infection *dl*922-947 alone because more effective translation with co-infection may falsely reduce the total copy number detected. Importantly, we did not evaluate possible differences between nuclear and cytoplasmic mRNA copy numbers following infection. L4 100K protein is known to affect translational efficiency, a role that may be related to its function of shuttling hexon monomers from the cytoplasm to the nucleus for trimerization (Oosterom-Dragon and Ginsberg 1981; Cepko and Sharp 1982; Cepko and Sharp 1983; Morin and Boulanger 1986; Hayes, Telling et al. 1990; Iacovides, O'Shea et al. 2007).The addition of Ad100K may increase the transportation rate of mRNA species from the nucleus to the cytoplasm and thus facilitate increased translational efficacy within the cytoplasm. The *in vivo* data supports this theory of increased translational efficiency: co-infection of MOSEC tumours in ICRF nude female

mice demonstrated hexon expression without significant increase in hexon transcription rates. However, hexon protein expression within tumour samples was much lower than those seen in the human tumour xenografts despite the fact that transcript copy numbers were approximately the same (10^7) in both human and murine xenograft experiments. Additionally, it was noted that hexon particles in the murine tumours were generally located within the cytoplasm, in contrast to human xenografts where hexon was predominantly nuclear.

Increased L4 100K expression was associated with increased cell cytotoxicity in MOSEC and MOVCAR7 cell lines *in vitro* but the mechanisms of death remain unclear. In view of the fact that only a partial rescue of late capsid protein expression was seen, greater cytotoxicity may result from a fatal inhibition of translation secondary to increase L4 100K expression rather than successful virion production. $TCID_{50}$ data from the MOSEC cell line demonstrate an increase in virion production with Ad 100K co-infection despite only a partial rescue of late protein expression on immunoblot but virion numbers remain much lower than those seen in the human cell lines and cannot account for the increased cytotoxicity seen at MTT with any certainty.

Latterly, work has been undertaken by Professor McNeish's team to examine L4 100K functionality and to identify which of its actions are aberrant in malignant murine cells. These data are contained within this thesis in the manuscript attached as Appendix I. Due to the intrinsic cytotoxicity seen with L4 100K co-expression, a novel inducible gene expression system in which L4 100K production lies under the control of a cumate-inducible promoter was used to evaluate the functional effectiveness of L4 100K co-expression (Mullick, Xu et al. 2006). This allowed tighter control of L4 100K expression and mitigated its cytotoxic effects. The mechanisms by which L4 100K promotes viral mRNA translation are complex and still incompletely understood: however, it binds to the C terminal of eIF4G and displaces Mnk-1 from the cap-binding

complex. L4 100K and Mnk-1 share a hydrophilically charged amino acid-rich sequence that is necessary for binding to eIF4G and is located between aa 280 and 345 (the RRK sequence). However, L4 100K has been shown to bind more avidly to eIF4G than either human or murine Mnk-1, thus displacing Mnk-1 (Cuesta, Xi et al. 2004). Successful displacement of Mnk-1 results in reduced eIF4E phosphorylation and theoretically permits increased viral mRNA translation. This in turn should reduce the number of viral mRNA transcripts in the cytosol and result in decreased PKR-mediated eIF2α phosphorylation. Using the cumate-inducible 100K system, a concomitant reduction of eIF4E and eIF2α phosphorylation in the presence of increased L4 100K and late capsid protein expression suggested that the exogenous L4 100K was functionally active and that the cap complex uncoupling function was intact in MOSEC cells. The integrity of this L4 100K function was demonstrated only within the cumate-induced L4 100K system so eIF4E and eIF2α phosphorylation states should also be assessed within Ad 100K co-infection lysates. However the fact that immunoblot of lysates with both cumate-induced 100K and Ad 100K co-expression demonstrated almost identical patterns of increased late protein expression in MOSEC cells strongly suggest that this L4 100K function is intact in both constructs and this is supported by the presence of phosphorylated eIF4E and eIF2α. It remains unclear why inducible/ over-expression of the human, adenoviral molecule L4 100K protein should increase viral mRNA translation within the murine cell lines. Until more is understood about the role of L4 100K in preferential viral mRNA translation this remains subject to conjecture. My data has shown that selected murine cell lines do effect some L4 100K expression following infection with *dl*922-947 without the aid of exogenous L4 100K constructs and therefore these murine ribosomes are able to translate the human viral mRNA, albeit inefficiently. Increased numbers of L4 100K mRNA transcripts may well result in increased L4 100K protein expression in the murine cell lines. If Mnk-1 displacement by L4 100K is concentration-dependent (Cuesta, Xi et al. 2004), it is possible that even a small increment in cytosolic L4 100K would lead to increased cap-

independent translation and thus increased late capsid protein expression. This rescue of viral protein production may be partial because L4 100K levels remain insufficient to effect maximal cap-independent translation. It is also possible that maximal viral mRNA translation is subject to a “threshold effect” whereby a minimum concentration of other viral products is required for effective late viral mRNA translation to take place. Thus overall inefficiency in L4 100K mRNA translation may lead to the abrogation of other translational functions.

L4 100K has particular mRNA binding properties and contains several functional domains to facilitate its interaction with eIF4G, mRNA and host cell ribosomes (Riley and Flint 1993; Cuesta, Xi et al. 2004; Xi, Cuesta et al. 2004). Therefore, further work was undertaken to examine the extent of ribosomal loading onto viral mRNA in the murine cell lines and compare it with that seen in the human control. Ribosomal fractionation studies indicated that, in human cells, viral infection increased the amount of total RNA associated with heavy polysomal fractions. Viral infection resulted in little change and even decreased total ribosomal RNA in the murine cells. Quantitative RT-PCR demonstrated fewer hexon transcripts across all fractions in the murine cells and especially in the polysomal fractions, suggesting that there was inhibition of ribosomal loading onto viral mRNA transcript in the murine cells.

In MOSEC cells expressing cumate-inducible L4 100K, the amount of RNA associated with ribosomes following *dl*922-947 infection increased in the presence of cumate, as did the amount of hexon mRNA associated with light ribosomal fractions, but not heavy fractions. Xi *et.al.* suggested that, within the process of ribosomal shunting, the reaction between L4 100K and the TPL includes only one eIF4G molecule per mRNA copy and also that it is likely that only one 40S ribosome subunit is involved per TPL strand/eIF4G molecule (Xi, Cuesta et al. 2004). Therefore, reduced ribosomal loading is not unexpected. This paper also suggests that high levels of PABP are required to

maintain the integrity of the eIF4G-100K-ribosomal complex as it is shunted down to the AUG start site. Therefore, evaluation of eIF4G and PABP levels associated with the various ribosomal fractions might also contribute to our understanding of this process.

Further work by the Xi group has examined the structural basis by which L4 100K is able to interact with so many molecules and performs multiple functions at this pivotal point in the adenoviral life cycle (**Error! Reference source not found.**). They identified two distinct potential RNA binding motifs; firstly an RNA recognition motif (RRM) situated between amino acid residues 348 and 446 and also an RGG-rich binding motif between residues 727 and 764 (RGG box). Both the RRM and the RGG have independent ability to bind RNA but the presence of both has previously been described in other RNA binding proteins such as nucleolin (Ghisolfi, Joseph et al. 1992). Nucleolin is an abundant nucleolar protein that is involved in the early stages of ribosome assembly. It may be that incompatibility of human adenoviral L4 100K RNA binding sites and murine pre-ribosomal RNA precludes or impairs ribosomal attachment to human viral mRNA. It has previously been noted that, although overall hAd5 100K and the putative MAV-1 100K DNA sequences show high levels of homogeneity (approximately 70%), the RRM sequence of these viruses demonstrates minimal similarity (Cauthen and Spindler 1996). RRM sequence variation may prevent effective translational complex formation because of limited interaction between hAd5 100K protein and murine ribosomes. Co-infection with MAV-1 may increase late human adenoviral protein expression by facilitating viral mRNA/ ribosomal interaction and hence increased translation via a species-specific MAV-1 100K RRM. The lower level of mRNA ribosomal loading demonstrated in the murine cells may result from inefficient or ineffective ribosomal shunting. Impaired TPL/ ribosomal interaction may prevent “fast-tracking” of the TPL/eIF4G/ribosome complex to the AUG codon. This in turn may prevent the loading of additional ribosomes. The process of ribosomal shunting requires phosphorylation of L4 100K tyrosine at Y365 and Y682. Successful

interaction of L4 100K with the viral mRNA TPL is phosphorylation-dependent (Xi, Cuesta et al. 2005) and it is possible that the tyrosine phosphorylation necessary for ribosomal shunting is inadequate in the murine cell lines. To date, we have been unable to assess phosphorylation levels at these sites due lack of reagents.

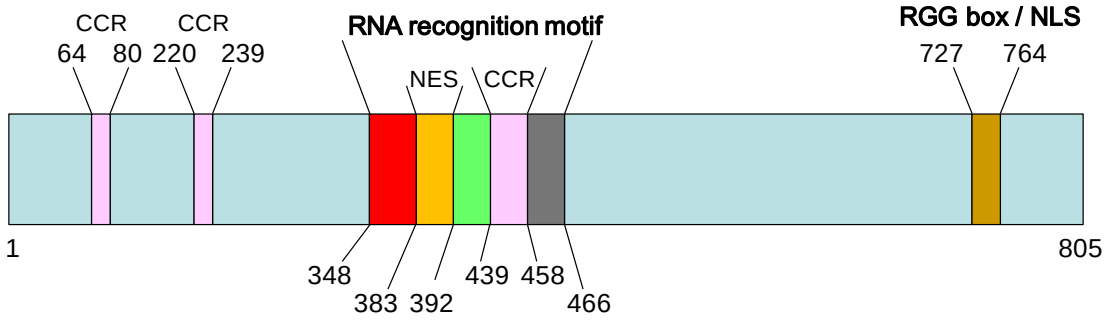

Figure 51 Predicted structural regions within the L4 100K protein.

Proposed functional domains within the human adenoviral L4 100K protein. Numbers refer to amino acid residue position; coiled-coiled region (CCR 439-458);RNA recognition motif (RRM 383-458); nuclear export signal (NES 383-392); RGG-rich RNA binding motif box and overlapping nuclear location signal (RGG / NLS 727-764). Adapted from Cuesta (Cuesta, Xi et al. 2004).

Little is known about the kinases that phosphorylate these residues and this requires further investigation. Multiple kinase pathways are activated following adenoviral infection (Suomalainen, Nakano et al. 2001; Liu, White et al. 2005; Rajala, Rajala et al. 2005). Of note, work by Schumann and Dobbelstein has identified ERK activity as central to successful viral replication and particularly important for late viral protein translation in H1299 cells (Schumann and Dobbelstein 2006). Blocking MEK/ERK signaling affected virus DNA replication and mRNA levels only weakly but strongly reduced viral protein production, mirroring the process seen in my work with the malignant murine cell lines. Importantly, the role of this kinase in viral protein translation appeared to be independent of PKR and Mnk-1 activity and also eIF4E/ eIF2α phosphorylation status, which would correlate with data presented here. Additionally, pharmacological inhibition of ERK phosphorylation reduced infectious

virion production by >100-fold in these cells, once again mirroring *dl*922-947 activity in malignant murine cells. Thus ERK and its activity in adenovirus-infected murine cells would be a candidate for further investigation.

Another important function of L4 100K is its orchestration of hexon trimerization. Each hexon capsomer is a trimer of three hexon monomers that are assembled in the cytoplasm before being imported to the nucleus for capsid assembly. L4 100K is required both for hexon trimerization and trimer entry into the nucleus (Cepko and Sharp 1982; Cepko and Sharp 1983; Hong, Szolajska et al. 2005). The effect of L4 100K co-expression on trimer formation has not been evaluated within this body of work. However, some evaluation of hexon nuclear transport has been undertaken and the results are presented in Appendix I. It was observed within the co-expression experiments that, whilst increased L4 100K expression did result in increased hexon expression in the murine xenograft models, the hexon was located predominantly in the cytoplasmic compartment of the cell on immunohistochemistry. This was in contrast to human xenografts infected with *dl*922-947, which demonstrated a predominantly nuclear distribution of hexon. It is possible that a failure of L4 100K export mechanisms and the consequent accumulation of cytoplasmic L4 100K in the murine cells prevent full rescue of late viral protein in the co-expression assays. Previous work has shown that viral proteins undergo extensive post-translational modification and that this is a mechanism that allows a switch in protein function. E1B 55K undergoes arginine methylation and this activates its function as a nuclear export protein (Kzhyshkowska, Schutt et al. 2001). Similarly L4 100K also undergoes extensive arginine methylation by protein-arginine methyltransferase-1 (PRMT1) at a site located in the RGG region in its C terminus and this is associated with increase viral replication (Kzhyshkowska, Kremmer et al. 2004; Koyuncu and Dobner 2009). Methylated L4 100K is exclusively nuclear and mutation of the RGG motif located between amino acids 741 -743 prevents L4 100K/hexon nuclear localization. Furthermore, inhibition of methylation

results in decreased late viral capsid protein expression and viral replication (Iacovides, O'Shea et al. 2007). Therefore there is a strong argument that L4 100K RGG methylation is required for L4 100K/hexon shuttling to the nucleus. It is possible that a deficit of arginine and/or arginine methylation in the murine cells results in the failure L4 100K/hexon shuttling to the nucleus. The consequent cytoplasmic accumulation of L4 100K may be sufficient to prevent full late gene expression and may explain why co-expression of L4 100K resulted in only a partial rescue of late viral protein expression in our work.

In summary, data presented in this chapter demonstrate that provision of a viral molecule in *trans* may be able to increase late viral protein expression. In my work, two candidate molecules, the adenoviral tripartite leader and L4 100K, were utilised in an attempt to overcome the hurdle to late adenoviral protein expression previously demonstrated in malignant murine cells. Manipulation of human and murine MLP and TPL constructs did not generate robust data, possibly due to incorrect sequencing of the mTPL. Work with L4 100K expression demonstrated that ectopic expression of hAd5 L4 100K in murine cell lines can augment viral protein expression. However, successful L4 100K co-expression resulted in only a partial rescue of late viral protein expression. Attempts to investigate the relationship between L4 100K and capsid protein expression have been undertaken by the McNeish team but are complicated by the functional complexity of this late viral molecule and the cytotoxicity of L4 100K over-expression. Concomitant dephosphorylation of eIF4E and eIF2-α suggest displacement of Mnk1 an uncoupling of host cell translational machinery occurs. However the formation of polysomes on viral mRNA is impaired in the murine cells. The reasons for this remain unclear and will form the basis for future work.

6. Final Discussion

6.1. Conclusions

The aims of this project were to identify the point at which human adenovirus fails to replicate within malignant murine cell lines and to engineer a solution to overcome that hurdle.

In this thesis I have presented data confirming that malignant murine cell lines are permissive to infection with human adenovirus type 5 vectors, which reinforces work published previously relating to infection of murine cell lines with human adenovirus wild types (Ganly, Mautner et al. 2000; Hallden, Hill et al. 2003). Data presented in Chapter 3 demonstrate not only that Ad5 vectors (as exemplified by the E1A CR2-deleted Ad5 *dl*922-947) can enter murine cells but also that viral DNA is transported to the nucleus where it is transcribed and undergoes active replication. Furthermore, the rate of viral DNA replication in murine cells can be equal to if not greater than that seen in a human control cell line OVCAR4. Furthermore, I have shown that murine cell lines are partially susceptible to cell death *in vitro* following infection with *dl*922-947 and the E1A wild-type control *dl*309 when evaluated using MTT assay but that these results are not reproducible in xenograft models of murine cancer. Furthermore $TCID_{50}$ data demonstrated that *in vitro* cytotoxicity cannot be attributed to lytic viral replication as murine cell lines with the lowest IC_{50} values do not produce infective viral progeny. It is therefore likely that cell death results from another cytotoxic process but what that is remains unclear and was not evaluated as part of this body of work.

Further investigation of why infectious viral progeny are not produced revealed significant reduction of viral protein expression in the murine cell lines *in vitro* and *in vivo*. Western blotting of lysates infected with *dl*309 demonstrated that reduced protein expression was not related to the 24 base pair deletion in E1A CR2 present in *dl*922-

947. Late viral proteins, especially the viral capsid proteins, were noted to be almost undetectable by immunoblot in the cell lysates of malignant murine cells infected with *dl*922-947 and infected xenograft models demonstrated a similar paucity of late capsid protein expression compared to human control.

Experiments described in Chapter 4 were undertaken as part of stepwise approach to establishing the cause of reduced protein expression. There was some cross-species variation in the rates of transcription at early time points post infection but by 48 hours post infection, transcript copy numbers for E1A matched if not exceeded their human counterpart. Of note, at MOI 100, E1A transcript numbers in the murine cells exceeded those in the human cells in a dose dependent fashion. This dose–dependent increase suggests that the mechanism of early viral gene transcription was not impaired in murine cell lines. However, it is also conceivable that impaired translation of E1A mRNA rather than efficient transcription accounts for their relative abundance in the murine cell lysates. Transcription of late genes, under the control of the MLP, was clearly reduced in the murine cell lines but, nonetheless, increased within the first 48 hours post infection and demonstrated a similar pattern of replication, albeit with reduced transcript copy numbers. L4 genes, under the control of the recently identified L4P promoter, demonstrated similar rates and patterns of transcription across human and murine cell lines early in infection but in the murine cell lines these began to decline from 48 hours post infection. The overall uniformity of the pattern of DNA replication and viral gene transcription across the species suggested that local factors, such as host cell transcription factors and DNA binding molecules, resulted in less efficient, but nonetheless extant replication of the viral components that could not account for the failure to produce infectious viral progeny. Moreover, regardless of relative rates of transcription within human and murine cells, the fact remains that, despite the presence of $>10^7$ copies of late viral genes/µg cDNA, these were demonstrably not translated into viral proteins. The integrity of viral mRNA cytosolic

transport mechanisms was demonstrated to be intact and there was no evidence to suggest that protein instability resulted in reduced viral protein expression.

Due to the disparity between their expression rates in murine cells, differences between early and late viral gene products became the focus of subsequent work. Unlike many early gene products, late gene mRNA transcripts undergo extensive alternate splicing, a process inherently prone to error and imperfections. Whilst my work did not demonstrate major qualitative defects in alternate splicing of the L4 gene products in murine cells, this evaluation was not exhaustive; the mRNA species examined were limited to L4 gene products, mRNA quantification was not undertaken and no functional analysis was performed. This is an area for future work and should include the analysis of other mRNA species. Genes of interest would include those that affect late viral gene expression such as E1A (including its various spliceoforms), intermediate molecules IVa_2 and pIX as well as L4 22K and L4 33K, all of which appear to be important for maximal MLP transactivation and late viral capsid formation (Tribouley, Lutz et al. 1994; Fessler and Young 1998; Fessler and Young 1999; Zhang and Imperiale 2000; Pardo-Mateos and Young 2004; Tormanen, Backstrom et al. 2006; Ali, LeRoy et al. 2007; Morris and Leppard 2009; Russell 2009; Backstrom, Kaufmann et al. 2010). Of particular interest would be the intermediate molecules IVa_2 and pIX, whose open reading frames are located between the E1 and MLTU genes on the 3'- 5' strand of the genome which suggests a role for them in the transition from early to late phases of infection. Whilst qualitatively there was no distinction between human and murine cell lines, PCR did suggest that there was an accumulation of L4 100K PCR product in the murine cell lines that was not present in the human control. This was of interest because it occurred on a background of reduced L4 100K gene transcription and pointed again at a possible failure of mRNA translation. In view of the hypothesis that the failure of human adenovirus to replicate in murine cells results from abrogation of L4 100K function, successful cytoplasmic export of its mRNA must be

established and requires further investigation. Subcellular fractionation of L4 100K mRNA should be undertaken to exclude a failure of L4 100K mRNA nuclear export. There was no evidence to support a failure of hexon mRNA nuclear export in my work. However, it is possible that cytoplasmic hexon mRNA levels are falsely elevated due translational failure. Evaluation of hexon mRNA subcellular fractions over several time points would give more information about how murine cells process this molecule as temporal factors may also be important.

Absence of a global failure of host translational machinery in conjunction with failed attenuation of host cell protein translation appeared to result in a concomitant up-regulation of PKR activity. Together with earlier data, this suggested that there was a failure of preferential viral mRNA translation. Subsequent work therefore focused on the viral factors executing this switch. Co-infection experiments using both the human adenoviral mutant *dl*922-947 and its murine counterpart MAV-1 were undertaken. These demonstrated an increase in the expression of human adenoviral capsid proteins suggesting that the murine virus provided a virally encoded molecule *in trans* that partially rescued late human adenoviral gene expression. Increased cytotoxicity was also noted with MAV-1 and *dl*922-947 co-infection, but it was not clear that this resulted directly from an increase in human adenoviral replication. Contamination of MAV-1 viral stocks precluded further investigation of these phenomena but future work could examine the effect of MAV-1 on transcription rates in order to establish that the increase of viral protein expression resulted from translational rather than transcriptional modification by the murine virus.

In view of the failure of late viral protein expression at the point of translation, strategies to overcome this hurdle focused on L4 gene products and specifically L4 100K. The role of the L4 non-structural proteins in late adenoviral infection has been discussed previously (section 1.8.3). The apparent accumulation of L4 100K mRNA in PCR

samples despite lower transcription rates and the pivotal role of this molecule in translation initiation, capsid protein shuttling to the nucleus and capsid formation made this viral protein particularly interesting. Plasmids encoding flag-tagged L4 22K, L4 33K and L4 22/33K were successfully transfected into MOVCAR7 cells and resulted in detectable protein expression on immunoblot for Flag. However, successful expression of these molecules on co-infection with *dl*922-947 did not result in increased viral capsid protein expression. Attempts to over-express flag-tagged L4 100K met with less success and stable plasmid transfection in the form of successful L4 100K protein expression could not be reliably demonstrated in either of the murine cell lines.

Attention therefore turned to the TPL as a target for manipulation in view of its role in late mRNA translation and ribosomal shunting (Yueh and Schneider 1996; Yueh and Schneider 2000). Attempts to increase protein expression in murine cells by combining human and murine adenoviral MLP and TPL sequences within a firefly luciferase reporter gene construct did not result in increased gene expression. Again, this work was hampered by a lack of molecular tools (in this case a confirmed sequence for the MAV-1 TPL) and it is possible that the MAV-1 TPL sequence used was incorrect.

Our attention returned to L4 100K for several reasons. Firstly, L4 100K alters cellular machinery to achieve preferential translation of viral mRNAs, initially by uncoupling host cell translational machinery and then by co-locating viral and host cell factors into an alternative translation complex (Hayes, Telling et al. 1990; Riley and Flint 1993; Cuesta, Xi et al. 2000; Cuesta, Xi et al. 2004; Xi, Cuesta et al. 2004; Xi, Cuesta et al. 2005). Coomassie staining had suggested that the process of switching off host cell mRNA translation was ineffective and this process is driven by L4 100K. Secondly, a possible accumulation of cytosolic L4 100K mRNA, seen in the PCR products, hinted further at a failure to translate this gene effectively in murine cells. Thirdly, L4 100K co-ordinates the nuclear accumulation of viral products for capsid assembly and is

necessary for successful hexon trimerization and its nuclear transport (Cepko and Sharp 1982). Finally, once in the nucleus, L4 100K acts as a scaffold molecule for the intranuclear assembly of adenoviral virions (Cepko and Sharp 1982; Morin and Boulanger 1984; Morin and Boulanger 1986; Hong, Szolajska et al. 2005). Thus insufficient nuclear L4 100K would certainly contribute to a failure to produce infectious virion progeny. In order to evaluate this molecule further, a specific L4 100K antibody was utilised. In view of previous difficulties with plasmid infection of CMT64 and MOVCAR7 cell lines, a third murine cell line, MOSEC was also included for evaluation. Following *dl*922-947 infection, CMT64 and MOSEC cell lines did support some L4 100K expression but at much lower levels than in human control, whilst there was no demonstrable expression MOVCAR7 cells. pCMV 100K transfection of the MOSEC cell line was successful and dramatically increased L4 100K expression. Crucially, co-infection of MOSEC cells with *dl*922-947 and pCMV 100K resulted in increased expression of the late viral capsid proteins hexon, penton and fibre.

In view of these encouraging data, a recombinant Ad5 vector encoding L4 100K was constructed to evaluate the its role and specifically to look for any improvement of late viral gene expression. Co-infection of MOSEC cells again resulted in an increased expression of hexon, penton and fibre. Maximal capsid protein expression at 72 hours p.i. coincided with reduced E1A and L4 100K levels suggesting that later viral molecules acted *in trans* to affect earlier viral gene expression. Further investigation demonstrated that co-infection with Ad100K resulted in reduced E1A gene transcription compared to *dl*922-947 alone, but did not alter hexon and L4 100K transcription rates. It is unclear whether this effect is a direct result of L4 100K expression or a sequelae of the increased expression of another late molecule mediated by L4 100K which in turn reduces E1A production. *In vivo* work correlated with *in vitro* analyses and co-infection of MOSEC tumours with *dl*922-947 and Ad 100K resulted in a partial rescue of late viral gene expression with detectable hexon expression within the tumour that was not

associated with increased in hexon transcription. However, hexon expression was significantly lower than that seen in the human control xenograft model IGROV1 and it was noted that hexon expression was predominantly cytoplasmic rather than the nuclear pattern observed in the human xenograft tumours. Differences between the location of hexon protein in the murine and human xenograft tumours suggested that nuclear import failed in the malignant murine cells.

Further investigation of L4 100K activity in MOSEC cells has been undertaken by the McNeish team and supports the hypothesis that an insufficiency of L4 100K or a functional failure of this molecule halts adenoviral replication in MOSEC cells. Uncoupling of the host cell cap binding complex appears to take place these cells, with a reduction in eIF4G and eIF2α phosphorylation. However, there is a reduction in the association of murine polyribosomes to human adenoviral mRNA and confocal microscopy confirms that L4 100K is found almost exclusively in the cytoplasm of MOSEC murine xenograft tumours in stark contrast to its nuclear location in IGROV1 human xenografts.

In summary, work presented in this thesis has identified a failure of viral protein translation as the major hurdle to the successful replication of the human adenoviral mutant *dl*922-947 in malignant murine cell lines. The human adenoviral protein L4 100K has a pivotal role in successful viral mRNA translation which is aberrant in the MOSEC cell line. Co-expression of L4 100K partially rescues late viral protein expression but does not result in full expression of late viral capsid proteins or the release of infective virion progeny. Investigation of L4 100K activity in MOSEC cells suggest that ineffective ribosomal loading, possibly in conjunction with impaired ribosomal shunting, and a failure of the L4 100K nuclear export function contribute to this. Future work should therefore focus on these areas.

6.2. Future Work

There are emerging data demonstrating that the ability of L4 100K to fulfil its multiple functions depends on post translational changes including phosphorylation and methylation. Tyrosine phosphorylation and arginine methylation have been identified to date and are important for successful mRNA/TPL/ribosome interaction and L4 100K/hexon shuttling to the nucleus respectively (Xi, Cuesta et al. 2005; Iacovides, O'Shea et al. 2007; Koyuncu and Dobner 2009). Both of these will require evaluation in the context of *dl*922-947 infection of malignant murine cell lines such as MOSEC. Arginine methylation of the L4 100K RGG region is important for L4 100K activity both in terms of hexon shuttling and L4 100K interaction with mRNA TPLs (Koyuncu and Dobner 2009) and therefore this area is of particular interest. Cellular arginine deficiency is a recognised feature of malignancy and results in a dependence on extracellular arginine termed 'arginine auxotrophy' (Delage, Fennell et al. 2010) and restriction of arginine availability has been identified as a potential anti-cancer therapy (Wheatley 2004). Methylation of amino acid residues in and around the L4 100K RGG site are important for its shuttling function. Quantitative evaluation of nuclear and cytoplasmic L4 100K mRNA should also be undertaken as part of this work as it is important to exclude an anomaly in this area. In view of the differences between MAV-1 and hAd5 RRM sequences, co-expression of plasmids encoding the MAV-1 RRM may also shed light on any possible role intra-species differences in this area may have on human adenoviral late mRNA translation in murine cells.

Work presented in this thesis has identified a failure of viral mRNA translation as the major hurdle to successful adenoviral replication in malignant murine cell lines. Aberrant L4 100K function has been identified as the likely cause of translational failure and initial investigation suggests that abrogation of post translational modification(s) to this protein may mediate this. Due to the multiplicity of L4 100K functions, it remains unclear whether one or all comprise(s) the rate-limiting step. Ineffective L4 100K

interaction with the viral mRNA TPL, reduced host cell ribosomal loading and aberrant nuclear shuttling of hexon molecules are all possible candidates and merit further evaluation. Possible roles for other L4 encoded proteins L4 22K and L4 33K and intermediate proteins IVa_2 and IX should also be considered. Once the molecule(s) and processes necessary to allow full and effective late viral protein expression to occur have been identified, steps can be taken to supply them exogenously and thus bring about full human adenoviral replication within malignant murine cells. Recent work in the field of hepatitis C virus (HCV) has shown that co-expression of human factors can be used to overcome hurdles to human viral infection in immunocompetent inbred mice. Murine humanisation was used to express factors required for human viral replication in immunocompetent inbred mice. SCARB1 is an essential human HCV entry factor in vivo. Rosa26-Fluc mice were crossed with $mSCARB1^{-/-}$ mice and offspring were injected with different combinations of adenoviral vectors expressing human SCARB1 and a selection of other human factors required for HCV entry. Absence of SCARB1 ($SCARB^{-/-}$) resulted in a 90% decrease in HCV infection rates compared to $SCARB^{+/+}$ mice and 50% less than $SCARB^{+/-}$ mice as evidenced by luciferase expression (Dorner, Horwitz et al. 2011). This is the first time that any step in the viral life cycle has been recapitulated in a mouse by the expression of human genes alone. The ultimate goal for our group would be the development of a transgenic mouse model that allowed controlled expression of molecule(s) essential for the replication of *dl*922-947 in an immunocompetent setting. I am hopeful that the work presented here on L4 100K takes us closer to the development of this and may ultimately allow us to take an important step forward in the development of this novel and promising therapy.

7. References

Ablack, J. N., P. Pelka, et al. (2010). "Comparison of E1A CR3 -dependent transcriptional activation across six different human adenovirus subgroups." J Virol **84**(24): 12771-12781.

Abou El Hassan, M. A., I. van der Meulen-Muileman, et al. (2004). "Conditionally replicating adenoviruses kill tumor cells via a basic apoptotic machinery-independent mechanism that resembles necrosis-like programmed cell death." J Virol **78**(22): 12243 -12251.

Adair, R. A., V. Roulstone, et al. (2012). "Cell carriage, delivery, and selective replication of an oncolytic virus in tumor in patients." Sci Transl Med **4**(138): 138ra177.

Adam, S. A. and G. Dreyfuss (1987). "Adenovirus proteins associated with mRNA and hnRNA in infected HeLa cells." J Virol **61**(10): 3276 -3283.

Ahmed, A. A., D. Etemadmoghadam, et al. (2010). "Driver mutations in TP53 are ubiquitous in high grade serous carcinoma of the ovary." J Pathol **221**(1): 49 -56.

Akusjarvi, G. (2008). "T emporal regulation of adenovirus major late alternative RNA splicing." Front Biosci **13**: 5006-5015.

Alba, R., A. C. Bradshaw, et al. (2009). "Identification of coagulation factor (F)X binding sites on the adenovirus serotype 5 hexon: effect of mutagenesis on FX interactions and gene transfer." Blood **114**(5): 965 -971.

Alberts, D. S., P. Y. Liu, et al. (1996). "Intraperitoneal cisplatin plus intravenous cyclophosphamide versus intravenous cisplatin plus intravenous cyclophosphamide for stage III ovarian cancer." N Engl J Med **335**(26): 1950-1955.

Alemany, R. and D. T. Curiel (2001). "CAR -binding ablation does not change biodistribution and toxicity of adenoviral vectors." Gene Ther **8**(17): 1347 -1353.

Alemany, R., K. Suzuki, et al. (2000). "Blood clearance rates of adenovirus type 5 in mice." J Gen Virol **81**(Pt 11): 2605 -2609.

Aletti, G. D., D. Nordquist, et al. (2010). "From randomized trial to practice: single institution experience using the GOG 172 i.p. chemotherapy regimen for ovarian cancer." Ann Oncol **21**(9): 1772 -1778.

Ali, H., G. LeRoy, et al. (2007). "The adenovirus L4 33 -kilodalton protein binds to intragenic sequences of the major late promoter required for late phase-specific stimulation of transcription." J Virol **81**(3): 1327 -1338.

Anderson, B. D., T. Nakamura, et al. (2004). "High CD46 receptor density determines preferential killing of tumor cells by oncolytic measles virus." Cancer Res **64**(14): 4919 -4926.

Armstrong, D. K., B. Bundy, et al. (2006). "Intraperitoneal cisplatin and paclitaxel in ovarian cancer." N Engl J Med **354**(1): 34 -43.

Asaoka, K., M. Tada, et al. (2000). "Dependence of efficient adenoviral gene delivery in malignant glioma cells on the expression levels of the Coxsackievirus and adenovirus receptor." J Neurosurg **92**(6): 1002 -1008.

Ashworth, A. (2008). "A synthetic lethal therapeutic approach: poly(ADP) ribose polymerase inhibitors for the treatment of cancers deficient in DNA double-strand break repair." J Clin Oncol **26**(22): 3785 -3790.

Audeh, M. W., J. Carmichael, et al. (2010). "Oral poly(ADP -ribose) polymerase inhibitor olaparib in patients with BRCA1 or BRCA2 mutations and recurrent ovarian cancer: a proof-of-concept trial." Lancet **376**(9737): 245 -251.

Auersperg, N., S. L. Maines-Bandiera, et al. (1994). "Characterization of cultured human ovarian surface epithelial cells: phenotypic plasticity and premalignant changes." Lab Invest **71**(4): 510 -518.

Backstrom, E., K. B. Kaufmann, et al. (2010). "Adenovirus L4-22K stimulates major late transcription by a mechanism requiring the intragenic late-specific transcription factor-binding site." Virus Res **151**(2): 220 -228.

Baird, S. K., J. L. Aerts, et al. (2008). "Oncolytic adenoviral mutants induce a no vel mode of programmed cell death in ovarian cancer." Oncogene **27**(22): 3081 -3090.

Baldwin, R. L., E. Nemeth, et al. (2000). "BRCA1 promoter region hypermethylation in ovarian carcinoma: a population-based study." Cancer Res **60**(19): 5329 -5333.

Ball, A. O., C. W. Beard, et al. (1989). "Genome organization of mouse adenovirus type 1 early region 1: a novel transcription map." Virology **170**(2): 523 -536.

Ball, A. O., M. E. Williams, et al. (1988). "Identification of mouse adenovirus type 1 early region 1: DNA sequence and a conserved transactivating function." J Virol **62**(11): 3947 -3957.

Banerjee, S. and S. Kaye (2011). "The role of targeted therapy in ovarian cancer." Eur J Cancer **47 Suppl 3**: S116-130.

Banerjee, S., S. B. Kaye, et al. (2010). "Making the best of PARP inhibitors in ovarian cancer." Nat Rev Clin Oncol **7**(9): 508 -519.

Barnes, M. N., C. J. Coolidge, et al. (2002). "Conditionally replicative adenoviruses for ovarian cancer therapy." Mol Cancer Ther **1**(6): 435 -439.

Beard, C. W., A. O. Ball, et al. (1990). "Transcription mapping of mouse adenovirus type 1 early region 3." Virology **175**(1): 81 -90.

Ben-Gary, H., R. L. McKinney, et al. (2002). "Systemic interleukin -6 responses following administration of adenovirus gene transfer vectors to humans by different routes." Mol Ther **6**(2): 287 -297.

Benedict, C. A., P. S. Norris, et al. (2001). "Three adenovirus E3 proteins cooperate to evade apoptosis by tumor necrosis factor-related apoptosis-inducing ligand receptor-1 and -2." J Biol Chem **276**(5): 3270 -3278.

Bergelson, J. M. (1999). "Receptors mediating adenovirus attachment and internalization." Biochem Pharmacol **57**(9): 975 -979.

Bergelson, J. M., J. A. Cunningham, et al. (1997). "Isolation of a common recept or for Coxsackie B viruses and adenoviruses 2 and 5." Science **275**(5304): 1320-1323.

Bergelson, J. M., A. Krithivas, et al. (1998). "The murine CAR homolog is a receptor for coxsackie B viruses and adenoviruses." J Virol **72**(1): 415 -419.

Berk, A. J. (2005). "Recent lessons in gene expression, cell cycle control, and cell biology from adenovirus." Oncogene **24**(52): 7673 -7685.

Berkner, K. L. and P. A. Sharp (1985). "Effect of the tripartite leader on synthesis of a non-viral protein in an adenovirus 5 recombinant." Nucleic Acids Res **13**(3): 841-857.

Bhat, N. R. and F. Fan (2002). "Adenovirus infection induces microglial activation: involvement of mitogen-activated protein kinase pathways." Brain Res **948**(1 - 2): 93 -101.

Bhrigu, V. and J. P. Trempe (2009). "Adeno -associated virus infection of murine fibroblasts with help provided by mouse adenovirus." Virology.

Bischoff, J. R., D. H. Kirn, et al. (1996). "An adenovirus mutant that replicates selectively in p53-deficient human tumor cells." Science **274**(5286): 373 -376.

Blackford, A. N. and R. J. Grand (2009). "Adenovirus E1B 55 -kilodalton protein: multiple roles in viral infection and cell transformation." J Virol **83**(9): 4000 - 4012.

Blair, G. E., S. C. Dixon, et al. (1989). "Restricted replication of human adenovirus type 5 in mouse cell lines." Virus Res **14**(4): 339 -346.

Blanchette, P., C. Y. Cheng, et al. (2004). "Both BC -box motifs of adenovirus protein E4orf6 are required to efficiently assemble an E3 ligase complex that degrades p53." Mol Cell Biol **24**(21): 9619 -9629.

Bluming, A. Z. and J. L. Ziegler (1971). "Regression of Burkitt's lymphoma in association with measles infection." Lancet **2**(7715): 105 -106.

Bocker, W. (2002). "[WHO cl assification of breast tumors and tumors of the female genital organs: pathology and genetics]." Verh Dtsch Ges Pathol **86**: 116-119.

Bookman, M. A., M. F. Brady, et al. (2009). "Evaluation of new platinum -based treatment regimens in advanced-stage ovarian cancer: a Phase III Trial of the Gynecologic Cancer Intergroup." J Clin Oncol **27**(9): 1419 -1425.

Bookman, M. A., H. Malmstrom, et al. (1998). "Topotecan for the treatment of advanced epithelial ovarian cancer: an open-label phase II study in patients treated after prior chemotherapy that contained cisplatin or carboplatin and paclitaxel." J Clin Oncol **16**(10): 3345 -3352.

Bookman, M. A., W. P. McGuire, 3rd, et al. (1996). "Carboplatin and paclitaxel in ovarian carcinoma: a phase I study of the Gynecologic Oncology Group." J Clin Oncol **14**(6): 1895 -1902.

Bos, J. L. (1989). "ras oncogenes in human cancer: a review." Cancer Res **49**(17): 4682 -4689.

Bosher, J., E. C. Robinson, et al. (1990). "Interactions between the adenovirus type 2 DNA polymerase and the DNA binding domain of nuclear factor I." New Biol **2**(12): 1083 -1090.

Bourke, M. G., S. Salwa, et al. (2011). "The emerging role of viruses in the t reatment of solid tumours." Cancer Treat Rev **37**(8): 618 -632.

Breitbach, C. J., J. Burke, et al. (2011). "Intravenous delivery of a multi -mechanistic cancer-targeted oncolytic poxvirus in humans." Nature **477**(7362): 99 -102.

Brink, M., A. F. de Goeij, et al. (2003). "K -ras oncogene mutations in sporadic colorectal cancer in The Netherlands Cohort Study." Carcinogenesis **24**(4): 703-710.

Bruning, A., T. Kohler, et al. (2001). "Adenoviral transduction efficiency of ovarian cancer cells can be limited by loss of integrin beta3 subunit expression and increased by reconstitution of integrin alphavbeta3." Hum Gene Ther **12**(4): 391-399.

Bullock, A. N. and A. R. Fersht (2001). "Rescuing the function of mutant p53." Nat Rev Cancer **1**(1): 68 -76.

Burger, R. A., M. F. Brady, et al. (2011). "Incorporation of bevacizumab in the primary treatment of ovarian cancer." N Engl J Med **365**(26): 2473 -2483.

Burger, R. A., P. J. DiSaia, et al. (1999). "Phase II trial of vinorelbine in recurrent and progressive epithelial ovarian cancer." Gynecol Oncol **72**(2): 148 -153.

Burgert, H. G., Z. Ruzsics, et al. (2002). "Subversion of host defense mechanisms by adenoviruses." Curr Top Microbiol Immunol **269**: 273-318.

Burstein, H. J. (2005). "The distinctive nature of HER2 -positive breast cancers." N Engl J Med **353**(16): 1652 -1654.

Cannistra, S. A. (2004). "Cancer of the ovary." N Engl J Med **351**(24): 2519 -2529.

Carlisle, R. C., Y. Di, et al. (2009). "Human erythrocytes bind and inactivate type 5 adenovirus by presenting Coxsackie virus-adenovirus receptor and complement receptor 1." Blood **113**(9): 1909 -1918.

Carmody, R. J., K. Maguschak, et al. (2006). "A novel me chanism of nuclear factor-kappaB regulation by adenoviral protein 14.7K." Immunology **117**(2): 188 -195.

Carson, C. T., N. I. Orazio, et al. (2009). "Mislocalization of the MRN complex prevents ATR signaling during adenovirus infection." EMBO J **28**(6): 652 -662.

Carter, B. J. (2005). "Adeno -associated virus vectors in clinical trials." Hum Gene Ther **16**(5): 541 -550.

Cartier, N., S. Hacein-Bey-Abina, et al. (2009). "Hematopoietic stem cell gene therapy with a lentiviral vector in X-linked adrenoleukodystrophy." Science **326**(5954): 818 -823.

Cassel, W. A. and R. E. Garrett (1965). "Newcastle Disease Virus as an Antineoplastic Agent." Cancer **18**: 863-868.

Cauthen, A. N. and K. R. Spindler (1996). "Sequence of the mouse adenovirus type -1 DNA encoding the 100-kDa, 33-kDa and DNA-binding proteins." Gene **168**(2): 183 -187.

Cepko, C. L. and P. A. Sharp (1982). "Assembly of adenovirus major capsid protein is mediated by a nonvirion protein." Cell **31**(2 Pt 1): 407 -415.

Cepko, C. L. and P. A. Sharp (1983). "Analysis of Ad5 hexon and 100K ts mutants using conformation-specific monoclonal antibodies." Virology **129**(1): 137 -154.

Chen, M., N. Mermod, et al. (1990). "Protein -protein interactions between adenovirus DNA polymerase and nuclear factor I mediate formation of the DNA replication preinitiation complex." J Biol Chem **265**(30): 18634 -18642.

Chen, M. J., B. Holskin, et al. (1987). "Induction by E1A oncogene expression of cellular susceptibility to lysis by TNF." Nature **330**(6148): 581 -583.

Chen, P. H., D. A. Ornelles, et al. (1993). "The adenovirus L3 23 -kilodalton proteinase cleaves the amino-terminal head domain from cytokeratin 18 and disrupts the cytokeratin network of HeLa cells." J Virol **67**(6): 3507 -3514.

Chen, S. H., H. D. Shine, et al. (1994). "Gene therapy for brain tumors: regression of experimental gliomas by adenovirus-mediated gene transfer in vivo." Proc Natl Acad Sci U S A **91**(8): 3054 -3057.

Chen, V. W., B. Ruiz, et al. (2003). "Pathology and classification of o varian tumors." Cancer **97**(10 Suppl): 2631 -2642.

Cheng, W., J. Liu, et al. (2005). "Lineage infidelity of epithelial ovarian cancers is controlled by HOX genes that specify regional identity in the reproductive tract." Nat Med **11**(5): 531 -537.

Chow, L. T., T. R. Broker, et al. (1979). "Complex splicing patterns of RNAs from the early regions of adenovirus-2." J Mol Biol **134**(2): 265 -303.

Chow, L. T., R. E. Gelinas, et al. (1977). "An amazing sequence arrangement at the 5' ends of adenovirus 2 messenger RNA." Cell **12**(1): 1 -8.

Chu, Y., D. Heistad, et al. (2001). "Vascular cell adhesion molecule -1 augments adenovirus-mediated gene transfer." Arterioscler Thromb Vasc Biol **21**(2): 238-242.

Clark-Knowles, K. V., M. K. Senterman, et al. (2009). "Conditional inactivatio n of Brca1, p53 and Rb in mouse ovaries results in the development of leiomyosarcomas." PLoS One **4**(12): e8534.

Coffey, M. C., J. E. Strong, et al. (1998). "Reovirus therapy of tumors with activated Ras pathway." Science **282**(5392): 1332 -1334.

Cohen, C. J., J. Gaetz, et al. (2001). "Multiple regions within the coxsackievirus and adenovirus receptor cytoplasmic domain are required for basolateral sorting." J Biol Chem **276**(27): 25392 -25398.

Colak, A., J. C. Goodman, et al. (1995). "Adenovirus -mediated gene therapy in an experimental model of breast cancer metastatic to the brain." Hum Gene Ther **6**(10): 1317 -1322.

Comer, M. T., H. J. Leese, et al. (1998). "Induction of a differentiated ciliated cell phenotype in primary cultures of Fallopian tube epithelium." Hum Reprod **13**(11): 3114 -3120.

Comins, C., L. Heinemann, et al. (2008). "Reovirus: viral therapy for cancer 'as nature intended'." Clin Oncol (R Coll Radiol) **20**(7): 548 -554.

Connell, C. M., A. Shibata, et al. (2011). "Genomic DNA damage and ATR -Chk1 signaling determine oncolytic adenoviral efficacy in human ovarian cancer cells." J Clin Invest **121**(4): 1283 -1297.

Connell, C. M., S. P. Wheatley, et al. (2008). "Nuclear survivin abrogates multip le cell cycle checkpoints and enhances viral oncolysis." Cancer Res **68**(19): 7923-7931.

Connolly, D. C., R. Bao, et al. (2003). "Female mice chimeric for expression of the simian virus 40 TAg under control of the MISIIR promoter develop epithelial ovarian cancer." Cancer Res **63**(6): 1389 -1397.

Cook, J. L., D. L. May, et al. (1989). "Role of tumor necrosis factor -alpha in E1A oncogene-induced susceptibility of neoplastic cells to lysis by natural killer cells and activated macrophages." J Immunol **142**(12): 4527 -4534.

Coughlan, L., S. Vallath, et al. (2009). "In vivo retargeting of adenovirus type 5 to alphavbeta6 integrin results in reduced hepatotoxicity and improved tumor uptake following systemic delivery." J Virol **83**(13): 6416 -6428.

Coura Rdos, S. and N. B. Nardi (2007). "The state of the art of adeno -associated virus-based vectors in gene therapy." Virol J **4**: 99.

CRUK (2007). http://info.cancerresearchuk.org/cancerstats/types/ovary/survival/#trends.

CRUK. (2011). "http://info.cancerresearchuk.org/cancerstats/incidence/commoncancers/#Top2 ", 2011.

Crum, C. P., R. Drapkin, et al. (2007). "Lessons from BRCA: the tubal fimbria emerges as an origin for pelvic serous cancer." Clin Med Res **5**(1): 35 -44.

Csatary, L. K., G. Gosztonyi, et al. (2004). "MTH -68/H oncolytic viral treatment in human high-grade gliomas." J Neurooncol **67**(1 -2): 83 -93.

Cuatrecasas, M., N. Erill, et al. (1998). "K -ras mutations in nonmucinous ovarian epithelial tumors: a molecular analysis and clinicopathologic study of 144 patients." Cancer **82**(6): 1088 -1095.

Cuesta, R., Q. Xi, et al. (2000). "Adenovirus -specific translation by displacement of kinase Mnk1 from cap-initiation complex eIF4F." EMBO J **19**(13): 3465 -3474.

Cuesta, R., Q. Xi, et al. (2001). "Preferential translation of adenovirus mRNAs in infected cells." Cold Spring Harb Symp Quant Biol **66**: 259-267.

Cuesta, R., Q. Xi, et al. (2004). "Structural basis for competitive inhibition of eIF4G -Mnk1 interaction by the adenovirus 100-kilodalton protein." J Virol **78**(14): 7707-7716.

Czernobilsky, B., R. Moll, et al. (1985). "Co -expression of cytokeratin and vimentin filaments in mesothelial, granulosa and rete ovarii cells of the human ovary." Eur J Cell Biol **37**: 175-190.

Dales, S. and Y. Chardonnet (1973). "Early events in the interaction of adenoviruses with HeLa cells. IV. Association with microtubules and the nuclear pore complex during vectorial movement of the inoculum." Virology **56**(2): 465 -483.

Dallaire, F., P. Blanchette, et al. (2009). "Identification of integrin alpha3 as a new substrate of the adenovirus E4orf6/E1B 55-kilodalton E3 ubiquitin ligase complex." J Virol **83**(11): 5329 -5338.

Davison, E., R. M. Diaz, et al. (1997). "Integrin alpha5be ta1-mediated adenovirus infection is enhanced by the integrin-activating antibody TS2/16." J Virol **71**(8): 6204 -6207.

Davison, E., I. Kirby, et al. (1999). "The human HLA -A*0201 allele, expressed in hamster cells, is not a high-affinity receptor for adenovirus type 5 fiber." J Virol **73**(5): 4513 -4517.

Davison, E., I. Kirby, et al. (2001). "Adenovirus type 5 uptake by lung adenocarcinoma cells in culture correlates with Ad5 fibre binding is mediated by alpha(v)beta1 integrin and can be modulated by changes in beta1 integrin function." J Gene Med **3**(6): 550 -559.

de Jong, R. N., P. C. van der Vliet, et al. (2003). "Adenovirus DNA replication: protein priming, jumping back and the role of the DNA binding protein DBP." Curr Top Microbiol Immunol **272**: 187-211.

De Pace, N. (1912). "Sulla scomparsa di un enorme cancer vegetante del callo dell'utero senza cura chirurgica." Ginecologia **9**: 82-88.

De Wever, O., P. Pauwels, et al. (2008). "Molecular and pathological signatures of epithelial-mesenchymal transitions at the cancer invasion front." Histochem Cell Biol **130**(3): 481 -494.

Debbas, M. and E. White (1993). "Wild -type p53 mediates apoptosis by E1A, which is inhibited by E1B." Genes Dev **7**(4): 546 -554.

Dechecchi, M. C., P. Melotti, et al. (2001). "Heparan sulfate glycosami noglycans are receptors sufficient to mediate the initial binding of adenovirus types 2 and 5." J Virol **75**(18): 8772 -8780.

Dechecchi, M. C., A. Tamanini, et al. (2000). "Heparan sulfate glycosaminoglycans are involved in adenovirus type 5 and 2-host cell interactions." Virology **268**(2): 382 -390.

Delage, B., D. A. Fennell, et al. (2010). "Arginine deprivation and argininosuccinate synthetase expression in the treatment of cancer." Int J Cancer **126**(12): 2762-2772.

DeWeese, T. L., H. van der Poel, et al. (2001). "A phase I trial of CV706, a replication-competent, PSA selective oncolytic adenovirus, for the treatment of locally recurrent prostate cancer following radiation therapy." Cancer Res **61**(20): 7464 -7472.

Dinulescu, D. M., T. A. Ince, et al. (2005). "Role of K -ras and Pten in the development of mouse models of endometriosis and endometrioid ovarian cancer." Nat Med **11**(1): 63 -70.

Dobbelstein, M., J. Roth, et al. (1997). "Nuclear export of the E1B 55 -kDa and E4 34-kDa adenoviral oncoproteins mediated by a rev-like signal sequence." Embo J **16**(14): 4276 -4284.

DobbelsteinM., J. Roth, et al. (1997). "Nuclear export of the E1B 55 -kDa and E4 34-kDa adenoviral oncoproteins mediated by a rev-like signal sequence." EMBO J **16**: 4276 ‑ 4284.

Dolph, P. J., V. Racaniello, et al. (1988). "The adenovirus tripartite leader may eliminate the requirement for cap-binding protein complex during translation initiation." J Virol **62**(6): 2059 -2066.

Dorner, M., J. A. Horwitz, et al. (2011). "A genetically humanized mouse model for hepatitis C virus infection." Nature **474**(7350): 208 -211.

Dosch, T., F. Horn, et al. (2001). "The adenovirus type 5 E1B -55K oncoprotein actively shuttles in virus-infected cells, whereas transport of E4orf6 is mediated by a CRM1-independent mechanism." J Virol **75**(12): 5677 -5683.

Drapkin, R., C. P. Crum, et al. (2004). "Expression of candidate tumor markers in ovarian carcinoma and benign ovary: evidence for a link between epithelial phenotype and neoplasia." Hum Pathol **35**(8): 1014 -1021.

Dubeau, L. (1999). "The cell of origin of ovarian epithelial tumors and the ovarian surface epithelium dogma: does the emperor have no clothes?" Gynecol Oncol **72**(3): 437 -442.

Duncan, S. J., F. C. Gordon, et al. (1978). "Infection of mouse liver by human adenovirus type 5." J Gen Virol **40**(1): 45 -61.

Eggerding, F. A. and W. C. Pierce (1986). "Molecular biology of adenovirus type 2 semipermissive infections. I. Viral growth and expression of viral replicative functions during restricted adenovirus infection." Virology **148**(1): 97 -113.

El-Deiry, W. S. (2003). "The role of p53 in chemosensitivity and radiosensitivity." Oncogene **22**(47): 7486 -7495.

Engler, H., T. Machemer, et al. (2004). "Acute hepatotoxicity of oncolytic adenoviruses in mouse models is associated with expression of wild-type E1a and induction of TNF-alpha." Virology **328**(1): 52 -61.

Evans, J. (2002). Adenoviral Replication. Adenoviral vectors for gene therapy. D. Curiel and J. Douglas, Academic press: 39-70.

Evans, J. D. and P. Hearing (2005). "Relocalization of the Mre11 -Rad50-Nbs1 complex by the adenovirus E4 ORF3 protein is required for viral replication." J Virol **79**(10): 6207 -6215.

Everitt, E., L. Lutter, et al. (1975). "Structural proteins of adenoviruses. XII. Location and neighbor relationship among proteins of adenovirion type 2 as revealed by enzymatic iodination, immunoprecipitation and chemical cross-linking." Virology **67**(1): 197-208.

Everitt, E., B. Sundquist, et al. (1973). "Structural proteins of adenoviruses. X. Isolation and topography of low molecular weight antigens from the virion of adenovirus type 2." Virology **52**(1): 130 -147.

Fang, L., J. L. Stevens, et al. (2004). " Requirement of Sur2 for efficient replication of mouse adenovirus type 1." J Virol **78**(23): 12888 -12900.

Farley, D. C., J. L. Brown, et al. (2004). "Activation of the early -late switch in adenovirus type 5 major late transcription unit expression by L4 gene products." J Virol **78**(4): 1782 -1791.

Farmer, C., P. E. Morton, et al. (2009). "Coxsackie adenovirus receptor (CAR) regulates integrin function through activation of p44/42 MAPK." Exp Cell Res **315**(15): 2637 -2647.

Felsani, A., A. M. Mileo, et al. (2006). "R etinoblastoma family proteins as key targets of the small DNA virus oncoproteins." Oncogene **25**(38): 5277 -5285.

Fessler, S. P. and C. S. Young (1998). "Control of adenovirus early gene expression during the late phase of infection." J Virol **72**(5): 4049-4056.

Fessler, S. P. and C. S. Young (1999). "The role of the L4 33K gene in adenovirus infection." Virology 263(2): 507 -516.

Fields, B. N., D. M. Knipe, et al. (2007). Fields' virology. Philadelphia, Pa. ; London, Wolters Kluwer/Lippincott Williams & Wilkins.

Flak, M. B., C. M. Connell, et al. "p21 Promotes oncolytic adenoviral activity in ovarian cancer and is a potential biomarker." Mol Cancer 9: 175.

Flak, M. B., C. M. Connell, et al. (2010). "p21 Promotes oncolytic adenoviral activity in ovarian cancer and is a potential biomarker." Mol Cancer 9: 175.

Flesken-Nikitin, A., K. C. Choi, et al. (2003). "Induction of carcinogenesis by concurrent inactivation of p53 and Rb1 in the mouse ovarian surface epithelium." Cancer Res 63(13): 3459 -3463.

Folkins, A. K., E. A. Jarboe, et al. (2008). "A candidate precursor to pelvic serous cancer (p53 signature) and its prevalence in ovaries and fallopian tubes from women with BRCA mutations." Gynecol Oncol 109(2): 168 -173.

Fong, P. C., D. S. Boss, et al. (2009). "In hibition of poly(ADP -ribose) polymerase in tumors from BRCA mutation carriers." N Engl J Med 361(2): 123 -134.

Fong, P. C., T. A. Yap, et al. (2010). "Poly(ADP) -ribose polymerase inhibition: frequent durable responses in BRCA carrier ovarian cancer correlating with platinum-free interval." J Clin Oncol 28(15): 2512 -2519.

Fong, Y., T. Kim, et al. (2009). "A herpes oncolytic virus can be delivered via the vasculature to produce biologic changes in human colorectal cancer." Mol Ther 17(2): 389 -394.

Forsyth, P., G. Roldan, et al. (2008). "A phase I trial of intratumoral administration of reovirus in patients with histologically confirmed recurrent malignant gliomas." Mol Ther 16(3): 627 -632.

Fotheringham, S., K. Levanon, et al. (2011). "Ex Vivo Culture of Primary Human Fallopian Tube Epithelial Cells." J Vis Exp(51).

Freeman, A. I., Z. Zakay-Rones, et al. (2006). "Phase I/II trial of intravenous NDV -HUJ oncolytic virus in recurrent glioblastoma multiforme." Mol Ther **13**(1): 221-228.

Fridman, J. S. and S. W. Lowe (2003). "Control of apoptosis by p53." Oncogene **22**(56): 9030 -9040.

Fujimoto, Y., T. Mizuno, et al. (2006). "Intratumoral injection of herpes simplex virus HF10 in recurrent head and neck squamous cell carcinoma." Acta Otolaryngol **126**(10): 1115 -1117.

Futterer, J., Z. Kiss-Laszlo, et al. (1993). "Nonlinear ribosome migration on cauliflower mosaic virus 35S RNA." Cell **73**(4): 789 -802.

Galanis, E., L. C. Hartmann, et al. (2010). "Phase I trial of intraperitoneal administration of an oncolytic measles virus strain engineered to express carcinoembryonic antigen for recurrent ovarian cancer." Cancer Res **70**(3): 875-882.

Gale, M., Jr., S. L. Tan, et al. (2000). "Translational control of viral gene expression in eukaryotes." Microbiol Mol Biol Rev **64**(2): 239 -280.

Ganly, I., D. Kirn, et al. (2000). "A phase I study of Onyx -015, an E1B attenuated adenovirus, administered intratumorally to patients with recurrent head and neck cancer." Clin Cancer Res **6**(3): 798 -806.

Ganly, I., V. Mautner, et al. (2000). "Productive replication of human adenoviruses in mouse epidermal cells." J Virol **74**(6): 2895 -2899.

Gelmon, K. A., M. Tischkowitz, et al. (2011). "Olaparib in patients with recurrent high-grade serous or poorly differentiated ovarian carcinoma or triple-negative breast cancer: a phase 2, multicentre, open-label, non-randomised study." Lancet Oncol **12**(9): 852-861.

Gemignani, M. L., A. C. Schlaerth, et al. (2003). "Role of KRAS and BRAF gene mutations in mucinous ovarian carcinoma." Gynecol Oncol **90**(2): 378 -381.

Gerlinger, M., A. J. Rowan, et al. (2012). "Intratumor heterogeneity and branched evolution revealed by multiregion sequencing." N Engl J Med **366**(10): 883 -892.

Ghisolfi, L., G. Joseph, et al. (1992). "The glycine -rich domain of nucleolin has an unusual supersecondary structure responsible for its RNA-helix-destabilizing properties." J Biol Chem **267**(5): 2955 -2959.

Gimenez-Alejandre, M., M. Cascallo, et al. (2008). "Coagulation factors determine tumor transduction in vivo." Hum Gene Ther **19**(12): 1415 -1419.

Ginsberg, H. S., L. L. Moldawer, et al. (1991). "A mouse model for investigating the molecular pathogenesis of adenovirus pneumonia." Proc Natl Acad Sci U S A **88**(5): 1651 -1655.

Gomella, L. G., M. J. Mastrangelo, et al. (2001). "Phase i study of intravesical vaccinia virus as a vector for gene therapy of bladder cancer." J Urol **166**(4): 1291-1295.

Goodrum, F. D. and D. A. Ornelles (1998). "p53 status does not determine outcome of E1B 55-kilodalton mutant adenovirus lytic infection." J Virol **72**(12): 9479 -9490.

Gordon, A. N., C. O. Granai, et al. (2000). "Phase II study of liposomal doxorubicin in platinum- and paclitaxel-refractory epithelial ovarian cancer." J Clin Oncol **18**(17): 3093 -3100.

Gore, M. E., V. Levy, et al. (1995). "Paclitaxel (Taxol) in relapsed and refractory ovarian cancer: the UK and Eire experience." Br J Cancer **72**(4): 1016 -1019.

Greber, U. F., M. Suomalainen, et al. (1997). "The role of the nuclear pore complex in adenovirus DNA entry." EMBO J **16**(19): 5998 -6007.

Greber, U. F., M. Willetts, et al. (1993). "Stepwise dismantling of adenovirus 2 during entry into cells." Cell **75**(3): 477 -486.

Guida, J. D., G. Fejer, et al. (1995). "Mouse adenovirus type 1 causes a fatal hemorrhagic encephalomyelitis in adult C57BL/6 but not BALB/c mice." J Virol **69**(12): 7674 -7681.

Hall, A. R., B. R. Dix, et al. (1998). "p53 -dependent cell death/apoptosis is required for a productive adenovirus infection." Nat Med **4**(9): 1068 -1072.

Hallden, G., R. Hill, et al. (2003). "Novel immunocompetent murine tumor models for the assessment of replication-competent oncolytic adenovirus efficacy." Mol Ther **8**(3): 412 -424.

Harada, J. N. and A. J. Berk (1999). "p53 -Independent and -dependent requirements for E1B-55K in adenovirus type 5 replication." J Virol **73**(7): 5333-5344.

Harrington, K., J. A. Bonner, et al. ⁀2010⁀. "Efficacy Study of REOLYSIN® in Combination With Paclitaxel and Carboplatin in Platinum-Refractory Head and Neck Cancers." Retrieved 01/04/2013, 2013, from http://clinicaltrials.gov/show/NCT01166542.

Harrington, K. J., M. Hingorani, et al. (2010). "Ph ase I/II study of oncolytic HSV GM-CSF in combination with radiotherapy and cisplatin in untreated stage III/IV squamous cell cancer of the head and neck." Clin Cancer Res **16**(15): 4005 -4015.

Harris, G. F. t., M. E. Anderson, et al. (2008). "The effect of p roteasome inhibition on p53 degradation and proliferation in tonsil epithelial cells." Arch Otolaryngol Head Neck Surg **134**(2): 157 -163.

Harrow, S., V. Papanastassiou, et al. (2004). "HSV1716 injection into the brain adjacent to tumour following surgical resection of high-grade glioma: safety data and long-term survival." Gene Ther **11**(22): 1648 -1658.

Hartley, J. W. and W. P. Rowe (1960). "A new mouse virus apparently related to the adenovirus group." Virology **11**: 645-647.

Hawkins, L. K., N. R. Lemoine, et al. (2002). "Oncolytic biotherapy: a novel therapeutic platform." Lancet Oncol **3**(1): 17 -26.

Hayes, B. W., G. C. Telling, et al. (1990). "The adenovirus L4 100 -kilodalton protein is necessary for efficient translation of viral late mRNA species." J Virol **64**(6): 2732 -2742.

Heise, C., I. Ganly, et al. (2000b). "Efficacy of a replication -selective adenovirus against ovarian carcinomatosis is dependent on tumor burden, viral replication and p53 status." Gene Ther **7**(22): 1925 -1929.

Heise, C., T. Hermiston, et al. (2000a). "An adenovirus E1A mutant that demonstrates potent and selective systemic anti-tumoral efficacy." Nat Med **6**(10): 1134 -1139.

Heise, C., M. Lemmon, et al. (2000). "Efficacy with a replication -selective adenovirus plus cisplatin-based chemotherapy: dependence on sequencing but not p53 functional status or route of administration." Clin Cancer Res **6**(12): 4908 -4914.

Heise, C. C., A. M. Williams, et al. (1999). "Intravenous administration of ONYX -015, a selectively replicating adenovirus, induces antitumoral efficacy." Cancer Res **59**(11): 2623 -2628.

Helt, A. M. and D. A. Galloway (2003). "Mechanisms by which DNA tumor virus oncoproteins target the Rb family of pocket proteins." Carcinogenesis **24**(2): 159-169.

Hemmi, S., R. Geertsen, et al. (1998). "The presence of human coxsackievirus and adenovirus receptor is associated with efficient adenovirus-mediated transgene expression in human melanoma cell cultures." Hum Gene Ther **9**(16): 2363 -2373.

Hemminki, A., A. Kanerva, et al. (2003). "A canine conditionally replicating adenovirus for evaluating oncolytic virotherapy in a syngeneic animal model." Mol Ther **7**(2): 163 -173.

Hennessy, B. T., K. M. Timms, et al. (2010). "Somatic mutations in BRCA1 and BRCA2 could expand the number of patients that benefit from poly (ADP ribose) polymerase inhibitors in ovarian cancer." J Clin Oncol **28**(22): 3570 -3576.

Henriksen, T., T. Tanbo, et al. (1990). "Epithelial cells from human fallopian tube in culture." Hum Reprod **5**(1): 25 -31.

Hermiston, T. W., R. Hellwig, et al. (1993). "Sequence and functional analysis of the human adenovirus type 7 E3-gp19K protein from 17 clinical isolates." Virology **197**(2): 593 -600.

Hermiston, T. W., R. A. Tripp, et al. (1993a). "Deletion mutation analysis of the adenovirus type 2 E3-gp19K protein: identification of sequences within the endoplasmic reticulum lumenal domain that are required for class I antigen binding and protection from adenovirus-specific cytotoxic T lymphocytes." J Virol **67**(9): 5289 -5298.

Hogdall, E. V., C. K. Hogdall, et al. (2003). "K -ras alterations in Danish ovarian tumour patients. From the Danish "Malova" Ovarian Cancer study." Gynecol Oncol **89**(1): 31 -36.

Hoggan, M. D., N. R. Blacklow, et al. (1966). "Studies of small DNA viruses found in various adenovirus preparations: physical, biological, and immunological characteristics." Proc Natl Acad Sci U S A **55**(6): 1467 -1474.

Hong, S. S., L. Karayan, et al. (1997). "Adenovirus type 5 fiber knob binds to MHC class I alpha2 domain at the surface of human epithelial and B lymphoblastoid cells." EMBO J **16**(9): 2294 -2306.

Hong, S. S., E. Szolajska, et al. (2005). "The 100K -chaperone protein from adenovirus serotype 2 (S ubgroup C) assists in trimerization and nuclear localization of hexons from subgroups C and B adenoviruses." J Mol Biol **352**(1): 125 -138.

Horwood, N. J., C. Smith, et al. (2002). "High -efficiency gene transfer into nontransformed cells: utility for studying gene regulation and analysis of potential therapeutic targets." Arthritis Res **4 Suppl 3**: S215-225.

Howe, J. A. and S. T. Bayley (1992). "Effects of Ad5 E1A mutant viruses on the cell cycle in relation to the binding of cellular proteins including the retinoblastoma protein and cyclin A." Virology **186**(1): 15 -24.

Hu, J. C., R. S. Coffin, et al. (2006). "A phase I study of OncoVEXGM -CSF, a second-generation oncolytic herpes simplex virus expressing granulocyte macrophage colony-stimulating factor." Clin Cancer Res **12**(22): 6737 -6747.

Huang, J. T. and R. J. Schneider (1991). "Adenovirus inhibition of cellular protein synthesis involves inactivation of cap-binding protein." Cell **65**(2): 271 -280.

Huang, S., T. Kamata, et al. (1996). "Adenovirus interaction with dis tinct integrins mediates separate events in cell entry and gene delivery to hematopoietic cells." J Virol **70**(7): 4502 -4508.

Huang, W. and S. J. Flint (1998). "The tripartite leader sequence of subgroup C adenovirus major late mRNAs can increase the efficiency of mRNA export." J Virol **72**(1): 225 -235.

Iacovides, D. C., C. C. O'Shea, et al. (2007). "Critical role for arginine methylation in adenovirus-infected cells." J Virol **81**(23): 13209 -13217.

ICON (2002). "Paclitaxel plus carboplatin versus standard chemot herapy with either single-agent carboplatin or cyclophosphamide, doxorubicin, and cisplatin in women with ovarian cancer: the ICON3 randomised trial." Lancet **360**(9332): 505-515.

Imperiale, M. J., G. Akusjnarvi, et al. (1995). "Post -transcriptional control of adenovirus gene expression." Curr Top Microbiol Immunol **199 (Pt 2)** : 139-171.

Imperiale, M. J., L. T. Feldman, et al. (1983). "Activation of gene expression by adenovirus and herpesvirus regulatory genes acting in trans and by a cis-acting adenovirus enhancer element." Cell **35**(1): 127 -136.

Ingemarsdotter, C. K., S. K. Baird, et al. "Low-dose paclitaxel synergizes with oncolytic adenoviruses via mitotic slippage and apoptosis in ovarian cancer." Oncogene **29**(45): 6051 -6063.

Ioannides, C. G., C. D. Platsoucas, et al. (1990). "T -cell functions in ovarian cancer patients treated with viral oncolysates: I. Increased helper activity to immunoglobulins production." Anticancer Res **10**(3): 645-653.

Iorio, M. V., R. Visone, et al. (2007). "MicroRNA signatures in human ovarian cancer." Cancer Res **67**(18): 8699 -8707.

Itamochi, H., J. Kigawa, et al. (2002). "Low proliferation activity may be associated with chemoresistance in clear cell carcinoma of the ovary." Obstet Gynecol **100**(2): 281 -287.

Ito, H., H. Aoki, et al. (2006). "Autophagic cell death of malignant glioma cells induced by a conditionally replicating adenovirus." J Natl Cancer Inst **98**(9): 625-636.

Janda, E., K. Lehmann, et al. (2002). "Ras and TGF[beta] cooperatively regulate epithelial cell plasticity and metastasis: dissection of Ras signaling pathways." J Cell Biol **156**(2): 299 -313.

Janeway C., T. P., Walport M, and Sclomik, M. (2005). Immunobiology, the immune system in health and disease, Oxfors: Garland Science Publishing.

Janke, M., B. Peeters, et al. (2007). "Recombinant Newcastle disease virus (NDV) with inserted gene coding for GM -CSF as a new vector for cancer immunogene therapy." Gene Ther **14**(23): 1639 -1649.

Jia, L. Q., M. Osada, et al. (1997). "Screening the p53 status of human cell lines using a yeast functional assay." Mol Carcinog **19**(4): 243 -253.

Jiang, H., E. J. White, et al. (2011). "Human adenovirus type 5 induces cell lysis through autophagy and autophagy-triggered caspase activity." J Virol **85**(10): 4720-4729.

Jogler, C., D. Hoffmann, et al. (2006). "Replication properties of human adenovirus in vivo and in cultures of primary cells from different animal species." J Virol **80**(7): 3549 -3558.

Johnson, L., A. Shen, et al. (2002). "Selectively replicating adenoviruses targeting deregulated E2F activity are potent, systemic antitumor agents." Cancer Cell **1**(4): 325 -337.

Jones, N. C., P. W. Rigby, et al. (1988). "Trans -acting protein factors and the regulation of eukaryotic transcription: lessons from studies on DNA tumor viruses." Genes Dev **2**(3): 267 -281.

Jordan, V. C. (1976). "Antiestrogenic and antitu mor properties of tamoxifen in laboratory animals." Cancer Treat Rep **60**(10): 1409 -1419.

Jurvansuu, J., K. Raj, et al. (2005). "Viral transport of DNA damage that mimics a stalled replication fork." J Virol **79**(1): 569 -580.

Kaelin, W. G., Jr. (2005). "The co ncept of synthetic lethality in the context of anticancer therapy." Nat Rev Cancer **5**(9): 689 -698.

Kalyuzhniy, O., N. C. Di Paolo, et al. (2008). "Adenovirus serotype 5 hexon is critical for virus infection of hepatocytes in vivo." Proc Natl Acad Sci U S A **105**(14): 5483-5488.

Kang, J., A. D. D'Andrea, et al. (2012). "A DNA repair pathway -focused score for prediction of outcomes in ovarian cancer treated with platinum-based chemotherapy." J Natl Cancer Inst **104**(9): 670 -681.

Kanopka, A., O. Muhlemann, et al. (1996). "Inhibition by SR proteins of splicing of a regulated adenovirus pre-mRNA." Nature **381**(6582): 535 -538.

Kanopka, A., O. Muhlemann, et al. (1998). "Regulation of adenovirus alternative RNA splicing by dephosphorylation of SR proteins." Nature **393**(6681): 185 -187.

Kao, C. C., P. R. Yew, et al. (1990). "Domains required for in vitro association between the cellular p53 and the adenovirus 2 E1B 55K proteins." Virology **179**(2): 806 -814.

Kao, H. T. and J. R. Nevins (1983). "Transcriptional activation and subsequent control of the human heat shock gene during adenovirus infection." Mol Cell Biol **3**(11): 2058 -2065.

Kaplitt, M. G., A. Feigin, et al. (2007). "Safety and tolerability of gene therapy with an adeno-associated virus (AAV) borne GAD gene for Parkinson's disease: an open label, phase I trial." Lancet **369**(9579): 2097 -2105.

Karapanagiotou, E. M., V. Roulstone, et al. (2012). "Phase I/II trial of carboplatin and paclitaxel chemotherapy in combination with intravenous oncolytic reovirus in patients with advanced malignancies." Clin Cancer Res **18**(7): 2080 -2089.

Karen, K. A., P. J. Hoey, et al. (2009). "Temporal regulation of the Mre11-Rad50-Nbs1 complex during adenovirus infection." J Virol **83**(9): 4565 -4573.

Karst, A. M. and R. Drapkin (2010). "Ovarian cancer pathogenesis: a model in evolution." J Oncol **2010**: 932371.

Kaye, S. B., M. Piccart, et al. (1997). "Phase II trials of docetaxel (Taxotere) in advanced ovarian cancer--an updated overview." Eur J Cancer **33**(13): 2167 -2170.

Kelkar, S. A., K. K. Pfister, et al. (2004). "Cytoplasmic dynein mediates adenovirus binding to microtubules." J Virol **78**(18): 10122 -10132.

Kemeny, N., K. Brown, et al. (2006). "Phase I, open-label, dose-escalating study of a genetically engineered herpes simplex virus, NV1020, in subjects with metastatic colorectal carcinoma to the liver." Hum Gene Ther **17**(12): 1214 -1224.

Kim, M., L. A. Sumerel, et al. (2003). "The coxsackievirus and adenovirus receptor acts as a tumour suppressor in malignant glioma cells." Br J Cancer **88**(9): 1411-1416.

Kimata, H., T. Imai, et al. (2006). "Pilot study of oncolytic viral therapy using mutant herpes simplex virus (HF10) against recurrent metastatic breast cancer." Ann Surg Oncol **13**(8): 1078 -1084.

Kimball, K. J., M. A. Preuss, et al. (2010). "A phase I study of a tropism -modified conditionally replicative adenovirus for recurrent malignant gynecologic diseases." Clin Cancer Res **16**(21): 5277 -5287.

Kindelberger, D. W., Y. Lee, et al. (2007). "Intraepi thelial carcinoma of the fimbria and pelvic serous carcinoma: Evidence for a causal relationship." Am J Surg Pathol **31**(2): 161 -169.

Kobel, M., S. E. Kalloger, et al. (2008). "Ovarian carcinoma subtypes are different diseases: implications for biomarker studies." PLoS Med **5**(12): e232.

Koizumi, N., K. Kawabata, et al. (2006). "Modified adenoviral vectors ablated for coxsackievirus-adenovirus receptor, alphav integrin, and heparan sulfate binding reduce in vivo tissue transduction and toxicity." Hum Gene Ther **17**(3): 264 -279.

Konstantinopoulos, P. A., D. Spentzos, et al. (2010). "Gene expression profile of BRCAness that correlates with responsiveness to chemotherapy and with outcome in patients with epithelial ovarian cancer." J Clin Oncol **28**(22): 3555-3561.

Kotin, R. M., R. M. Linden, et al. (1992). "Characterization of a preferred site on human chromosome 19q for integration of adeno-associated virus DNA by non-homologous recombination." EMBO J **11**(13): 5071 -5078.

Kovesdi, I., R. Reichel, et al. (1986). "E1A transcription induction: enhanced binding of a factor to upstream promoter sequences." Science **231**(4739): 719 -722.

Koyuncu, O. O. and T. Dobner (2009). "Arginine methylation of human adenovirus type 5 L4 100-kilodalton protein is required for efficient virus production." J Virol **83**(10): 4778 -4790.

Krajcsi, P., T. Dimitrov, et al. (1996). "The adenovirus E3 -14.7K protein and the E3-10.4K/14.5K complex of proteins, which independently inhibit tumor necrosis factor (TNF) -induced apoptosis, also independently inhibit TNF-induced release of arachidonic acid." J Virol **70**(8): 4904 -4913.

Kring, S. C., A. O. Ball, et al. (1992). "Transcription mapping of mouse adenovirus type 1 early region 4." Virology **190**(1): 248 -255.

Kring, S. C., C. S. King, et al. (1995). "Susce ptibility and signs associated with mouse adenovirus type 1 infection of adult outbred Swiss mice." J Virol **69**(12): 8084 -8088.

Krishnamurthy, S., T. Takimoto, et al. (2006). "Differentially regulated interferon response determines the outcome of Newcastle disease virus infection in normal and tumor cell lines." J Virol **80**(11): 5145 -5155.

Kzhyshkowska, J., E. Kremmer, et al. (2004) . "Protein arginine methylation during lytic adenovirus infection." Biochem J **383**(Pt 2): 259 -265.

Kzhyshkowska, J., H. Schutt, et al. (2001). "Heterogeneous nuclear ribonucleoprotein E1B-AP5 is methylated in its Arg-Gly-Gly (RGG) box and interacts with human arginine methyltransferase HRMT1L1." Biochem J **358**(Pt 2): 305 -314.

Landen, C. N., Jr., M. J. Birrer, et al. (2008). "Early events in the pathogenesis of epithelial ovarian cancer." J Clin Oncol **26**(6): 995 -1005.

Lanuti, M., G. P. Gao, et al. (1999). "Eva luation of an E1E4-deleted adenovirus expressing the herpes simplex thymidine kinase suicide gene in cancer gene therapy." Hum Gene Ther **10**(3): 463 -475.

Larsson, S., C. Svensson, et al. (1992). "Control of adenovirus major late gene expression at multiple levels." J Mol Biol **225**(2): 287 -298.

Laurie, S. A., J. C. Bell, et al. (2006). "A phase 1 clinical study of intravenous administration of PV701, an oncolytic virus, using two-step desensitization." Clin Cancer Res **12**(8): 2555 -2562.

Lazar, I., B. Yaacov, et al. (2010). "The oncolytic activity of Newcastle disease virus NDV-HUJ on chemoresistant primary melanoma cells is dependent on the proapoptotic activity of the inhibitor of apoptosis protein Livin." J Virol **84**(1): 639-646.

Ledermann, J., P. Harter, et al. (2012). "Olaparib maintenance therapy in platinum -sensitive relapsed ovarian cancer." N Engl J Med **366**(15): 1382 -1392.

Ledermann J.A , H. P., Gourley C, Friedlander M, Vergote I. B, Rustin G. J. S, Scott C, Meier W,Shapira-Frommer R, Safra T, Matei D, Macpherson E, Watkins C, Carmichael J, Matulonis U (2011). Phase II Randomised placebo -controlled study of olaparib (AZD2281) in patients with platinum -sensitive relapsed serous ovarian cancer (PSR SOC). ASCO, J.Clin.Oncol. **29**.

Lee, Y., A. Miron, et al. (2007). "A candidate precursor to serous carcinoma that originates in the distal fallopian tube." J Pathol **211**(1): 26 -35.

Lenaerts, L., D. Daelemans, et al. (2006). "Mouse adenovirus type 1 attachment is not mediated by the coxsackie-adenovirus receptor." FEBS Lett **580**(16): 3937-3942.

Lenaerts, L., J. H. McVey, et al. (2009). "Mouse adenovirus type 1 and human adenovirus type 5 differ in endothelial cell tropism and liver targeting." J Gene Med **11**(2): 119 -127.

Leopold, P. L., G. Kreitzer, et al. (2000). "Dy nein- and microtubule-mediated translocation of adenovirus serotype 5 occurs after endosomal lysis." Hum Gene Ther **11**(1): 151 -165.

Leppard, K. N. and R. D. Everett (1999). "The adenovirus type 5 E1b 55K and E4 Orf3 proteins associate in infected cells and affect ND10 components." J Gen Virol **80 (Pt 4)** : 997-1008.

Li, E., S. L. Brown, et al. (2001). "Integrin alpha(v)beta1 is an adenovirus coreceptor." J Virol **75**(11): 5405 -5409.

Li, E., D. Stupack, et al. (1998b). "Adenovirus endocytosis requires actin cytoskeleton reorganization mediated by Rho family GTPases." J Virol **72**(11): 8806 -8812.

Li, E., D. Stupack, et al. (1998a). "Adenovirus endocytosis via alpha(v) integrins requires phosphoinositide-3-OH kinase." J Virol **72**(3): 2055 -2061.

Li, N. F., S. A. Gayther, et al. (2005). A cellular model for studying human ovarian surface epithelium carcinognenesis. , Proc Am Assoc Cancer Res.

Li, Y., J. Kang, et al. (1998). "Interaction of an adenovirus E3 14.7 -kilodalton protein with a novel tumor necrosis factor alpha-inducible cellular protein containing leucine zipper domains." Mol Cell Biol **18**(3): 1601 -1610.

Lichtenstein, D. L., K. Doronin, et al. (2004). "Adenovirus E3 -6.7K protein is required in conjunction with the E3-RID protein complex for the internalization and degradation of TRAIL receptor 2." J Virol **78**(22): 12297 -12307.

Lichtenstein, D. L., K. Toth, et al. (2004). "Functions and mechanisms of action of the adenovirus E3 proteins." Int Rev Immunol **23**(1 -2): 75 -111.

Lieber, A., C. Y. He, et al. (1997). "The role of Kupffer cell activation and viral gene expression in early liver toxicity after infusion of recombinant adenovirus vectors." J Virol **71**(11): 8798 -8807.

Lindström, L. ⁀2005⁀. Enhanced cellular uptake of virus by increased expression levels of the coxsackie-and adenovirus receptor. Ph.D Ph.D, Sveriges lantbruksuniversitet.

Linette, G. P., D. Zhang, et al. (2005). "Immunization using autologous dendritic cells pulsed with the melanoma-associated antigen gp100-derived G280-9V peptide elicits CD8+ immunity." Clin Cancer Res **11**(21): 7692 -7699.

Liu, Q., L. R. White, et al. (2005). "Akt/protein kinase B activation by adenovirus vectors contributes to NFkappaB-dependent CXCL10 expression." J Virol **79**(23): 14507 -14515.

Liu, Y., H. Wang, et al. (2009). "Transduction of liver metastases after intravenous injection of Ad5/35 or Ad35 vectors with and without factor X-binding protein pretreatment." Hum Gene Ther **20**(6): 621 -629.

Lockley, M. (2007). Activity of adenoviral E1A CR2 deletion mutants in ovarian cancer. PhD, Queen Mary, University of London.

Lockley, M., M. Fernandez, et al. (2006). "Activity of the adenoviral E1A deletion mutant dl922-947 in ovarian cancer: comparison with E1A wild-type viruses, bioluminescence monitoring, and intraperitoneal delivery in icodextrin." Cancer Res **66**(2): 989 -998.

Logan, J. and T. Shenk (1984). "Adenovirus tripartite leader sequence enhances translation of mRNAs late after infection." Proc Natl Acad Sci U S A **81**(12): 3655-3659.

Lohr, F., Q. Huang, et al. (2001). "Systemic vector leakage and transgene expression by intratumorally injected recombinant adenovirus vectors." Clin Cancer Res **7**(11): 3625 -3628.

Lolkema, M. P., H. T. Arkenau, et al. (2010). "A phase I study of the combination of intravenous reovirus type 3 Dearing and gemcitabine in patients with advanced cancer." Clin Cancer Res **17**(3): 581 -588.

Lowe, S. W. and H. E. Ruley (1993). "Stabilization of the p53 tumor suppressor is induced by adenovirus 5 E1A and accompanies apoptosis." Genes Dev **7**(4): 535-545.

Luckey, M., J. Hernandez, et al. (2000). "A peptide from the adenovirus fiber shaft forms amyloid-type fibrils." FEBS Lett **468**(1): 23 -27.

Lutz, P. and C. Kedinger (1996). "Properties of the adenovirus IVa2 gene product, an effector of late-phase-dependent activation of the major late promoter." J Virol **70**(3): 1396 -1405.

Makower, D., A. Rozenblit, et al. (2003). "Phase II clinical trial of in tralesional administration of the oncolytic adenovirus ONYX-015 in patients with hepatobiliary tumors with correlative p53 studies." Clin Cancer Res **9**(2): 693-702.

Manickan, E., J. S. Smith, et al. (2006). "Rapid Kupffer cell death after intravenous injection of adenovirus vectors." Mol Ther **13**(1): 108 -117.

Markert, J. M., P. G. Liechty, et al. (2009). "Phase Ib trial of mutant herpes simplex virus G207 inoculated pre-and post-tumor resection for recurrent GBM." Mol Ther **17**(1): 199 -207.

Markman, M., B. N. Bundy, et al. (2001). "Phase III trial of standard -dose intravenous cisplatin plus paclitaxel versus moderately high-dose carboplatin followed by intravenous paclitaxel and intraperitoneal cisplatin in small-volume stage III ovarian carcinoma: an intergroup study of the Gynecologic Oncology Group, Southwestern Oncology Group, and Eastern Cooperative Oncology Group." J Clin Oncol **19**(4): 1001 -1007.

Markman, M., A. Kennedy, et al. (2000). "Phase 2 trial of liposomal doxorubicin (40 mg/m(2)) in platinum/paclitax el-refractory ovarian and fallopian tube cancers and primary carcinoma of the peritoneum." Gynecol Oncol **78**(3 Pt 1): 369 -372.

Mastrangelo, M. J., H. C. Maguire, Jr., et al. (1999). "Intratumoral recombinant GM - CSF-encoding virus as gene therapy in patients with cutaneous melanoma." Cancer Gene Ther **6**(5): 409 -422.

Mathews, M. B. (1980). "Binding of adenovirus VA RNA to mRNA: a possible role in splicing?" Nature **285**(5766): 575 -577.

Mautner, V. and H. G. Pereira (1971). "Crystallization of a second adenovirus protein (the fibre)." Nature 230(5294): 456 -457.

McDonald, D., L. Stockwin, et al. (1999). "Coxsackie and adenovirus receptor (CAR) -dependent and major histocompatibility complex (MHC) class I -independent uptake of recombinant adenoviruses into human tumour cells." Gene Ther 6(9): 1512 -1519.

McNeish, I. A., T. Tenev, et al. (2001). "Herpes simplex virus thymidine kinase/ganciclovir-induced cell death is enhanced by co-expression of caspase-3 in ovarian carcinoma cells." Cancer Gene Ther 8(4): 308 -319.

Medeiros, F., M. G. Muto, et al. (2006). "The tubal fimbria is a preferred site for early adenocarcinoma in women with familial ovarian cancer syndrome." Am J Surg Pathol 30(2): 230 -236.

Meier, O., K. Boucke, et al. (2002). "Adenovirus triggers macropinocy tosis and endosomal leakage together with its clathrin-mediated uptake." J Cell Biol 158(6): 1119 -1131.

Meissner, J. D., G. N. Hirsch, et al. (1997). "Completion of the DNA sequence of mouse adenovirus type 1: sequence of E2B, L1, and L2 (18 -51 map units). " Virus Res 51(1): 53 -64.

Miller, C. R., D. J. Buchsbaum, et al. (1998). "Differential susceptibility of primary and established human glioma cells to adenovirus infection: targeting via the epidermal growth factor receptor achieves fiber receptor-independent gene transfer." Cancer Res 58(24): 5738 -5748.

Miller, G., S. Lahrs, et al. (2002). "Adenovirus infection enhances dendritic cell immunostimulatory properties and induces natural killer and T-cell-mediated tumor protection." Cancer Res 62(18): 5260 -5266.

Mittereder, N., K. L. March, et al. (1996). "Evaluation of the concentration and bioactivity of adenovirus vectors for gene therapy." J Virol 70(11): 7498 -7509.

Mizuno, M., J. Yoshida, et al. (1998). "Adeno -associated virus vector containing the herpes simplex virus thymidine kinase gene causes complete regression of intracerebrally implanted human gliomas in mice, in conjunction with ganciclovir administration." Jpn J Cancer Res **89**(1): 76 -80.

Mohr, I. (2005). "To replicate or not to replicate: achieving selective oncolytic virus replication in cancer cells through translational control." Oncogene **24**(52): 7697-7709.

Morgan, R. J., Jr., R. D. Alvarez, et al. (2012). "Ovarian cancer, version 3.2012." J Natl Compr Canc Netw **10**(11): 1339 -1349.

Morin, N. and P. Boulanger (1984). "Morphogenesis of human adenovirus type 2: sequence of entry of proteins into previral and viral particles." Virology **136**(1): 153 -167.

Morin, N. and P. Boulanger (1986). "Hexon trimerization occurring in an assembly -defective, 100K temperature-sensitive mutant of adenovirus 2." Virology **152**(1): 11 -31.

Morris, S. J. and K. N. Leppard (2009). "Adenovirus serotype 5 L4 -22K and L4-33K proteins have distinct functions in regulating late gene expression." J Virol **83**(7): 3049 -3058.

Morris, S. J., G. E. Scott, et al. (2010). "Adenovirus late -phase infection is controlled by a novel L4 promoter." J Virol **84**(14): 7096 -7104.

Mosmann, T. (1983). "Rapid colorimetric assay for cellular growth and survival: application to proliferation and cytotoxicity assays." J Immunol Methods **65**(1 -2): 55 -63.

Muggia, F. M., P. S. Braly, et al. (2000). "Phase III randomized study of cisplatin versus paclitaxel versus cisplatin and paclitaxel in patients with suboptimal stage III or IV ovarian cancer: a gynecologic oncology group study." J Clin Oncol **18**(1): 106 -115.

Mukhopadhyay, A., A. Elattar, et al. (2010). "Development of a functional assay for homologous recombination status in primary cultures of epithelial ovarian tumor and correlation with sensitivity to poly(ADP -ribose) polymerase inhibitors." Clin Cancer Res **16**(8): 2344 -2351.

Mul, Y. M., C. P. Verrijzer, et al. (1990). "Transcription factors NFI and NFIII/oct -1 function independently, employing different mechanisms to enhance adenovirus DNA replication." J Virol **64**(11): 5510 -5518.

Mullick, A., Y. Xu, et al. (2006). "The cumate g ene-switch: a system for regulated expression in mammalian cells." BMC Biotechnol **6**: 43.

Mulvihill, S., R. Warren, et al. (2001). "Safety and feasibility of injection with an E1B -55 kDa gene-deleted, replication-selective adenovirus (ONYX -015) into primary carcinomas of the pancreas: a phase I trial." Gene Ther **8**(4): 308 -315.

Murdoch, W. J. and J. F. Martinchick (2004). "Oxidative damage to DNA of ovarian surface epithelial cells affected by ovulation: carcinogenic implication and chemoprevention." Exp Biol Med (Maywood) **229**(6): 546 -552.

Muruve, D. A. (2004). "The innate immune response to adenovirus vectors." Hum Gene Ther **15**(12): 1157 -1166.

Nagata, K., R. A. Guggenheimer, et al. (1983). "Specific binding of a cellular DNA replication protein to the origin of replication of adenovirus DNA." Proc Natl Acad Sci U S A **80**(20): 6177 -6181.

Neijt, J. P., S. A. Engelholm, et al. (2000). "Exploratory phase III study of paclitaxel and cisplatin versus paclitaxel and carboplatin in advanced ovarian cancer." J Clin Oncol **18**(17): 3084 -3092.

Nemunaitis, J., C. Cunningham, et al. (2001). "Intravenous infusion of a replication -selective adenovirus (ONYX -015) in cancer patients: safety, feasibility and biological activity." Gene Ther **8**(10): 746 -759.

Nemunaitis, J., I. Ganly, et al. (2000). "Selective replication and oncolysis in p53 mutant tumors with ONYX-015, an E1B-55kD gene-deleted adenovirus, in patients with advanced head and neck cancer: a phase II trial." Cancer Res **60**(22): 6359 -6366.

Nemunaitis, J., F. Khuri, et al. (2001). "Phase II trial of intratumoral administration of ONYX-015, a replication-selective adenovirus, in patients with refractory head and neck cancer." J Clin Oncol **19**(2): 289 -298.

Nevins, J. R. (1986). "Control of cellular and viral transcription du ring adenovirus infection." CRC Crit Rev Biochem **19**(4): 307 -322.

Nordqvist, K., K. Ohman, et al. (1994). "Human adenovirus encodes two proteins which have opposite effects on accumulation of alternatively spliced mRNAs." Mol Cell Biol **14**(1): 437 -445.

O'Connor, P. M., J. Jackman, et al. (1997). "Characterization of the p53 tumor suppressor pathway in cell lines of the National Cancer Institute anticancer drug screen and correlations with the growth-inhibitory potency of 123 anticancer agents." Cancer Res **57**(19): 4285 -4300.

O'Shea, C., K. Klupsch, et al. (2005). "Adenoviral proteins mimic nutrient/growth signals to activate the mTOR pathway for viral replication." Embo J **24**(6): 1211-1221.

O'Shea, C. C., S. Choi, et al. (2005). "Adenovirus overrides cellular ch eckpoints for protein translation." Cell Cycle **4**(7): 883 -888.

O'Shea, C. C., L. Johnson, et al. (2004). "Late viral RNA export, rather than p53 inactivation, determines ONYX-015 tumor selectivity." Cancer Cell **6**(6): 611 -623.

O ' Reilly D, M. L., Luckow V (19 94). Appendix 6. Baculovirus Expression Vectors: A laboratory Manual, Oxford University Press

Obata, K., S. J. Morland, et al. (1998). "Frequent PTEN/MMAC mutations in endometrioid but not serous or mucinous epithelial ovarian tumors." Cancer Res **58**(10): 2095-2097.

Ohman, K., K. Nordqvist, et al. (1993). "Two adenovirus proteins with redundant activities in virus growth facilitates tripartite leader mRNA accumulation." Virology **194**(1): 50 -58.

Oosterom-Dragon, E. A. and H. S. Ginsberg (1981). "Characterizat ion of two temperature-sensitive mutants of type 5 adenovirus with mutations in the 100,000-dalton protein gene." J Virol **40**(2): 491 -500.

Orsulic, S., Y. Li, et al. (2002). "Induction of ovarian cancer by defined multiple genetic changes in a mouse model system." Cancer Cell **1**(1): 53 -62.

Ostapchuk, P., M. E. Anderson, et al. (2006). "The L4 22 -kilodalton protein plays a role in packaging of the adenovirus genome." J Virol **80**(14): 6973 -6981.

Ostapchuk, P. and P. Hearing (2005). "Control of adenovirus packagi ng." J Cell Biochem **96**(1): 25 -35.

Ozols, R. F., B. N. Bundy, et al. (2003). "Phase III trial of carboplatin and paclitaxel compared with cisplatin and paclitaxel in patients with optimally resected stage III ovarian cancer: a Gynecologic Oncology Group study." J Clin Oncol **21**(17): 3194 -3200.

Pardo-Mateos, A. and C. S. Young (2004). "Adenovirus IVa2 protein plays an important role in transcription from the major late promoter in vivo." Virology **327**(1): 50 -59.

Park, B. H., T. Hwang, et al. (2008). "Use of a t argeted oncolytic poxvirus, JX-594, in patients with refractory primary or metastatic liver cancer: a phase I trial." Lancet Oncol **9**(6): 533 -542.

Park, S. M., R. Schickel, et al. (2005). "Nonapoptotic functions of FADD -binding death receptors and their signaling molecules." Curr Opin Cell Biol **17**(6): 610-616.

Parker, A. L., J. H. McVey, et al. (2007). "Influence of coagulation factor zymogens on the infectivity of adenoviruses pseudotyped with fibers from subgroup D." J Virol **81**(7): 3627 -3631.

Parker, A. L., S. N. Waddington, et al. (2006). "Multiple vitamin K -dependent coagulation zymogens promote adenovirus-mediated gene delivery to hepatocytes." Blood **108**(8): 2554 -2561.

Pecora, A. L., N. Rizvi, et al. (2002). "Phase I trial of intravenous adm inistration of PV701, an oncolytic virus, in patients with advanced solid cancers." J Clin Oncol **20**(9): 2251 -2266.

Pelka, P., J. N. Ablack, et al. (2008). "Intrinsic structural disorder in adenovirus E1A: a viral molecular hub linking multiple diverse processes." J Virol **82**(15): 7252-7263.

Pelletier, J. and N. Sonenberg (1988). "Internal initiation of translation of eukaryotic mRNA directed by a sequence derived from poliovirus RNA." Nature **334**(6180): 320 -325.

Perez-Cruet, M. J., T. W. Trask, et al. (1994). "Adenovirus-mediated gene therapy of experimental gliomas." J Neurosci Res **39**(4): 506 -511.

Perez-Romero, P., K. E. Gustin, et al. (2006). "Dependence of the encapsidation function of the adenovirus L1 52/55-kilodalton protein on its ability to bind the packaging sequence." J Virol **80**(4): 1965 -1971.

Perren, T. J., A. M. Swart, et al. (2011). "A phase 3 trial of bevacizumab in ovarian cancer." N Engl J Med **365**(26): 2484 -2496.

Piccart, M. J., K. Bertelsen, et al. (2000). "Randomized intergroup trial of cispla tin-paclitaxel versus cisplatin-cyclophosphamide in women with advanced epithelial ovarian cancer: three-year results." J Natl Cancer Inst **92**(9): 699 -708.

Piek, J. M., P. J. van Diest, et al. (2001). "Dysplastic changes in prophylactically removed Fallopian tubes of women predisposed to developing ovarian cancer." J Pathol **195**(4): 451 -456.

Piver, M. S., S. B. Lele, et al. (1988). "The impact of aggressive debulking surgery and cisplatin-based chemotherapy on progression-free survival in stage III and IV ovarian carcinoma." J Clin Oncol **6**(6): 983 -989.

Polos, P. G. and W. R. Gallaher (1981). "A quantitative assay for cytolysis induced by Newcastle disease virus." J Gen Virol **52**(Pt 2): 259 -265.

Press, J. Z., A. De Luca, et al. (2008). "Ovarian carcinomas with genetic and epigenetic BRCA1 loss have distinct molecular abnormalities." BMC Cancer **8**: 17.

Pujade-Lauraine, E., U. Wagner, et al. "Pegylated liposomal Doxorubicin and Carboplatin compared with Paclitaxel and Carboplatin for patients with platinum-sensitive ovarian cancer in late relapse." J Clin Oncol **28**(20): 3323 -3329.

Rajala, M. S., R. V. Rajala, et al. (2005). "Corneal cell survival in adenovirus type 19 infection requires phosphoinositide 3-kinase/Akt activation." J Virol **79**(19): 12332-12341.

Raki, M., M. Sarkioja, et al. (2008). "Oncolytic adenovirus Ad5/3 -delta24 and chemotherapy for treatment of orthotopic ovarian cancer." Gynecol Oncol **108**(1): 166 -172.

Raman, S., T. H. Hsu, et al. (20 09). "Usage of integrin and heparan sulfate as receptors for mouse adenovirus type 1." J Virol **83**(7): 2831 -2838.

Raper, S. E., M. Yudkoff, et al. (2002). "A pilot study of in vivo liver -directed gene transfer with an adenoviral vector in partial ornithine transcarbamylase deficiency." Hum Gene Ther **13**(1): 163 -175.

Reach, M., L. X. Xu, et al. (1991). "Transcription from the adenovirus major late promoter uses redundant activating elements." EMBO J **10**(11): 3439 -3446.

Reichel, R., S. D. Neill, et al. (1989). "The adenovirus E4 gene, in addition to the E1A gene, is important for trans-activation of E2 transcription and for E2F activation." J Virol **63**(9): 3643 -3650.

Reid, T. R., S. Freeman, et al. (2005). "Effects of Onyx -015 among metastatic colorectal cancer patients that have failed prior treatment with 5-FU/leucovorin." Cancer Gene Ther **12**(8): 673 -681.

Relph, K. L., K. J. Harrington, et al. (2005). "Adenoviral strategies for the gene therapy of cancer." Semin Oncol **32**(6): 573 -582.

Riley, D. and S. J. Flint (1993). "RNA -binding properties of a translational activator, the adenovirus L4 100-kilodalton protein." J Virol **67**(6): 3586 -3595.

Rissoan, M. C., V. Soumelis, et al. (1999). "Reciprocal control of T helper cell and dendritic cell differentiation." Science **283**(5405): 1183 -1186.

Roberts, M. S., R. M. Lorence, et al. (2006). "Naturally oncolytic viruses." Curr Opin Mol Ther **8**(4): 314 -321.

Roelvink, P. W., A. Lizonova, et al. (1998). "The coxsackievirus -adenovirus receptor protein can function as a cellular attachment protein for adenovirus serotypes from subgroups A, C, D, E, and F." J Virol **72**(10): 7909 -7915.

Roelvink, P. W., G. Mi Lee, et al. (1999). "Identification of a conserved receptor -binding site on the fiber proteins of CAR-recognizing adenoviridae." Science **286**(5444): 1568 -1571.

Rose, P. G., J. A. Blessing, et al. (1998). "Prolonged oral etoposide as second -line therapy for platinum-resistant and platinum-sensitive ovarian carcinoma: a Gynecologic Oncology Group study." J Clin Oncol **16**(2): 405 -410.

Routes, J. M., S. Ryan, et al. (2000). "Adenovirus E1A oncogene expression in tumor cells enhances killing by TNF-related apoptosis-inducing ligand (TRAIL)." J Immunol **165**(8): 4522 -4527.

Russell, W. C. (2009). "Adenoviruses: update on structure and function." J Gen Virol **90**(Pt 1): 1 -20.

Russell, W. C. and G. E. Blair (1977). "Polypeptide phosphorylation in adenovirus -infected cells." J Gen Virol **34**(1): 19 -35.

Saban, S. D., M. Silvestry, et al. (2006). "Visualization of alpha -helices in a 6-angstrom resolution cryoelectron microscopy structure of adenovirus allows refinement of capsid protein assignments." J Virol **80**(24): 12049 -12059.

Sabbah, M., S. Emami, et al. (2008). "Molecular signature and therapeutic perspective of the epithelial-to-mesenchymal transitions in epithelial cancers." Drug Resist Updat **11**(4 -5): 123 -151.

Salone, B., Y. Martina, et al. (2003). "Integrin alpha3beta1 is an a lternative cellular receptor for adenovirus serotype 5." J Virol **77**(24): 13448 -13454.

Santis, G., V. Legrand, et al. (1999). "Molecular determinants of adenovirus serotype 5 fibre binding to its cellular receptor CAR." J Gen Virol **80 (Pt 6)** : 1519-1527.

Sato, N., H. Tsunoda, et al. (2000). "Loss of heterozygosity on 10q23.3 and mutation of the tumor suppressor gene PTEN in benign endometrial cyst of the ovary: possible sequence progression from benign endometrial cyst to endometrioid carcinoma and clear cell carcinoma of the ovary." Cancer Res **60**(24): 7052 -7056.

Sauthoff, H., J. Hu, et al. (2003). "Intratumoral spread of wild -type adenovirus is limited after local injection of human xenograft tumors: virus persists and spreads systemically at late time points." Hum Gene Ther **14**(5): 425 -433.

Schirrmacher, V. (1999). "In situ analysis of tumor -specific CTL effector and memory responses elicited by tumor vaccination." Int J Oncol **15**(2): 217 -227.

Schneider-Brachert, W., V. Tchikov, et al. (2006). "Inhibition of TNF receptor 1 internalization by adenovirus 14.7K as a novel immune escape mechanism." J Clin Invest **116**(11): 2901 -2913.

Schumann, M. and M. Dobbelstein (2006). "Adenovirus -induced extracellular signal-regulated kinase phosphorylation during the late phase of infection enhances viral protein levels and virus progeny." Cancer Res **66**(3): 1282 -1288.

Schwartz, D. R., S. L. Kardia, et al. (2002). "Gene expression in ovarian cancer reflects both morphology and biological behavior, distinguishing clear cell from other poor-prognosis ovarian carcinomas." Cancer Res **62**(16): 4722 -4729.

Seidman, J. D. and R. J. Kurman (1996). "Subclassification of serous borderline tumors of the ovary into benign and malignant types. A clinicopathologic study of 65 advanced stage cases." Am J Surg Pathol **20**(11): 1331 -1345.

Shao, R., M. C. Hu, et al. (1999). "E1A sensitizes cells to tumor necrosis factor -induced apoptosis through inhibition of IkappaB kinases and nuclear factor kappaB activities." J Biol Chem **274**(31): 21495 -21498.

Shashkova, E. V., K. Doronin, et al. (2008). "Macrophage depletion combined with anticoagulant therapy increases therapeutic window of systemic treatment with oncolytic adenovirus." Cancer Res **68**(14): 5896 -5904.

Shaw, C. A., P. C. Holland, et al. (2004). "Isof orm-specific expression of the Coxsackie and adenovirus receptor (CAR) in neuromuscular junction and cardiac intercalated discs." BMC Cell Biol **5**(1): 42.

Shayakhmetov, D. M., A. Gaggar, et al. (2005). "Adenovirus binding to blood factors results in liver cell infection and hepatotoxicity." J Virol **79**(12): 7478 -7491.

Shen, Y. and J. Nemunaitis (2005). "Fighting cancer with vaccinia virus: teaching new tricks to an old dog." Mol Ther **11**(2): 180 -195.

Shenk, T. (2001). Adenoviridae: The Viruses and Their Replication. Fields Virology. D. Knipe, Howley, P, Lippincott Williams and Wilkins**:** 2265-2301.

Sherr, C. J. and F. McCormick (2002). "The RB and p53 pathways in cancer." Cancer Cell **2**(2): 103 -112.

Shih Ie, M. and R. J. Kurman (2004). "Ovarian tumorigenesis: a proposed model based on morphological and molecular genetic analysis." Am J Pathol **164**(5): 1511 -1518.

Shisler, J., C. Yang, et al. (1997). "The adenovirus E3 -10.4K/14.5K complex mediates loss of cell surface Fas (CD95) and resistance to Fas -induced apoptosis." J Virol **71**(11): 8299 -8306.

Siemens, C. H. and N. Auersperg (1988). "Serial propagation of human ovarian surface epithelium in tissue culture." J Cell Physiol **134**(3): 347 -356.

Silverstein, G. and W. A. Strohl (1986). "Restricted replication of adenovirus type 2 in mouse Balb/3T3 cells." Arch Virol **87**(3 -4): 241 -264.

Singer, G., R. Oldt, 3rd, et al. (2003). "Mutations in BRAF and KRAS characterize the development of low-grade ovarian serous carcinoma." J Natl Cancer Inst **95**(6): 484 -486.

Singer, G., R. Stohr, et al. (2005). "Patterns of p53 mutations separate ovarian serous borderline tumors and low- and high-grade carcinomas and provide support for a new model of ovarian carcinogenesis: a mutational analysis with immunohistochemical correlation." Am J Surg Pathol **29**(2): 218 -224.

Sinkovics, J. G. and J. C. Horvath (2000). "Newcastle disease virus (NDV): brief history of its oncolytic strains." J Clin Virol **16**(1): 1 -15.

Small, E. J., M. A. Carducci, et al. (2006). "A phase I trial of intravenous CG7870, a replication-selective, prostate-specific antigen-targeted oncolytic adenovirus, for the treatment of hormone-refractory, metastatic prostate cancer." Mol Ther **14**(1): 107 -117.

Smith Sehdev, A. E., P. S. Sehdev, et al. (2003). "Noninvasive and invasive micropapillary (low -grade) serous carcinoma of the ovary: a clinicopathologic analysis of 135 cases." Am J Surg Pathol **27**(6): 725 -736.

Smith, T. A., N. Idamakanti, et al. (20 03). "Adenovirus serotype 5 fiber shaft influences in vivo gene transfer in mice." Hum Gene Ther **14**(8): 777 -787.

Soiffer, R., T. Lynch, et al. (1998). "Vaccination with irradiated autologous melanoma cells engineered to secrete human granulocyte-macrophage colony-stimulating factor generates potent antitumor immunity in patients with metastatic melanoma." Proc Natl Acad Sci U S A **95**(22): 13141 -13146.

Soloway, P. D. and T. Shenk (1990). "The adenovirus type 5 i -leader open reading frame functions in cis to reduce the half-life of L1 mRNAs." J Virol **64**(2): 551 -558.

Song, B., S. L. Hu, et al. (1996). "Conservation of DNA sequence in the predicted major late promoter regions of selected mastadenoviruses." Virology **220**(2): 390-401.

Song, B. and C. S. Young (1997) . "Functional characterization of the major late promoter of mouse adenovirus type 1." Virology **235**(1): 109 -117.

Sorensen, C. S., R. G. Syljuasen, et al. (2003). "Chk1 regulates the S phase checkpoint by coupling the physiological turnover and ionizing radiation-induced accelerated proteolysis of Cdc25A." Cancer Cell **3**(3): 247 -258.

South, S. A., H. Vance, et al. (2009). "Consideration of hereditary nonpolyposis colorectal cancer in BRCA mutation-negative familial ovarian cancers." Cancer **115**(2): 324 -333.

Steel, J. C., B. J. Morrison, et al. (2007). "Immunocompetent syngeneic cotton rat tumor models for the assessment of replication-competent oncolytic adenovirus." Virology **369**(1): 131 -142.

Stone, D., Y. Liu, et al. (2007). "Adenovirus -platelet interaction in blood causes virus sequestration to the reticuloendothelial system of the liver." J Virol **81**(9): 4866-4871.

Stracker, T. H., C. T. Carson, et al. (2002). "Adenovirus oncoproteins inactivate the Mre11-Rad50-NBS1 DNA repair complex." Nature **418**(6895): 348-352.

Strijker, R., D. T. Fritz, et al. (1989). "Adenovirus VAI -RNA regulates gene expression by controlling stability of ribosome-bound RNAs." EMBO J **8**(9): 2669-2675.

Strom, A. C., P. Ohlsson, et al. (1998). "AR1 is an integral part of the adenovirus type 2 E1A-CR3 transactivation domain." J Virol **72**(7): 5978 -5983.

Strong, J. E., M. C. Coffey, et al. (1998). "The molecular basis of viral oncolysis: usurpation of the Ras signaling pathway by reovirus." EMBO J **17**(12): 3351 -3362.

Su, Q., S. Wang, et al. (2 006). "Tyrosine phosphorylation acts as a molecular switch to full-scale activation of the eIF2alpha RNA-dependent protein kinase." Proc Natl Acad Sci U S A **103**(1): 63 -68.

Subramanian, T., S. Vijayalingam, et al. (2006). "Genetic identification of adenovir us type 5 genes that influence viral spread." J Virol **80**(4): 2000 -2012.

Sugiyama, T., T. Kamura, et al. (2000). "Clinical characteristics of clear cell carcinoma of the ovary: a distinct histologic type with poor prognosis and resistance to platinum-based chemotherapy." Cancer **88**(11): 2584 -2589.

Sumikawa, T., Y. Shigeoka, et al. (2008). "Dexamethasone interferes with trastuzumab-induced cell growth inhibition through restoration of AKT activity in BT-474 breast cancer cells." Int J Oncol **32**(3): 683 -688.

Suomalainen, M., M. Y. Nakano, et al. (2001). "Adenovirus -activated PKA and p38/MAPK pathways boost microtubule-mediated nuclear targeting of virus." EMBO J **20**(6): 1310 -1319.

Suomalainen, M., M. Y. Nakano, et al. (1999). "Microtubule -dependent plus- and minus end-directed motilities are competing processes for nuclear targeting of adenovirus." J Cell Biol **144**(4): 657 -672.

Suzuki, K., R. Alemany, et al. (2002). "The presence of the adenovirus E3 region improves the oncolytic potency of conditionally replicative adenoviruses." Clin Cancer Res **8**(11): 3348 -3359.

Swiersz, L. M. (2002). "Role of endometriosis in cancer and tumor development." Ann N Y Acad Sci **955**: 281-292; discussion 293-285, 396-406.

Symington, J. S., L. A. Lucher, et al. (1986). "Biosynthesis of adenovirus type 2 i - leader protein." J Virol **57**(3): 848 -856.

Tao, N., G. P. Gao, et al. (2001). "Sequestration of adenoviral vector by Kupffer cells leads to a nonlinear dose response of transduction in liver." Mol Ther **3**(1): 28-35.

Taqi, A. M., M. B. Abdurrahman, et al. (1981). "Regression of Hodgkin's disease after measles." Lancet **1**(8229): 1112.

TCGA (2011). "Integrated genomic analyses of ovarian carcinoma." Nature **474**(7353): 609 -615.

Thirukkumaran, C. M., M. J. Nodwell, et al. (2010). "Oncolytic viral therapy for prostate cancer: efficacy of reovirus as a biological therapeutic." Cancer Res **70**(6): 2435 -2444.

Thomas, M. A., J. F. Spencer, et al. (2006). "Syrian hamster as a permissive immunocompetent animal model for the study of oncolytic adenovirus vectors." Cancer Res **66**(3): 1270 -1276.

Tibbles, L. A., J. C. Spurrell, et al. (2002). "Activation of p38 and ERK signaling during adenovirus vector cell entry lead to expression of the C-X-C chemokine IP-10." J Virol **76**(4): 1559 -1568.

Tollefson AE, S. A., Hermiston TW, Ryerse JS, Wold LJ, Wold WS. (1996). "The adenovirus death protein (E3 -11.6K) is required at very late stages of infection for efficient cell lysis and release of adenovirus from infected cells." J Virol **70**(4): 2296 -2306.

Tomko, R. P., C. B. Johansson, et al. (2000). "Expression of the adenovirus receptor and its interaction with the fiber knob." Exp Cell Res **255**(1): 47 -55.

Tomko, R. P., R. Xu, et al. (1997). "HCAR and MCAR: the huma n and mouse cellular receptors for subgroup C adenoviruses and group B coxsackieviruses." Proc Natl Acad Sci U S A **94**(7): 3352 -3356.

Tormanen, H., E. Backstrom, et al. (2006). "L4 -33K, an adenovirus-encoded alternative RNA splicing factor." J Biol Chem **281**(48): 36510 -36517.

Toth, K., J. F. Spencer, et al. (2005). "Cotton rat tumor model for the evaluation of oncolytic adenoviruses." Hum Gene Ther **16**(1): 139 -146.

Toth, K., J. F. Spencer, et al. (2007). "Immunocompetent, semi -permissive cotton rat tumor model for the evaluation of oncolytic adenoviruses." Methods Mol Med **130**: 157-168.

Trask, T. W., R. P. Trask, et al. (2000). "Phase I study of adenoviral delivery of the HSV-tk gene and ganciclovir administration in patients with current malignant brain tumors." Mol Ther **1**(2): 195 -203.

Tribouley, C., P. Lutz, et al. (1994). "The product of the adenovirus intermediate gene IVa2 is a transcriptional activator of the major late promoter." J Virol **68**(7): 4450 -4457.

Tubiana, M. and E. Malaise (1976). "Comparison of c ell proliferation kinetics in human and experimental tumors: response to irradiation." Cancer Treat Rep **60**(12): 1887 -1895.

Turner, N., A. Tutt, et al. (2004). "Hallmarks of 'BRCAness' in sporadic cancers." Nat Rev Cancer **4**(10): 814 -819.

van den Hengel, S. K., J. de Vrij, et al. "Truncating the i-leader open reading frame enhances release of human adenovirus type 5 in glioma cells." Virol J **8**: 162.

van Raaij, M. J., E. Chouin, et al. (2000). "Dimeric structure of the coxsackievirus and adenovirus receptor D1 domain at 1.7 A resolution." Structure **8**(11): 1147-1155.

Vasey, P. A. (2005). "Intraperitoneal chemotherapy for epithelial ovarian carcinoma." Future Oncol **1**(3): 289 -292.

Vasey, P. A., L. N. Shulman, et al. (2002). "Phase I trial of intraperitoneal inject ion of the E1B-55-kd-gene-deleted adenovirus ONYX-015 (dl1520) given on days 1 through 5 every 3 weeks in patients with recurrent/refractory epithelial ovarian cancer." J Clin Oncol **20**(6): 1562 -1569.

Vidal, L., H. S. Pandha, et al. (2008). "A phase I study of intravenous oncolytic reovirus type 3 Dearing in patients with advanced cancer." Clin Cancer Res **14**(21): 7127 -7137.

Vigant, F., D. Descamps, et al. (2008). "Substitution of hexon hypervariable reg ion 5 of adenovirus serotype 5 abrogates blood factor binding and limits gene transfer to liver." Mol Ther **16**(8): 1474 -1480.

von Minckwitz, G., T. Bauknecht, et al. (1999). "Phase II study of gemcitabine in ovarian cancer." Ann Oncol **10**(7): 853 -855.

Vorburger, S. A. and K. K. Hunt (2002). "Adenoviral gene therapy." Oncologist **7**(1): 46 -59.

Waddington, S. N., J. H. McVey, et al. (2008). "Adenovirus serotype 5 hexon mediates liver gene transfer." Cell **132**(3): 397 -409.

Waddington, S. N., A. L. Parker, et al. (2007). "Targeting of adenovirus serotype 5 (Ad5) and 5/47 pseudotyped vectors in vivo: fundamental involvement of coagulation factors and redundancy of CAR binding by Ad5." J Virol **81**(17): 9568-9571.

Wang, H. G., G. Draetta, et al. (1991). "E1A induce s phosphorylation of the retinoblastoma protein independently of direct physical association between the E1A and retinoblastoma products." Mol Cell Biol **11**(8): 4253 -4265.

Wang, K., S. Huang, et al. (1998). "Adenovirus internalization and infection require dynamin." J Virol **72**(4): 3455 -3458.

Wang, Y., R. Gangeswaran, et al. (2009). "CEACAM6 attenuates adenovirus infection by antagonizing viral trafficking in cancer cells." J Clin Invest **119**(6): 1604-1615.

Wang, Y., G. Hallden, et al. (2003). "E3 gene manipul ations affect oncolytic adenovirus activity in immunocompetent tumor models." Nat Biotechnol **21**(11): 1328 -1335.

Wang, Y., J. K. Hu, et al. (2003). "Systemic dissemination of viral vectors during intratumoral injection." Mol Cancer Ther **2**(11): 1233 -1242.

Webster, L. C. and R. P. Ricciardi (1991). "trans -dominant mutants of E1A provide genetic evidence that the zinc finger of the trans-activating domain binds a transcription factor." Mol Cell Biol **11**(9): 4287 -4296.

Weitzman, M. D. (2005a). "Functions of the adenovirus E4 proteins and their impact on viral vectors." Front Biosci **10**: 1106-1117.

Weitzman, M. D. and D. A. Ornelles (2005b). "Inactivating intracellular antiviral responses during adenovirus infection." Oncogene **24**(52): 7686 -7696.

Wheatley, D. N. (2 004). "Controlling cancer by restricting arginine availability -- arginine-catabolizing enzymes as anticancer agents." Anticancer Drugs **15**(9): 825 -833.

White, E. (2001). "Regulation of the cell cycle and apoptosis by the oncogenes of adenovirus." Oncogene **20**(54): 7836 -7846.

Wickham, T. J., P. Mathias, et al. (1993). "Integrins alpha v beta 3 and alpha v beta 5 promote adenovirus internalization but not virus attachment." Cell **73**(2): 309-319.

Wiethoff, C. M., H. Wodrich, et al. (2005). "Adenovirus protein VI m ediates membrane disruption following capsid disassembly." J Virol **79**(4): 1992 -2000.

Wolff, G., S. Worgall, et al. (1997). "Enhancement of in vivo adenovirus -mediated gene transfer and expression by prior depletion of tissue macrophages in the target organ." J Virol **71**(1): 624 -629.

Workman, P., A. Balmain, et al. (1988). "UKCCCR guidelines for the welfare of animals in experimental neoplasia." Lab Anim **22**(3): 195 -201.

Xi, Q., R. Cuesta, et al. (2004). "Tethering of eIF4G to adenoviral mRNAs by viral 100k protein drives ribosome shunting." Genes Dev **18**(16): 1997 -2009.

Xi, Q., R. Cuesta, et al. (2005). "Regulation of translation by ribosome shunting through phosphotyrosine-dependent coupling of adenovirus protein 100k to viral mRNAs." J Virol **79**(9): 5676 -5683.

Xu, Z., J. Tian, et al. (2008). "Clearance of adenovirus by Kupffer cells is mediated by scavenger receptors, natural antibodies, and complement." J Virol **82**(23): 11705-11713.

Yang, T. C. and N. K. Maluf "Self-association of the adenoviral L4-22K protein." Biochemistry **49**(45): 9830 -9838.

Yew, P. R., C. C. Kao, et al. (1990). "Dissection of functional domains in the adenovirus 2 early 1B 55K polypeptide by suppressor-linker insertional mutagenesis." Virology **179**(2): 795 -805.

Ying, B., K. Toth, et al. (2009). "INGN 007, an oncolytic adenovirus vector, replicates in Syrian hamsters but not mice: comparison of biodistribution studies." Cancer Gene Ther.

You, Z., D. C. Fischer, et al. (2001). "Coxsackievirus -adenovirus receptor expression in ovarian cancer cell lines is associated with increased adenovirus transduction efficiency and transgene expression." Cancer Gene Ther **8**(3): 168-175.

Young, A. and I. A. McNeish (2009). "Oncolytic a denoviral gene therapy in ovarian cancer: why we are not wasting our time." Future Oncol **5**(3): 339 -357.

Yu, G. Y. and M. M. Lai (2005). "The ubiquitin -proteasome system facilitates the transfer of murine coronavirus from endosome to cytoplasm during virus entry." J Virol **79**(1): 644 -648.

Yueh, A. and R. J. Schneider (1996). "Selective translation initiation by ribosome jumping in adenovirus-infected and heat-shocked cells." Genes Dev **10**(12): 1557-1567.

Yueh, A. and R. J. Schneider (2000). "Translation by ribosome shunting on adenovirus and hsp70 mRNAs facilitated by complementarity to 18S rRNA." Genes Dev **14**(4): 414 -421.

Yun, C. O., E. Kim, et al. (2005). "ADP -overexpressing adenovirus elicits enhanced cytopathic effect by induction of apoptosis." Cancer Gene Ther **12**(1): 61 -71.

Zhang, W. and M. J. Imperiale (2000). "Interaction of the adenovirus IVa2 protein with viral packaging sequences." J Virol **74**(6): 2687 -2693.

Zhang, Y., P. J. Dolph, et al. (1989). "Secondary structure analysis of adenovirus tripartite leader." J Biol Chem **264**(18): 10679 -10684.

Zorn, K. K., T. Bonome, et al. (2005). "Gene expression profiles of serous, endometrioid, and clear cell subtypes of ovarian and endometrial cancer." Clin Cancer Res **11**(18): 6422 -6430.

8. Appendix 1: Publications